Selected problems of ship dynamics and hydrodynamics

Избранные задачи теории корабля

Serge Sutulo

Сергей Валентинович Сутуло

Centre for Marine Technology and Ocean Engineering (CENTEC), Instituto Superior Técnico, Universidade de Lisboa, Portugal

St. Petersburg, April 2023

List of topics

1. Development of a multi-model offline manoeuvring simulation code MANIST
2. Regression analysis and optimized experimental designs in ship manoeuvrability
3. Hydrodynamic interaction---HYDINTER code
4. 3D linear frequency-domain seakeeping code SEAKIST
5. Hydrodynamic characteristics of ship sections
6. Manoeuvring in waves
7. Identification
8. Episodes:

- Kinematical prediction
- Nomoto-type model
- Full-scale trials and observations
- Fractional model
- 4-quadrant model, wind-tunnel, CFD

Features of the OO Manoeuvring Code MANIST

1. Priority of research and teaching purposes
2. Full access at the source level is presumed
3. The class system should be as natural and logical as possible
4. The code must be reasonably safe
5. Implementation of various mathematical models is envisaged
6. Almost arbitrary configuration

Main Manoeuvring Classes--1

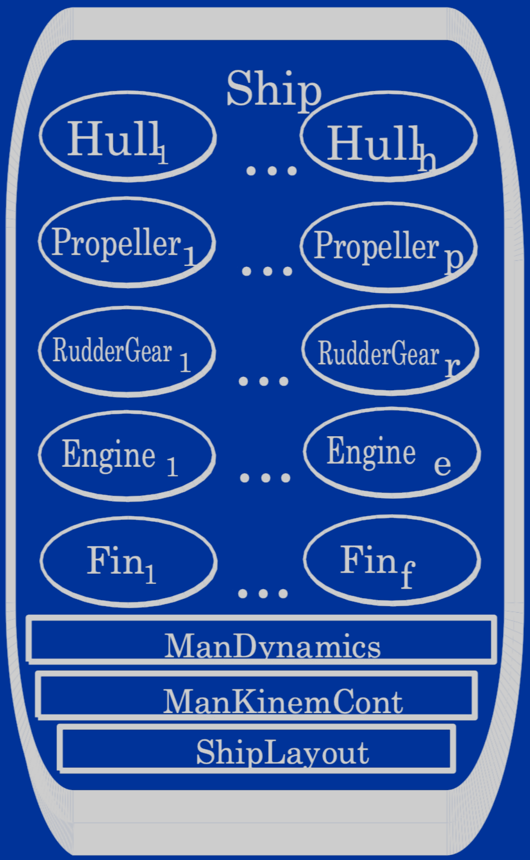


```
class  Ship
{
  public:
    ~Ship();
     Ship();
…………………
  private: //  Ship subclasses:

    ShipLayout     theLayout;
    ManKinemCont   theKinCon;
    ManDynamics   theForces;

    Hull             * theHulls;
    Propeller      * thePropellers;
    RudderGear * theRudders;
    Engine          * theEngines;
    Fin               * theFins;
};
```

Main Manoeuvring Classes--2

```
class  Ship
{
 public:
………………………………..
   void SetShip( const   String &  aShipDatabase );

   void PlayTurn( double  hlmDg,    const String &  filename,   double  outSprite = -
      1.0);
   void PlaySpiral( double mxHlmDg,  double RelRpmPc,   const String &   filename);
   void PlayZigZag( double hlmDg,  double hdnDg,     double RelRpmPc,
        const String & filename,  int numZeros = 5     );
   void   NextState();
   void  OutHistTecpl( const String & fname, int  heading_represent_option  = 0 );
   void  OutSpiralTecpl( const String & fname  );
   void  OutTurnParamTex(   const String & fname, double results[2][6] );
………………………………..
};
```

Main Manoeuvring Classes--3

```
class  RudderGear
{
 public:
  ~RudderGear();
    RudderGear();
   void  SetData( int rud_number, const ShipLayout &   aLayout );
   void  LinkToHull( const Hull &  aHull );
   void  LinkToProp( const Propeller &  aPropeller );
   void  ForcesMoments(   double  aDeflctn,          // rudder's deflection angle
                          double  aSrg_vel,          // rudder's surge velocity
                          double  aSwy_vel,          // rudder's sway  velocity
                          double  anInflow,          // inflow magnitude
                          double  aSidewash,         // sidewash  angle
                          double  aSlip,             // propeller's slip
                          double  aLoading,          // propeller's loading cft
                          double  aThrust,           // propeller's thrust
                          double  & surgeForce,
                          double  & swayForce,
                          double  & hydroAbscissa  );
    double  GearAction(    double  anOrder,         // rudder order
                           double  aDeflctn  );     // rudder's deflection angle
 private:
  ........................................................
};
```

Main Manoeuvring Classes--4

```
void main()
{
   Ship  ship_A, ship_B;   Ship  target_ships[30];

   ship_A.SetShip( “ship_A_input_file.dat” );
   ship_B.SetShip( “ship_B_input_file.dat” );

   ship_A.PlayTurn( helmdg, GenericFileNameA,
    image_period, final_time );
   ship_B.PlaySpiral( 35.0, 100.0, GenericFileNameB );
}
```

INSTITUTO SUPERIOR TÉCNICO

Mathematical Model: Common Part

$$(m+\mu_{11})\dot{u}+(mz_G+\mu_{15})\dot{q}-mvr$$
$$-mx_Gr^2+mz_Gpr+mwq-mx_Gq^2=X,$$
$$(m+\mu_{22})\dot{v}-(mz_G+\mu_{24})\dot{p}+(mx_G+\mu_{26})\dot{r}$$
$$+mur-mur-mwp+mx_Gpq+mz_Gqr=Y,$$
$$(m+\mu_{33})\dot{w}-(mx_G+\mu_{35})\dot{q}-muq$$
$$-mz_Gq^2+mvp+mx_Gpr-mz_Gp^2=Z,$$
$$-(mz_G+\mu_{24})\dot{v}+(I_{xx}+\mu_{44})\dot{p}-(I_{xz}+\mu_{46})\dot{r}$$
$$+mz_Gwp+(I_{zz}-I_{yy})qr-mz_Gur-I_{xz}pq=K,$$
$$(mz_G+\mu_{15})\dot{u}-(mx_G+\mu_{35})\dot{w}+(I_{yy}+\mu_{55})\dot{q}$$
$$+mx_Guq+mz_Gwq+(I_{xx}-I_{zz})pr$$
$$+I_{xz}(p^2-r^2)-mz_Gvr-mx_Gvp=M,$$
$$(mx_G+\mu_{26})\dot{v}-(I_{xz}+\mu_{46})\dot{p}+(I_{zz}+\mu_{66})\dot{r}$$
$$+mx_Gur-mx_Gwp+(I_{yy}-I_{xx})pq+I_{xz}qr=N,$$

$$\begin{aligned}
\dot{\xi} &= u\cos\psi\cos\theta \\
&\quad + v(\cos\psi\sin\theta\sin\varphi-\sin\psi\cos\varphi) \\
&\quad + w(\cos\psi\sin\theta\cos\varphi-\sin\psi\sin\varphi), \\
\dot{\eta} &= u\sin\psi\cos\theta \\
&\quad + v(\sin\psi\sin\theta\sin\varphi+\cos\psi\cos\varphi) \\
&\quad + w(\cos\psi\sin\theta\cos\varphi-\cos\psi\sin\varphi), \\
\dot{\zeta} &= -u\sin\theta+v\cos\theta\sin\varphi+w\cos\theta\cos\varphi, \\
\dot{\psi} &= q\frac{\sin\varphi}{\cos\theta}+r\frac{\cos\varphi}{\cos\theta}, \\
\dot{\theta} &= q\cos\varphi-r\sin\varphi, \\
\dot{\varphi} &= p+q\tan\theta\sin\varphi+r\tan\theta\cos\varphi.
\end{aligned}$$

Mathematical Model: Unified Internal Representation

$$\mathbf{L}\dot{\mathbf{X}} = \mathbf{R}(\mathbf{X}) + \Phi(\mathbf{X}, t),$$

$$\dot{\mathbf{X}} = \mathbf{L}^{-1}(\mathbf{R} + \Phi).$$

$$\mathbf{L} = \mathrm{diag}(\mathbf{M}, \mathbf{E})$$

$$\mathbf{X} = (u, v, w, p, q, r, \xi_C, \eta_C, \zeta_C, \varphi, \theta, \psi)^T$$

$$\Phi = (\mathbf{F}^{\mathbf{T}}, \mathbf{0})^{\mathbf{T}},$$

$$\mathbf{F_H} = \mathbf{F_{HD}} + \mathbf{F_{HS}} + \mathbf{F_D},$$

$$\mathbf{F} = (X, Y, Z, K, M, N)^T$$

$$\mathbf{F_{HD}} = \frac{\rho}{2} L^{\alpha} T V_H^2 \mathbf{F}'_{\mathbf{H}}(\mathbf{X}'),$$

$$\mathbf{F} = \mathbf{F_H} + \mathbf{F_F} + \mathbf{F_P} + \mathbf{F_R},$$

Currently Implemented Models---1

Hull forces:

1. A holistic 3DOF model based on published *Mariner* coefficients
2. Inoue et al. 4DOF model (1981)
3. Extension of the Inoue model to the low-speed manoeuvres domain (1994)
4. Matsunaga 3DOF model (1993)
5. Kijima 3DOF model (2001)
6. 3DOF and 6DOF models for a catamaran
7. Pershitz (1960—1985)
8. Pershitz—Tumashic (4 quadrant)
9. 3 catamaran models

Drag submodels for modular models:

1. Series 60
2. Holtrop

Currently Implemented Models---2

Rudder:

1. Polynomial as part of the holistic model
2. Inoue
3. Ogawa
4. Söding extended to 4 quadrants / Molland
5. Pershitz
6. Tumashik (4 quadrants)
7. Steering nozzle

Propeller:

1. Oosterveld—Ossannen (B and BB)
2. Oltmann—Sharma (4 quadrant)
3. 4 quadrant MARIN data: ∃ ANN code → make portable trigonometric approximations

Currently Implemented Models---3

Engine

1. Constant rpm
2. Diesel simplified
3. Steam turbine (all regimes)

To implement:

1. Diesel (all regimes)
2. Gas turbine
3. Electric drive

Polynomial regression model---1

$$X_q = X'_q \frac{\rho V^2}{2} LT, \quad Y_q = Y'_q \frac{\rho V^2}{2} LT, \quad N_q = N'_q \frac{\rho V^2}{2} L^2 T,$$

$$X'_q = X'_{uu} u'^2 + X'_{vr} v' r' + X'_{\delta\delta} \delta_R^2,$$

$$Y'_q = Y'_0 + Y'_v v' + Y'_r r' + Y'_{vvv} v'^3 + Y'_{vvr} v'^2 r' + Y'_\delta \delta_R + Y'_{vv\delta} v'^2 \delta_R + Y'_{v\delta\delta} v' \delta_R^2,$$

$$N'_q = N'_0 + N'_v v' + N'_r r' + N'_{vvv} v'^3 + N'_{vvr} v'^2 r' + N'_\delta \delta_R + N'_{vv\delta} v'^2 \delta_R + N'_{v\delta\delta} v' \delta_R^2 + N'_{\delta\delta\delta} \delta_R^3,$$

How to determine the regression coefficients ("manoeuvring derivatives")?

1. Munk method + cross-flow drag concept
2. Empiric methods
3. Captive-model tests in PMM, CPMC, rotating arm
4. The same tests simulated with CFD
5. No need if you can run inline CFD

Representation of quasi-steady characteristics

1. Grid functions/multi-entry tables + interpolation function:

   Require direct measurements of forces in CMT and full-factorial designs with sufficiently large number of runs

2. Regression models:

   --- linear vs nonlinear;

   --- algebraic (moderate manoeuvres) vs trigonometric (arbitrary manoeuvres) polynomials;

Minimum number of test runs == number of regression parameters $\ll$ number of runs in a full-factorial design

Number of factors k	1	2	3	4	5	6	7
Classic 3-level	3	9	27	81	243	729	2,187
Classic 5-level	5	25	125	625	3,125	15,625	78,125
Classic 7-level	7	49	343	2,401	16,807	117,649	823,543
Saturated 3-polynomial	4	10	20	35	56	84	122

Types of captive-model tests---1

1. Harmonic excitation (PMM, CPMC)

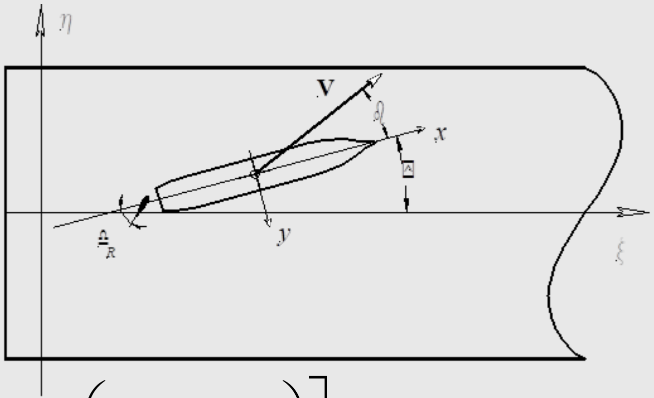

$$V = \mathrm{Fn}\sqrt{gL}, \quad \mathrm{Sn} = \omega L / V$$

$$\dot{\xi} = V\left[\cos\beta\cos\left(\frac{r_0}{\omega}\sin\omega t\right) - \sin\beta\sin\left(\frac{r_0}{\omega}\sin\omega t\right)\right],$$

$$\dot{\eta} = V\left[\cos\beta\sin\left(\frac{r_0}{\omega}\sin\omega t\right) + \sin\beta\cos\left(\frac{r_0}{\omega}\sin\omega t\right)\right],$$

$$r = \frac{r'V}{L}$$

$$\dot{\psi} = r(t) = r_0\cos\omega t,$$

$(\beta, r_0) \in \{(\beta, r_0)_1, (\beta, r_0)_2, \ldots, (\beta, r_0)_N\}$ ---sway-yaw tests,

$\beta \equiv 0$ ---pure yaw tests,

$\dot{\xi}_C = \sqrt{V^2 - v_0^2\cos^2\omega t}$, ---pure sway test: for μ_{22} only!

$\dot{\eta}_C = v_0 \sin\omega t$

Types of captive-model tests---2

2. Circular motion tests CMT (CPMC, Rotating Arm)

$$(\beta, r) \in \{(\beta, r)_1, (\beta, r)_2, \ldots, (\beta, r)_N\}$$

$\exists r'_{\min} : |r'_{\min}| \geq \varepsilon > 0$ ---on rotating arm

Strictly steady, oblique towing at $\beta = 0$

3. Unsteady transients (PMM, CPMC): Scragg, Rhee, Eloot
4. Generalized quasi-steady one-run test: Quadvlieg
   ~a “continuous” sequence of CMTs
5. Can be simulated in CFD

Optimized experimental designs: formulation

1. Only possible when the structure of regression models is set a priori
2. Ideally, the minimum required number of test runs is equal to the number of regression parameters to be defined (saturated design)
3. The higher is the number of the factors (variables the regression depends on), the greater is the efficiency of the approach
4. The quality of the estimates of the regression parameters and the value of the resulting regression model depends on the experimental design i.e. on the set of locations of the test runs in the factor space
5. There are regular algorithms for optimizing response-surface experimental designs

Optimized designs for polynomial regressions

1. Karulin E., Sutulo S. *Optimized Experimental Designs for Estimating Ship Hydrodynamic Derivatives.* Proc. 19th Scientific and Methodological Seminar on Ship Hydrodynamics "Advanced Experimental Techniques and CAD-CAM Methods in Ship Hydrodynamics and Aerodynamics", Varna, Bulgaria. 1—6 October 1990, Vol. 2, pp. 5.1-5.11.

2. Sutulo S., Kim S.-Y. *Systematic Approach to PMM/Rotating Arm Experiment Planning, Parameter Estimation, and Uncertainty Analysis*, MAN'98: Proceedings of the Symposium on Forces Acting on a Manoeuvring Vessel. Val de Reuil, France. September 16–18, 1998, pp. 57–67.

3. Sutulo S, Guedes Soares C. *An algorithm for optimized design of maneuvering experiments.* J Ship Res., 2002, 46: pp. 214—227

4. Sutulo S, Guedes Soares C. *Synthesis of experimental designs of maneuvering captive-model tests with a large number of factors.* J Mar Sci Technol, 2004, Vol.9, pp.32–42

Full-factorials fro 2 factors

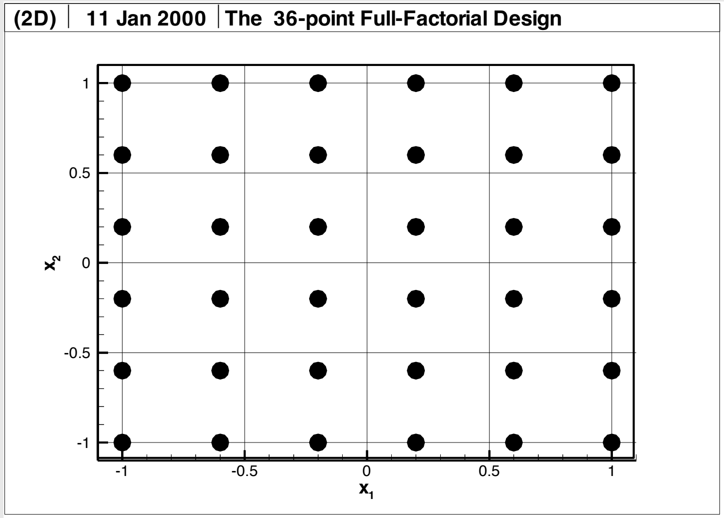

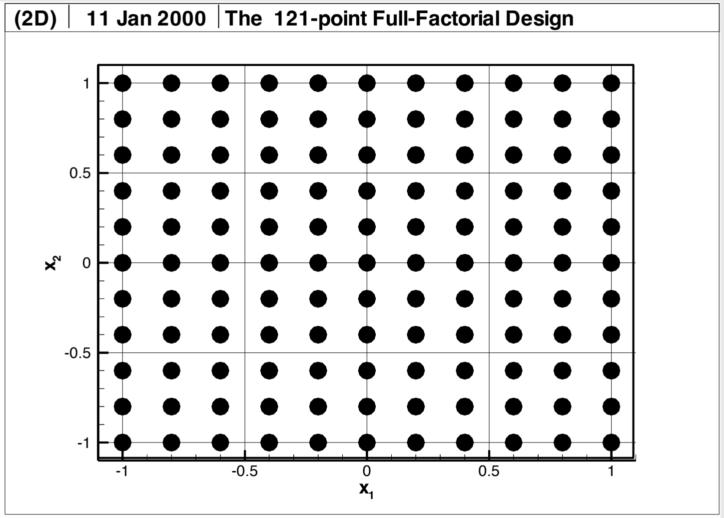

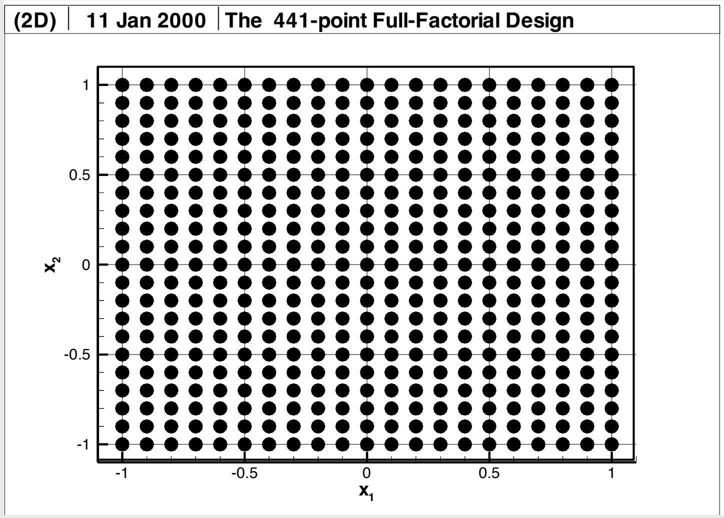

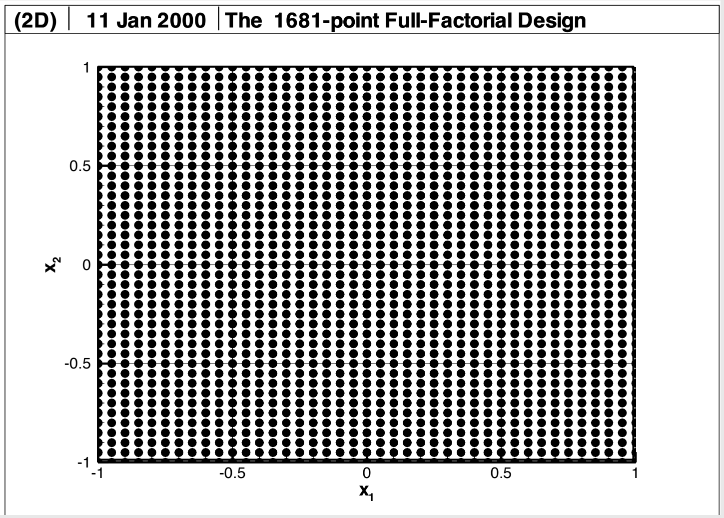

Full-factorials for 3 factors

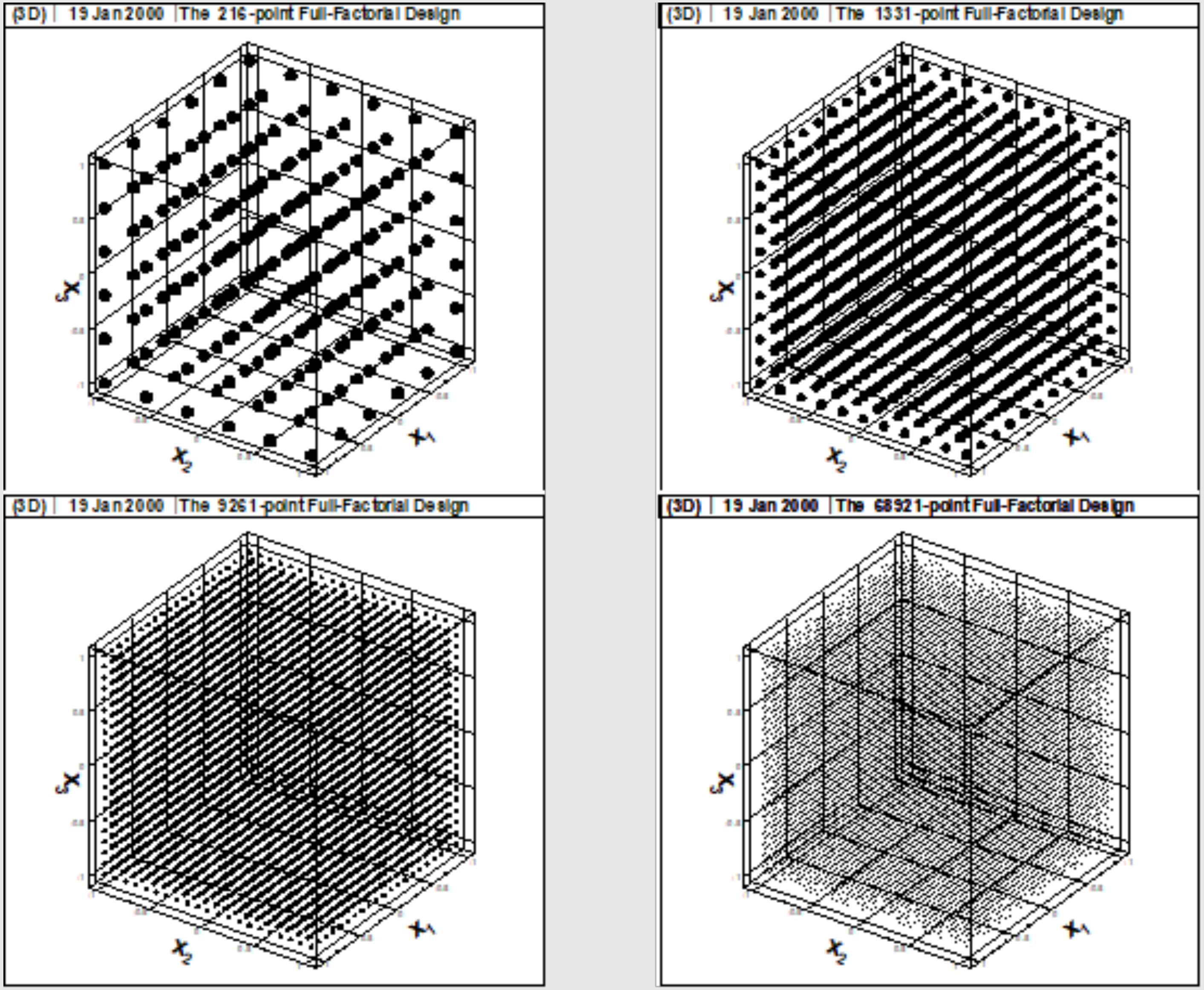

Random saturated 6/11-level designs

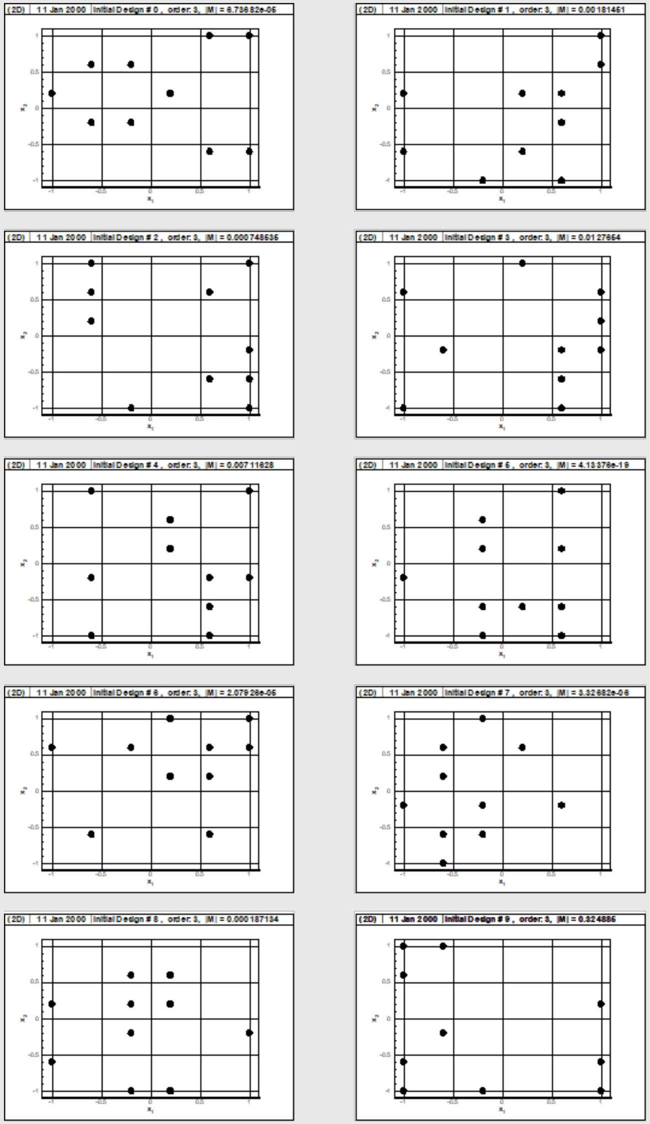

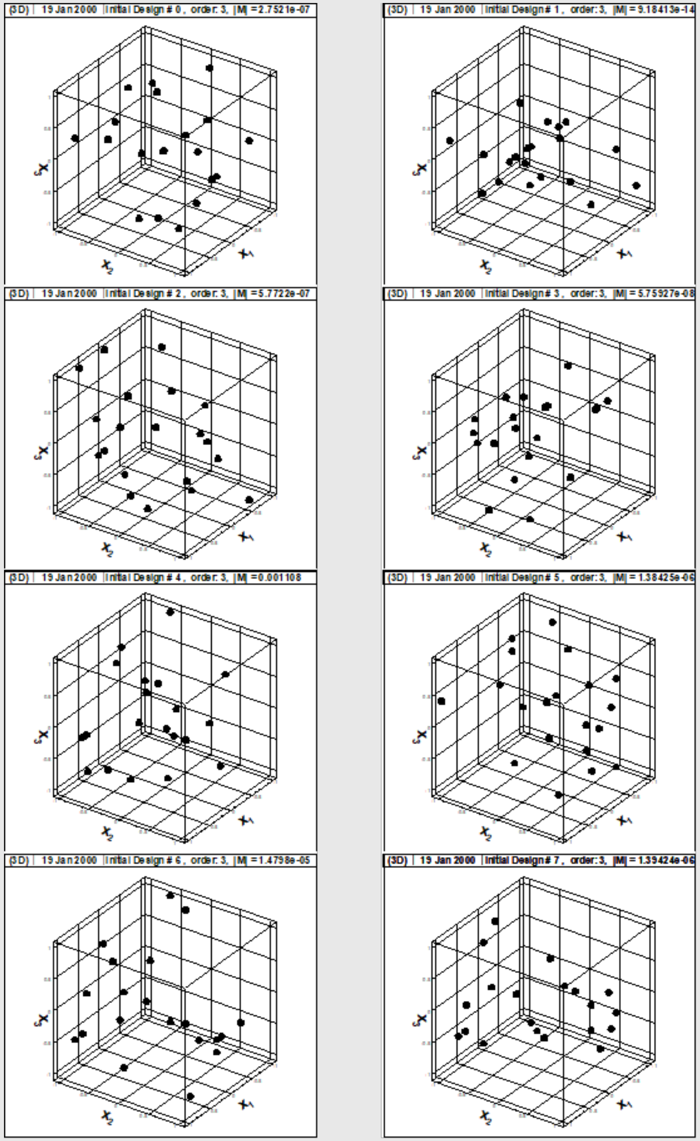

LS regression analysis and ANOVA

$$y_i = \mathbf{f}(\mathbf{x}_i)\mathbf{b} + \varepsilon_i, \quad i = 1,\ldots,N \qquad \mathbf{f}(\mathbf{x}_i) = \left[f_1(\mathbf{x}_i),\ldots,f_m(\mathbf{x}_i) \right]^T$$

$$\mathbf{b} = \left[b_1,\ldots,b_m \right]^T \qquad \mathbf{x} = \left[x_1,\ldots,x_k \right]^T$$

$$\mathbf{y} = \mathbf{F}\mathbf{b} + \varepsilon \qquad \mathbf{y} = \left[y_1,\ldots,y_N \right]^T; \quad \varepsilon = \left[\varepsilon_1,\ldots,\varepsilon_N \right]^T$$

$$\mathbf{F} = \left[\mathbf{f}^T(\mathbf{x}_1),\mathbf{f}^T(\mathbf{x}_2),\ldots,\mathbf{f}^T(\mathbf{x}_N) \right]^T = \begin{bmatrix} f_1(\mathbf{x}_1) & \cdots & f_m(\mathbf{x}_1) \\ \vdots & \ddots & \vdots \\ f_1(\mathbf{x}_N) & \cdots & f_m(\mathbf{x}_N) \end{bmatrix}$$

$$\hat{\mathbf{b}} = \mathbf{D}\mathbf{F}^T\mathbf{y} \qquad \mathbf{D} = \mathbf{M}^{-1} \qquad \mathbf{M} = \mathbf{F}^T\mathbf{F}$$

$$\hat{y}(\mathbf{x}) = \mathbf{f}(\mathbf{x})\hat{\mathbf{b}} \qquad \mathbf{D}_b = \mathbf{D}\sigma^2 \qquad d(\mathbf{x}) = \mathbf{f}^T(\mathbf{x})\mathbf{D}\mathbf{f}(\mathbf{x})$$

Synthesis of D-optimal designs

$$X^D = \operatorname{argmin}|\mathbf{D}| = \operatorname{argmax}|M|, \quad (16)$$

$$X^G = \operatorname{argmin}\left[\max_{\mathbf{x}\in X_O} d(\mathbf{x})\right], \quad (17)$$

$$X^V = \operatorname{argmin} V, \quad (18)$$

$$V = \frac{1}{N_0}\sum_{i=1}^{N_0} d(\mathbf{x}_i). \quad (19)$$

Step 1. An initial design $X_N^0 \subset X_C$ such as $\mathbf{D}(X_N^0)$ 0 is somehow selected. The following steps are iterated.

Step 2. For any iteration $i = 0, 1, \ldots$ a prediction point $\boldsymbol{x}+_i$ with the largest value of the prediction variance (i.e. such as $d(\mathbf{x}+_i) = \max_{\mathbf{x}\in X_C} d(\mathbf{x})$ is found using some optimum searching procedure.

Step 3. The point found at the previous step is added to the current design forming a temporary augmented design $X_{N+1}{}^i = X_N{}^i \cup \{\boldsymbol{x}+_i\}$.

Step 4. The best prediction point $\boldsymbol{x}-_i \in \boldsymbol{X}^i_{N+1}$ such that $d(\mathbf{x}-_i) = \min_{\mathbf{x}\in X_{N+1}} d(\mathbf{x})$ is searched in the current augmented design.

Step 5. The point $\boldsymbol{x}-_i$ is detached from the current design resulting in $X_N^{i+1} = X_{N+1}^i \{ \mathbf{x}-_i \}$.

Step 6. The four previous steps are iterated until $\boldsymbol{M}(\boldsymbol{X}_N{}^{i+1}) = \boldsymbol{M}(\boldsymbol{X}_N{}^i)$.

Optimized saturated 6/11 level designs

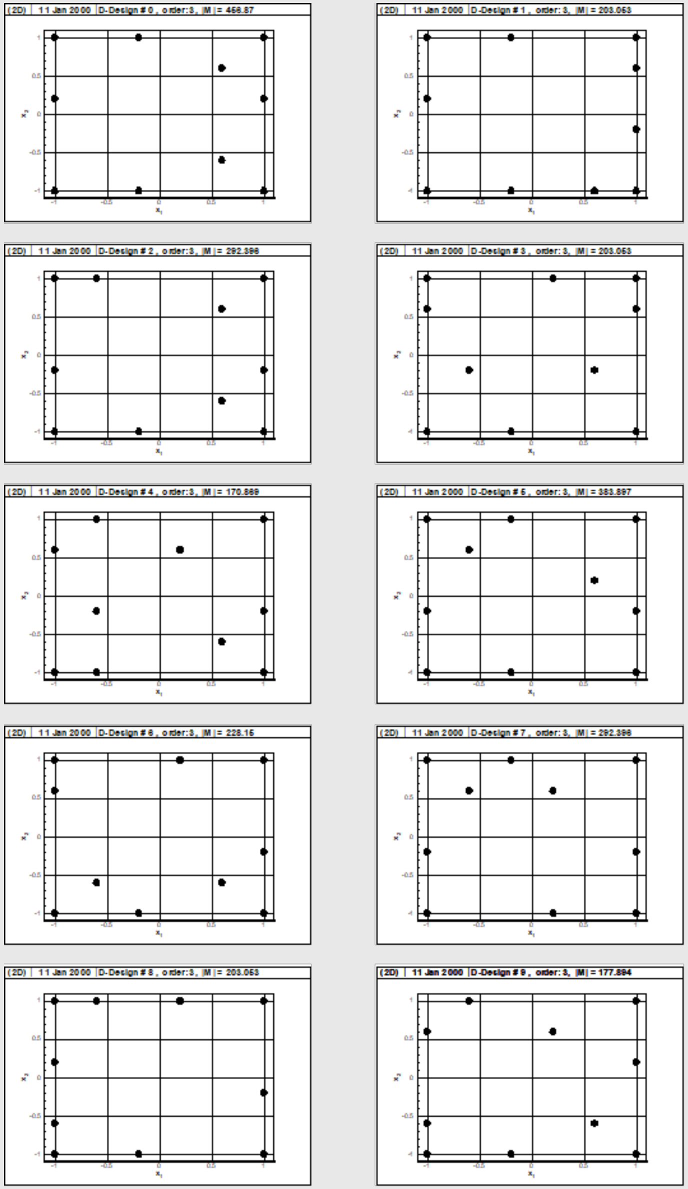

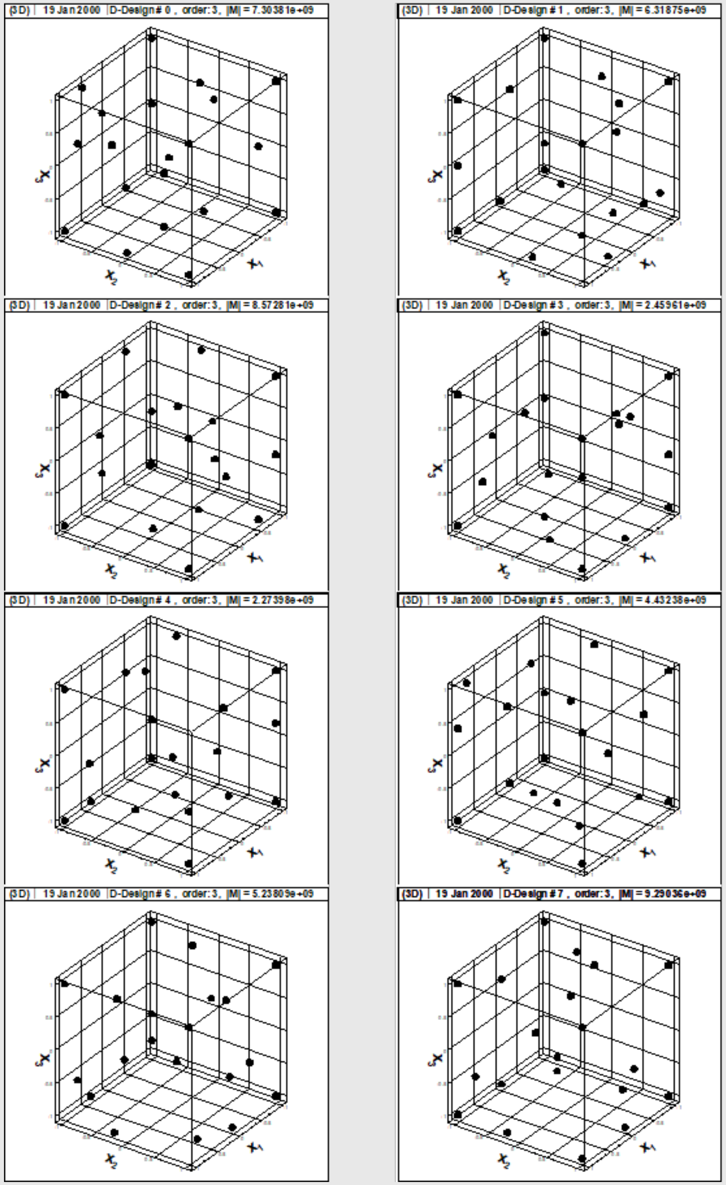

Effect due to optimization

Traces of $\tilde{S} = \sqrt[2m]{|\mathbf{D}|},$ for:

5 factors, exhaustive search

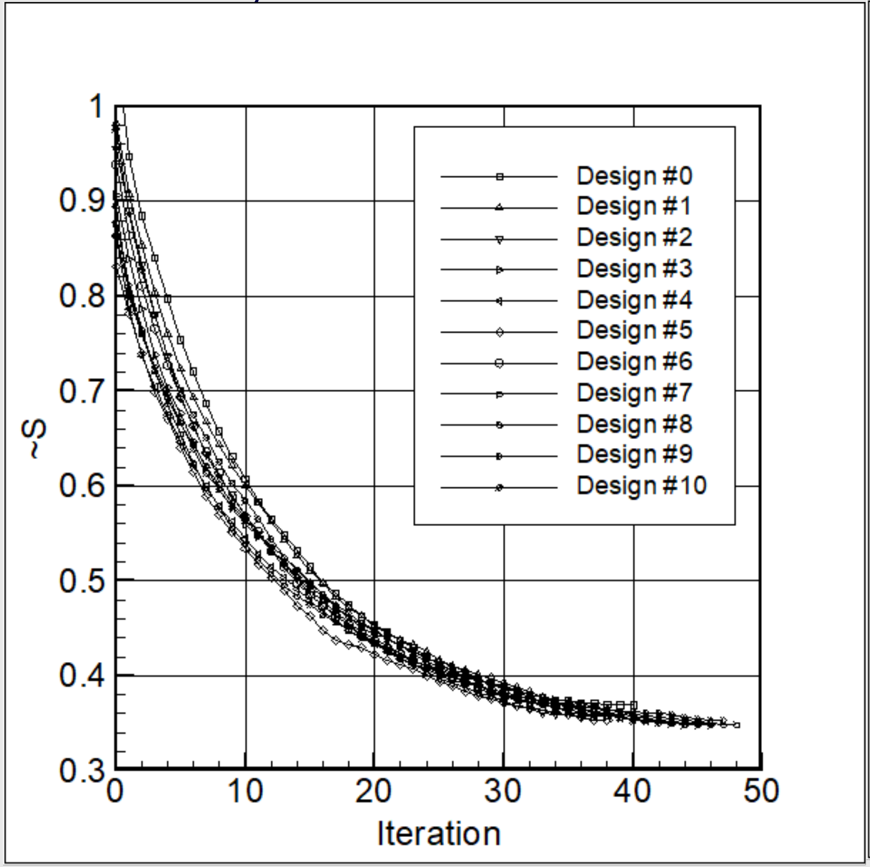

8 factors, GA optimization

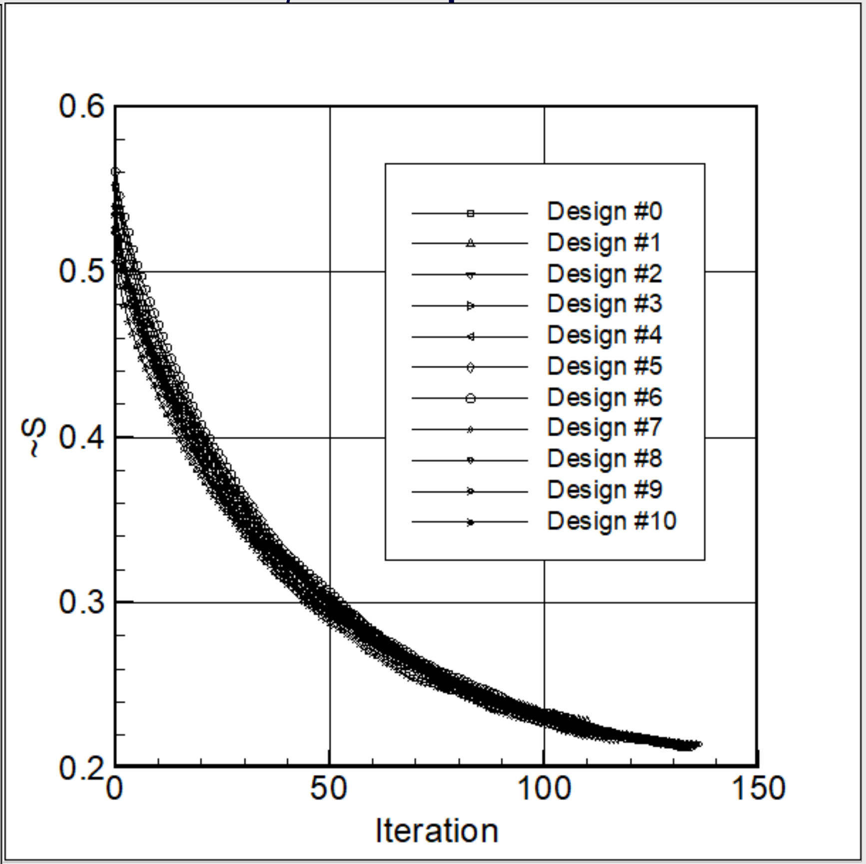

Conclusions regarding optimized designs

1. Application of optimized experimental designs may save time
2. In case of 1,2, and 3 factors the gain is not significant and full-factorials should then be preferred
3. In case of 5 factors no reasonable full-factorial is feasible
4. 4 factors --- grey zone
5. Optimized designs require higher experimentation culture
6. Saturated designs should not be used: recommended redundancy factor is 3
7. Besides the LS regression analysis and ANOVA, robust methods (e.g. least median) may be preferable especially when appearance of outliers cannot be prevented
8. However, robust methods may be incapable to perform ANOVA and sort out insignificant regressors
9. Makes little sense to combine with CFD

Sway force regression coefficients estimates

178 point full-factorial

20 point D-optimized saturated

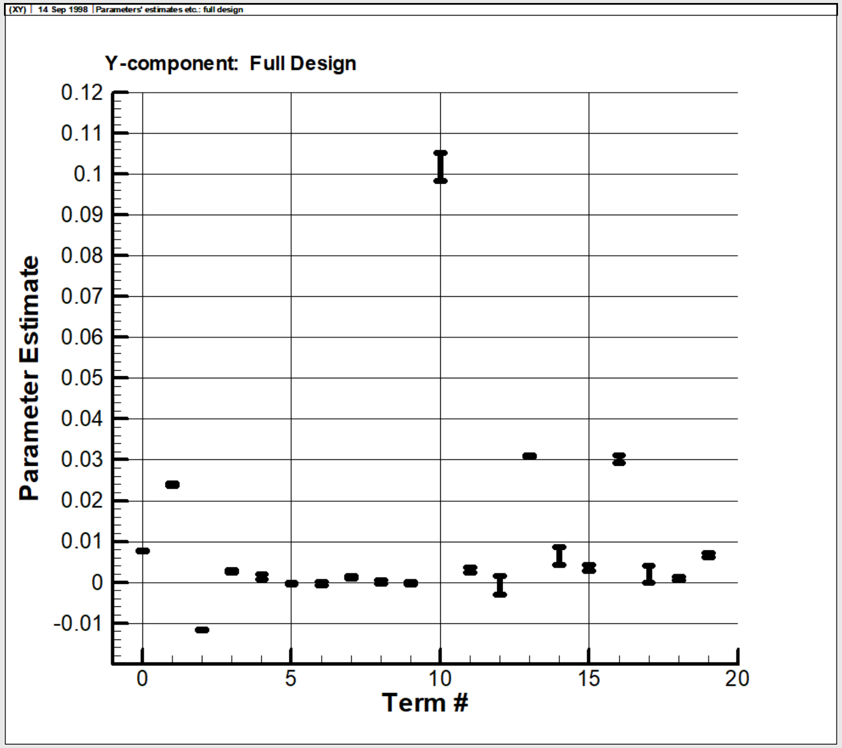

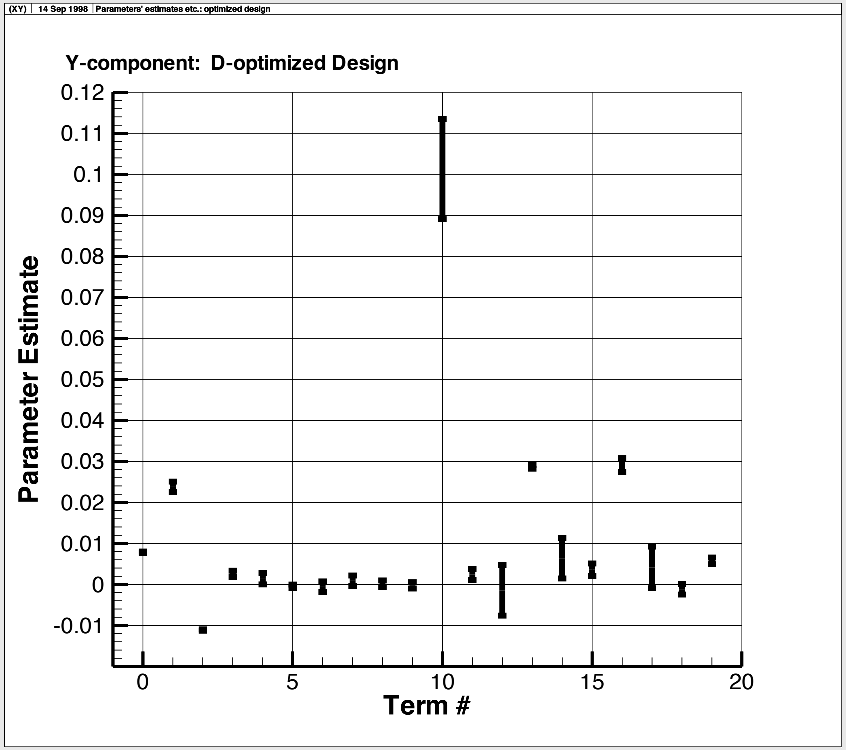

Primary responses for sway force

178 point full-factorial

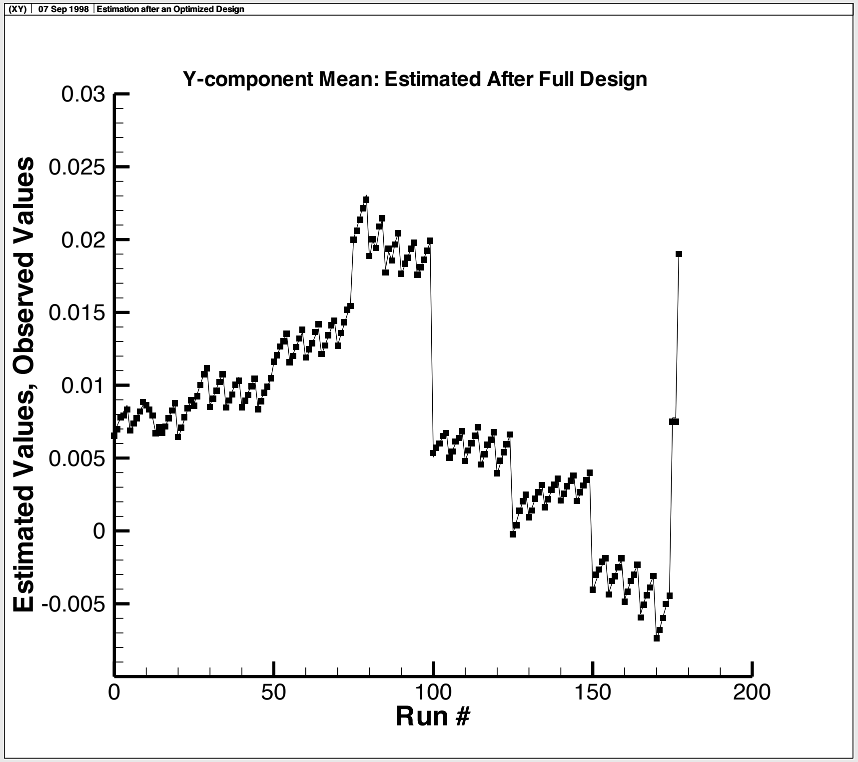

20 point D-optimized saturated

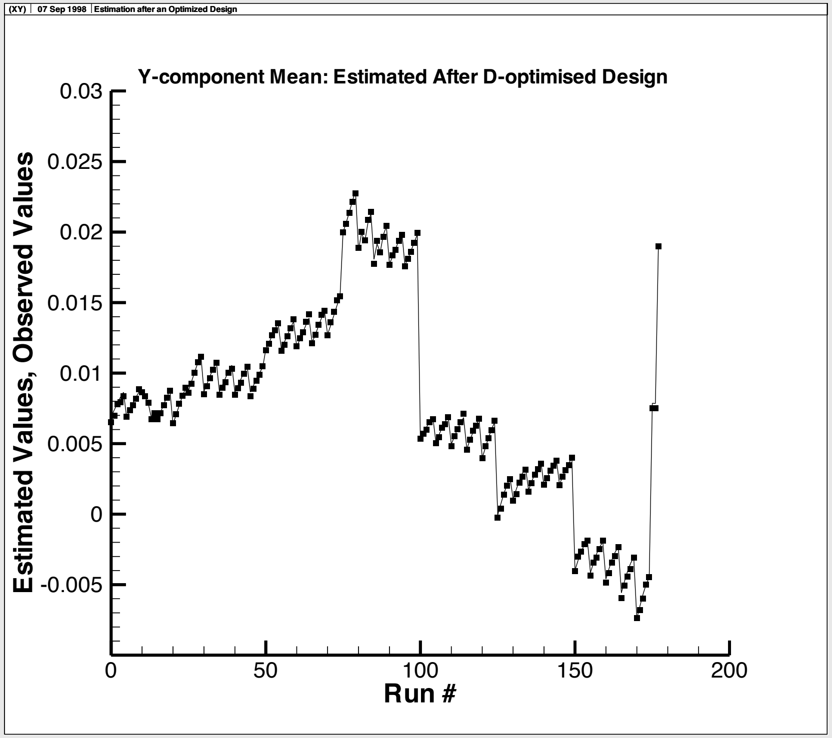

Conclusions regarding oscillatory tests

1. Are of significant historical value and cannot be avoided when using mechanical PMMs
2. Combined sway-yaw tests are the main option sufficient for estimating all regression coefficients of interest
3. Second-order harmonics had been useful for separation of the defining set of equations when the obsolete elementary processing method was used (PNA) but do not have value nowadays: neglecting them typically improves the estimates
4. While the oscillatory tests look at first sight more informative, there advantage is illusory and the CMTs must be preferred whenever possible i.e. using CPMC, when the rotating arm is available or when CFD is used.

Post-processing

1. Time responses are filtered and averaged when necessary
2. Steady tests --- required values are obtained directly
3. Oscillatory tests --- low-level identification, see

Sutulo S, Guedes Soares C. *Contribution of Higher-Order Harmonics for Estimating Manoeuvring Derivatives from Oscillatory Tests.* International Shipbuilding Progress, 2007, Vol.54, pp. 1–24.

$$F_{MEAN} = \mathrm{F}_{MEAN}[F(t)] = \frac{1}{nT}\int_0^{nT} F(t)\mathrm{d}t,$$

$$F_{IN\lambda} = \mathrm{F}_{IN\lambda}[F(t)] = \frac{2}{nT}\int_0^{nT} F(t)\sin\lambda\omega t\,\mathrm{d}t,$$

$$F_{OUT\lambda} = \mathrm{F}_{OUT\lambda}[F(t)] = \frac{2}{nT}\int_0^{nT} F(t)\cos\lambda\omega t\,\mathrm{d}t,$$

$$\lambda = 1, 2$$

Further processing is based on a priori regression models

Example of 5-factor design for a catamaran

Sutulo S., Guedes Soares C. *Development of a Multi-Factor Regression Model of Ship Maneuvering Forces Based on Optimized Captive-Model Tests.* J. Ship Research, 2006, Vol.50, No. 4, pp.311–333.

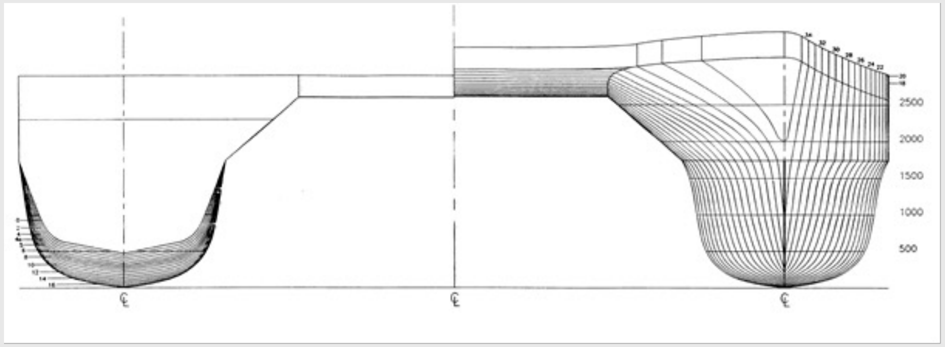

Oscillatory CPMC tests at CEHIPAR

6 force/moment components measured

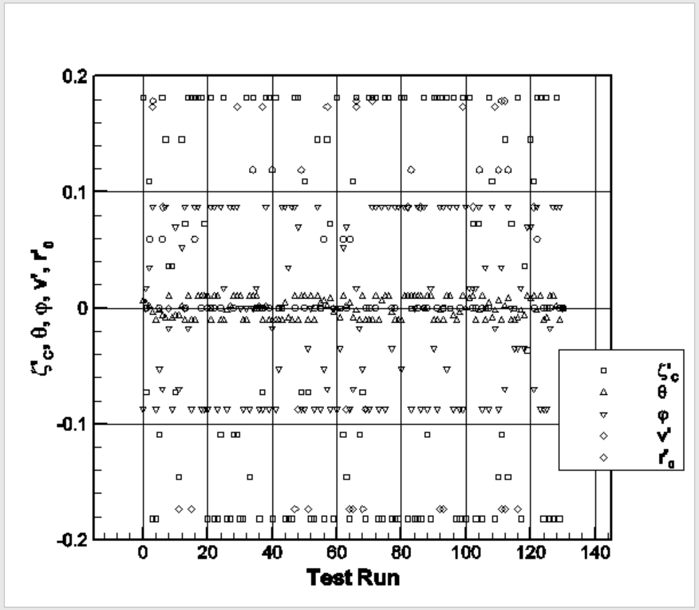

--- optimized design with redundancy 3

$$X'_H = X'_0 + X'_\theta \theta + X'_{\theta\theta}\theta^2 + X'_{vv} v'^2 + X'_{rr} r'^2 + X'_{\zeta\theta}\zeta'\theta$$
$$+ X'_{\varphi r}\varphi r' + X'_{vr} v'r' + X'_{\zeta vv}\zeta' v'^2 + X'_{\theta\varphi r}\theta\varphi r' + X'_{\theta vr}\theta v' r',$$

$$Y'_H = Y'_v v' + Y'_r r' + Y'_{\zeta\varphi}\zeta'\varphi + Y'_{\zeta v}\zeta' v' + Y'_{\zeta r}\zeta' r' + Y'_{\theta v}\theta v'$$
$$+ Y'_{\theta r}\theta r' + Y'_{vvv} v'^3 + Y'_{rrr} r'^3 + Y'_{\theta\theta v}\theta^2 v' + Y'_{vvr} v'^2 r'$$
$$+ Y'_{\varphi vv}\varphi v'^2 + Y'_{\varphi rr}\varphi r'^2 + Y'_{\zeta\theta\varphi}\zeta'\theta\varphi + Y'_{\zeta\theta r}\zeta'\theta r',$$

Main Particulars

Waterline Length	44.25m
Length Overall	46.25m
Breadth Overall	11.80m
Waterline Breadth (single hull)	2.68m
Distance between centre planes	9m
Depth	2.90m
Design Draught	1.35m
Draught at trials (forward/aft)	0.92-1.01/1.17-1.25
Displacement (full)	176m^3
Block coefficient	0.548
LCB	-8.14%
Design Speed	25kn
Service Speed	20kn
Propellers (each of 2)	waterjets LIPS
Steering devices	deflectable nozzles
Stopping devices	reversing buckets
Maximum nozzle deflection angle	32deg

Table 1: Main particulars of the Catamaran tested

Observed vs estimated responses

no outliers removed,
complete sets of regressors,
no a priori information used

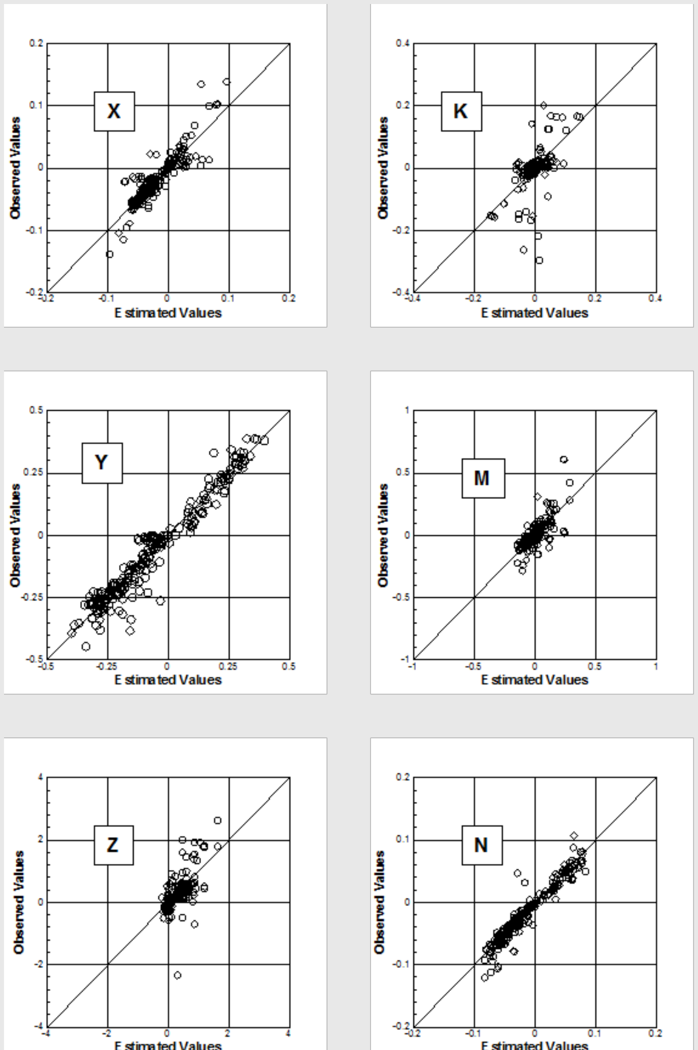

outliers removed,
insignificant regressors eliminated,
maximum a priori information used

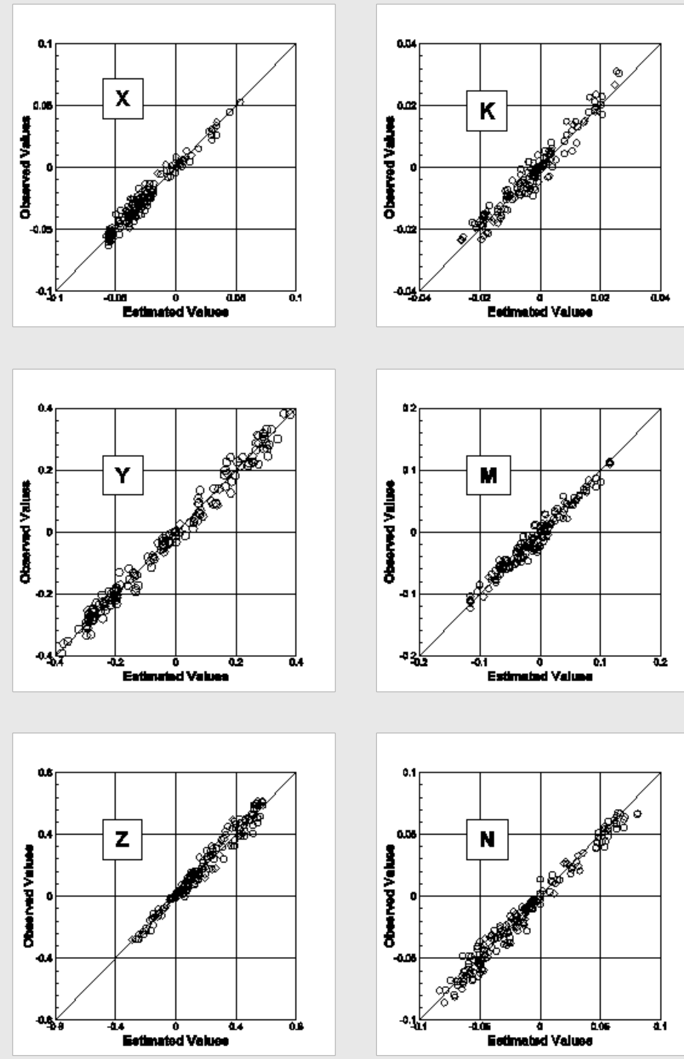

Final quasi-steady estimated responses

$$\zeta_C = -0.2, \theta = 0.6\deg, \varphi = -5\deg$$

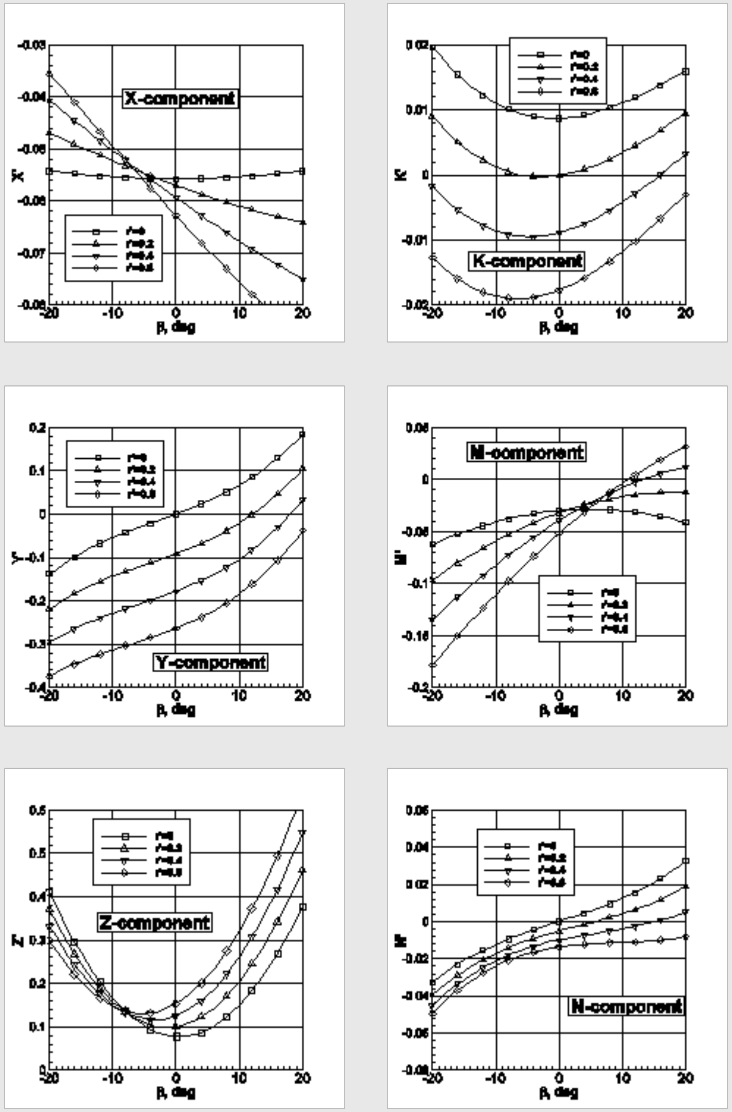

$$\zeta_C = 0.2, \theta = -0.6\deg, \varphi = 5\deg$$

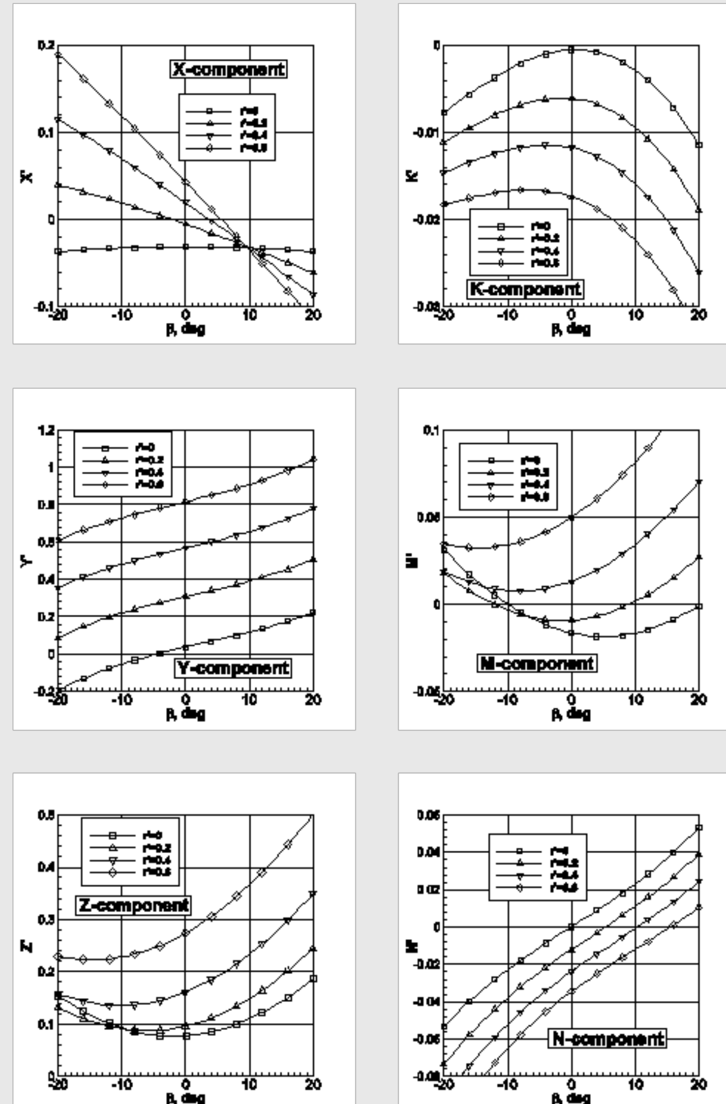

Model for arbitrary manoeuvres

Sutulo S, Guedes Soares C. Development of a core mathematical model for arbitrary maneuvers of a shuttle tanker, Applied Ocean Research, 2015, Vol. 51, pp. 293–308

$$r'' = \frac{rL}{\sqrt{V^2 + r^2 L^2}} = \frac{r'}{\sqrt{1 + r'^2}}$$

$$\beta = \begin{cases} -\operatorname{asin} v' & \text{at} \quad u \geq 0, \\ -\pi \operatorname{sign} v + \operatorname{asin} v' & \text{at} \quad u < 0; \end{cases}$$

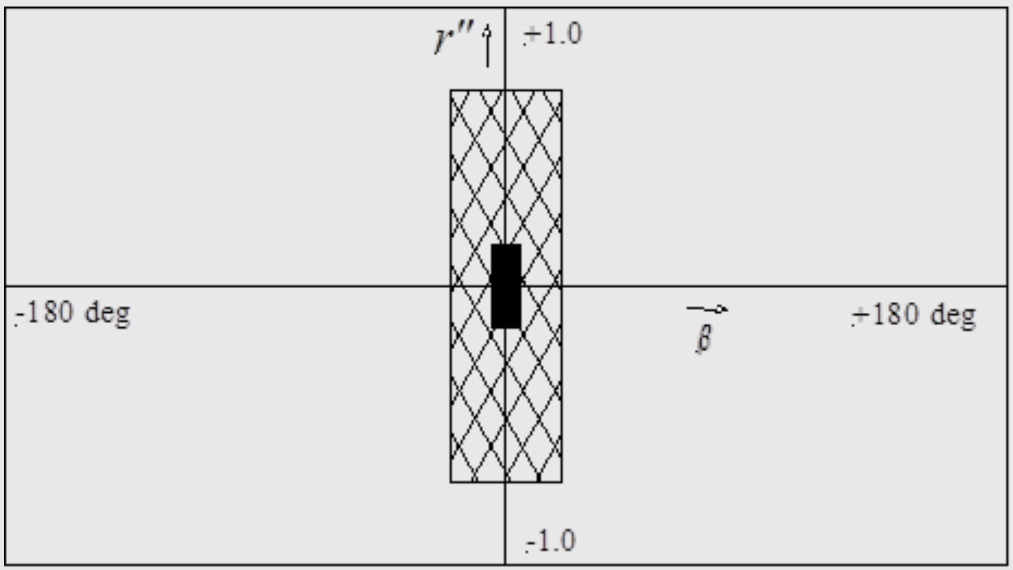

$$X_H = X'' \frac{\rho}{2} (V^2 + L^2 r^2) LT,$$

$$Y_H = Y'' \frac{\rho}{2} (V^2 + L^2 r^2) LT,$$

$$N_H = N'' \frac{\rho}{2} (V^2 + L^2 r^2) L^2 T,$$

Regressions for arbitrary manoeuvres

$$X''_H = -\frac{2R_T(u)r_{AS}(u)}{\rho V^2 LT}\cos\beta\,|\cos\beta|\,(1-r''^2) - \frac{2C_m\mu_{22}}{\rho L^2 T}\sin\beta\, r''\sqrt{1-r''^2}$$

$$Y''(\beta,r'') = c_{y0}r'' + c_{y1}\sin\beta\sin\pi r''\,\mathrm{sign}\,r'' + c_{y2}\sin\beta\cos\frac{\pi}{2}r'' + c_{y3}\sin 2\beta\cos\frac{\pi}{2}r''$$
$$+c_{y4}\cos\beta\sin\pi r'' + c_{y5}\cos 2\beta\sin\pi r'' + c_{y6}\cos\beta\left(\cos\frac{\pi}{2}r'' - \cos\frac{3\pi}{2}r''\right)\mathrm{sign}\,r''$$
$$+c_{y7}\left(\cos 2\beta - \cos 4\beta\right)\cos\frac{\pi}{2}r''\,\mathrm{sign}\,\beta + c_{y8}\sin 3\beta\cos\frac{\pi}{2}r'';$$

$$N''(\beta,r'') = c_{n0}r'' + c_{n1}\sin 2\beta\cos\frac{\pi}{2}r'' + c_{n2}\sin\beta\cos\frac{\pi}{2}r'' + c_{n3}\cos 2\beta\sin\pi r''$$
$$+c_{n4}\cos\beta\sin\pi r'' + c_{n5}\left(\cos 2\beta - \cos 4\beta\right)\sin\pi r'' + c_{n6}\cos\beta\left(\cos\beta - \cos 3\beta\right)\mathrm{sign}\,r''$$
$$+c_{n7}\sin 2\beta\left(\cos\frac{\pi}{2}r'' - \cos\frac{3\pi}{2}r''\right) + c_{n8}\sin\beta\left(\cos\frac{\pi}{2}r'' - \cos\frac{3\pi}{2}r''\right)$$
$$+c_{n9}\sin 2\beta\left(\cos\frac{\pi}{2}r'' - \cos\frac{3\pi}{2}r''\right)\mathrm{sign}\,r''.$$

Modelo Matemático do Catamarã: Casco

Representação das forças:

$$F_{HULL} = \frac{\rho}{2} L^{\alpha} T V_L^2 F''(\beta, r''), \; V_L = \sqrt{V^2 + L^2 r^2}$$

Definições do ângulo de deriva e da velocidade de guinada não dimensional generalizada:

$$\beta = \begin{cases} -\operatorname{asin} \overline{v}' & \text{at} \quad \overline{u} \geq 0, \\ -\pi \operatorname{sign} \overline{v} + \operatorname{asin} \overline{v}' & \text{at} \quad \overline{u} < 0; \end{cases}$$

$$r'' = \frac{r'}{\sqrt{1 + r'^2}}, \quad r' = rL/V, \quad v' = v/V$$

Modelo Matemático do Catamaran: Modelos de Regressão

Coeficiente da força de avanço:

$$X'' = X_0 \cos\frac{\pi}{2} r'' \cos\beta + X_1 \sin^2 \pi r'' \cos\beta + X_2 \sin \pi r'' \sin\beta + X_3 \cos\frac{\pi}{2} r'' \cos 3\beta,$$

da força de deriva:

$$Y'' = X_0 \cos\frac{\pi}{2} r'' \sin\beta + X_1 \cos\frac{\pi}{2} r'' \sin^3 \beta + X_2 \cos\frac{\pi}{2} r'' \sin^5 \beta + X_3 \sin \pi r'' \cos\beta$$
$$+ X_4 \sin^3 \pi r'' \cos\beta + X_5 \sin^2 \pi r'' \sin\beta + X_6 \sin \pi r'' \sin^2 \beta,$$

do momento de guinada:

$$N'' = N_0 r'' + N_1 \sin \pi r'' + N_2 \sin^3 \pi r'' + N_3 \cos\frac{\pi}{2} r'' \sin 2\beta$$
$$+ N_4 \cos\frac{\pi}{2} r'' \sin^3 2\beta + N_5 \sin \pi r'' \sin^2 2\beta + N_6 \sin^2 \pi r'' \sin 2\beta.$$

Modelo Matemático do Catamaran

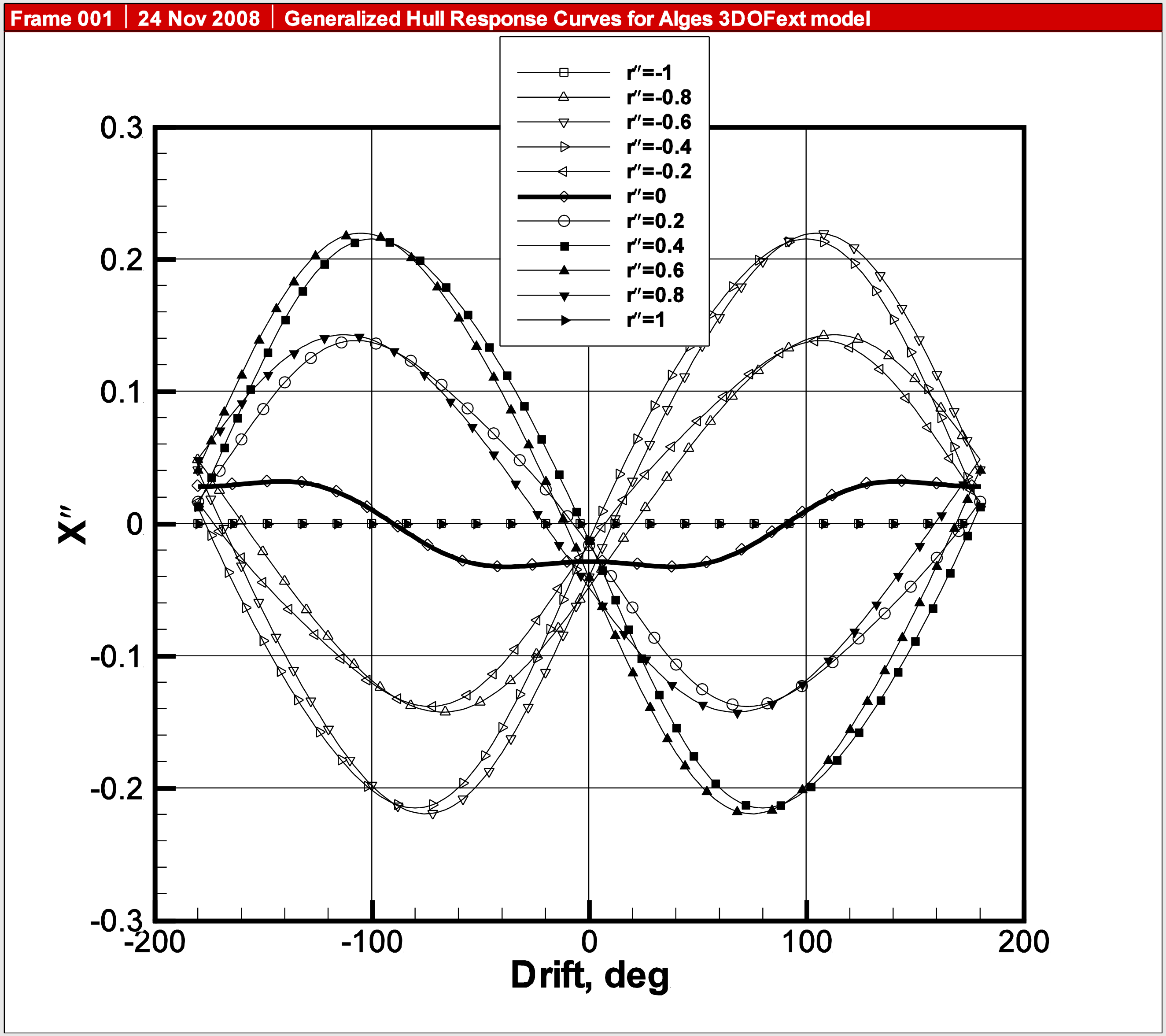

Modelo Matemático do Catamaran

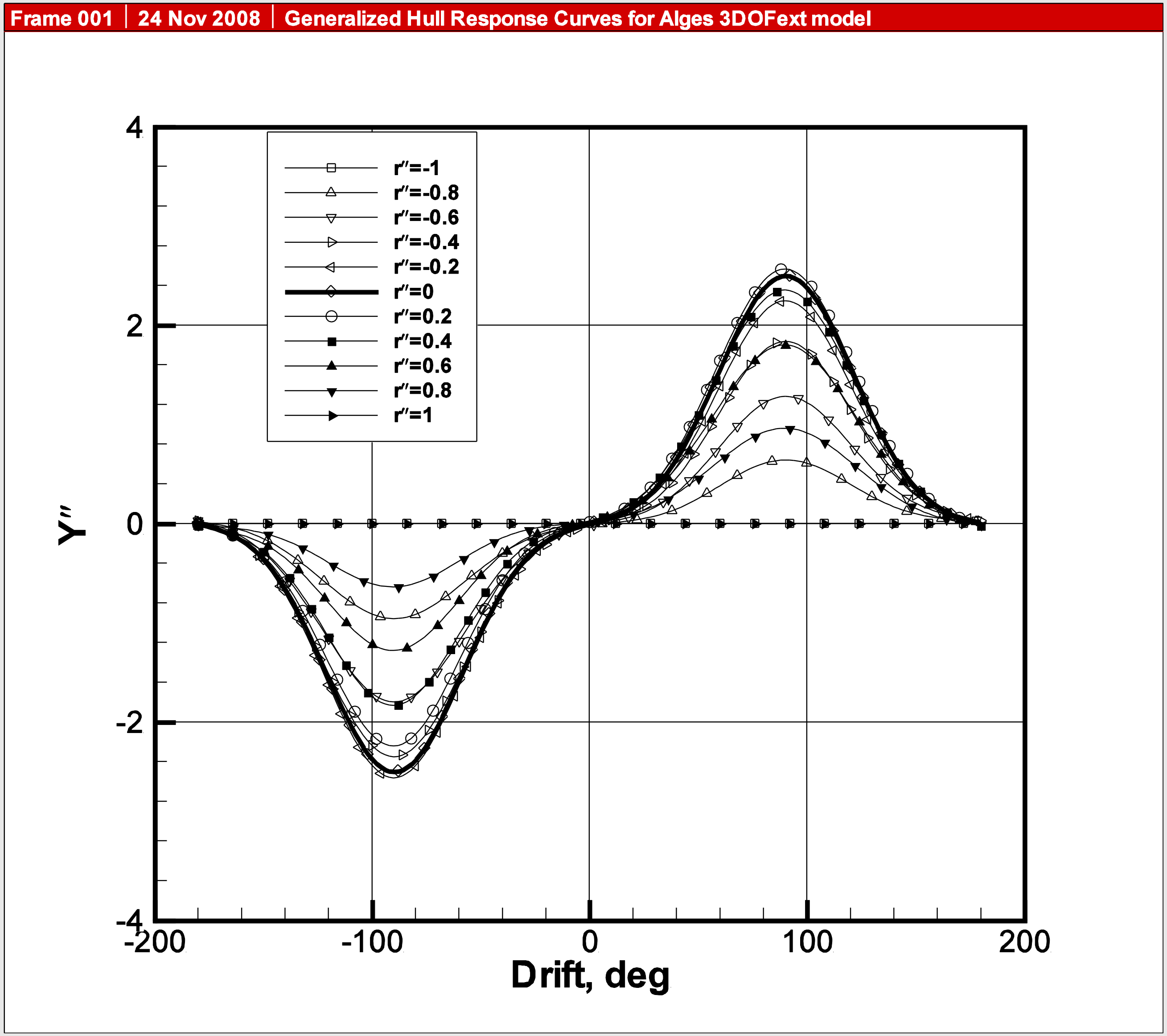

Modelo Matemático do Catamaran

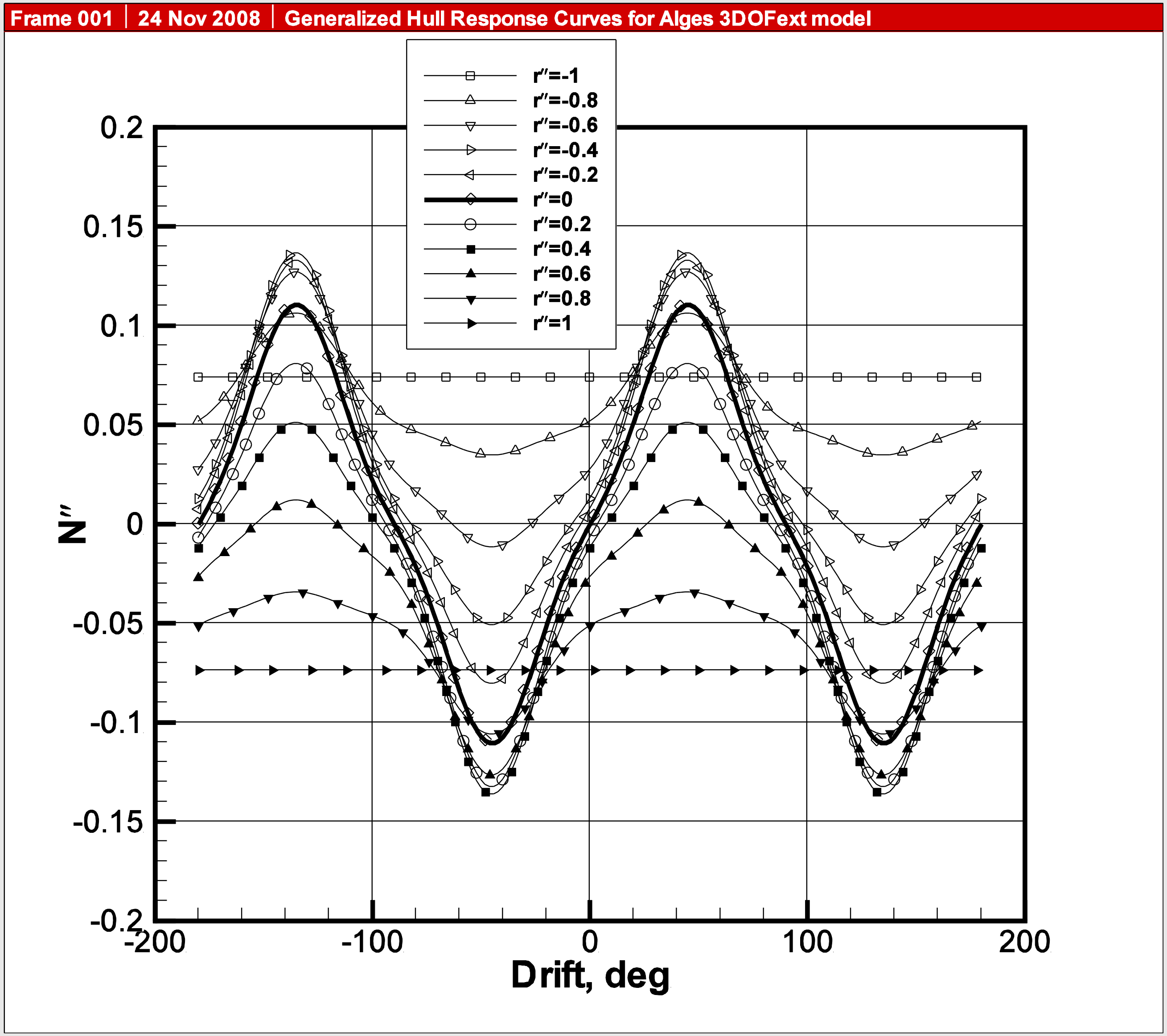

Descrição do ambiente gráfico

- Corresponde representação virtual dum espaço físico existente
- Inclui os objectos virtuais considerados relevantes para a simulação com correspondência directa no mundo real
- Inclui objectos abstractos (sem correspondência real) representados sobre o cenário

- Meio de comunicação entre o utilizador e o Ambiente Gráfico
- Consola de controlo do Catamaran
- Painel de visualização e controlo de ferramentas de análise de resultados

Descrição do ambiente gráfico

Interface com o Utilizador

Sincronizador dos propulsores BB/EB

Paragem dos motores

Controladores dos propulsores

Indicador de RPM

Sincronizador dos ângulos dos propulsores

Alinhamento dos propulsores

Controladores do ângulo de viragem

Indicadores do ângulo dos propulsores

Indicador do ângulo de rumo

Indicador da velocidade de avanço

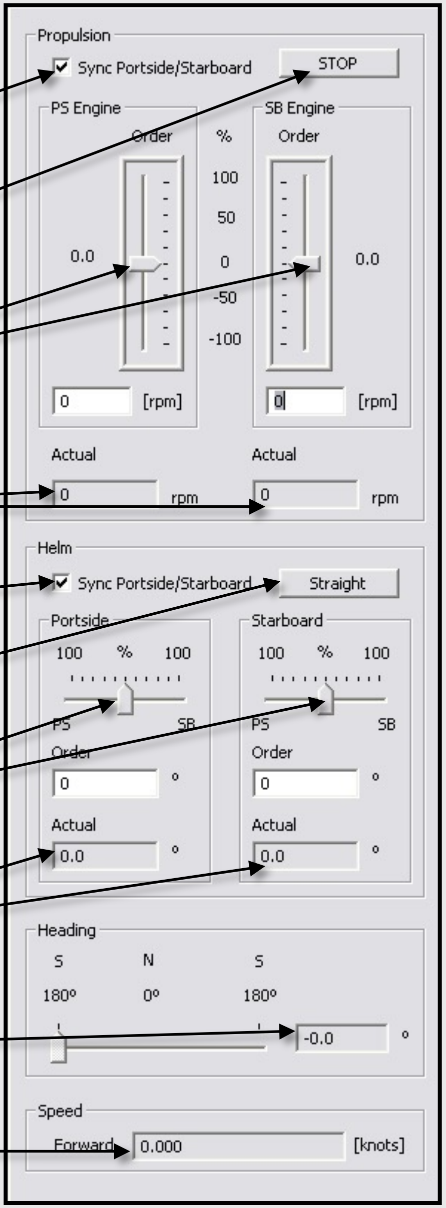

Sincronização dos diferentes ciclos

- Processamento gráfico (*pipeline* gráfico - *GPU*)
  - Extremamente rápido
  - Tempos de ciclo variáveis
- Comportamento dos objectos virtuais (ambiente virtual - *CPU)*
  - Mais lento
  - Tempos de ciclo com grandes variações
- Cálculos de manobrabilidade (motor físico – *CPU*)
  - Computacionalmente mais pesado
  - Tempo mínimo admissível

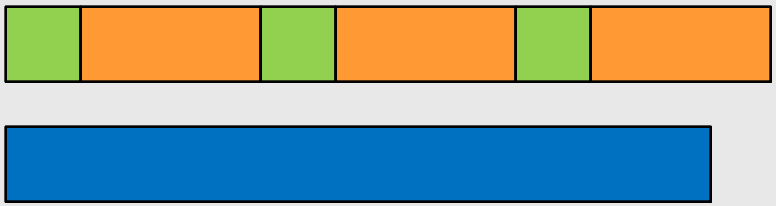

Transferência de dados

rpm order stbd
rpm order poort
bucket port
rudder ordr stbd
rudder ordr port
ruddr ordr port
stbd thruster ordr
port thruster ordr

Input

up
right
heading
speed,
roll,
yawrate,
drift
rpmStbd,
rpmPort
bucketStbd
bucketPort
deflStbd
deflPort
thrustStbdRel
thrustPortRel

Output

Ferramentas de Visualização de Resultados

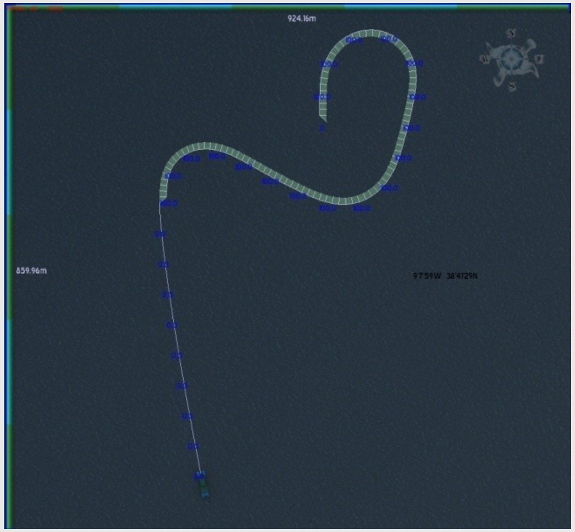

Hydrodynamic Interaction: Frames of Reference and Formulation

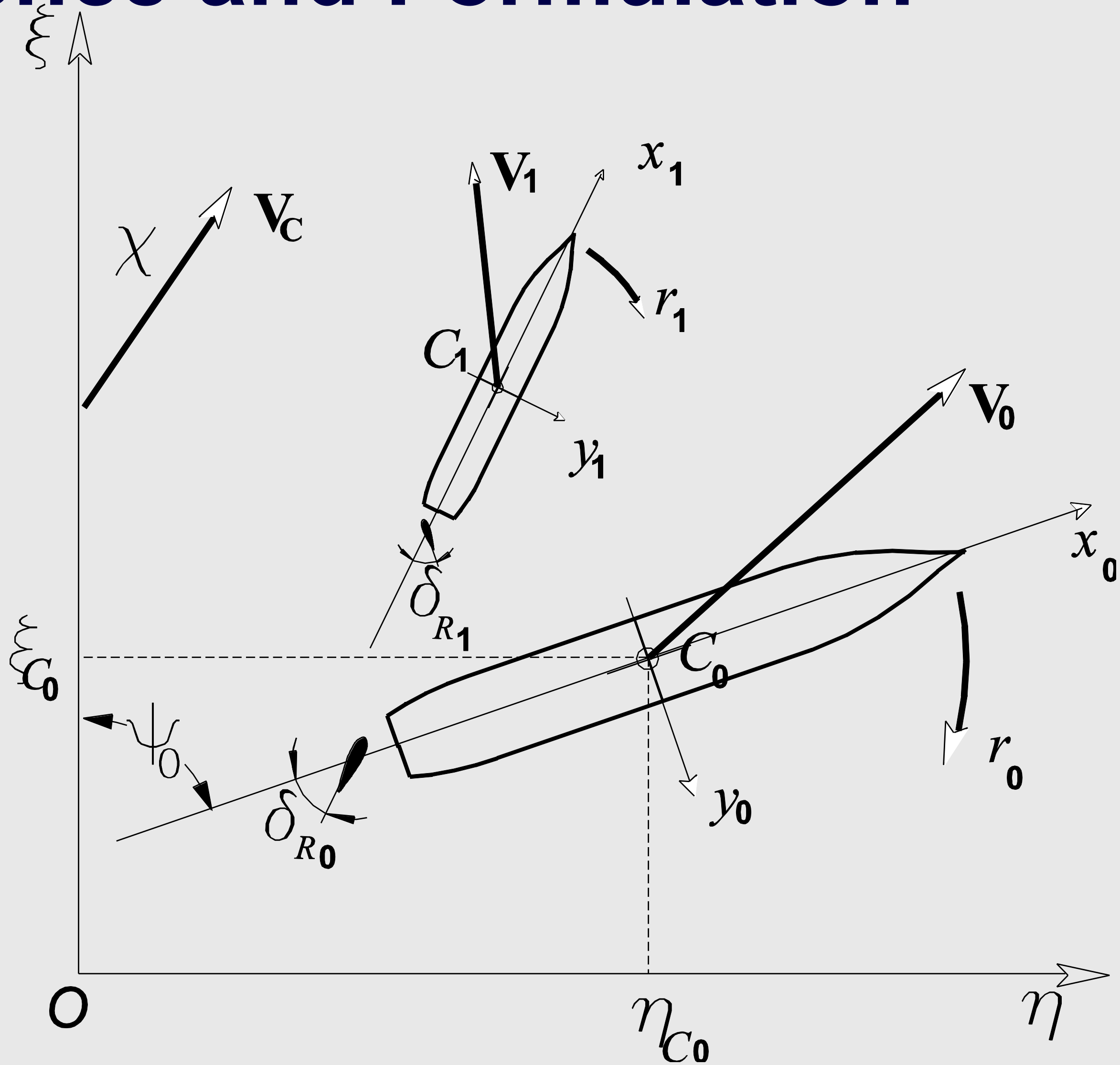

Sources of Inspiration and Motivation

- **Manoeuvring simulators need mathematical models for hydrodynamic interaction; these models seem sometimes too crude**
- **Often used empiric methods (e.g. Varyani) are inevitably limited in the number of covered combinations of kinematic parameters and experimentation of this kind is tedious**
- **Nonlinear CFD codes based on RANSE or even Euler equations are too slow to be used online**
- **Many data indicate that double-body potential flow approximation provides reasonable estimates in many cases of low-speed interaction (the Havelock hypothesis)**
- **The Hess & Smith method was successfully used offline by Ivan Vassilev Ivanov in 1981**
- **Progress in computer hardware since 1981 opens way to using similar methods online**

INSTITUTO SUPERIOR TÉCNICO

Formulation of the Potential Interaction Problem

Governing equation for absolute velocity potential: $\Delta\Phi = 0$

Perturbation velocity potential: $\phi = \Phi - (V_{\xi\mathrm{cur}}\xi + V_{\eta\mathrm{cur}}\eta)$

Low Froude number free-surface condition: $\dfrac{\partial\phi}{\partial\zeta} = 0 \quad \text{at} \quad \zeta = 0$

Body surface boundary condition

$$\frac{\partial\phi}{\partial n} = \mathbf{V}_r \cdot \mathbf{n},$$

where

$$\mathbf{V}_r = \mathbf{V} - \mathbf{V}_{\mathrm{cur}}, \quad \mathbf{V}(P) = \mathbf{V}_{C_i} + \mathbf{\Omega}_i \times \mathbf{r}_{C_i P},$$

Equation for Single Layer's Density

$$2\pi\sigma(M) + \int_S \sigma(P)\frac{\partial G(M,P)}{\partial n_M}\,\mathrm{d}S(P) = f(M),$$

where in deep fluid:

$$G(x,y,z,x',y',z') = \frac{1}{r} + \frac{1}{\bar{r}}, \quad r = \sqrt{(x-x')^2 + (y-y')^2 + (z-z')^2}, \quad \bar{r} = \sqrt{(x-x')^2 + (y-y')^2 + (z+z')^2}$$

at constant finite depth:

$$G(x,y,z,x',y',z') = \sum_{i=-\infty}^{\infty}\left(\frac{1}{r_i} + \frac{1}{\bar{r}_i}\right), \quad r = \sqrt{(x-x')^2 + (y-y')^2 + (z-z'+2iH)^2}, \quad \bar{r} = \sqrt{(x-x')^2 + (y-y')^2 + (z+z'+2iH)^2}$$

Absolute induced velocity and perturbation potential:

$$\mathbf{V}_I(M) = \int_S \sigma(P)\nabla_M G(M,P)\,\mathrm{d}S(P),$$

$$\phi(M) = \int_S \sigma(P)G(M,P)\,\mathrm{d}S(P).$$

Dynamic Pressure and Total Hydrodynamic Inertial Forces

Pressure:

$$p = \rho\left[-\frac{\partial\phi}{\partial t} + \frac{1}{2}\left(\mathbf{V}_r^2 - \mathbf{V}_p^2\right)\right],$$

where $\mathbf{V}_p = \mathbf{V}_I - \mathbf{V}_r$

Total inertial force and moment:

$$\mathbf{F}_{pi} = -\int_{S_i} p\,\mathbf{n}\,\mathrm{d}S; \quad \mathbf{M}_{pi} = -\int_{S_i} p\,\mathbf{r}\times\mathbf{n}\,\mathrm{d}S.$$

Net interaction surge and sway forces and yaw moment:

$$X_I = X_p - X_e; \quad Y_I = Y_p - Y_e; \quad N_I = N_p - N_e.$$

Alternatives…

Estimation of Proper Hydrodynamic Inertial Loads

- Concurrent solution for the set of interacting bodies and for each body is if it were isolated though moving with the same velocities and accelerations---always applicable
- Preliminary estimation of added mass coefficients and application of the Kirchhof equations technique:

$$
\begin{aligned}
X_e &= -\mu_{11}\dot{u} + \mu_{22} v_w r, \\
Y_e &= -\mu_{22}\dot{v} - \mu_{26}\dot{r} - \mu_{11} u_w r, \\
N_e &= -\mu_{26}\dot{v} - \mu_{66}\dot{r} + (\mu_{11} - \mu_{22}) u_w v_w - \mu_{26} u_w r,
\end{aligned}
$$

---only usable in constant (finite or infinite) depth case

INSTITUTO SUPERIOR TÉCNICO

Panel methods: typical implementations

- Quadrilateral displaced flat elements with constant source density (Hess & Smith)
- Higher-order methods: curvilinear elements with linear source density distribution
- “Patch” method (Söding 1993): desingularized, sub-surface point sources, non-penetration condition satisfied in the integral sense on triangular panels

Accuracy vs robustness…

Distribution of Panels: 172 (left), 360 (right)

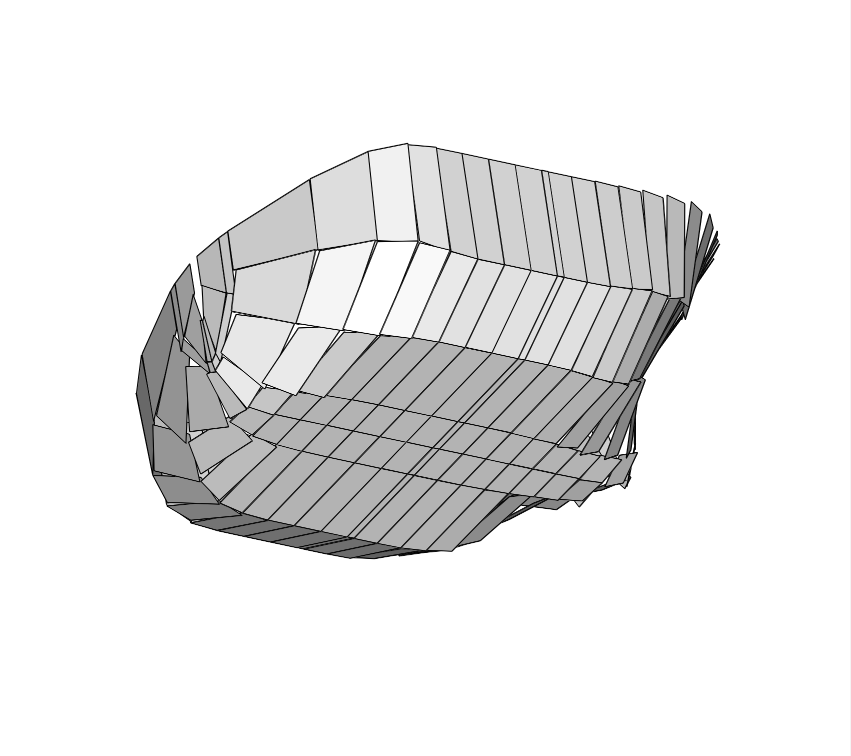

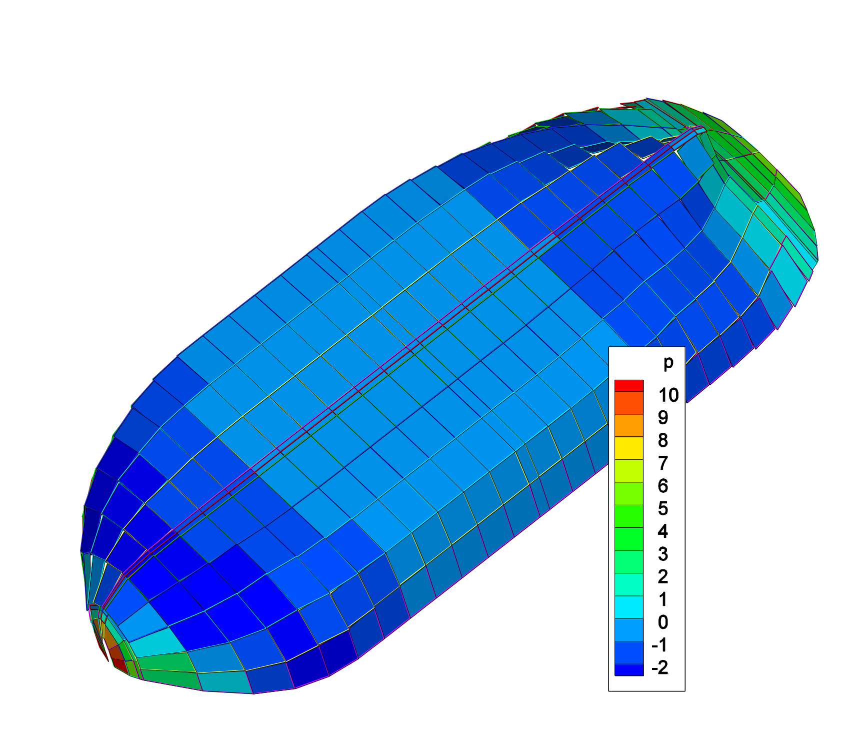

Oblique motion: 45deg drift---residual loads 3-7%

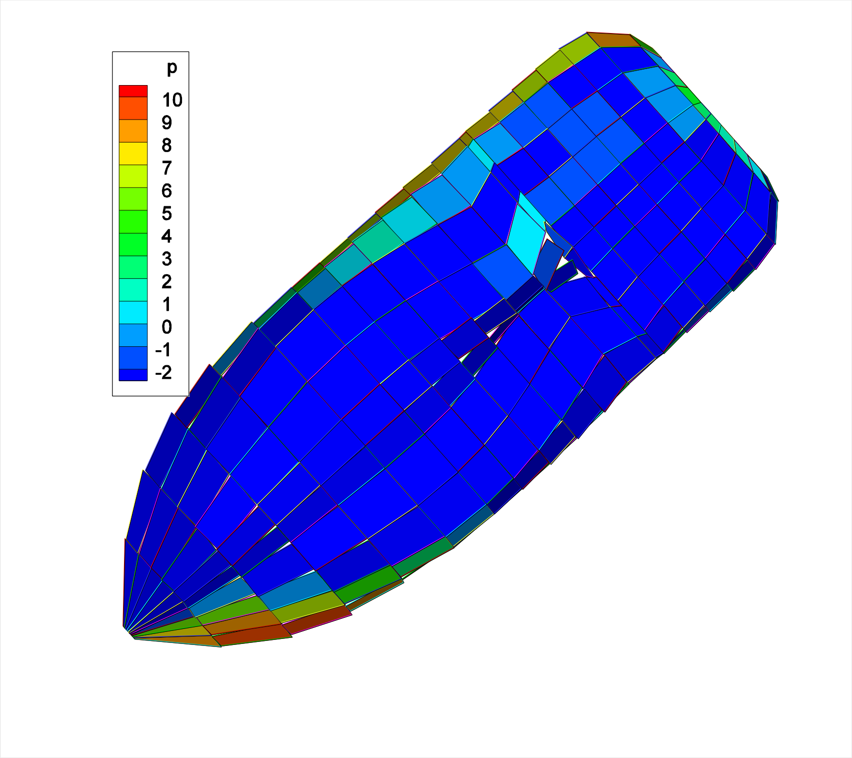

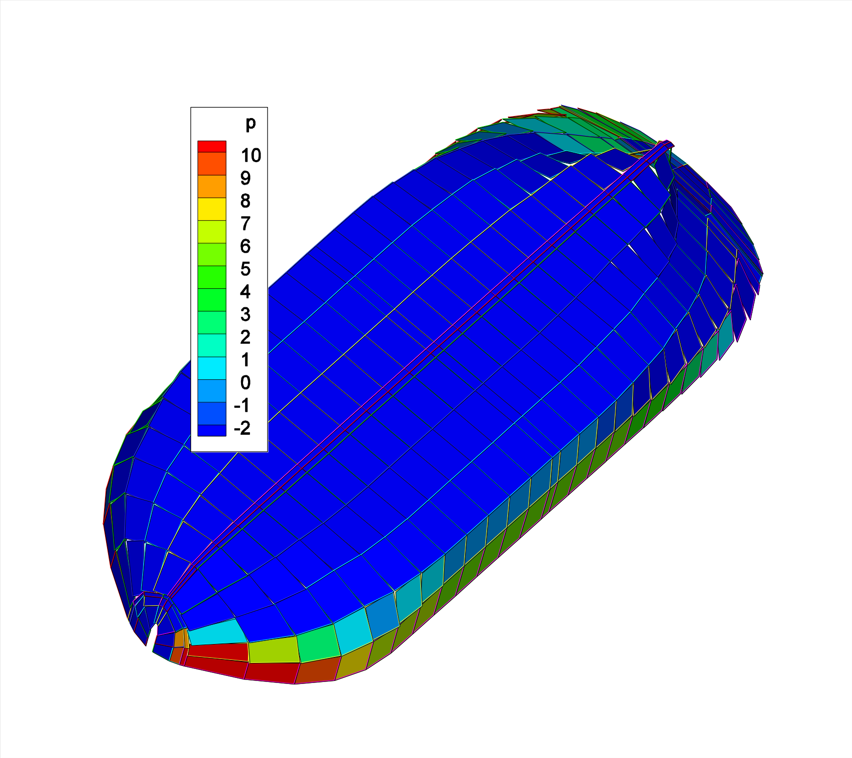

INSTITUTO SUPERIOR TÉCNICO

Verification against Brix' Method---X

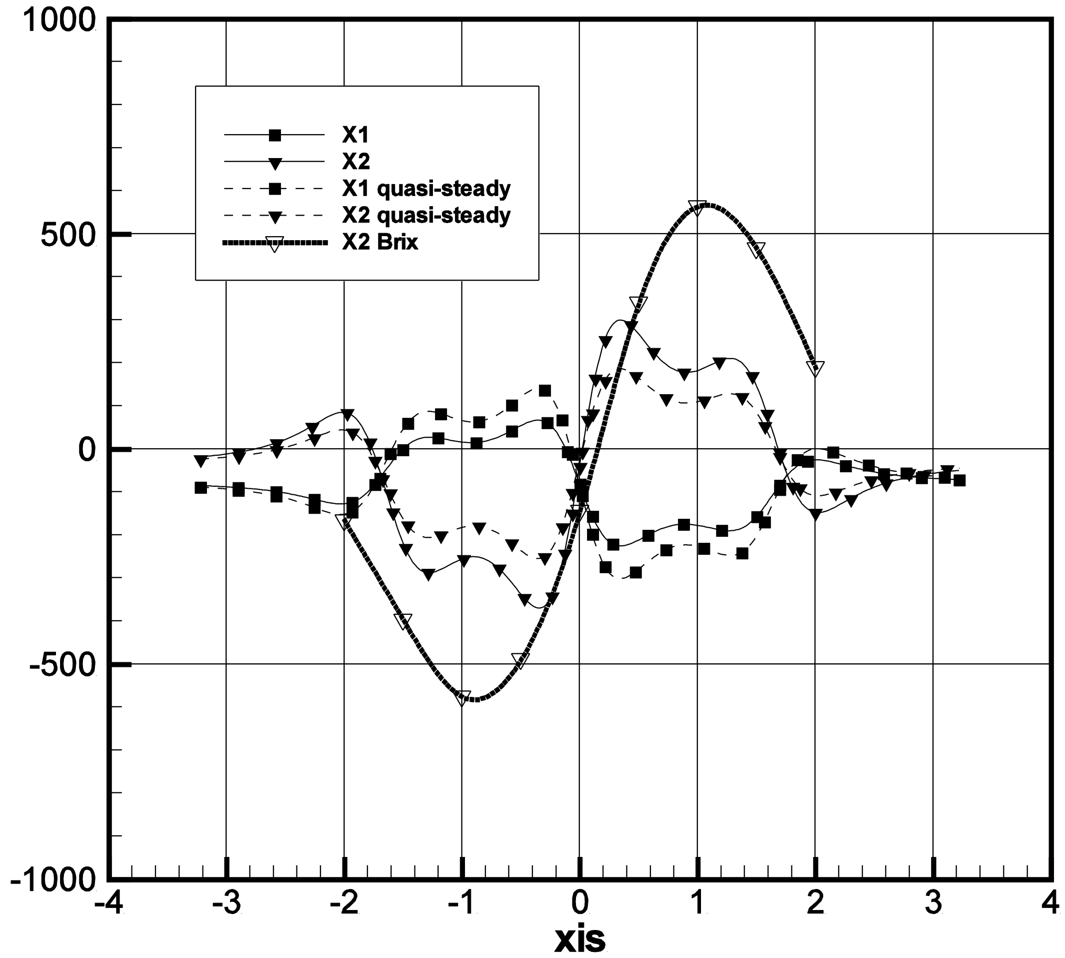

Verification against Brix' Method---Y

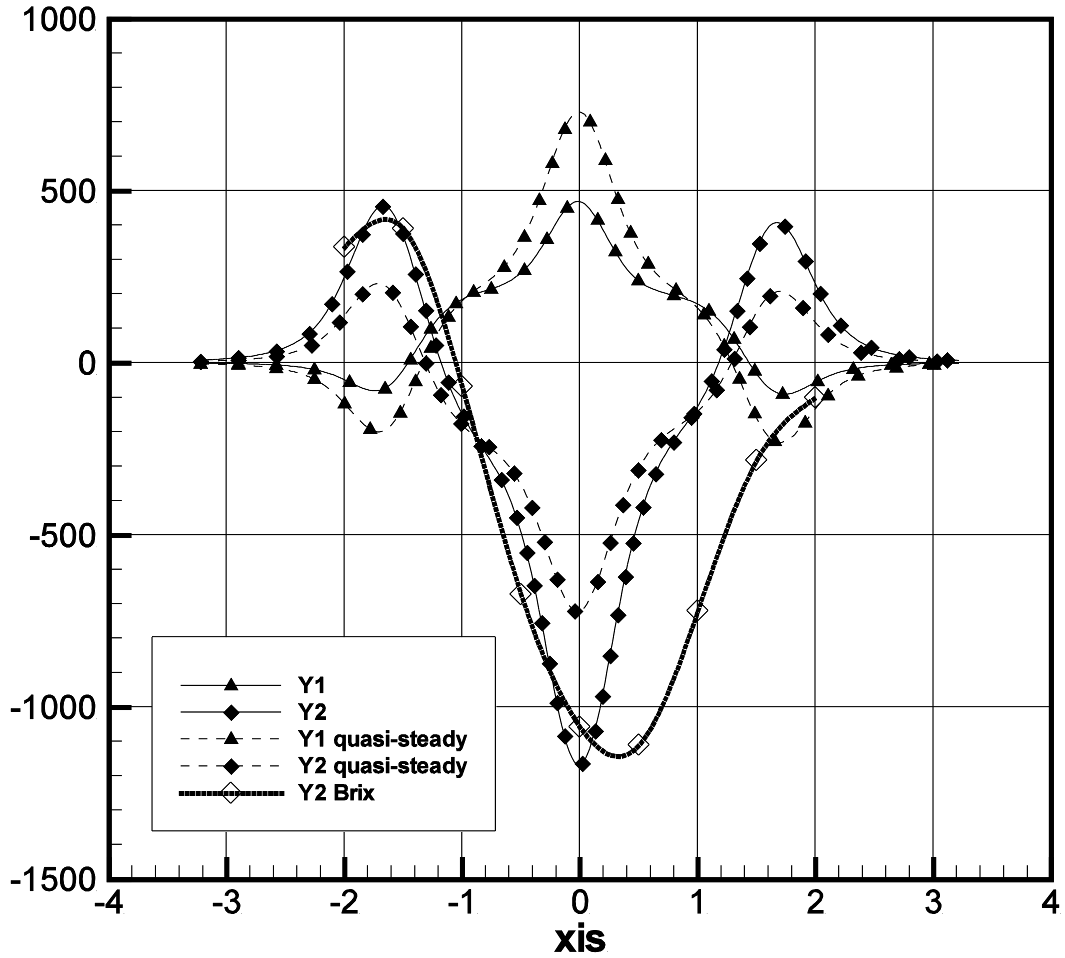

Verification against Brix' Method---N

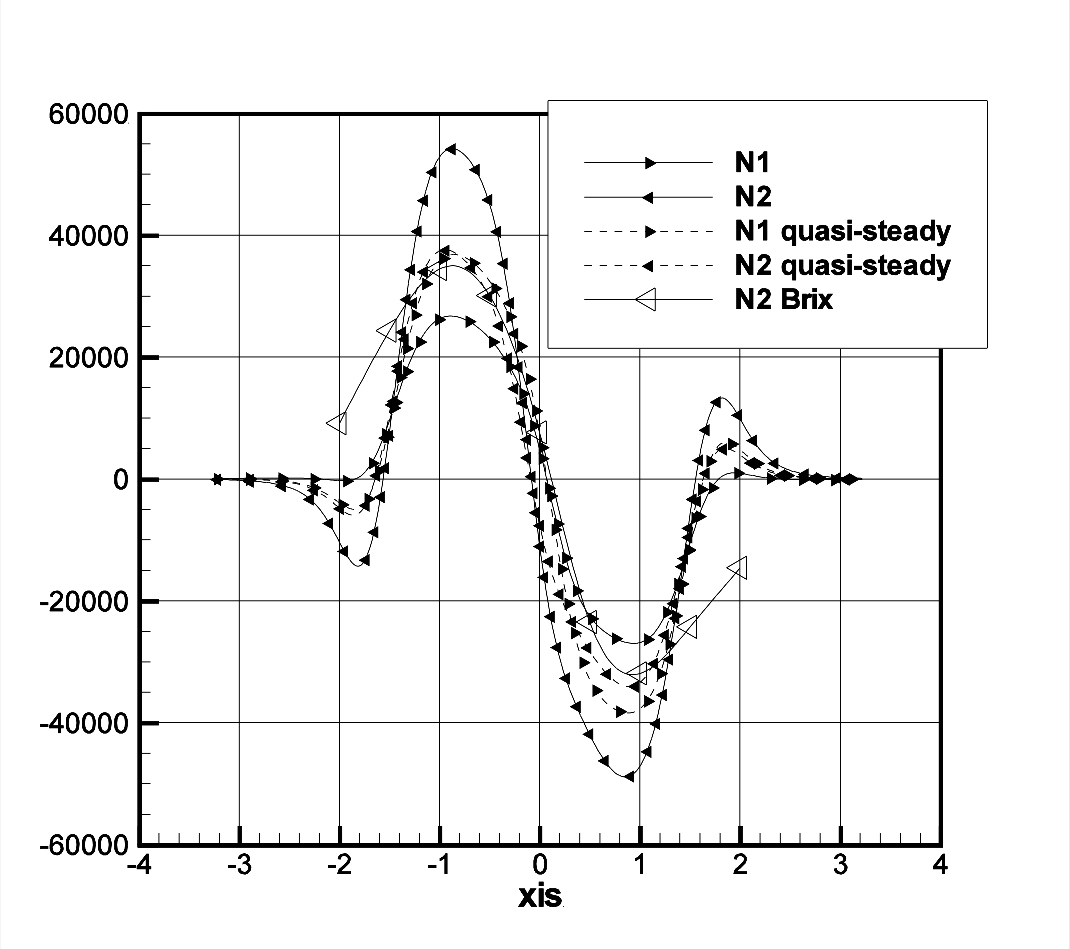

+ some other validation

Some Details of Program Implementation

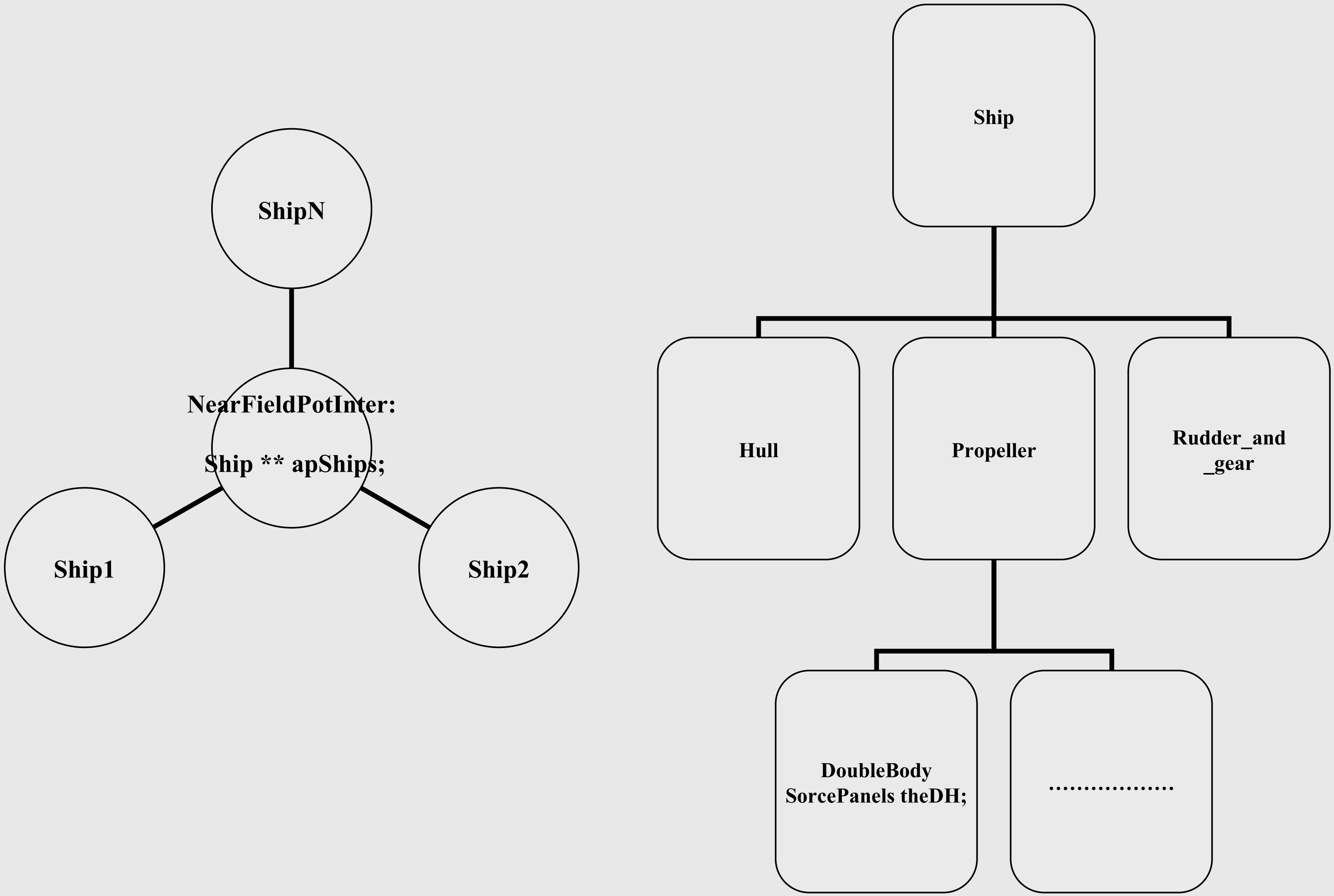

Trajectories in Overtaking: Left---Rudders Fixed, Right---PD-control

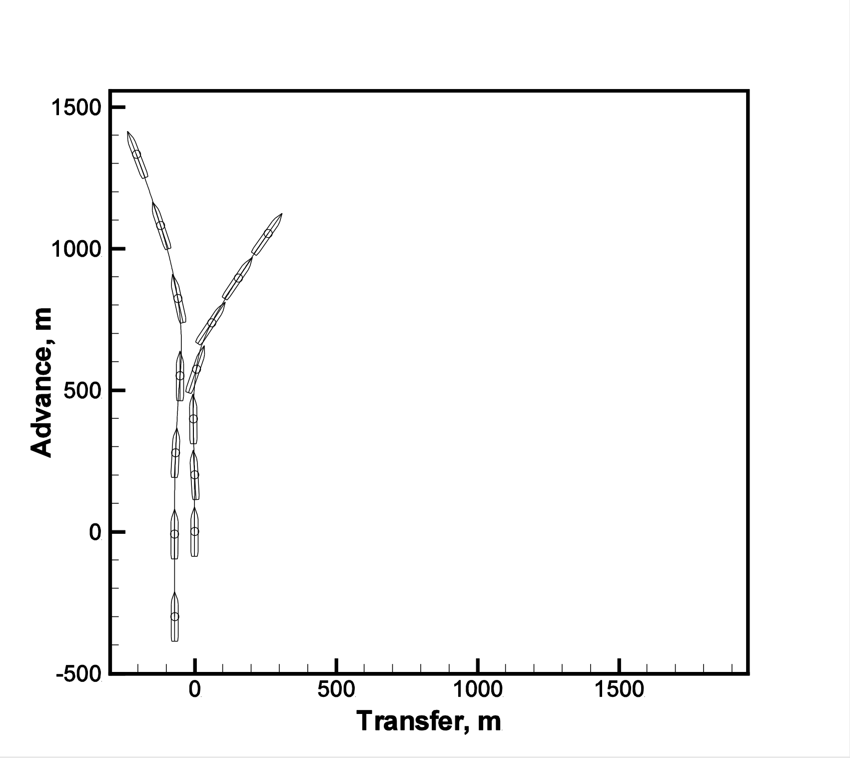

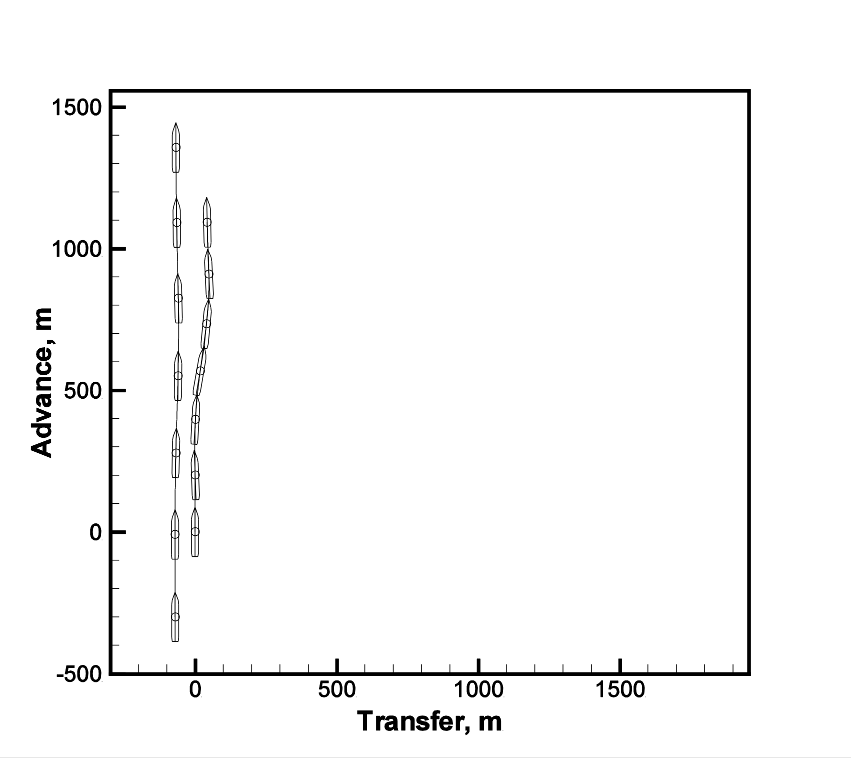

Further developments

- Extension to the case of arbitrary bathymetry: “moving patch method”
- Improvement of the panel method using some ideas of the patch method: the dihedral panel method
- Study of applicability of the double-body potential method to estimation of actual interaction forces through comparisons with CFD (Fonfach, Wnęk)
- CFD computations with high drift angle of one of interacting ships (up to crabbing motion)

INSTITUTO SUPERIOR TÉCNICO

SEAKIST history

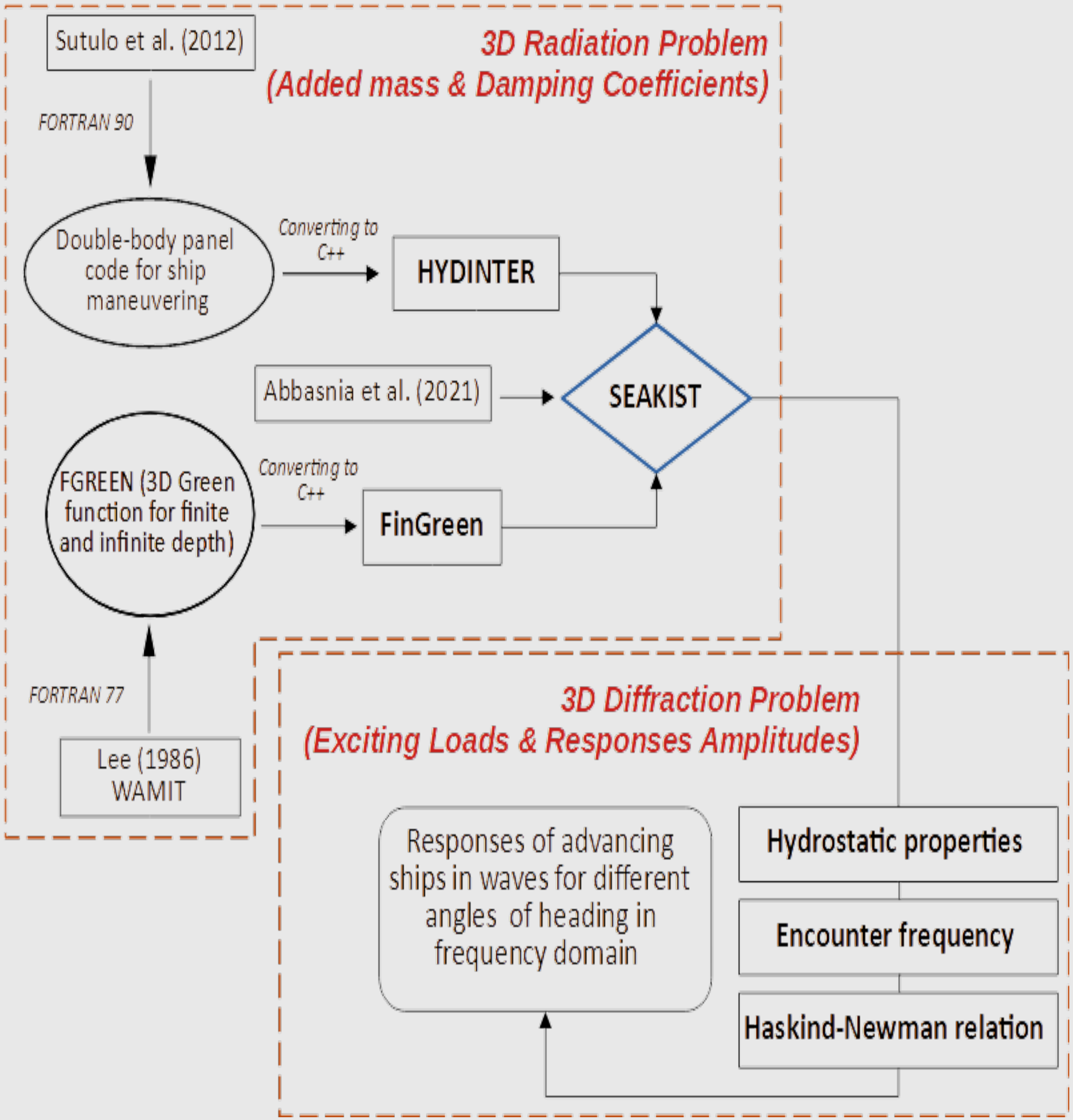

Mathematical formulation

Assumptions:

- ***Inviscid and incompressible fluid***
- ***Irrotationa flow***
- ***Rigid and impermeable body***

Potential flow theory

Wave amplitude

Diffraction potential function

$$\phi_D = \phi_w + \phi_s$$

Incident wave potential function

Scattering potential function

$$\Phi(x,y,z,t) = \mathrm{Re}\left[\zeta\phi_D(x,y,z)e^{i\omega_e t} + \sum_{j=1}^{6}\left\{X_j\phi_j(x,y,z)\right\}e^{i\omega_e t}\right]$$

$$G(\vec{P},\vec{q},\omega_e) = \frac{1}{r} + \frac{1}{r'} + \tilde{G}(\vec{P},\vec{q},\omega_e)$$

Ship wetted surface

$$2\pi\sigma(\vec{P}) + \int_\Gamma \sigma(\vec{q})\frac{\partial G(\vec{P},\vec{q})}{\partial n_q}dS = \psi(\vec{P})$$

Radiation potential function

Ship response amplitudes in six-degree of freedom

Mathematical formulation

Equation of motion for a rigid body in six DOF:

$$\sum_{j=1}^{6} X_j \left[-\omega_e^{\,2} \left(M^{kj} + A^{kj} \right) + i\omega_e D^{kj} + C^{kj} \right] = F_k,\ k, j = 1, 2, \ldots, 6$$

Ship hydrostatic properties

Mass matrix ***Restoring matrix***

Haskind–Newman relation

$$F_k = -\rho \int_{\Gamma} \left(\phi_w \psi^k - \phi^k \frac{\partial \phi_w}{\partial n} \right) dS,\ k = 1, 2, \ldots, 6$$

Numerical implementation

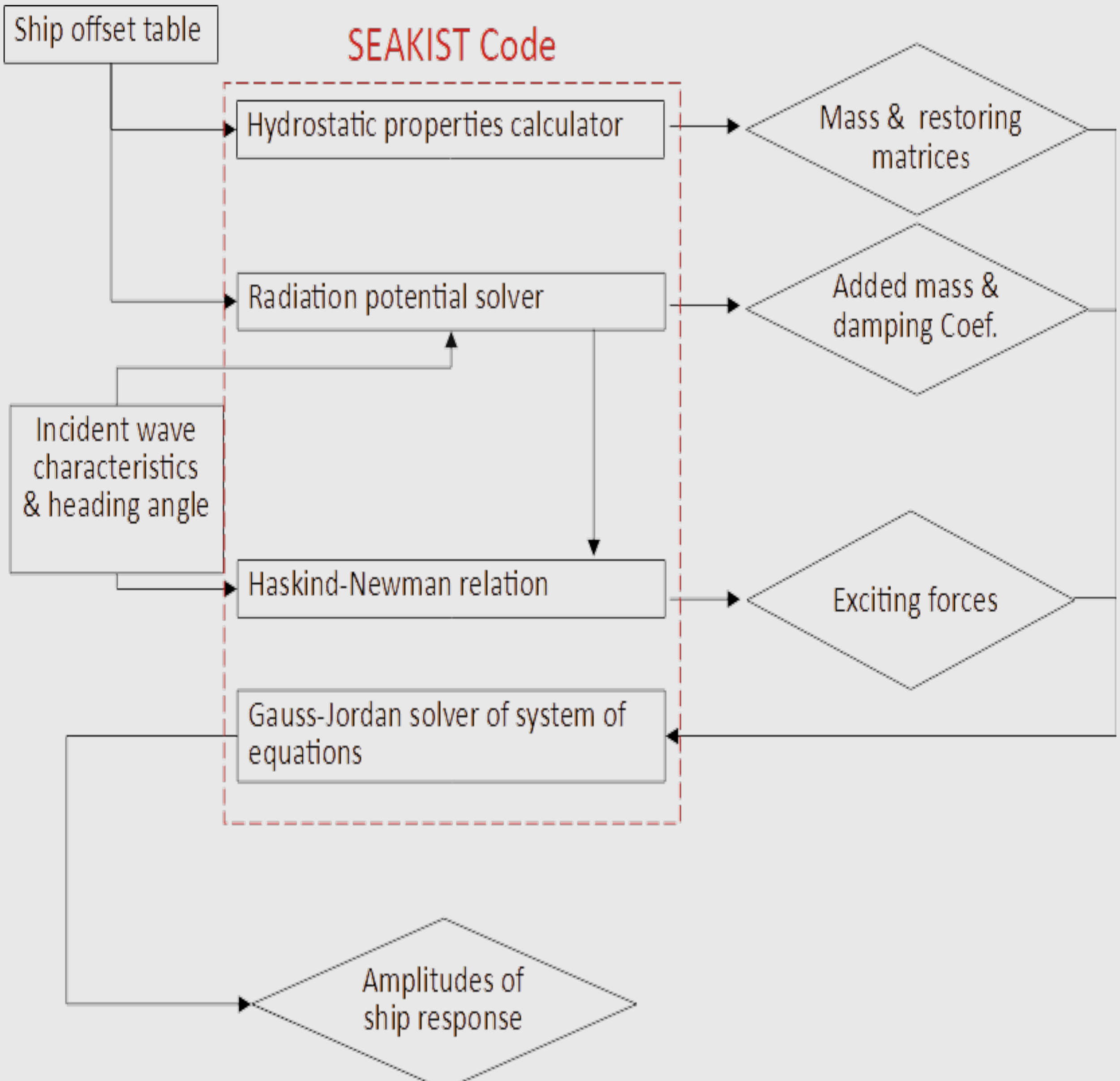

Verification of Green's function (FinGreen) for short wave lengths

$h = 1.0\text{m}$

$\omega = 4.43\text{rad/s}$

$z = 0.0\text{m}$

$z' = 0.1\text{m}$

$R = \sqrt{(x-x')+(y-y')}$

- ***Near field***

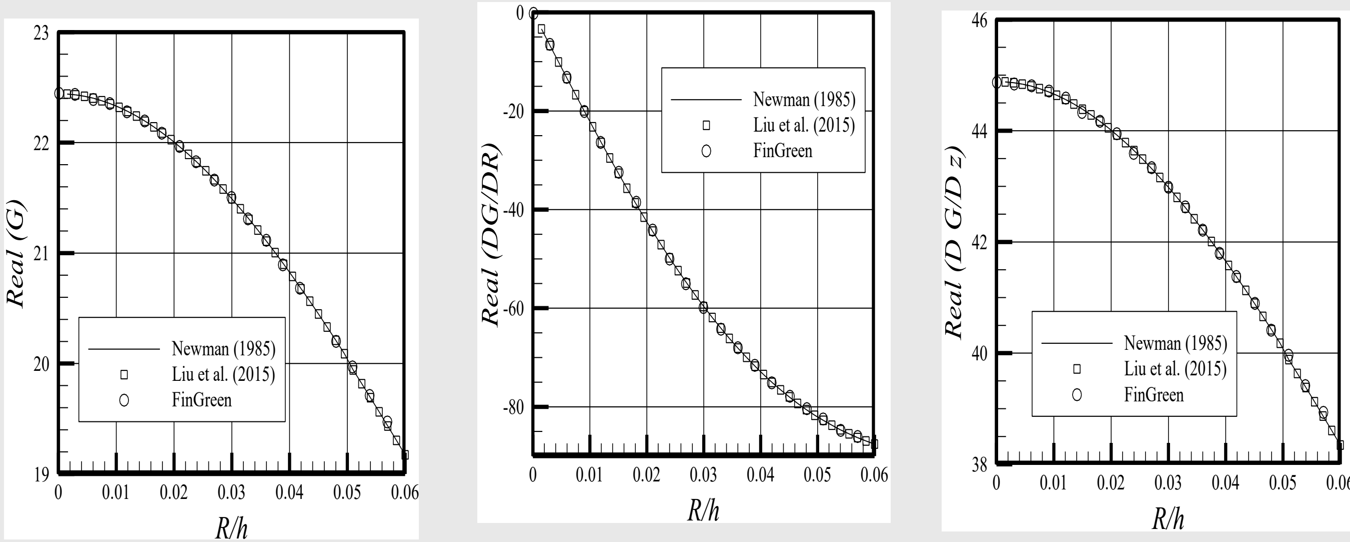

- ***Far field***

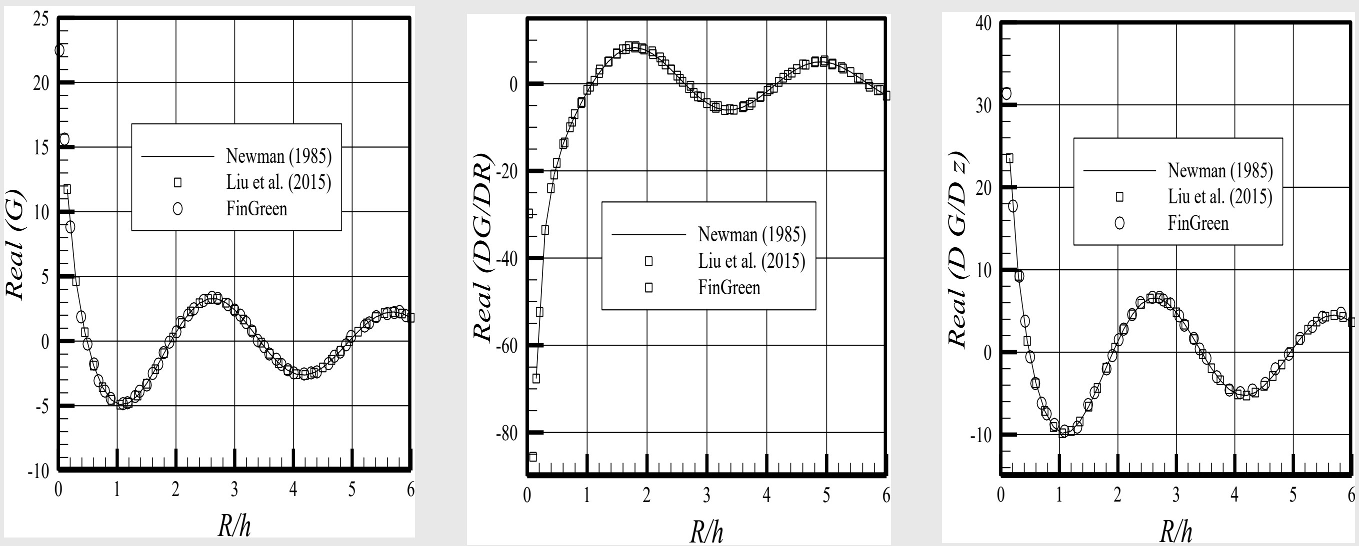

Validation of SEAKIST for an oscillating hemisphere in heave

Features of SEAKIST:

- *Flat quadrilateral panel*
- *Constant source density on panels*
- *Direct Gauss-Jordan solver (Press et al., 1992)*
- *Zero speed of advance (Limitation of FinGreen*

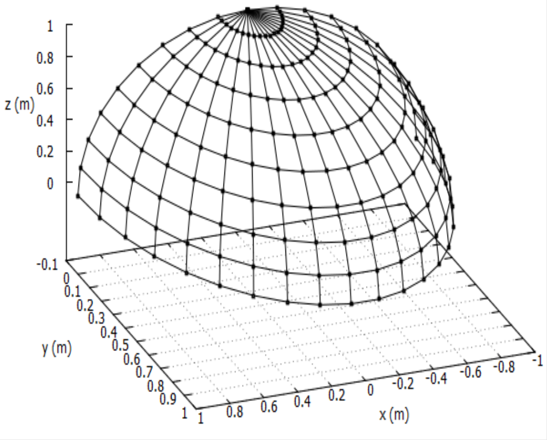

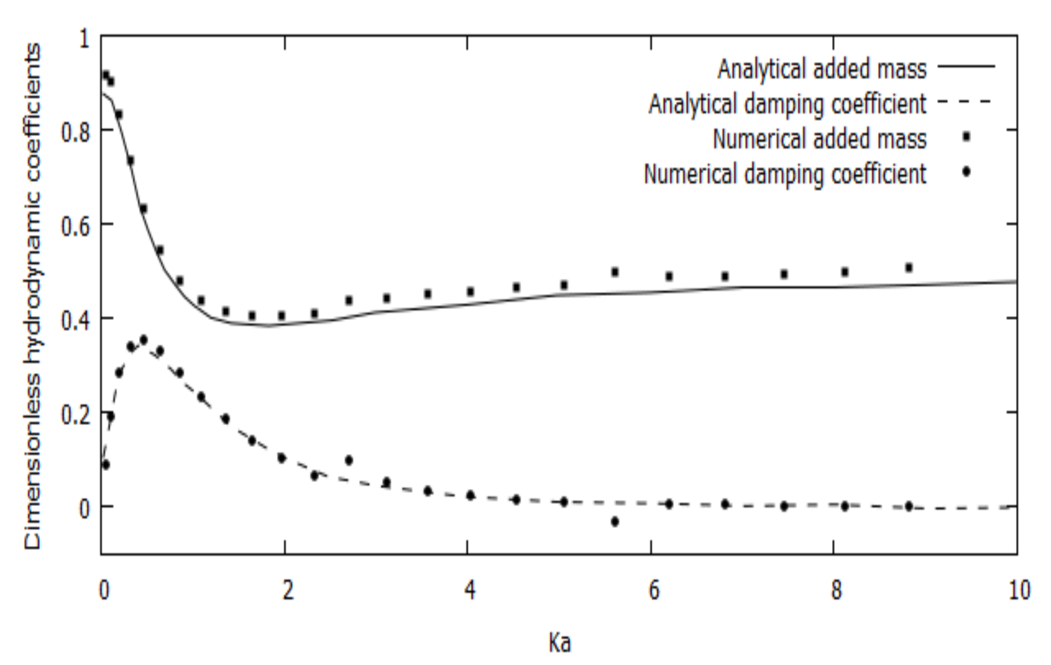

$K = \omega^2 / g$

a : *Radius of hemisphere*

V : *Volume of displacement*

$A^{33} / \rho V$: *Dimensionless added mass*

$D^{33} / \rho \omega V$: *Dimesionless damping coefficient*

$M = 684$

Comparative study for a real ship

Incident wave characteristics and advancing real ship properties:

$$0.232 \leq \omega_0 \leq 0.942$$

$$F_n = V \Big/ \sqrt{g L_{pp}} = 0.275$$

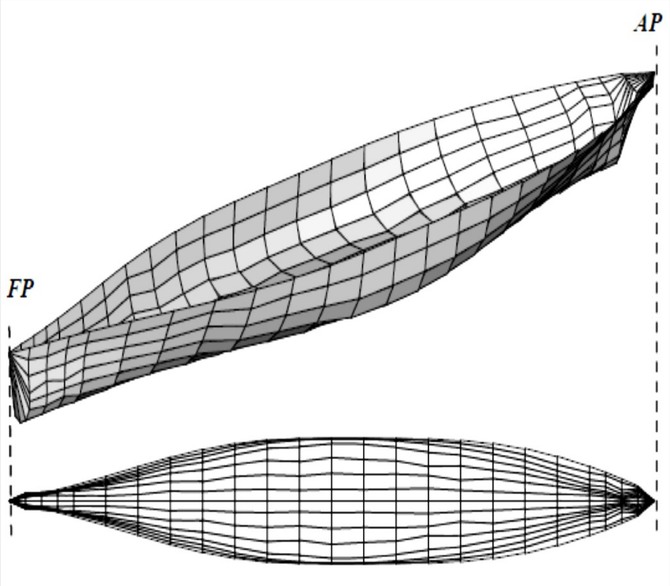

25 cross sections along the length
8 vertices along the draft
336 flat panels

S-175 container ship		
Length between perpendicular (m)	L_{pp}	175
Beam (m)	B	25.40
Depth (m)	D	15.40
Draft (m)	T	9.50
Mass (tone)	Δ	24,742
Longitudinal center of gravity (m)*	LCG	-2.4
Block coefficient	C_B	0.572
Roll radius gyration	k_{xx}/B	0.328
Pitch radius gyration	k_{yy}/L_{pp}	0.24
Keel to the centre of gravity (m)	KG	9.52
* From amid-ship		

INSTITUTO SUPERIOR TÉCNICO

Comparative study for a real ship

- For $\beta = 0^{\circ}$

X_1 / A $\quad$ X_3 / A $\quad$ X_5 / AK

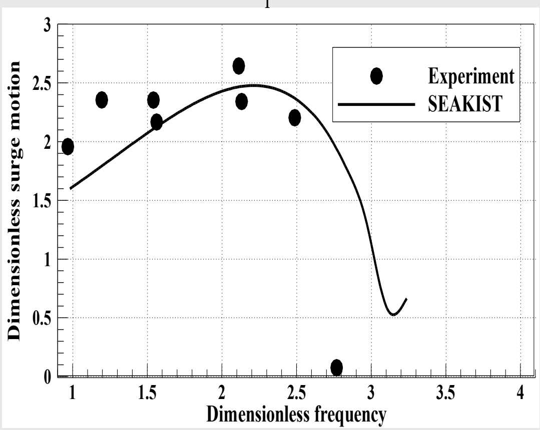

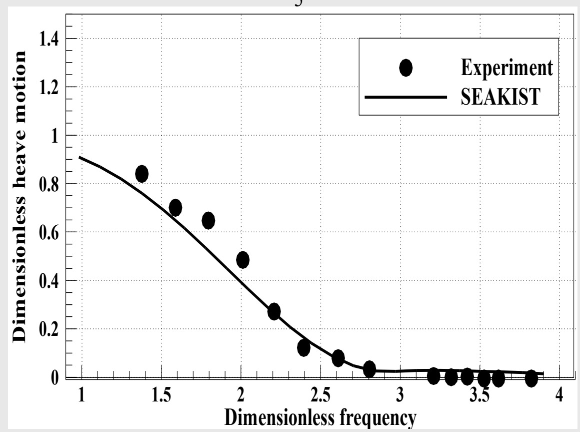

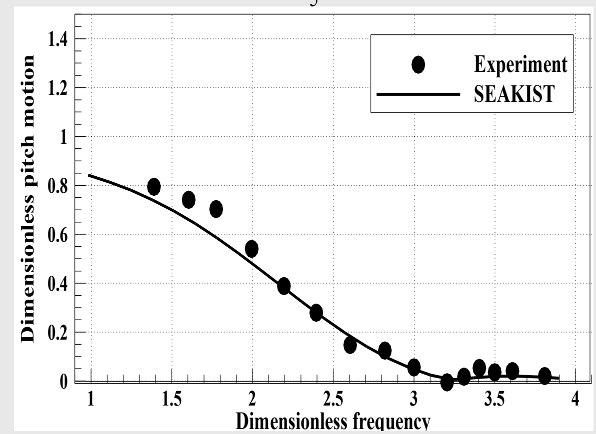

$$\omega_0 \sqrt{L_{pp} / g}$$

- For $\beta = 60^{\circ}$

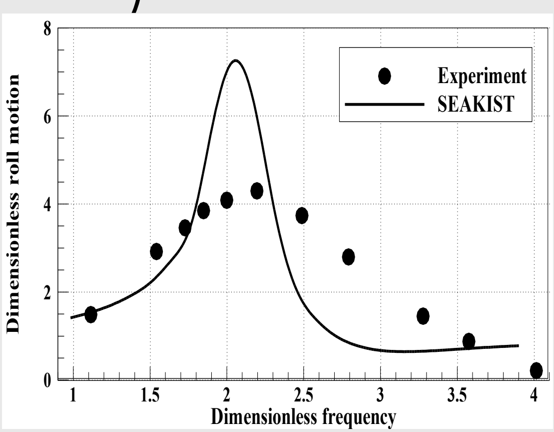

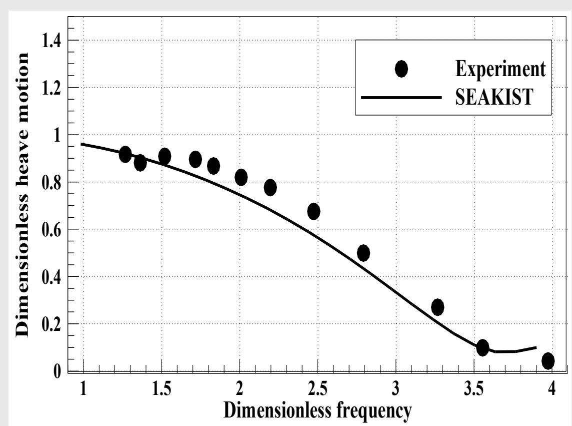

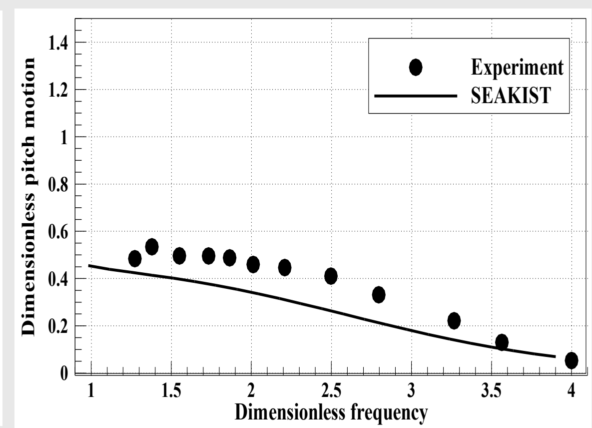

INSTITUTO SUPERIOR TÉCNICO

- For $\beta = 90^\circ$

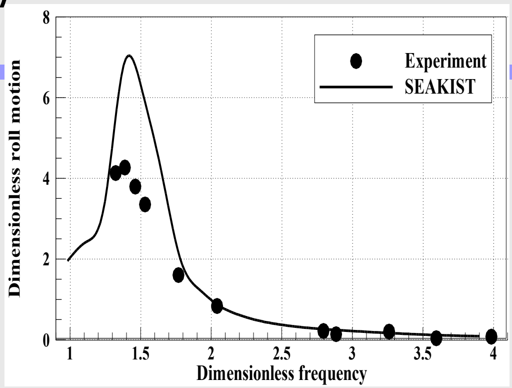

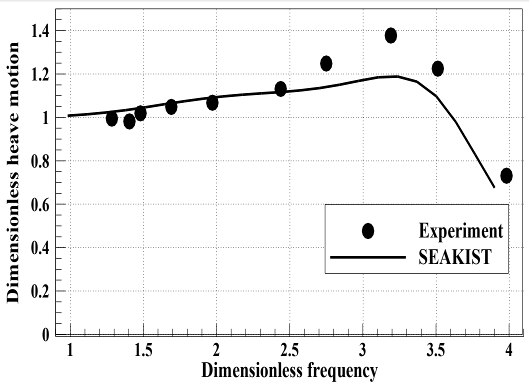

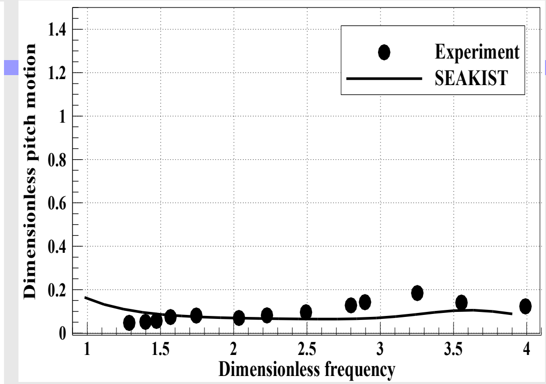

- For $\beta = 120^\circ$

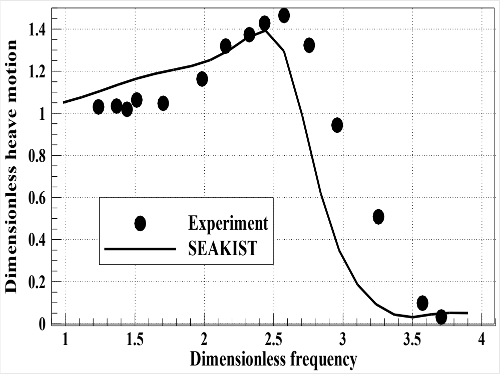

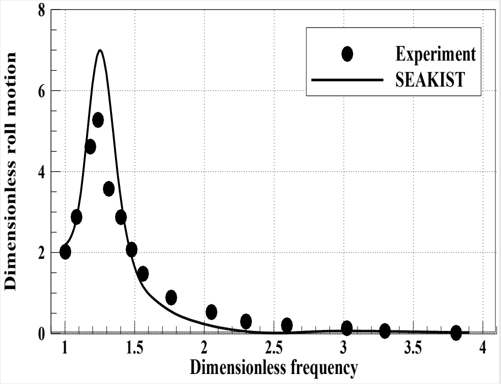

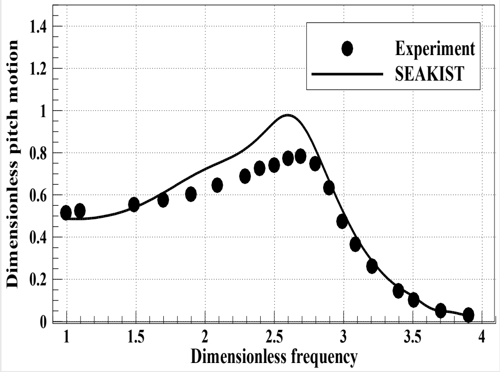

- For $\beta = 180^\circ$

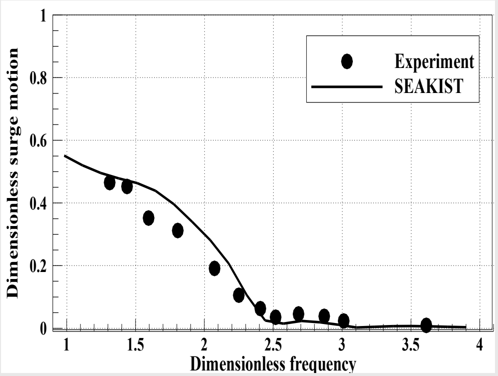

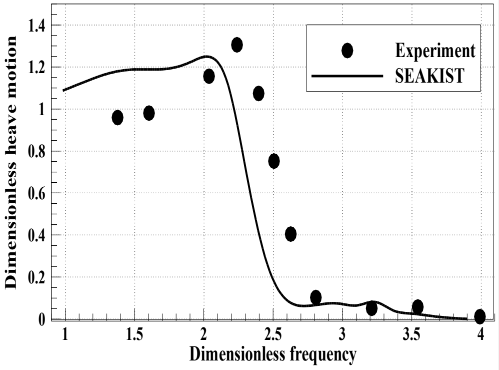

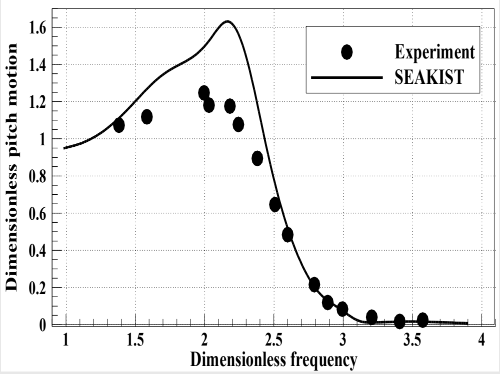

Hydrodynamics of vibrating ship sections---1

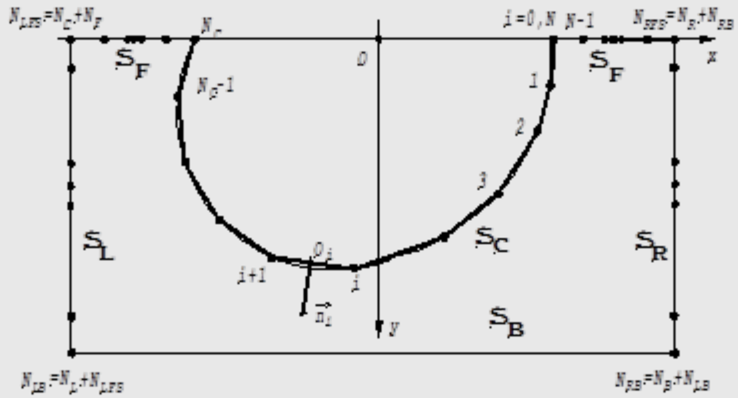

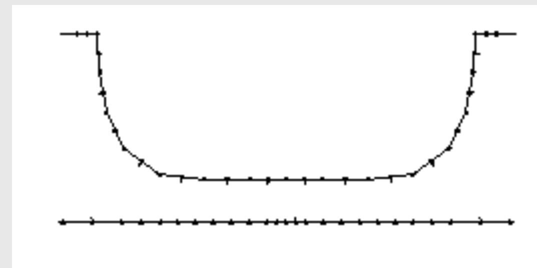

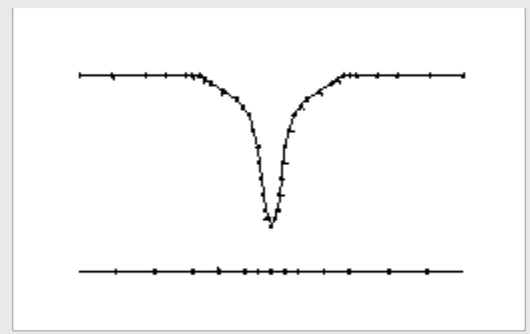

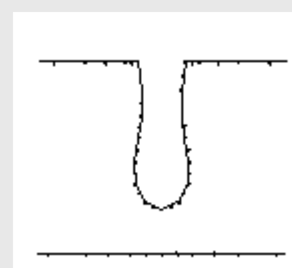

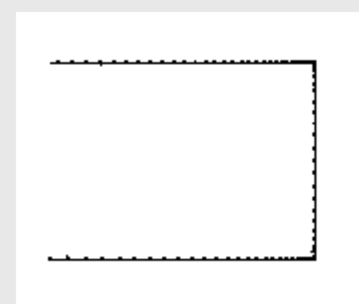

$$\frac{\partial \Phi^*}{\partial y} + k_0 \Phi^* = 0,$$

$$\frac{\partial \Phi^*}{\partial n}(x_{R,L}, y) = -i k_{R,L} \Phi^*(x_{R,L}, y), \quad \text{at} \quad y \in (0, h_{R,L}),$$

$$k_{R,L} \tanh k_{R,L} h_{R,L} = k_0.$$

$$\frac{\partial \varphi_2}{\partial n} = f_2 = n_x; \quad \frac{\partial \varphi_3}{\partial n} = f_3 = n_y;$$

$$\frac{\partial \varphi_4}{\partial n} = f_4 = x n_y - y n_x.$$

Hydrodynamics of vibrating ship sections---2

$$\pi\varphi(P) + \int_S \varphi(Q)\, K(P,Q)\, \mathrm{d}S(Q) = \int_{S_C} f(Q) \log r\, \mathrm{d}S(Q),$$

$$K(P,Q) = \begin{cases} \dfrac{\partial \log r}{\partial n_Q} & \text{if} \quad Q \in S_C \cup S_B, \\ \dfrac{\partial \log r}{\partial n_Q} + k_0 \log r & \text{if} \quad Q \in S_F, \\ -\dfrac{\partial \log r}{\partial n_Q} - ik_{R,L} \log r & \text{if} \quad Q \in S_{R,L} \end{cases}$$

$$\pi \bar{S}_i \varphi_i + \sum_{j=0}^{N-1} K_{ij} \varphi_j = F_i \equiv \sum_{j=0}^{N_C - 1} F_{ij}, \quad i = 0, \ldots, N-1,$$

$$K_{ij} = \int_{S_i} K_j(P)\, \mathrm{d}S(P); \quad F_{ij} = \int_{S_i} F_j(P)\, \mathrm{d}S(P).$$

Hydrodynamics of vibrating ship sections---3

$$F_{ij}^{(4)} = \tfrac{1}{2}(n_{yj}x_{O_i} - n_{xj}y_{O_i})I_0 - \tfrac{1}{2}I_1, \qquad I_{\begin{Bmatrix}0\\1\end{Bmatrix}} = \int_{-\bar{S}_i/2}^{\bar{S}_i/2} \mathrm{d}x \int_{-\bar{S}_j/2}^{\bar{S}_j/2} \log\left[(b_{ij} - s_{ij}x)^2 + (a_{ij} + c_{ij}x - \xi)^2\right]\begin{Bmatrix}1\\ \xi\end{Bmatrix}\mathrm{d}\xi,$$

$$I_1 = H^0(\bar{S}_i/2, \bar{S}_j/2,) - H^0(-\bar{S}_i/2, \bar{S}_j/2,) - H^0(\bar{S}_i/2, -\bar{S}_j/2,) + H^0(-\bar{S}_i/2, -\bar{S}_j/2,),$$

$$H^0(x,y) = H_0^0(x,y) + H_1^0(x,y) + H_2^0(x,y) + H_3^0(x,y)$$

$$H_0^0(x,y) = \log\left|b_{ij}\right| x(y^2 + b_{ij}^2); \quad H_1^0(x,y) = -2a_{ij}b_{ij}H_{10}^0(x,y) - 2c_{ij}b_{ij}H_{11}^0(x,y);$$

$$H_{10}^0(x,y) = x\,\mathrm{atan}\,\frac{a_{ij} - y + c_{ij}x}{b_{ij}} - c_{ij}(a_{ij} - y)\,\mathrm{atan2x}\,(b_{ij}, a_{ij} - y + c_{ij}x)$$

$$-\tfrac{1}{2}c_{ij}b_{ij}\log[b_{ij}^2 + (a_{ij} - y + c_{ij}x)^2];$$

$$H_{11}^0(x,y) = \frac{1}{2}\left\{-c_{ij}b_{ij}x + x^2\,\mathrm{atan}\,\frac{a_{ij} - y + c_{ij}x}{b_{ij}}\right.$$

$$+[(a_{ij} - y)^2 - b_{ij}^2]\,\mathrm{atan2x}\,(b_{ij}, a_{ij} - y + c_{ij}x)$$

$$\left. + b_{ij}(a_{ij} - y)\log[b_{ij}^2 + (a_{ij} - y + c_{ij}x)^2]\right\}$$

$$\mathrm{atan2x}\,(x,y) = \begin{cases} \mathrm{atan2}(x,y) & \text{at} \quad y \geq 0 \\ \pi\,\mathrm{sign}\,x + \mathrm{atan}\,\dfrac{x}{y} & \text{at} \quad y < 0 \end{cases},$$

$$\mathrm{atan2}(x,y) = \begin{cases} \mathrm{atan}\,\dfrac{x}{y} & \text{at} \quad y \neq 0 \\ \dfrac{\pi}{2}\,\mathrm{sign}\,x & \text{at} \quad y = 0 \end{cases}$$

Hydrodynamics of vibrating ship sections---4

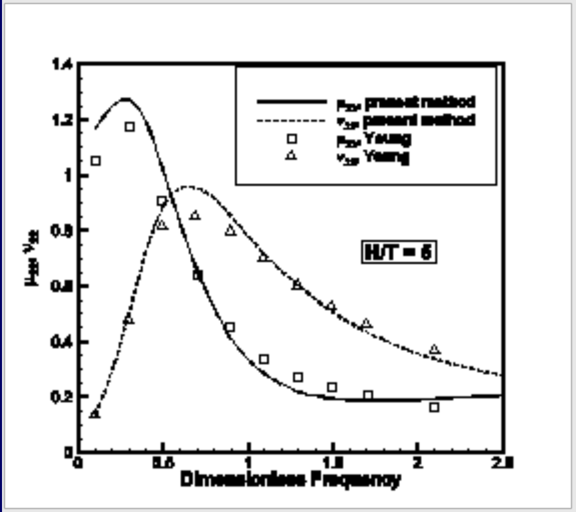

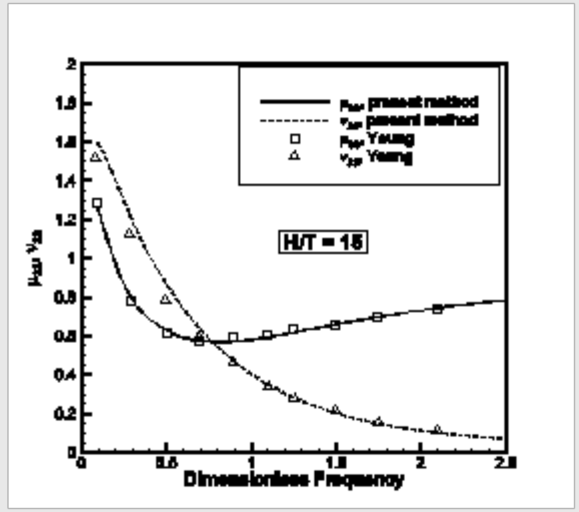

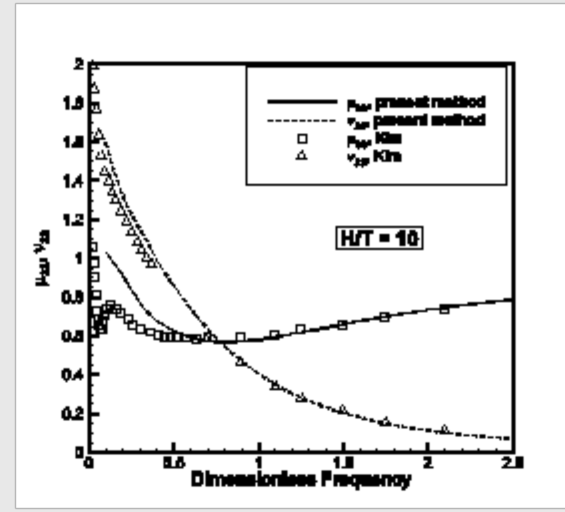

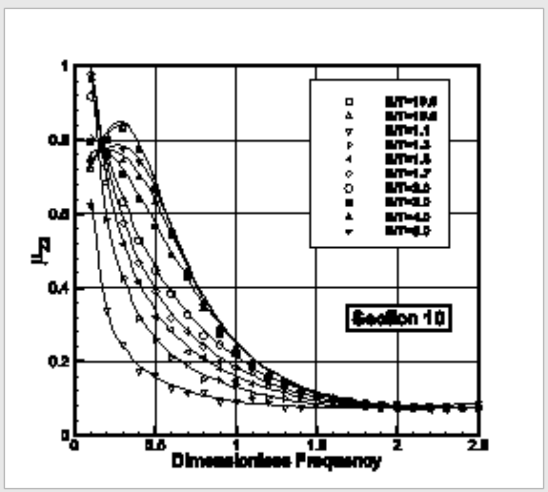

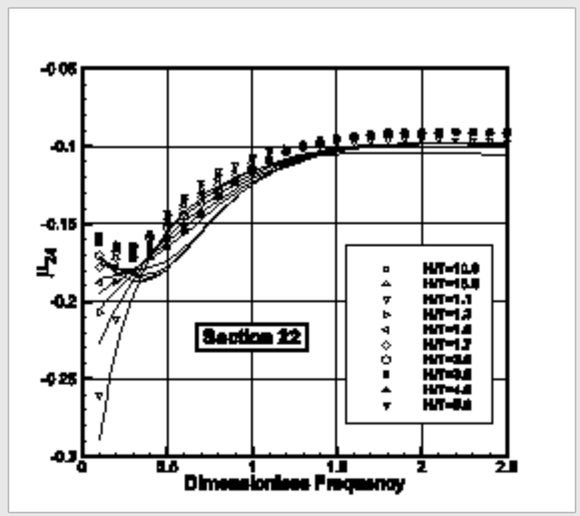

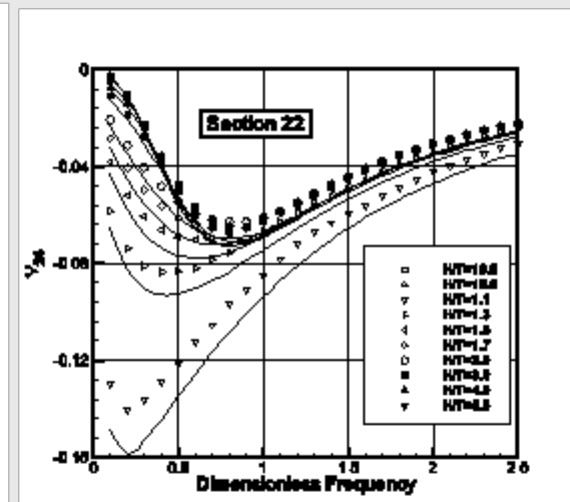

Lines---Soeding

Hydrodynamics of vibrating ship sections---5

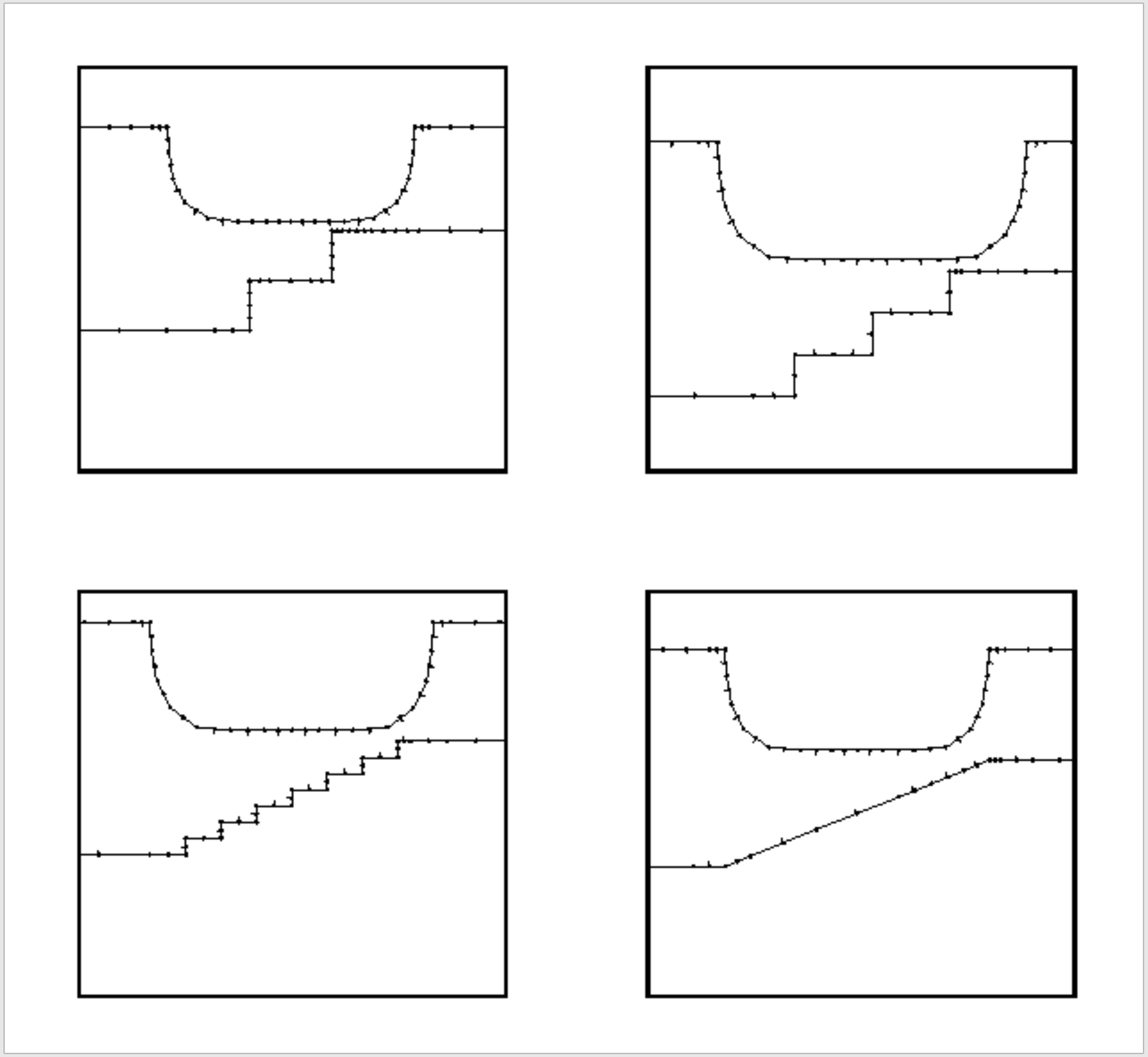

Hydrodynamics of vibrating ship sections---6

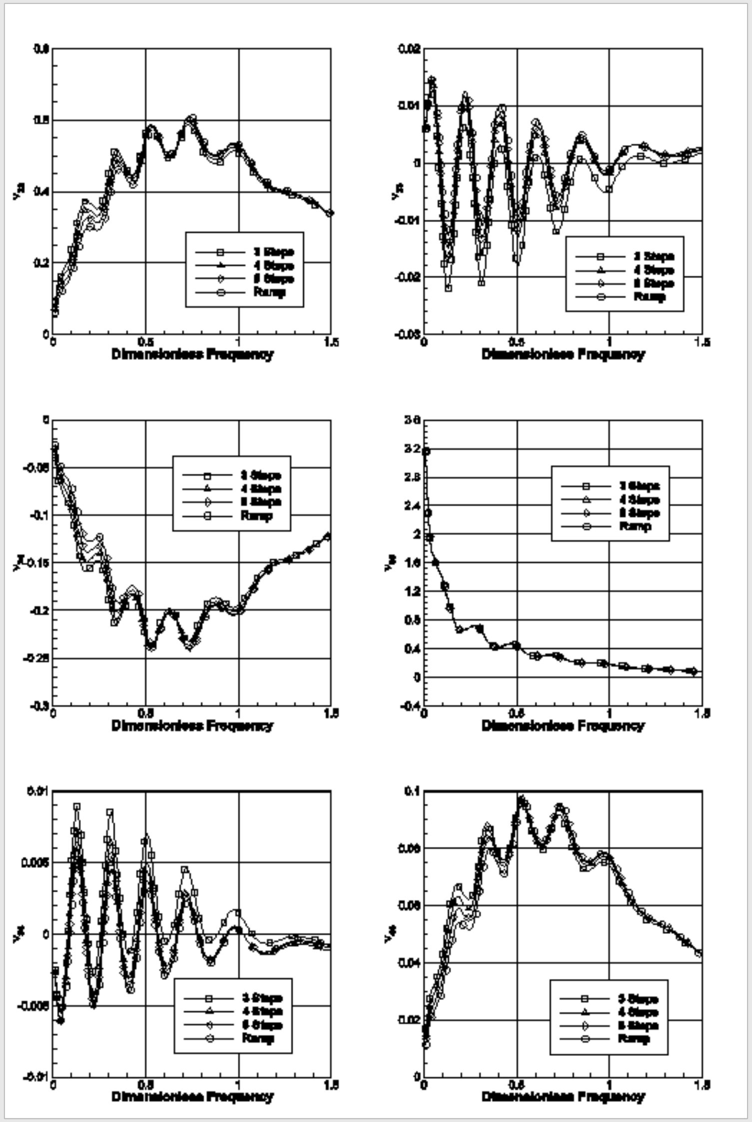

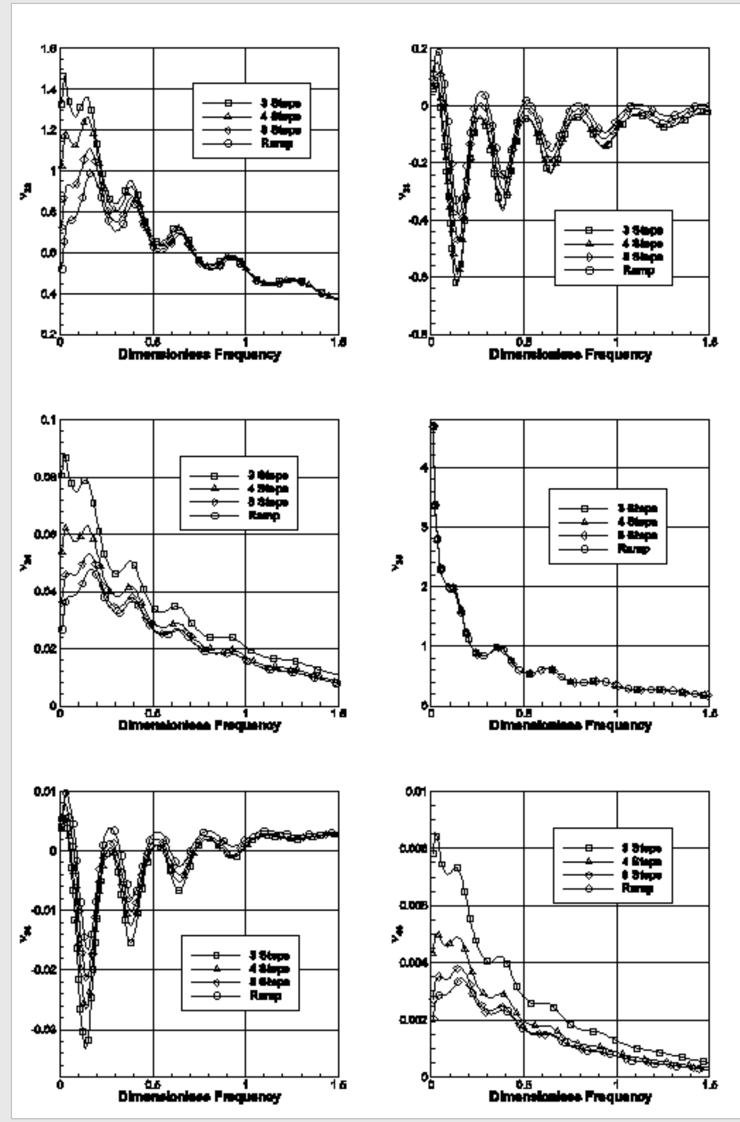

Hydrodynamics of vibrating ship sections---7

Advantage of the BIE method:

- No limitations on the domain
- No singular frequencies

Disadvantage: relatively slow.

Planned but not realised:

Implementation of the faster Frank method (Green function, single layer) with lids preventing appearance of singular frequencies (original Frank's f77 code available).

Introduction-1:

Problems Faced When Combining Seakeeping and Manoeuvring Mathematical Models

1. **Potential Forces** estimated theoretically dominate in the seakeeping

2. **Viscous Forces** usually estimated experimentally dominate in the manoeuvring but these always contain a potential component (e.g. the Munk moment)

3. Attempts of mechanical superposition of usual manoeuvring and seakeeping loads may result in **double account** for some components

4. Attempts of creating really consistent mathematical models equally suitable for manoeuvring and seakeeping calculations can only result in RANSE CFD codes

Introduction-2:

Approaches to Creating Approximate Manoeuvring & Seakeeping Models

- Basing on a still-water manoeuvring MM approximate wave excitation loads are added (usually 3DOF): Afremov (1967, linear), Ananyev & Gorbachova (1966—1993, linear)
- A 6DOF seakeeping model is augmented with seakeeping elements (certainly or likely): Ottosson & Bystrom (1991), Bailey et al. (1997, linear), Lee (2000, linear), Ayaz et al. (2003), Nishimura & Hirayama (2003, long waves)

Requirements to an Approximate Unified Mathematical Model

1. Reduces to a recognized seakeeping MM in straight run (strip method)
2. Reduces to a recognized manoeuvring MM in still-water manoeuvring (e.g. based on captive-model tests)
3. Accounts for all significant and treatable non-linearities and cross-coupling effects
4. Remains valid at any value of the instantaneous encounter frequency

INSTITUTO SUPERIOR TÉCNICO

MM Description—1: Frames of Reference

1. Earth-fixed frame $O_0\xi_0\eta_0\zeta_0$
2. Body-fixed frame $Cxyz$
3. Body-semi-fixed frame $O\xi\eta\zeta$ (as previous but not involved into heave, pitch, and roll)
4. Body-semi-fixed still-water frame $O_1\xi_1\eta_1\zeta_1$ (as previous but not involved into surge, sway, and yaw caused by waves)

MM Description: Equations of Motion

$$(m+\mu_{11})\dot{u}+(mz_G+\mu_{15})\dot{q}-mvr$$
$$-mx_Gr^2+mz_Gpr+mwq-mx_Gq^2=X_g+X,$$
$$(m+\mu_{22})\dot{v}-(mz_G+\mu_{24})\dot{p}+(mx_G+\mu_{26})\dot{r}$$
$$+mur-mur-mwp+mx_Gpq+mz_Gqr=Y_g+Y,$$
$$(m+\mu_{33})\dot{w}-(mx_G+\mu_{35})\dot{q}-muq$$
$$-mz_Gq^2+mvp+mx_Gpr-mz_Gp^2=Z_g+Z,$$
$$-(mz_G+\mu_{24})\dot{v}+(I_{xx}+\mu_{44})\dot{p}-(I_{xz}+\mu_{46})\dot{r}$$
$$+mz_Gwp+(I_{zz}-I_{yy})qr-mz_Gur-I_{xz}pq=K_g+K,$$
$$(mz_G+\mu_{15})\dot{u}-(mx_G+\mu_{35})\dot{w}+(I_{yy}+\mu_{55})\dot{q}$$
$$+mx_Guq+mz_Gwq+(I_{xx}-I_{zz})pr$$
$$+I_{xz}(p^2-r^2)-mz_Gvr-mx_Gvp=M_g+M,$$
$$(mx_G+\mu_{26})\dot{v}-(I_{xz}+\mu_{46})\dot{p}+(I_{zz}+\mu_{66})\dot{r}$$
$$+mx_Gur-mx_Gwp+(I_{yy}-I_{xx})pq+I_{xz}qr=N_g+N,$$

$$\begin{aligned}
\dot{\xi} &= u\cos\psi\cos\theta \\
&+ v(\cos\psi\sin\theta\sin\varphi-\sin\psi\cos\varphi) \\
&+ w(\cos\psi\sin\theta\cos\varphi-\sin\psi\sin\varphi), \\
\dot{\eta} &= u\sin\psi\cos\theta \\
&+ v(\sin\psi\sin\theta\sin\varphi+\cos\psi\cos\varphi) \\
&+ w(\cos\psi\sin\theta\cos\varphi-\cos\psi\sin\varphi), \\
\dot{\zeta} &= -u\sin\theta+v\cos\theta\sin\varphi+w\cos\theta\cos\varphi, \\
\dot{\psi} &= q\frac{\sin\varphi}{\cos\theta}+r\frac{\cos\varphi}{\cos\theta}, \\
\dot{\theta} &= q\cos\varphi-r\sin\varphi, \\
\dot{\varphi} &= p+q\tan\theta\sin\varphi+r\tan\theta\cos\varphi.
\end{aligned}$$

MM Description: Forces--1

- Gravity Forces:

$$
\begin{aligned}
X_g &= -mg\sin\theta, & K_g &= -mg z_G \cos\theta\sin\varphi,\\
Y_g &= \quad mg\cos\theta\sin\varphi, & M_g &= -mg x_G \cos\theta\cos\varphi - mg z_G \cos\theta\sin\varphi,\\
Z_g &= \quad mg\cos\theta\cos\varphi, & N_g &= \quad mg x_G \cos\theta\sin\varphi.
\end{aligned}
$$

- Hydrodynamic Forces' Decomposition--1:

$$F(\mathbf{W},\mathbf{M}) = F_{WM}(\mathbf{W},\mathbf{M}) - F_{WM}(\mathbf{0},\mathbf{M}) + F_M(\mathbf{M}).$$

- Hydrodynamic Forces' Decomposition--2:

$$F = F_{MAN} + F_{HS+FK} + F_R + F_D$$

Generalized Seakeeping Forces—1:

Velocity potential:

$$\phi(\xi_0, \eta_0, \zeta_0) = \phi_B + \phi_w + \phi_d,$$

Body boundary condition:

$$\frac{\partial \phi_B}{\partial n} = [\mathbf{V}(t) + \mathbf{\Omega}(t) \times \mathbf{r}(t)] \cdot \mathbf{n} \quad \text{on } S_B(t),$$

Incident wave's potential:

$$\phi_w = \mathrm{Re}\left[\frac{iga_w}{\omega} e^{-k\zeta_0 - i(k_1\xi_0 + k_2\eta_0)} e^{i\omega t} \right],$$

Generalized Seakeeping Forces—2:

- Local velocity:

$$\mathbf{V}(x,y,z,t) = \mathbf{V}_0(x,y,z,t) + \mathbf{V}_1(x,y,z,t)$$
$$= \mathbf{V}_{C0}(t) + \mathbf{V}_{C1}(t) + [\mathbf{\Omega}_0(t) + \mathbf{\Omega}_1(t)] \times \mathbf{r}(x,y,z),$$

- Bernoulli pressure equation in semi-fixed axes

$$p = -\rho \frac{\partial \phi}{\partial t} - \frac{\rho}{2}(\nabla \phi)^2 + \rho g \zeta + \rho \mathbf{V} \cdot \nabla \phi.$$

Pressure Components

- Total pressure: $p = p_{hs} + p_0 + p_{01} + p_1 + p_2,$ where
- $p_{hs} = \rho g \zeta$ ---hydrostatic pressure,
- $p_0 = \rho \mathbf{V_0} \cdot \nabla \phi_0 - \frac{\rho}{2}(\nabla \phi_0)^2$ ---quasi-steady contribution,
- $p_{01} = \rho \mathbf{V_1} \cdot \nabla \phi_0 - \rho \nabla \phi_0 \cdot \nabla \phi_1$ ---quasi-steady-unsteady interaction,
- $p_1 = -\rho \frac{\partial \phi_1}{\partial t} + \rho \mathbf{V_0} \cdot \nabla \phi_1$ ---1st-order unsteady pressure,
- $p_2 = -\frac{\rho}{2}(\nabla \phi_1)^2 + \rho \mathbf{V_1} \cdot \nabla \phi_1$ ---2nd-order pressure (part of)

First-Order Forces

- Potential's and forces' representation:

$$\mathbf{F} = -\int_{S(t)/S_0} p\mathbf{n}\,\mathrm{d}S; \qquad \mathbf{M} = -\int_{S(t)/S_0} p\mathbf{r}\times\mathbf{n}\,\mathrm{d}S,$$

$$\phi_1 = \phi_r + \phi_w + \phi_d,$$

$$F_1 = F_r + F_w + F_d,$$

- Radiation force:

$$F_r = \rho\int_S \frac{\partial\phi_r}{\partial t} n_F\,\mathrm{d}S - \rho V_{0\xi}\int_S \frac{\partial\phi_r}{\partial\xi} n_F\,\mathrm{d}S,$$

Escaping to the Frequency Domain

by means of the Fourier transform:

$$\phi_r(t) = \frac{1}{2\pi}\int_{-\infty}^{+\infty} e^{i\omega t}\hat{\phi}(\omega)\,\mathrm{d}\,\omega, \quad \Rightarrow$$

$$X_{ri} = \rho\int_S\left(\frac{\partial}{\partial t} - V_{0\xi}\frac{\partial}{\partial\xi}\right)\phi_r n_i\,\mathrm{d}\,S,\ \ i = 1,\ldots,6$$

$$\leftrightarrow \quad \hat{X}_{ri}(\omega) = i\omega\rho\int_S \hat{\phi}_r n_i\,\mathrm{d}\,S - \rho V_{0\xi}\int_S \frac{\partial\hat{\phi}_r}{\partial\xi} n_i\,\mathrm{d}\,S,$$

INSTITUTO SUPERIOR TÉCNICO

Forces in Frequency Domain---1

- Radiation functions and sectional loads:

$$\hat{\phi}_r = \sum_{i=1}^{6} \hat{\phi}_i \hat{U}_i, \quad \hat{U}_j = i\omega \hat{\xi}_j,\ j = 1,4,5,6; \quad \hat{U}_2 = i\omega \hat{\xi}_2 - V_{0\xi} \hat{\xi}_6; \quad \hat{U}_3 = i\omega \hat{\xi}_3 + V_{0\xi} \hat{\xi}_5$$

$$\hat{X}_{rj} = \int_{L'} \hat{R}_j(\xi)\,\mathrm{d}\xi, \quad j = 2,\ldots,4; \quad \hat{X}_{r5} = -\int_{L'} \xi \hat{R}_3(\xi)\,\mathrm{d}\xi, \quad \hat{X}_{r6} = \int_{L'} \xi \hat{R}_2(\xi)\,\mathrm{d}\xi,$$

$$\hat{R}_k = -i\omega \sum_{\ell=2}^{4} \hat{\mu}_{k\ell}(\xi)\hat{u}_\ell(\xi) + V_{0\xi} \sum_{\ell=2}^{4} \frac{\partial}{\partial \xi}[\hat{\mu}_{k\ell}(\xi)\hat{u}_\ell(\xi)],\ k = 2,3,4.$$

$$\hat{u}_2(\xi) = \hat{U}_2 + \xi \hat{U}_6 - \frac{V_{0\xi}}{i\omega}\hat{U}_6, \quad \hat{u}_3(\xi) = \hat{U}_3 - \xi \hat{U}_5 + \frac{V_{0\xi}}{i\omega}\hat{U}_5, \quad \hat{u}_4(\xi) \equiv \hat{U}_4.$$

Forces in Frequency Domain---2

Final representation in frequency domain:

$$\hat{X}_{rj}(\omega) = \sum_{k=2}^{6} \hat{A}_{jk}(\omega)\hat{U}_k(\omega), \quad j = 2,3,\ldots,6,$$

$$\hat{A}_{jk} = -i\omega\hat{\mu}_{jk} + V_{0\xi}\hat{\bar{\mu}}_{jk}, \quad k = 2,3,4;$$

$$\hat{A}_{j5} = -i\omega\hat{\mu}_{j5} + V_{0\xi}\hat{\bar{\mu}}_{j5} - 2V_{0\xi}\hat{\mu}_{j3} + \frac{V_{0\xi}^2}{i\omega}\hat{\bar{\mu}}_{j3},$$

$$\hat{A}_{j6} = -i\omega\hat{\mu}_{j6} + V_{0\xi}\hat{\bar{\mu}}_{j6} + 2V_{0\xi}\hat{\mu}_{j2} - \frac{V_{0\xi}^2}{i\omega}\hat{\bar{\mu}}_{j2},$$

Return to Time Domain: ASV method

- Fractional approximation to complex added masses:

$$\hat{\mu}_{jk}(\omega) = \mu_{jk\infty} + \frac{i\omega F + G}{(i\omega)^3 + (i\omega)^2 B + i\omega C + D},$$

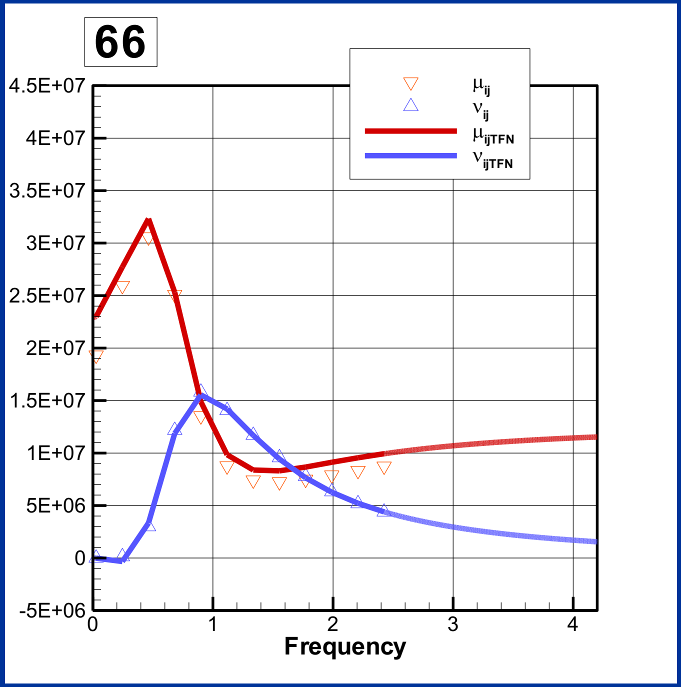

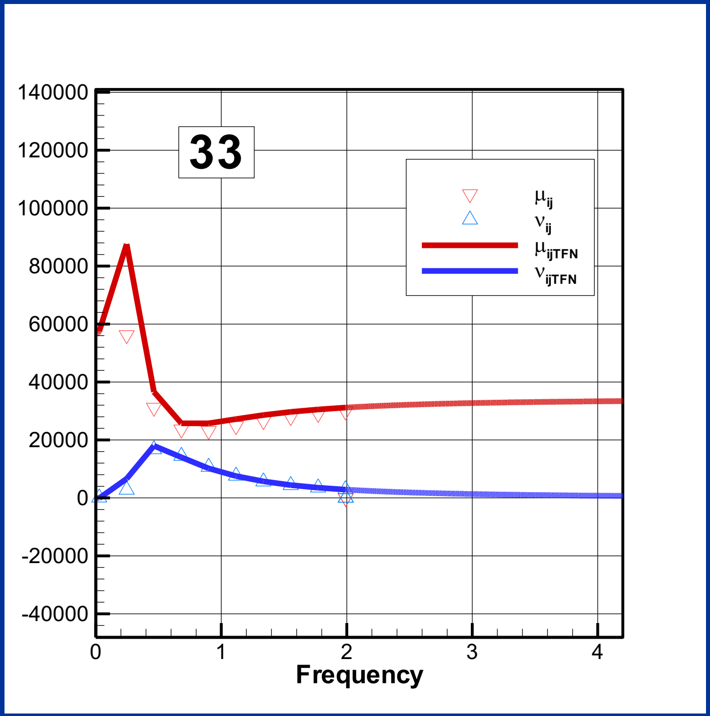

Return to Time Domain: Example

$$\hat{X}_{jk}(\omega) = -i\omega\hat{\mu}_{jk}(\omega) \quad \leftrightarrow \quad X_{jk}(t) = X_{jk}^{(1)}(t) + X_{jk}^{(2)}(t),$$

$$X_{jk}^{(1)}(t) = -\mu_{jk\infty}\dot{U}_k(t),$$

$$\dddot{X}_{jk}^{(2)} + B\ddot{X}_{jk}^{(2)} + C\dot{X}_{jk}^{(2)} + DX_{jk}^{(2)} = -F\ddot{U}_k - G\dot{U}_k, \quad \Leftrightarrow$$

$$X_{jk}^{(2)} = x_1, \quad \dot{x}_1 = x_2 - FU,$$

$$\dot{x}_2 = x_3 + (FB - G)U,$$

$$\dot{x}_3 = -Dx_1 - Cx_2 - Bx_3 + (CF + BG - FB^2)U;$$

The “Munk” forces (at $\omega = 0$ or $t \to \infty$)

$$X_{0i}(t) = V_{0\xi}\left[\sum_{j=2}^{6}\bar{\mu}_{ij}(0)U_j(t) - \mu_{i3}(0)U_5(t) + \mu_{i2}(0)U_6(t)\right], \quad i = 2,\ldots,6$$

Hydrostatic and Froude—Krylov Forces

---the wave surface:

$$\zeta_w = -a_w e^{i[\omega t + \Phi(t)]} e^{-ik[\xi\cos(\chi_{w0}-\psi)+\eta\sin(\chi_{w0}-\psi)]},$$

---the total wave phase:

$$\Phi = -k(\xi_{C0}\cos\chi_{w0} + \eta_{C0}\sin\chi_{w0})$$

---the force

$$X_{hsk} + X_{wk} = -\rho g \int_S \zeta \,\mathrm{d}S - \rho g a_w e^{i[\omega t + \Phi(t)]} \int_S e^{-k\zeta - ik[\xi\cos(\chi_{w0}-\psi)+\eta\sin(\chi_{w0}-\psi)]} n_k \,\mathrm{d}S.$$

Diffraction Forces

are: $$X_{dk}(t) = \hat{X}_{dk} e^{i\omega_e t}, \quad \omega_e = \omega - k(V_{0\xi}\cos\chi_w + V_{0\eta}\sin\chi_w)$$

$$\hat{X}_{dk} = \int_L f_{dk}^{(1)}(\xi)\,\mathrm{d}\xi + f_{dk}^{(2)}(\xi_m), \quad k = 2,3,4;$$

$$\hat{X}_{d5} = -\int_L f_{d3}^{(1)}(\xi)\xi\,\mathrm{d}\xi - \int_{L'} f_{d3}^{(2)}(\xi)\xi\,\mathrm{d}\,\xi - \xi_m f_{d3}^{(2)}(\xi_m),$$

$$\hat{X}_{d6} = \int_L f_{d2}^{(1)}(\xi)\xi\,\mathrm{d}\xi + \int_{L'} f_{d2}^{(2)}(\xi)\xi\,\mathrm{d}\,\xi + \xi_m f_{d2}^{(2)}(\xi_m),$$

where

$$f_{dk}^{(1)} = i\omega f_{dk}, \quad f_{dk}^{(2)} = V_{0\xi} f_{dk},$$

$$f_{dk} = -\rho\omega a_w e^{i\Phi} e^{-ik\xi\cos(\chi_w-\psi)} \int_C [n_2\sin(\chi_w-\psi) - in_3] e^{-k\zeta - ik\eta\sin(\chi_w-\psi)} \hat{\phi}_k\,\mathrm{d}C,$$

Numerical Example

- Containership S-175

- Length WL 175m
- Breadth 25.4m
- Draught 9.5m
- Mass 24,570t

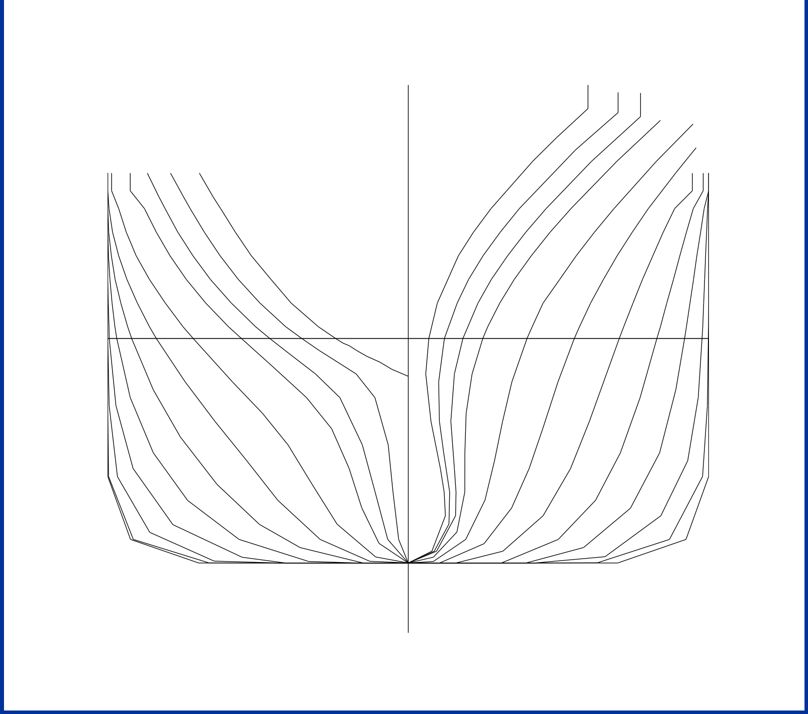

Submerged Part of the Hull

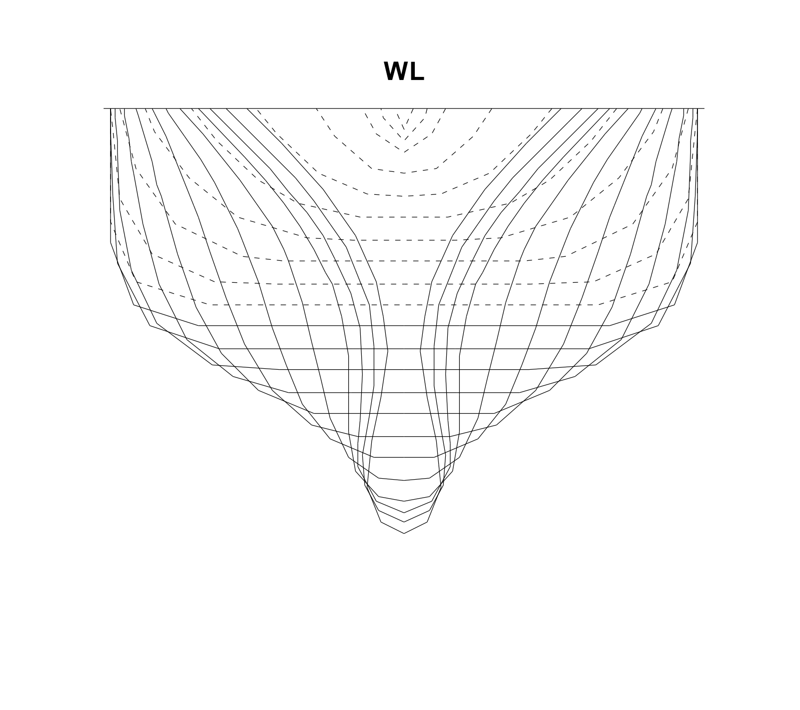

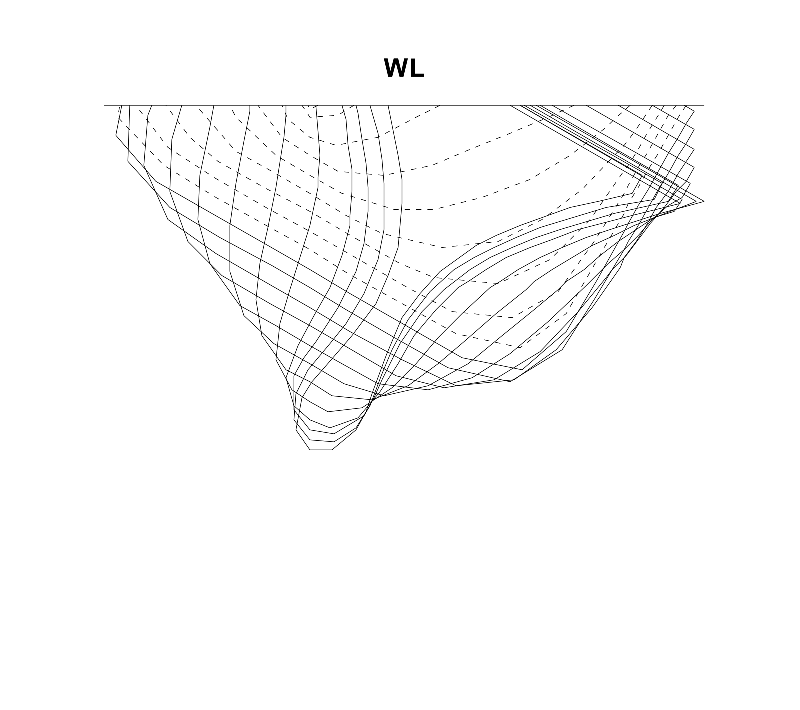

Submerged Hull in Waves and Spiral Curve in Still Water

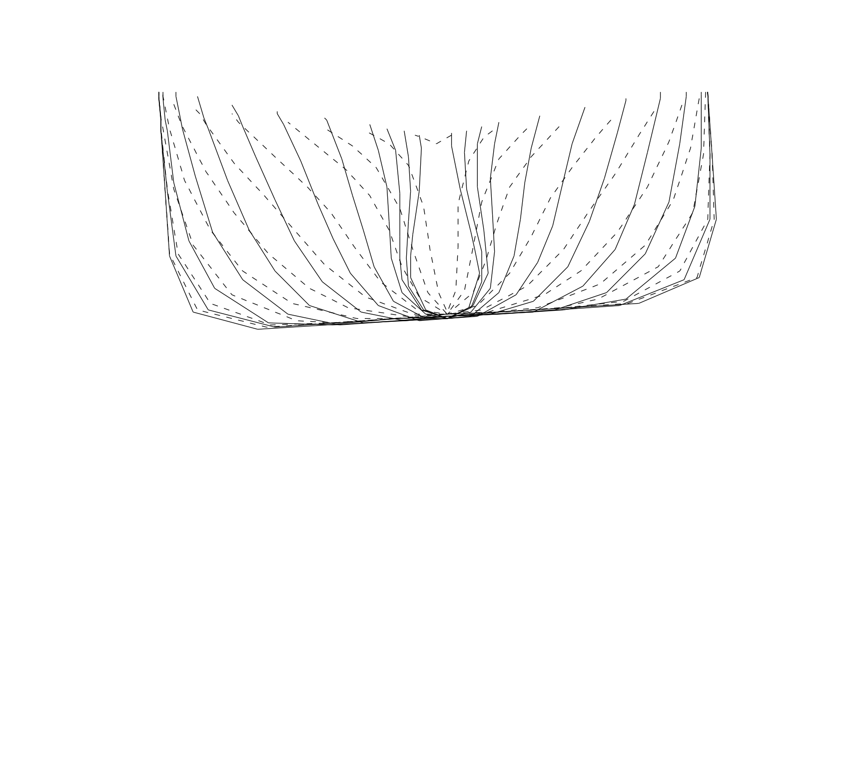

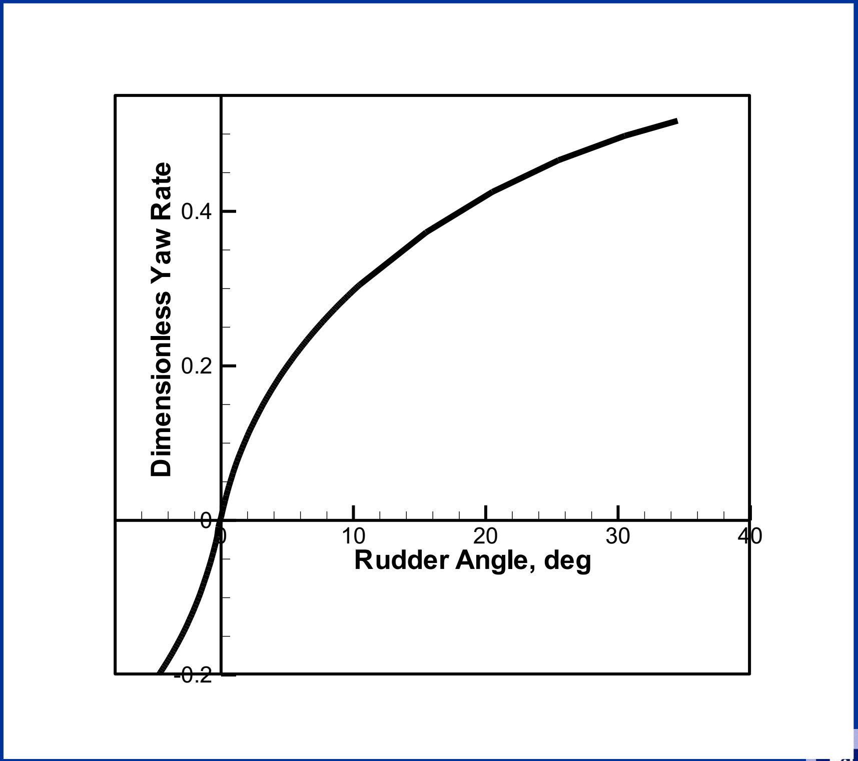

Turning manoeuvre: Trajectories

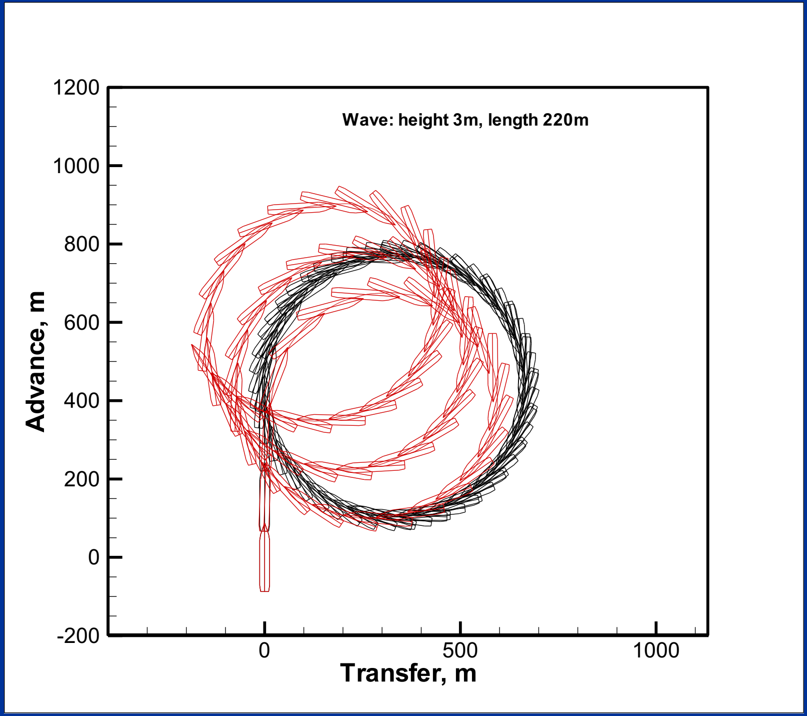

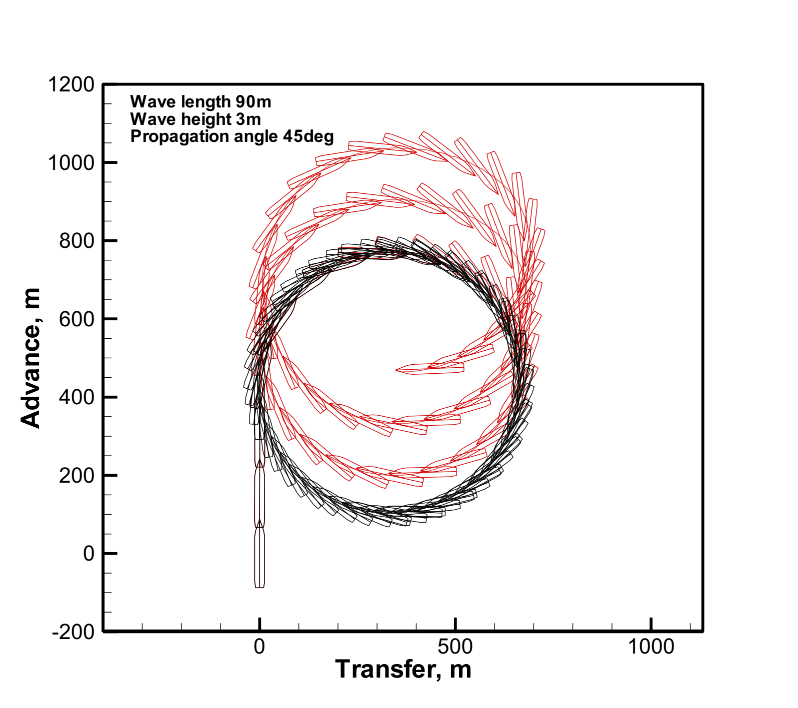

Turning Manoeuvre: Time Histories in Still Water

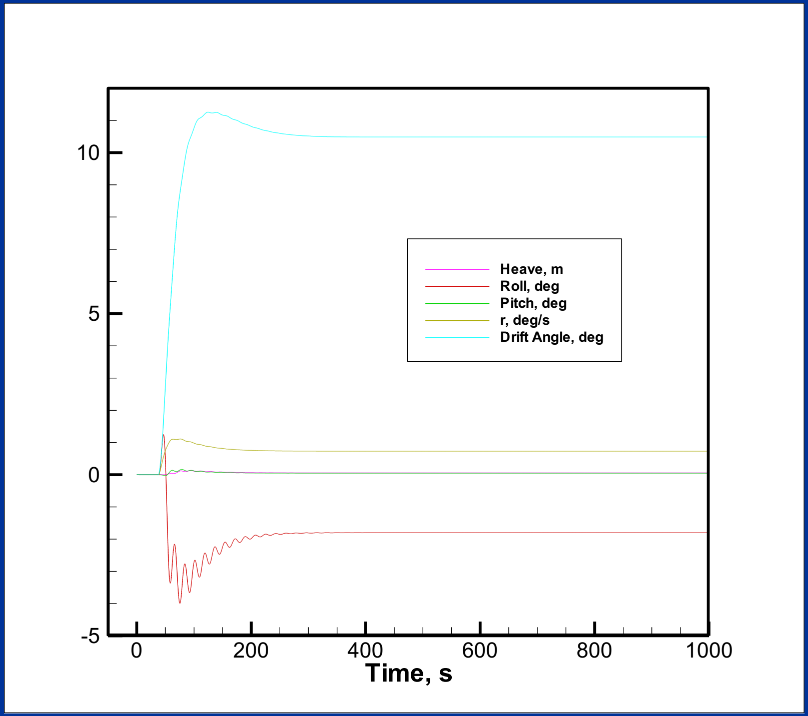

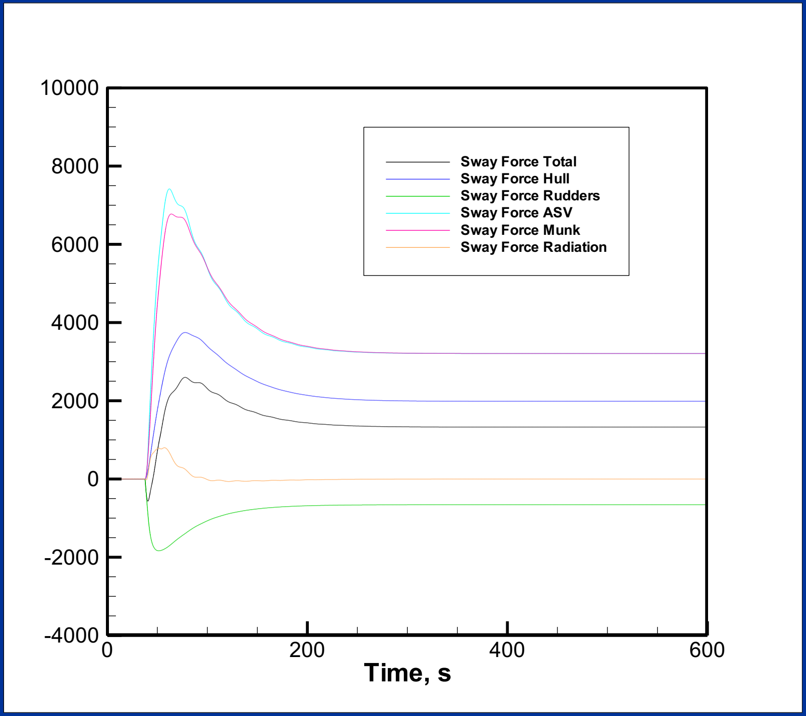

INSTITUTO SUPERIOR TÉCNICO

Turning Manoeuvre: Time Histories in Wave 220m/3m/45deg

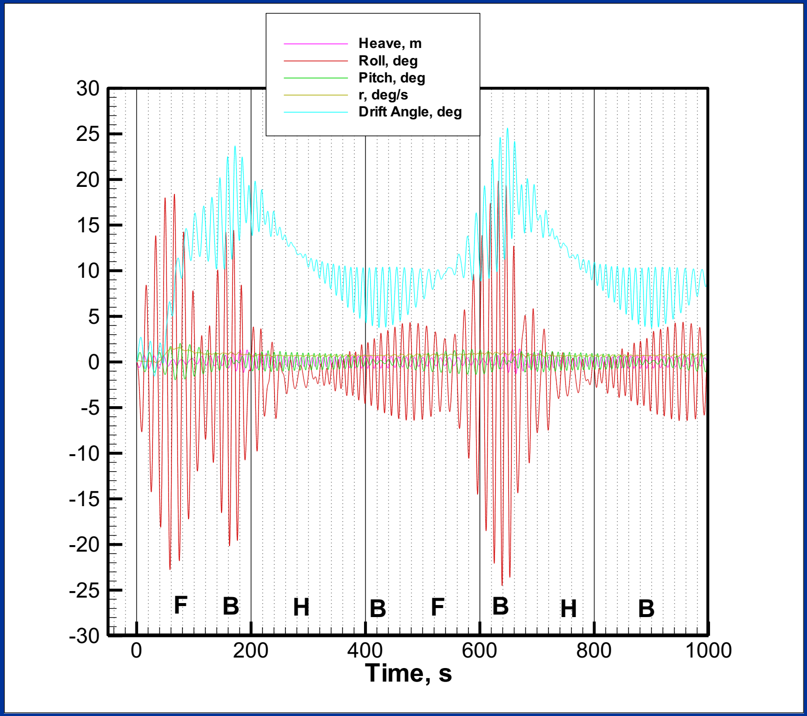

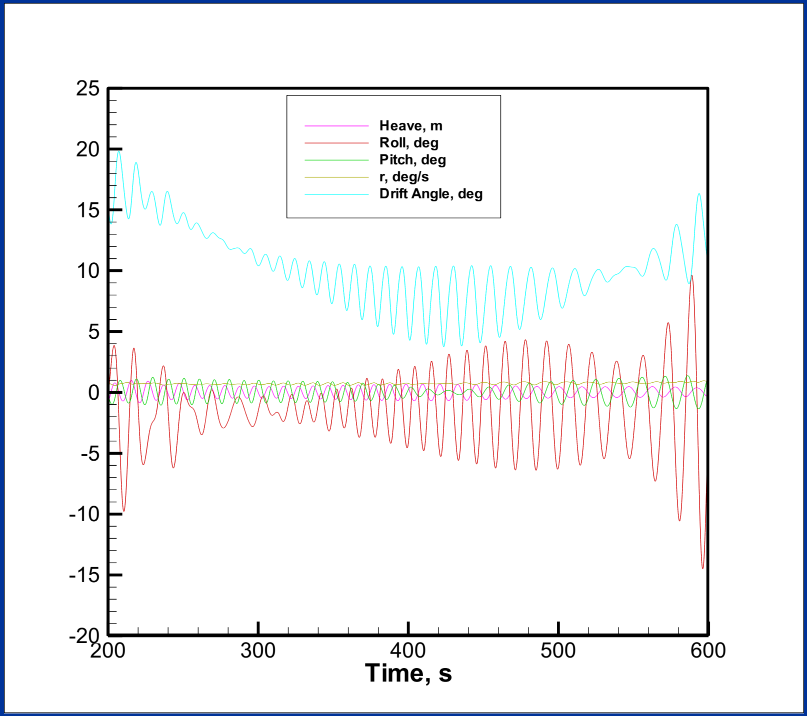

Turning Manoeuvre: Sway Force Histories in Wave 220m/3m/45deg

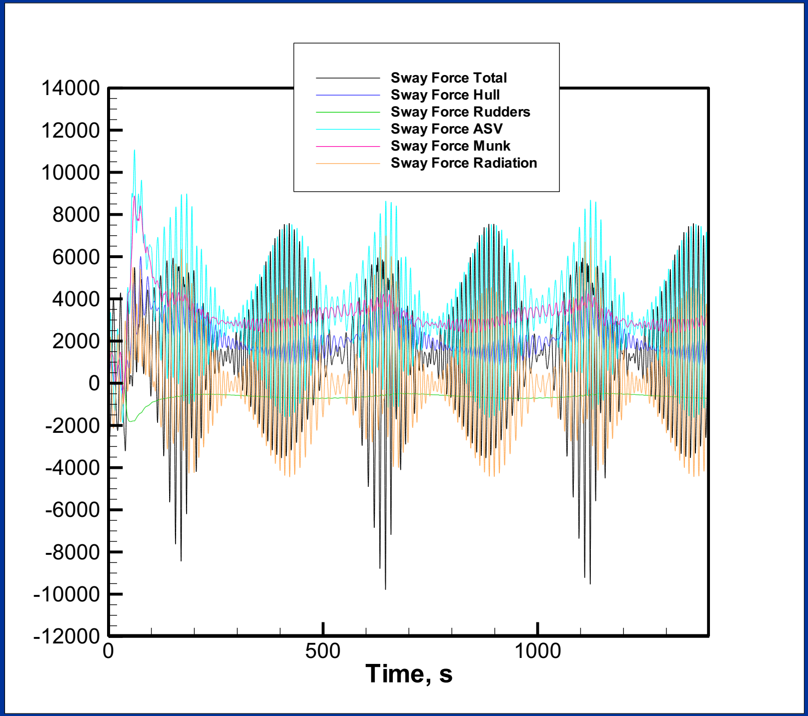

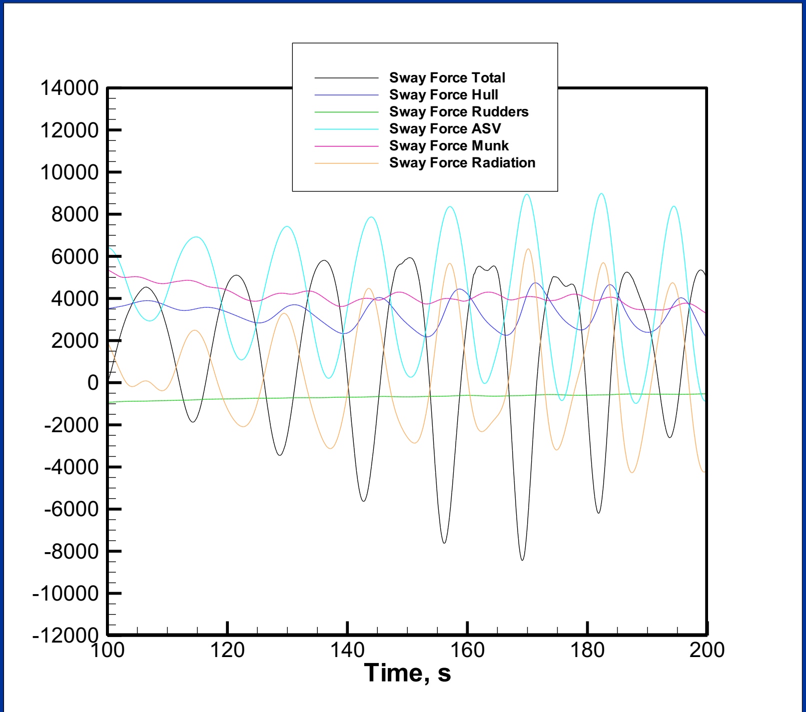

INSTITUTO SUPERIOR TÉCNICO

Zig-Zag 10deg—10deg

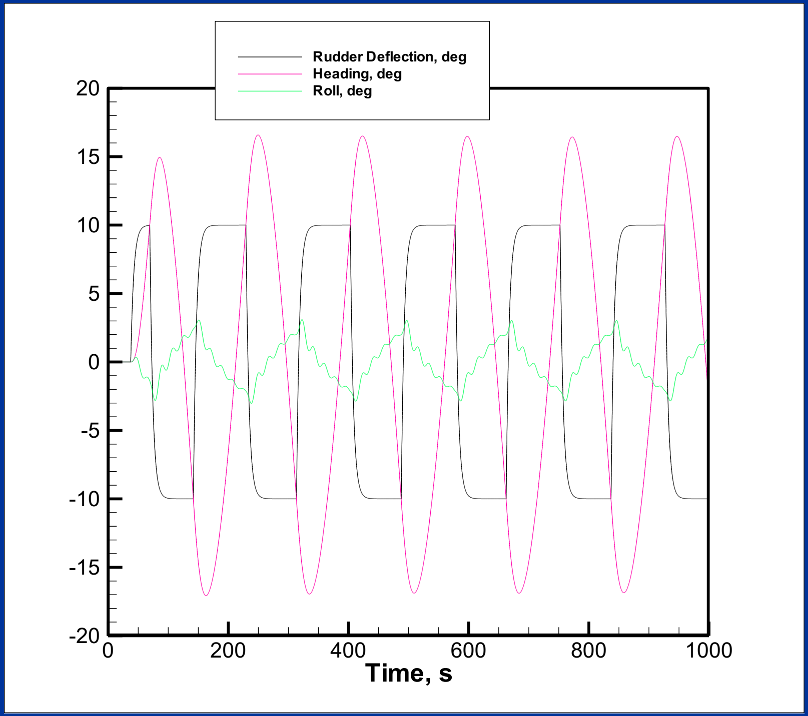

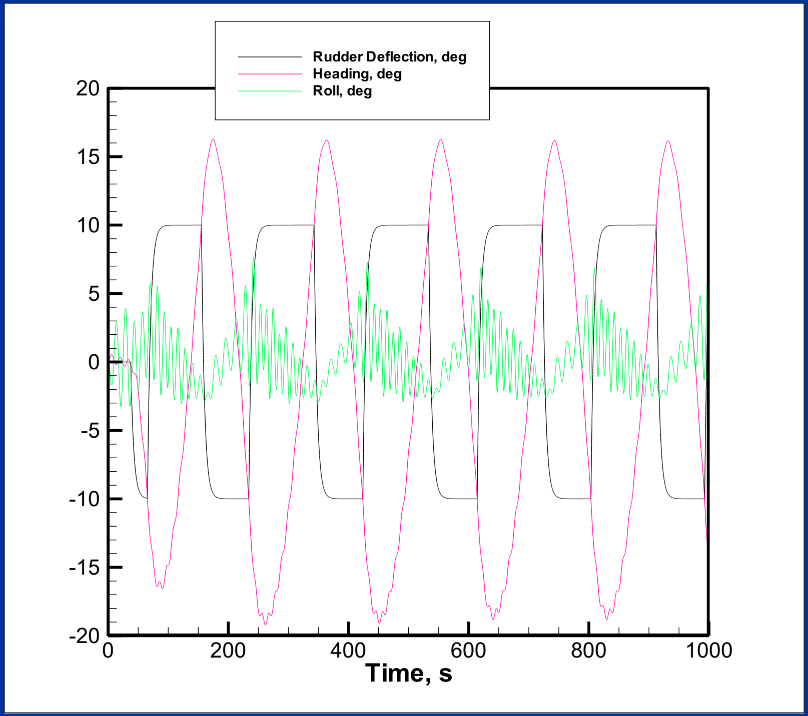

Zig-Zag 5deg—5deg

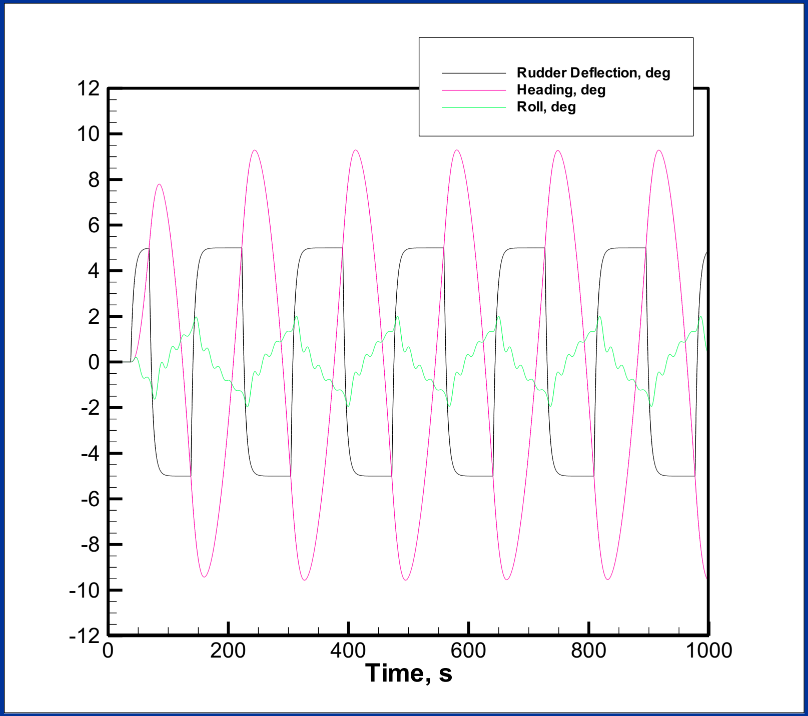

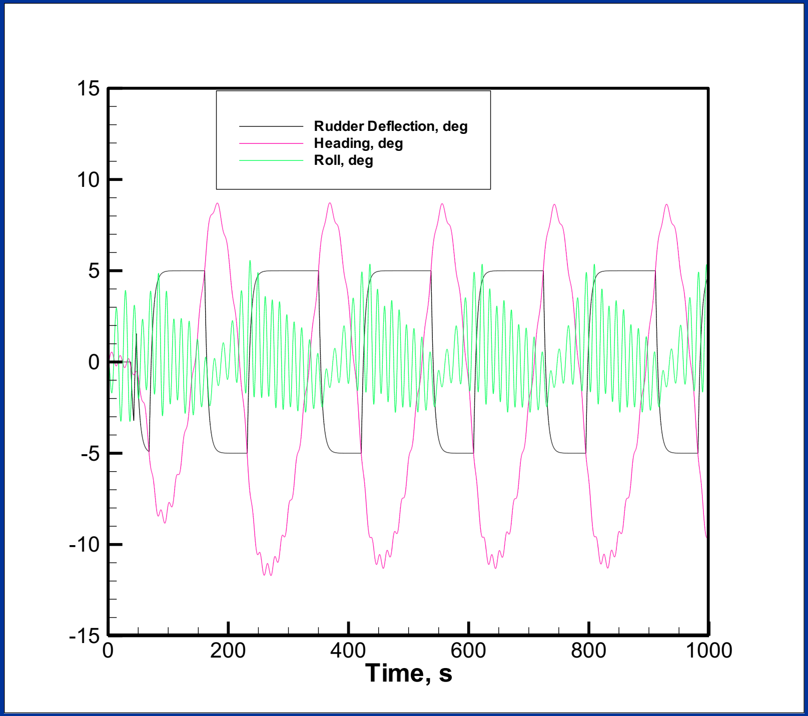

Zig-Zag 5dg—5dg in 220m waves and Resonance Roll Straight Run

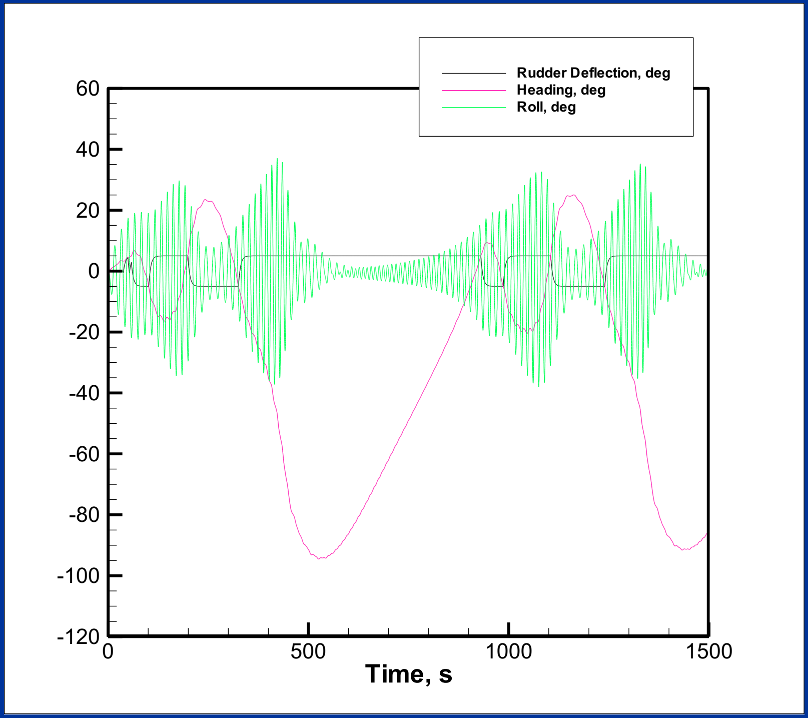

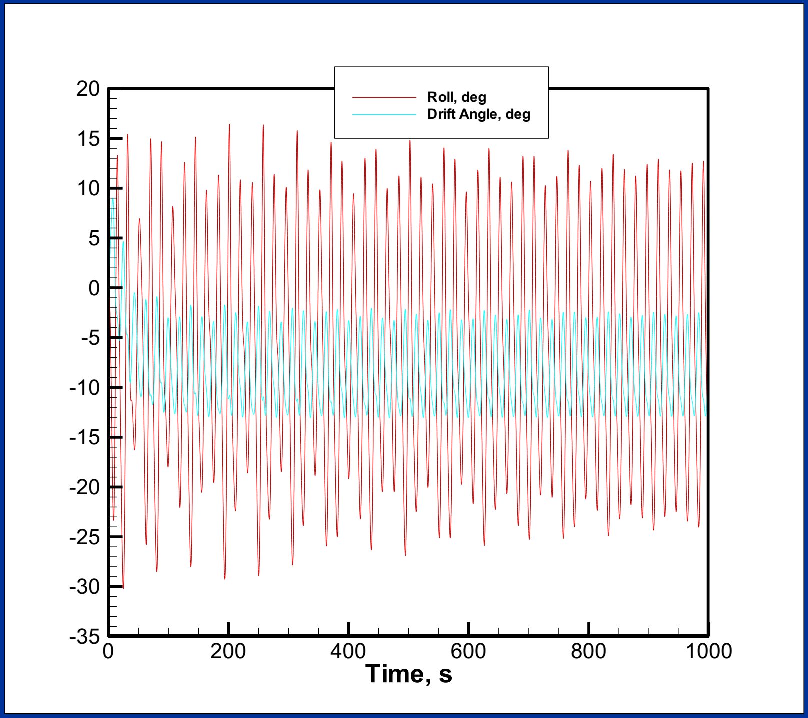

Required Properties of the Model

- Must give reasonable results for arbitrary ship motion in regular waves remaining valid at any instantaneous encounter frequency
- Must reduce to a common (namely, Salvesen—Tuck--Faltinsen) linear seakeeping model in constant-speed straight run
- Must allow accounting for the wetted hull’s deformation due to quasi-steady heel
- Must reduce to the usual Munk model for linear force/moment components in absence of waves

Additional Remarks

- Speed requirements exclude 3D models, hence the strip method
- Zero-frequency limit corresponds to still water manoeuvring---can be subtracted and substituted with any experiment-based still-water manoeuvring model
- This study focuses on inertial and damping hydrodynamic forces on a slender hull

Frames of Reference

- $O_0\xi_0\eta_0\zeta_0$ ---Earth-fixed frame;
- $Cxyz$ ---body-fixed frame;
- $O\xi\eta\zeta$ ---body-semi-fixed frame: as previous but not involved into heave, pitch and roll;
- $O_1\xi_1\eta_1\zeta_1$ ---"generalized seakeeping" frame: as previous but also not involved into waves-induced sway and yaw. Is quasi-inertial.

Motion Decomposition

- 0-motion---manoeuvring motion “as it were in still water”;
- 1-motion---additional motion caused by waves;

- **Some examples of 0-motion:**

1. Straight run---classic seakeeping formulation;
2. Steady turn
3. Spiral as continuous sequence of steady turns

General Boundary-Value Problem Formulation

- Laplace equation $\Delta\phi(\xi_0, \eta_0, \zeta_0, t) = 0, \quad \forall t > 0$
- Hull boundary condition

$$\left.\frac{\partial \phi}{\partial n}\right|_{S(t)} = [\mathbf{V}_C(t) + \mathbf{\Omega}(t) \times \mathbf{r}(t)] \cdot \mathbf{n}(t) \quad \forall t,$$

- Free-surface linearized boundary condition

$$\left.\frac{\partial^2 \phi}{\partial t^2} - g\frac{\partial \phi}{\partial \zeta_0}\right|_{\zeta_0 = 0} = 0$$

- +boundary conditions at infinity and initial conditions (Guo 1981)

Potential's Decomposition

- Oncoming waves $$\phi_w = \mathrm{Re}\left[\frac{iga_w}{\omega} e^{-k\zeta_0 - i(k_1\xi_0 + k_2\eta_0)} e^{i\omega t} \right],$$

- Natural decomposition $$\phi = \phi_0 + \phi_{skp} = \phi_0 + \phi_1 + \phi_w + \phi_d\,,$$
- Body boundary condition

$$\frac{\partial}{\partial n}(\phi_0 + \phi_1 + \phi_d)(P) = \mathbf{V}(P,t)\cdot \mathbf{n}(P) - \frac{\partial \phi_w}{\partial n}(P), \quad P \in S(t),$$

where

$$\mathbf{V}(P,t) = \mathbf{V}_0(P,t) + \mathbf{V}_1(P,t) = \mathbf{V}_{C0}(t) + \mathbf{\Omega}_0(t)\times \mathbf{r}(P) + \mathbf{V}_{C1}(t) + \mathbf{\Omega}_1(t)\times \mathbf{r}(P).$$

Hence

$$\frac{\partial \phi_0}{\partial n} = \mathbf{V}_0 \cdot \mathbf{n}, \quad \frac{\partial \phi_1}{\partial n} = \mathbf{V}_1 \cdot \mathbf{n}, \quad \frac{\partial \phi_d}{\partial n} = -\frac{\partial \phi_w}{\partial n}.$$

Pressure

- Bernoulli's integral in $O\xi\eta\zeta$

$$\frac{p}{\rho}+\frac{1}{2}(\nabla\phi)^2-g\zeta+\frac{\partial\phi}{\partial t}-\mathbf{V}\cdot\nabla\phi=C(t),$$

- Dynamic pressure

$$p=-\rho\frac{\partial\phi_0}{\partial t}-\frac{\rho}{2}(\nabla\phi_0)^2+\rho\mathbf{V}\cdot\nabla\phi_0$$
$$-\rho\frac{\partial\phi_{skp}}{\partial t}-\frac{\rho}{2}(\nabla\phi_{skp})^2+\rho\nabla\phi_0\cdot\nabla\phi_{skp}+\rho\mathbf{V}\cdot\nabla\phi_{skp}.$$

- Its decomposition:

$$p=p_0+p_{0skp}+p_1+p_2,$$

Pressure Components

- Quasi-steady contribution

$$p_0 = \rho \mathbf{V_0} \cdot \nabla \phi_0 - \tfrac{\rho}{2} (\nabla \phi_0)^2$$

- Steady-unsteady interaction

$$p_{0skp} = \rho \mathbf{V_1} \cdot \nabla \phi_0 - \rho \nabla \phi_{skp} \cdot \nabla \phi_0$$

- First-order seakeeping part

$$p_1 = -\rho \frac{\partial \phi_{skp}}{\partial t} + \rho \mathbf{V_0} \cdot \nabla \phi_{skp}$$

- Second-order seakeeping part

$$p_2 = -\tfrac{\rho}{2} (\nabla \phi_{skp})^2 + \rho \mathbf{V_1} \cdot \nabla \phi_{skp}$$

Hydrodynamic Forces

- General: $\mathbf{F} = -\int_S p\,\mathbf{n}\,\mathrm{d}S; \quad \mathbf{M} = -\int_S p\,\mathbf{r}\times\mathbf{n}\,\mathrm{d}S$
- Decomposed as

$$\mathbf{F}_1 = \mathbf{F}_{10} + \mathbf{F}_{11\xi} + \mathbf{F}_{11\eta},$$

where

$$\mathbf{F}_{10} = \rho\int_S \frac{\partial\phi_{skp}}{\partial t}\mathbf{n}\,\mathrm{d}S, \quad \mathbf{F}_{11\xi} = -\rho\int_S u_0(P)\frac{\partial\phi_{skp}}{\partial\xi}\mathbf{n}\,\mathrm{d}S, \quad \mathbf{F}_{11\eta} = -\rho\int_S v_0(P)\frac{\partial\phi_{skp}}{\partial\eta}\mathbf{n}\,\mathrm{d}S,$$

or

$$X_j(t) = \rho\int_S \frac{\partial\phi_{skp}}{\partial t}n_j\,\mathrm{d}S - \rho u_0\int_S \frac{\partial\phi_{skp}}{\partial t}n_j\,\mathrm{d}S = X_j^r + X_j^w + X_j^d.$$

CENTEC

INSTITUTO SUPERIOR TÉCNICO

Radiation Forces

- Temporary assumtion $S(t) \approx S_0(t) - \text{slowly varying;}$
- Then

$$X_j^r = \rho \int_{S_0} \left(\frac{\partial}{\partial t} - u_0 \frac{\partial}{\partial \xi} \right) \phi_1 n_j \, \mathrm{d}S.$$

- The Fourier transform

$$\mathrm{F}[f(t)] \equiv \hat{f}(\omega) = \int_{-\infty}^{\infty} f(t) \, \mathrm{e}^{-i\omega t} \mathrm{d}t \qquad \mathrm{F}^{-1}[\hat{f}(\omega)] \equiv f(t) = \frac{1}{2\pi} \int_{-\infty}^{\infty} \hat{f}(\omega) \, \mathrm{e}^{i\omega t} \mathrm{d}t$$

yields forces' images---complex amplitudes

$$\hat{X}_j^r(\omega) = i\omega\rho \int_{S_0} \hat{\phi}_1(\omega) n_j \, \mathrm{d}S - \rho u_0 \int_{S_0} \frac{\partial \hat{\phi}_1}{\partial \xi}(\omega) n_j \, \mathrm{d}S,$$

Further Evaluations

- Radiation potential's decomposition: $\hat{\phi}_1 = \hat{\phi}^j \hat{U}_j,$
- Quasi-velocities:

$$\begin{aligned}
\hat{U}_2 &= i\omega\hat{\xi}_2 - u_0\hat{\xi}_6, \\
\hat{U}_3 &= i\omega\hat{\xi}_3 + u_0\hat{\xi}_5, \\
\hat{U}_j &= i\omega\hat{\xi}_j, \quad j = 4,5,6
\end{aligned}$$

- Forces and moments

$$\hat{X}_j^r = \int_L \hat{R}_j(\xi)\,\mathrm{d}\xi, \qquad j = 2,\ldots,4$$

$$\hat{X}_5^r = -\int_L \xi \hat{R}_3(\xi)\,\mathrm{d}\xi, \quad \hat{X}_6^r = \int_L \xi \hat{R}_2(\xi)\,\mathrm{d}\xi,$$

Sectional Loads and Velocities

- Loads at the strip

$$\hat{R}_k(\xi) = -i\omega \sum_{\ell=2}^{4} \hat{\mu}_{k\ell}(\omega,\xi)\hat{u}_\ell(\xi) + u_0 \sum_{\ell=2}^{4} \lambda_{k\ell}(\xi)\,\hat{\mu}'_{k\ell}(\omega,\xi)\,\hat{u}_\ell(\xi) + u_0 \sum_{\ell=2}^{4} \hat{\mu}_{k\ell}(\omega,\xi)\hat{u}'_\ell(\xi), \qquad k = 2,3,4,$$

- Local velocities

$$\hat{u}_2(\xi) = \hat{U}_2 + \xi\hat{U}_6, \quad \hat{u}_3(\xi) = \hat{U}_3 - \xi\hat{U}_5, \quad \hat{u}_4(\xi) = \hat{U}_4.$$

- Load correction factor

$$\lambda_{21} = \begin{cases} 1 & \text{at} \quad \xi \geq \xi_{\mathrm{m}}, \\ 0 & \text{at} \quad \xi < \xi_{\mathrm{m}}; \end{cases} \quad \lambda_{31} = \begin{cases} 1 & \text{at} \quad \xi > \xi_{\mathrm{aft}}, \\ 0 & \text{at} \quad \xi = \xi_{\mathrm{aft}}, \end{cases}$$

Forces in frequency domain

$$\hat{X}_j^r(\omega) = \sum_{k=2}^{6} \hat{A}_{jk}(\omega)\hat{U}_k(\omega), \quad j = 2,3,\ldots,6,$$

- Complex amplitude functions

$$\hat{A}_{jk} = -i\omega\hat{\mu}_{jk} + u_0\hat{\bar{\mu}}_{jk}, \quad k = 2,3,4;$$

$$\hat{A}_{j5} = -i\omega\hat{\mu}_{j5} + u_0\hat{\bar{\mu}}_{j5} - u_0\hat{\mu}_{j3},$$

$$\hat{A}_{j6} = -i\omega\hat{\mu}_{j6} + u_0\hat{\bar{\mu}}_{j6} + u_0\hat{\mu}_{j2},$$

- Complex added masses

$$\hat{\mu}_{jk}(\omega) = \int_L \hat{\mu}_{r1}(\xi,\omega)\, w_{jkr1}(\xi)\,\mathrm{d}\,\xi,$$

$$\hat{\bar{\mu}}_{jk}(\omega) = \int_L \lambda_{r1}(\xi)\,\hat{\mu}'_{r1}(\xi,\omega)\, w_{jkr1}(\xi)\,\mathrm{d}\,\xi,$$

Return to time domain

- Rational approximation of complex added mass

$$\hat{\mu}_{jk}(\omega) = \mu_{jk\infty} + \frac{i\omega F_{jk} + G_{jk}}{(i\omega)^3 + (i\omega)^2 B_{jk} + i\omega C_{jk} + D_{jk}},$$

- Radiation forces in time domain

$$X_j^r = \sum_{k=2}^{6} X_{jk}, \quad X_{jk} = X_{jk}^{11} + X_{jk}^{21} + X_{jk}^{31} + X_{jk}^{12} + X_{jk}^{22} + X_{jk}^{32} - \text{next slide}$$

- Limiting zero-frequency case (Munk's case)

$$X_{0j}(t) = u_0 \left[\sum_{k=2}^{6} \bar{\mu}_{0jk} U_k(t) - \mu_{0j3} U_5(t) + \mu_{0j2} U_6(t) \right],$$

$$j = 2, \ldots, 6$$

Time-domain representation

- Defining ODE

$$X^{11}_{jk}(t) = -\mu_{jk\infty}\dot{U}_k(t), \qquad k = 2,\dots,6$$

$$X^{21}_{jk}(t) = u_0\bar{\mu}_{jk\infty}U_k(t),$$

$$X^{31}_{j5}(t) = -u_0\mu_{j3\infty}U_5(t),$$

$$X^{31}_{j6}(t) = \ u_0\mu_{j2\infty}U_6(t),$$

$$\dddot{X}^{12}_{jk} + B_{jk}\ddot{X}^{12}_{jk} + C_{jk}\dot{X}^{12}_{jk} + D_{jk}X^{12}_{jk} = -F_{jk}\ddot{U}_k - G_{jk}\dot{U}_k,$$

$$\dddot{X}^{22}_{jk} + \bar{B}_{jk}\ddot{X}^{22}_{jk} + \bar{C}_{jk}\dot{X}^{22}_{jk} + \bar{D}_{jk}X^{22}_{jk} = \ u_0(\bar{F}_{jk}\dot{U}_k - \bar{G}_{jk}U_k),$$

$$\dddot{X}^{32}_{j5} + B_{j3}\ddot{X}^{32}_{j5} + C_{j3}\dot{X}^{32}_{j5} + D_{j3}X^{32}_{j5} = -u_0(F_{j3}\dot{U}_5 - G_{j3}U_5),$$

$$\dddot{X}^{32}_{j6} + B_{j2}\ddot{X}^{32}_{j6} + C_{j2}\dot{X}^{32}_{j6} + D_{j2}X^{32}_{j6} = -u_0(F_{j2}\dot{U}_6 - G_{j2}U_6).$$

- Equivalent ODE set in terms of ASV (example)

$$\dot{x}_1 = x_2 - FU(t),$$

$$\dot{x}_2 = x_3 + (BF - G)U(t),$$

$$\dot{x}_3 = -Dx_1 - Cx_2 - Bx_3 + (CF + BG - FB^2)U(t),$$

Numerical Example 1: Turn in Still Water

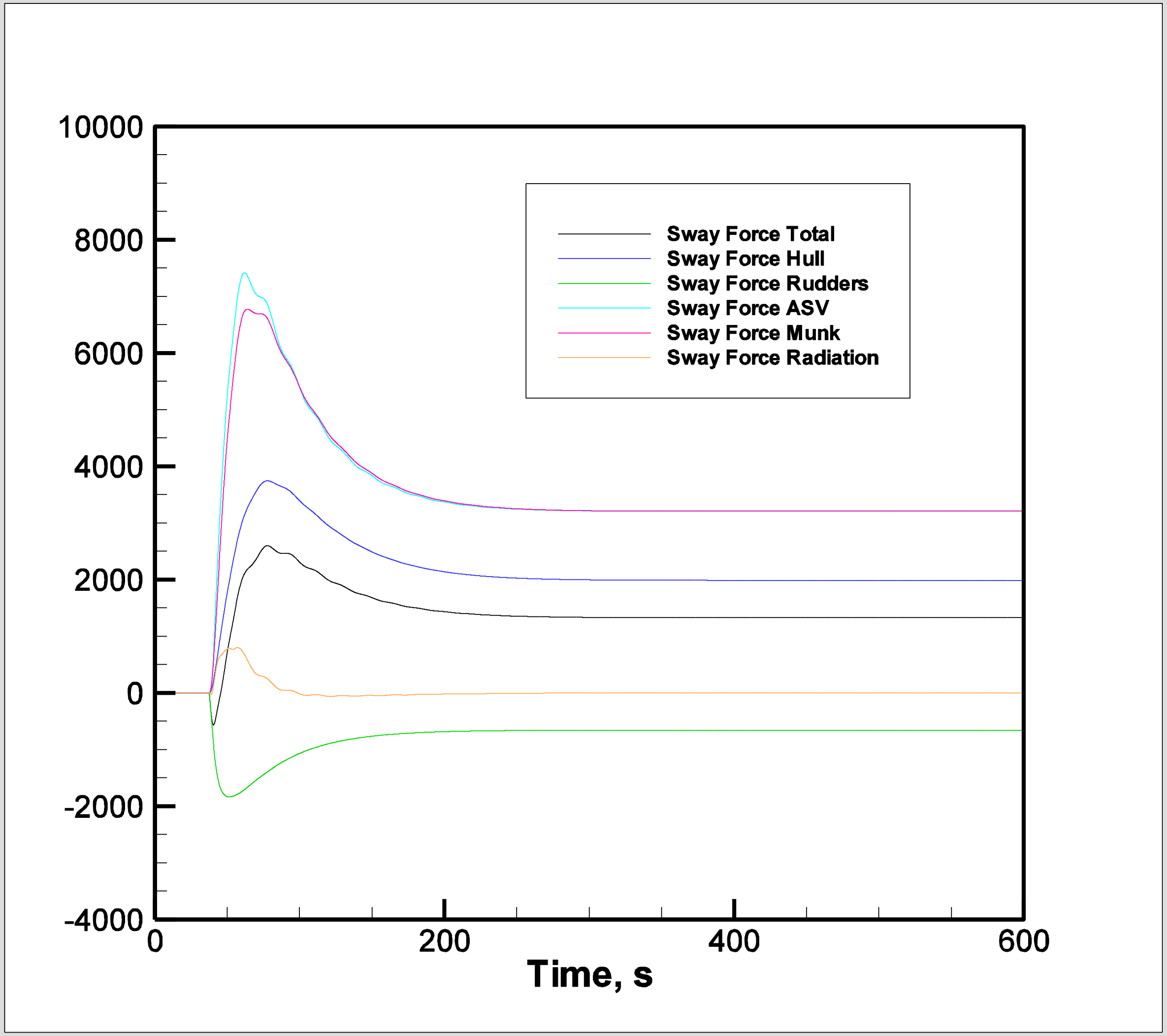

$$X_j^{\text{NET RADIATION}}(t) = X_j^r(t) - X_{0j}(t)$$

$S-175$ Ship

Numerical Example 2: Turn in Regular Waves

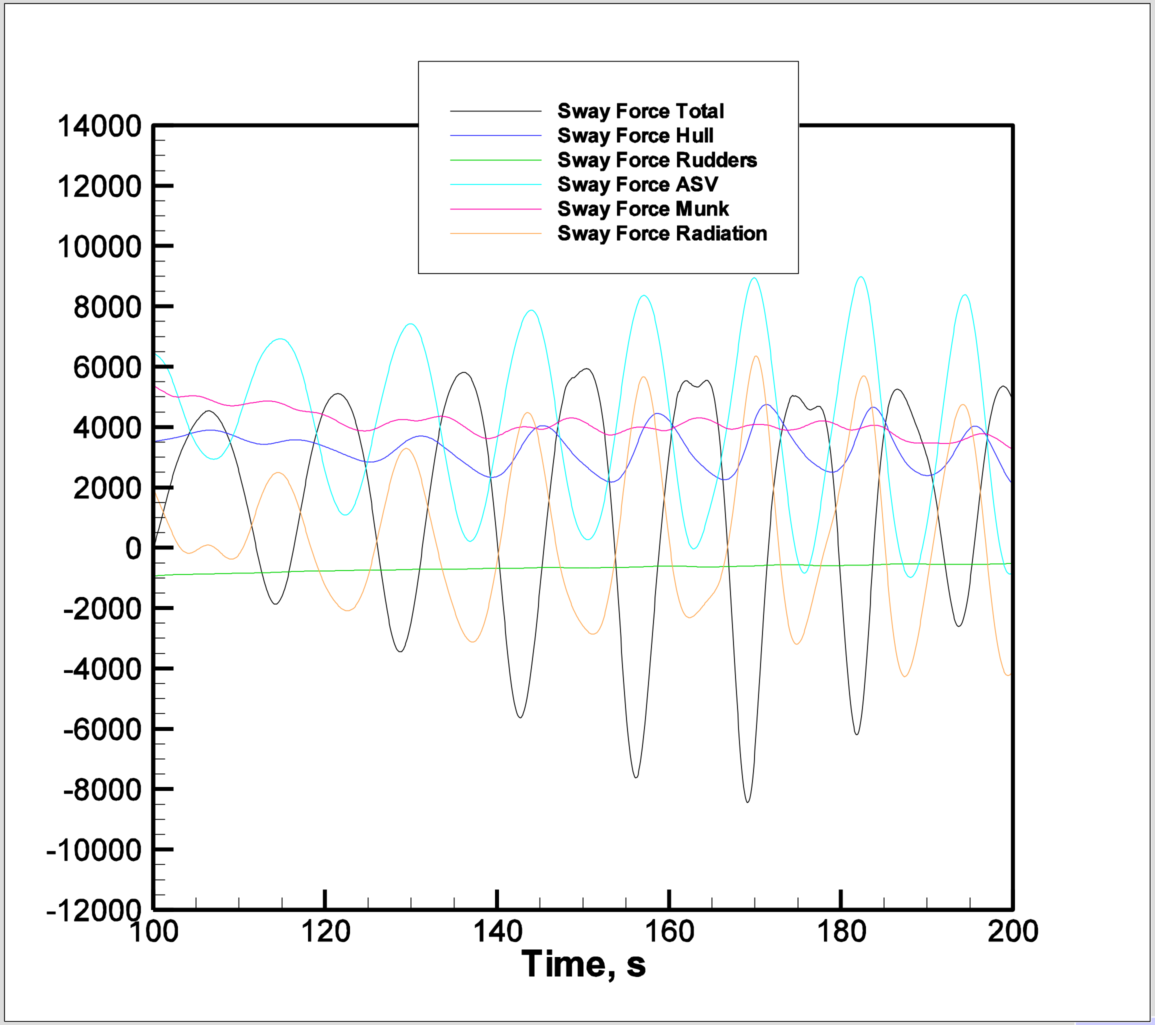

Identification from kinematical measurements

1. No alternative in case of full scale
2. Parametric vs structural (rare)
3. Online (with ~EKF) vs offline (a wide spectrum of methods)
4. Problem of adequacy of the model's structure
5. Identification of simplified manoeuvring models (Nomoto--Norrbin) is close to trivial but the resulting model is rarely consistent
6. Identification of moderately complex model on the basis of high-quality low-noise measurements (e.g. CPMC in tracking mode, Oltmann) is relatively easy
7. Identification of the same model on the basis of typical real-world noisy measurements becomes extremely difficult and is an example of an ill-posed problem

Sutulo S, Guedes Soares C. An Algorithm for Offline Identification of Ship Manoeuvring Mathematical Models from Free-Running Tests, Ocean Engineering, 2014, Vol. 79, pp. 10–25.

Basic formulation

Identification in manoeuvrability:

1. Assume some ship mathematical model (MM) with finite number of parameters
2. Real-world identification: possessing kinematical records obtained in full-scale trials or free-running model tests estimate values of the parameters such that simulated responses match the observed ones
3. Test identification: training responses are computed using the adopted MM, the responses are corrupted in some way; the corrupted responses are used for estimating the parameters; simulated responses are compared with the training ones.

Passing the test identication is conditio sine qua non for recognition of any identification algorithm!

Salient features of the identification method

1. Trajectories are not used for identification
2. Only one training manoeuvre is used: 30—30 zigzag
3. The following 4 kinematic responses are used: velocity of surge, velocity of sway, angular velocity of yaw, actual rudder angle.
4. The objective function is defined as scalarisation of 4 distances in the selected metric
5. The Hausdorff metric is used as the main option
6. A global optimization algorithm is used for minimizing the objective function’s values
7. The identified model can be linear or nonlinear with respect to adjusted parameters

Ship mathematical model -- 1

Equations of motion for 3DOF:

$$\mathbf{M}\dot{\mathbf{x}} = \mathbf{F}\left(\mathbf{x}, \boldsymbol{\theta}, \delta^*\right)$$

where

$$\boldsymbol{\theta} = \left(\kappa_1, \kappa_2, \ldots, \kappa_{19}\right)$$

$$\mathbf{M} = \begin{pmatrix} m+\mu_{11} & 0 & 0 & 0 \\ 0 & m+\mu_{22} & mx_G+\mu_{26} & 0 \\ 0 & mx_G+\mu_{26} & I_{zz}+\mu_{66} & 0 \\ 0 & 0 & 0 & 1 \end{pmatrix}$$

$$\mathbf{x} = \left(u, v, r, \delta_R\right)^T$$

$$\mathbf{F} = \begin{pmatrix} mvr + mx_G r^2 + X_P + X_H\left(V, v', r', \delta_R; \boldsymbol{\theta}\right) \\ -mur + Y_H\left(V, v', r', \delta_R; \boldsymbol{\theta}\right) \\ -mx_G ur + N_H\left(V, v', r', \delta_R; \boldsymbol{\theta}\right) \\ F_\delta\left(\delta_R, \delta^*\right) \end{pmatrix}$$

Ship mathematical model -- 2

Kinematic relations:

$$V = \sqrt{u^2 + v^2} \qquad v' = v/V, \quad r' = rL/V$$

$$\dot{\xi}_C = u\cos\psi - v\sin\psi,$$

$$\dot{\eta}_C = u\sin\psi + v\cos\psi,$$

$$\dot{\psi} = r,$$

Hydrodynamic forces:

$$X_H = X'_H \frac{\rho V^2}{2} LT, \qquad Y_H = Y'_H \frac{\rho V^2}{2} LT,$$

$$N_H = N'_H \frac{\rho V^2}{2} L^2 T,$$

Quasi-steady Hydrodynamic forces (holistic)

$$X'_H = \kappa_1 X'_{uu} u'^2 + \kappa_2 X'_{vr} v' r' + \kappa_3 X'_{\delta\delta} \delta_R^2,$$

$$Y'_q = Y'_0 + \kappa_4 Y'_v v' + \kappa_5 Y'_r r' + \kappa_6 Y'_{vvv} v'^3 + \kappa_7 Y'_{vvr} v'^2 r'$$
$$+ \kappa_8 Y'_\delta \delta_R + \kappa_9 Y'_{vv\delta} v'^2 \delta_R + \kappa_{10} Y'_{v\delta\delta} v' \delta_R^2 + \kappa_{11} Y'_{\delta\delta\delta} \delta_R^3,$$

$$N'_q = N'_0 + \kappa_{12} N'_v v' + \kappa_{13} N'_r r' + \kappa_{14} N'_{vvv} v'^3 + \kappa_{15} N'_{vvr} v'^2 r'$$
$$+ \kappa_{16} N'_\delta \delta_R + \kappa_{17} N'_{vv\delta} v'^2 \delta_R + \kappa_{18} N'_{v\delta\delta} v' \delta_R^2$$
$$+ \kappa_{19} N'_{\delta\delta\delta} \delta_R^3,$$

Identification on artificial data

1. "Clean" training responses $\tilde{u}(t), \tilde{v}(t), \tilde{r}(t), \tilde{\delta}_R(t)$ are obtained from 30—30deg zigzag at $\kappa_1 = \ldots = \kappa_{19} = 1$
2. "Polluted" responses: high-level Gauss white noise added
3. Initial values for adjustment factors are random, uniformly distributed within the hypercube $[0.5, 1.5]^{\times 19}$
4. An optimization algorithm is launched aiming at minimizing

$$\rho_w = w_u \rho\left[u(t), \tilde{u}(t)\right] + w_v \rho\left[v(t), \tilde{v}(t)\right]$$
$$+ w_r \rho\left[r(t), \tilde{r}(t)\right] + w_\delta \rho\left[\delta_R(t), \tilde{\delta}_R(t)\right]$$

5. With the reached quasi-optimal values of κ_i three standard validation manoeuvres are simulated:

   20—20deg zigzag; Dieudonné spiral

   35deg helm turn;

Metrics used

- Euclidean $$\rho_2(y,\tilde{y}) \triangleq \|y-\tilde{y}\|_{\mathbf{L}_2} = \left[\int_0^T \big(y(t)-\tilde{y}(t)\big)^2 \mathrm{d}\,t\right]^{1/2}$$
- Uniform $$\rho_\infty(y,\tilde{y}) \triangleq \|y-\tilde{y}\|_{\mathbf{L}_\infty} = \max_{t\in[0,T]} |y(t)-\tilde{y}(t)|$$
- Hausdorff $$\rho_H\big(\{t, y(t)\},\ \{t, \tilde{y}(t)\}\big)$$ $$\equiv \rho_H(y,\tilde{y}) \triangleq \max\left\{\begin{array}{l} \sup\limits_{t_1\in[0,T]} \inf\limits_{t_2\in[0,T]} r\big(y(t_1),\tilde{y}(t_2)\big), \\ \sup\limits_{t_2\in[0,T]} \inf\limits_{t_1\in[0,T]} r\big(y(t_1),\tilde{y}(t_2)\big) \end{array}\right\}$$

where the submetric:

$$r\big(y(t_1),\tilde{y}(t_2)\big) \triangleq \sqrt{(t_1-t_2)^2 + \big(y(t_1)-\tilde{y}(t_2)\big)^2}$$

or

$$r\big(y(t_1),\ \tilde{y}(t_2)\big) \triangleq \max\left\{\tfrac{1}{\alpha}|t_1-t_2|, |y(t_1)-\tilde{y}(t_2)|\right\},$$

Hausdorff metric: learning steps

First acquaintance: occasionally (!) hit upon the book written for schoolchildren Skvortsov, V.A., *Examples of Metric Spaces,* Moscow Centre for Continuous Mathematical Education, Moscow 2002 (in Russian)

Some additional information mainly from Wikipedia

After 2014 read the monograph Sendov B. *Hausdorff approximations,* Kluwer Academic Publishers, Dordrecht, 1990 (de facto used the original Bulgarian edition in Russian published in Sofia in 1986)

Optimization algorithms used

1. Direct quasi-random search with Sobol sequences mainly with 10,000 shots (QR)

2. Binary genetic algorithm (GA) with 100 individuals in the population, crossover rate 0.6, mutation rate 0.003, maximum number of generations 5000, non-improvement base 2000, two selection schemes: deterministic (d) and tournament (t). Its enhanced version (+): 300—06—0.001—15,000--5000

3. ABC algorithm with 100 sources, 30 source improvement attempts, 3,000 iterations

Numerical results: training records

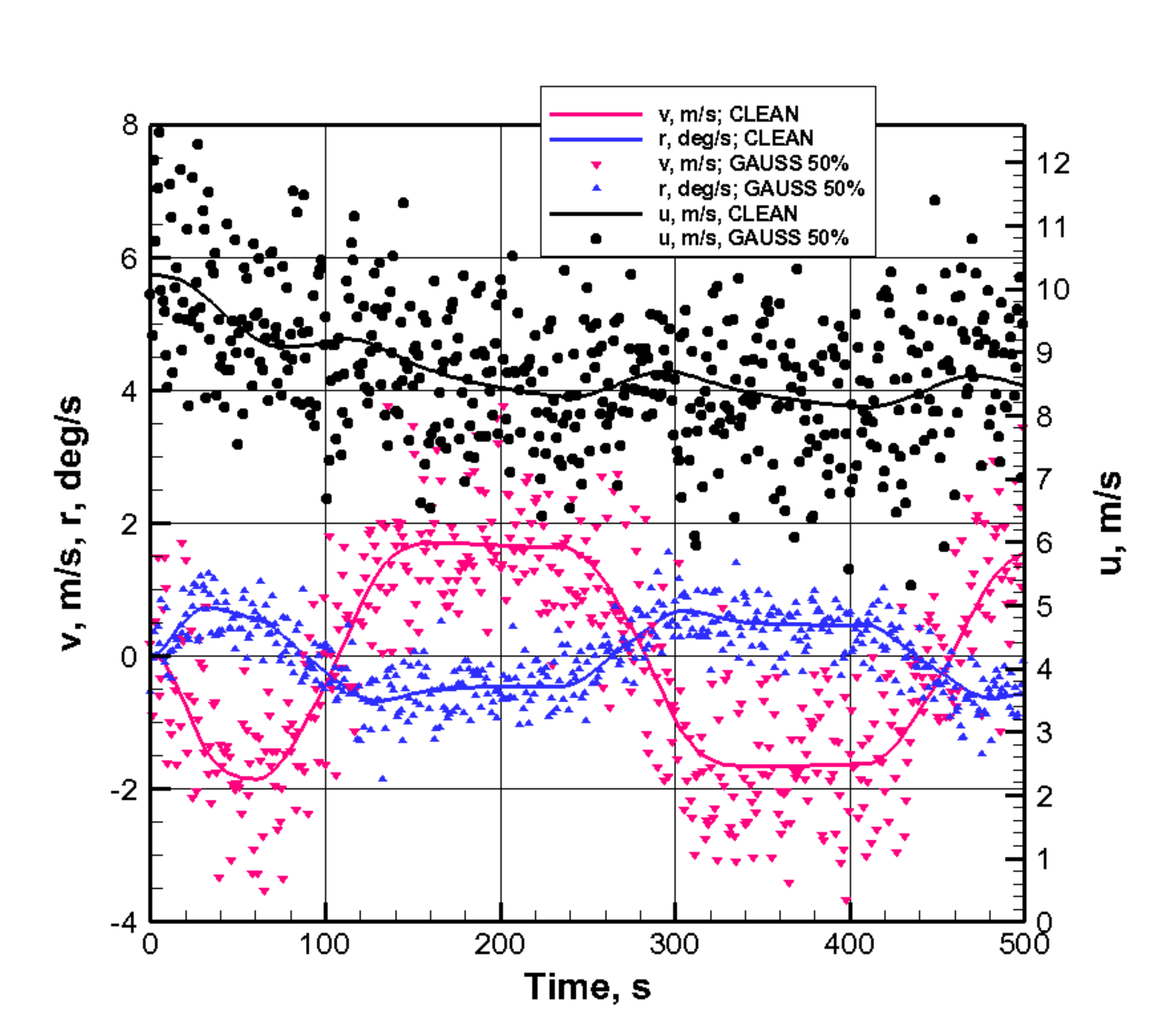

Manoeuvres and responses

Training: a zigzag

"Observed" (used) state variables:

$$u(t), v(t), r(t), \delta_R(t)$$

Validating:

1. 35deg turn
2. Spiral

All responses

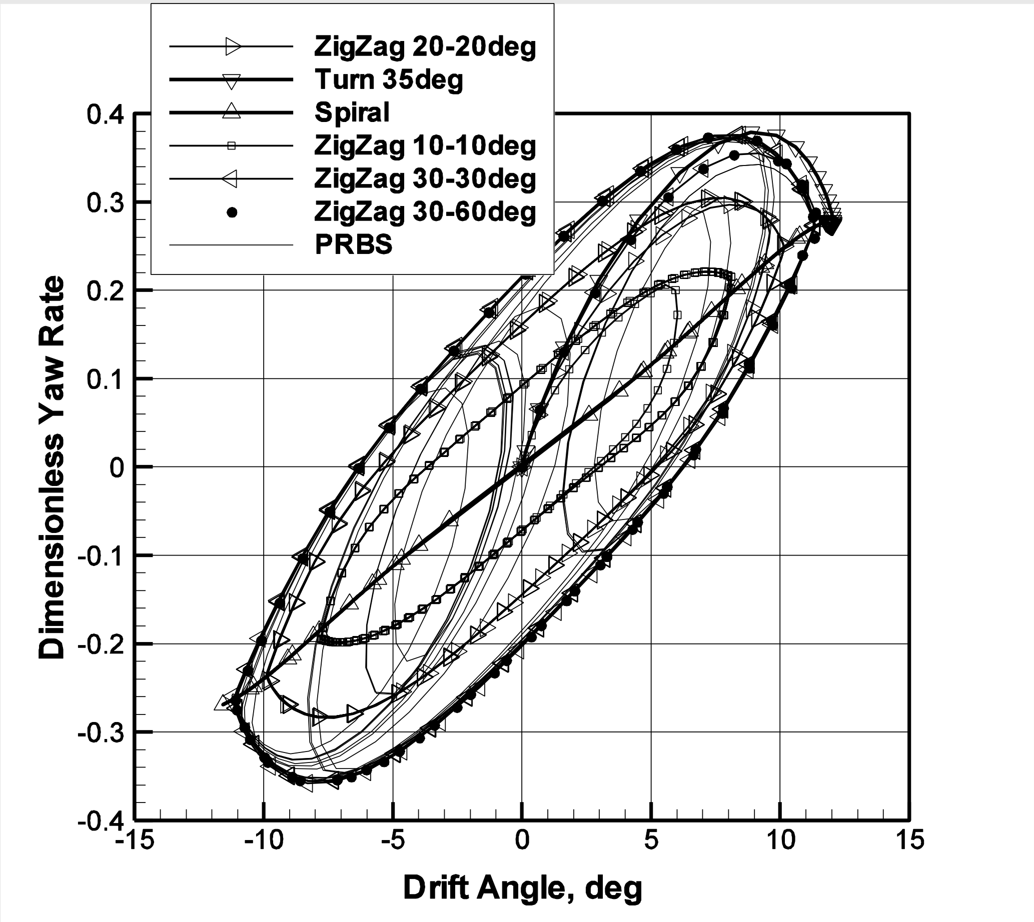

$$U_1 \leftrightarrow 20^\circ - 20^\circ \quad \text{or} \quad 30^\circ - 30^\circ \text{ zigzag}$$

$$U_2 \leftrightarrow \text{Dieudonne' spiral and turning}$$

Numerical results: 20—20 zigzag, QR

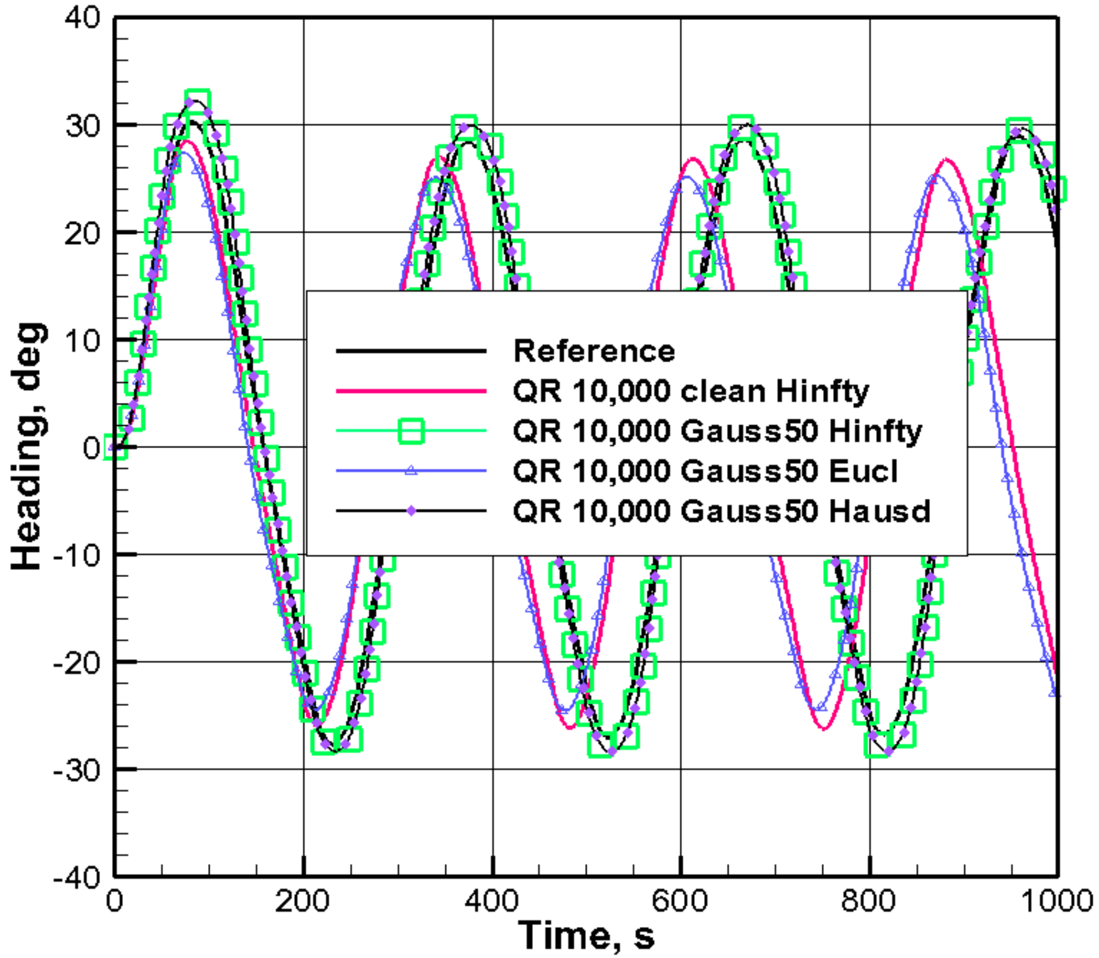

Numerical results: 20-20 zigzag, GA and ABC

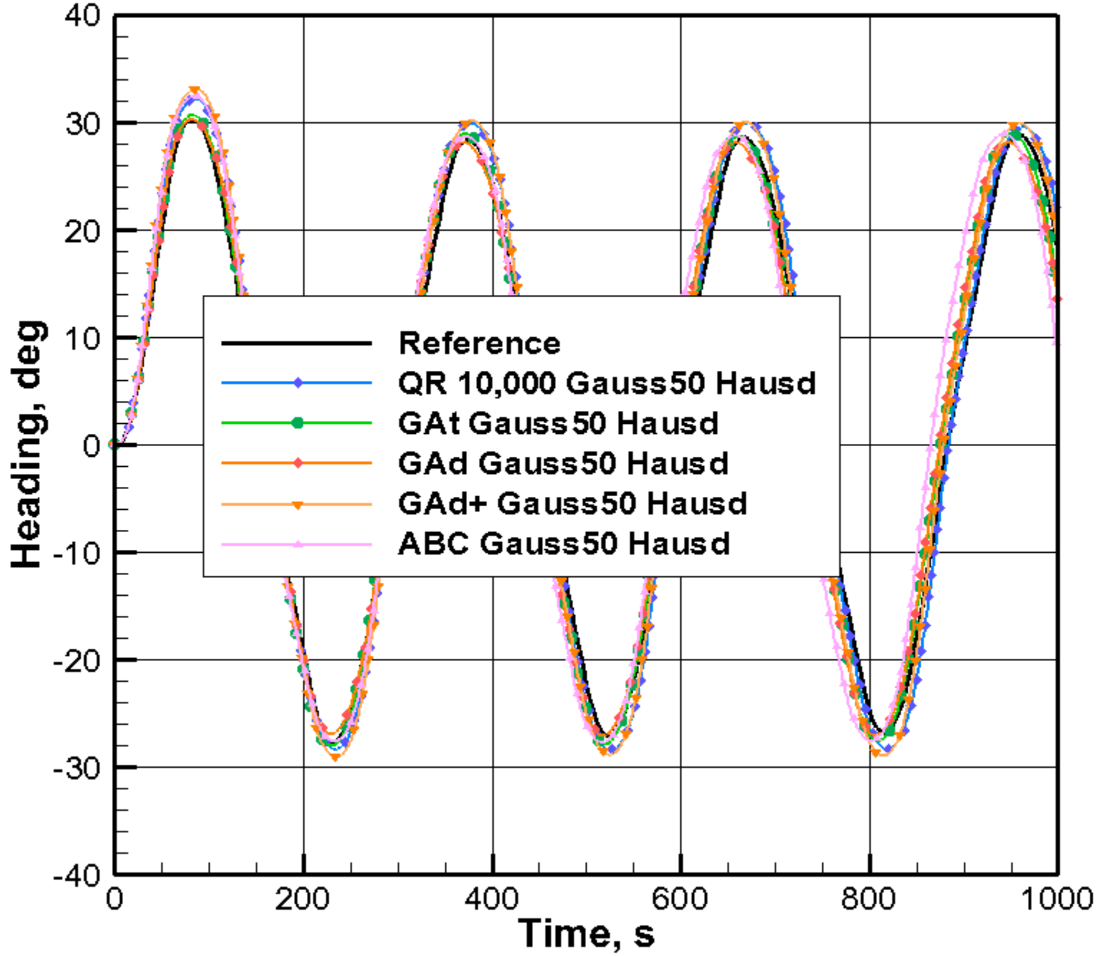

Numerical results: 20-20 zigzag, GA and ABC

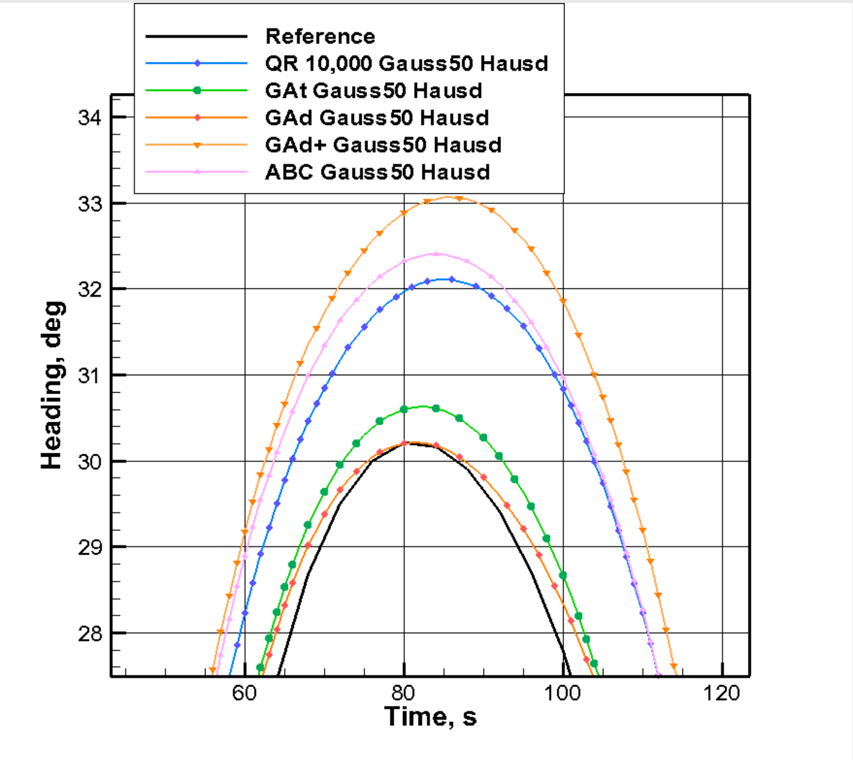

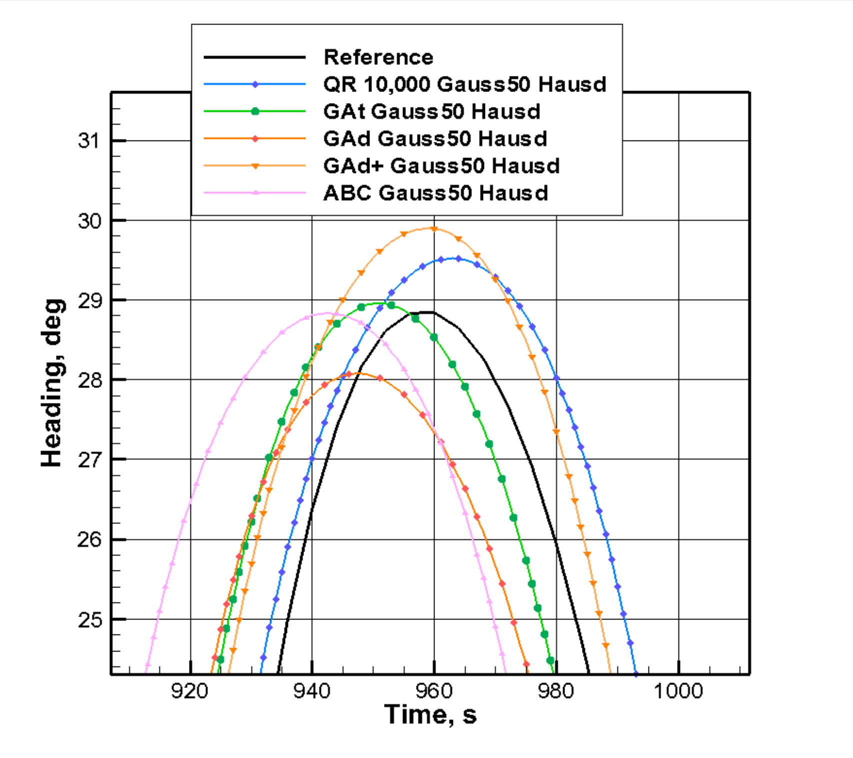

Numerical results: 35deg turn, yaw rate

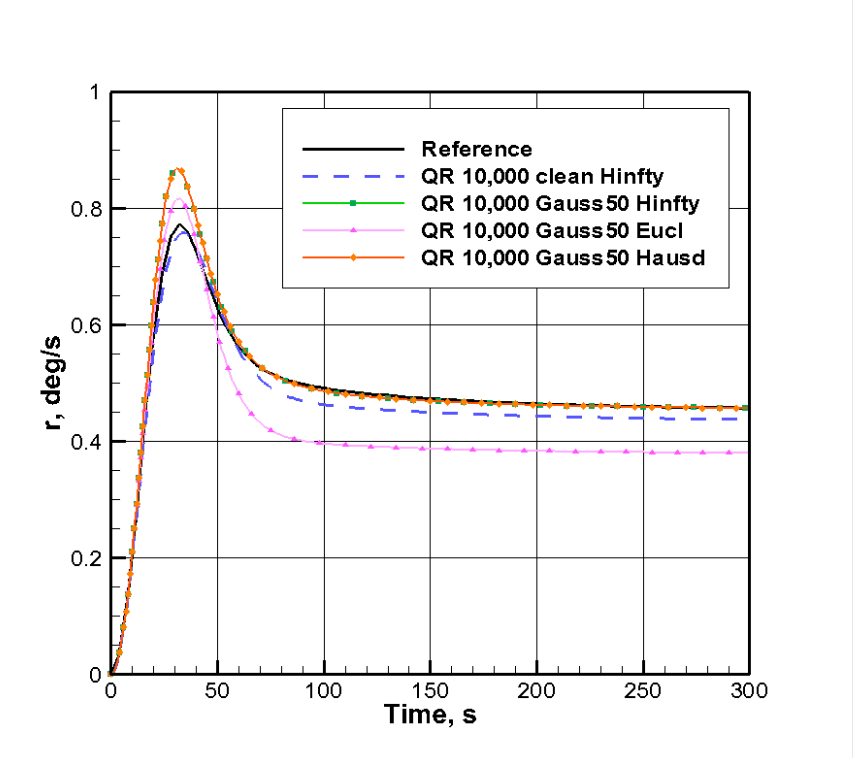

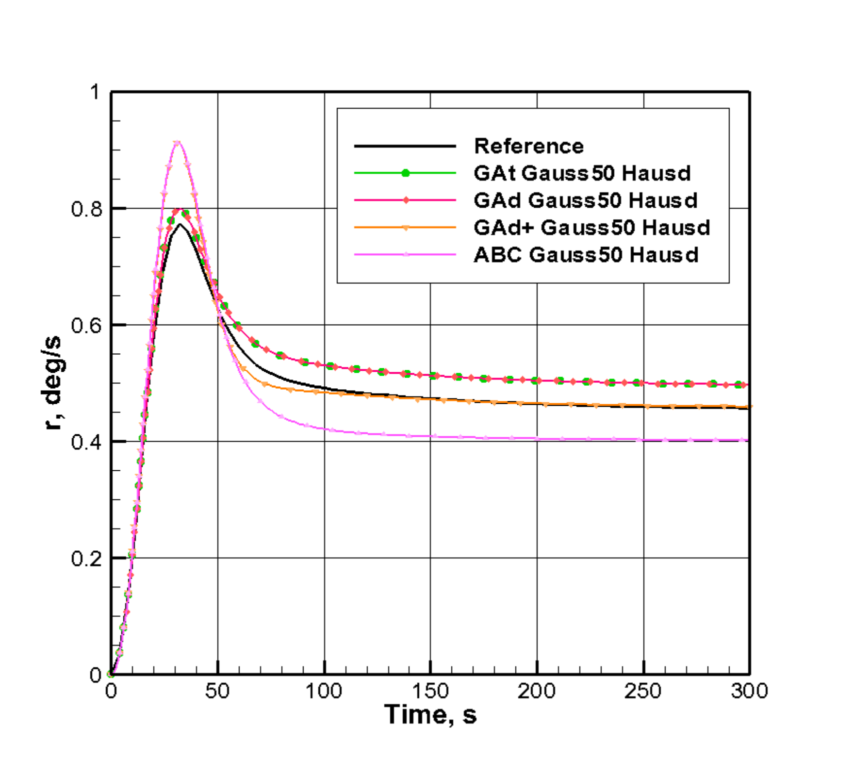

Numerical results: 35deg turn, drift angle

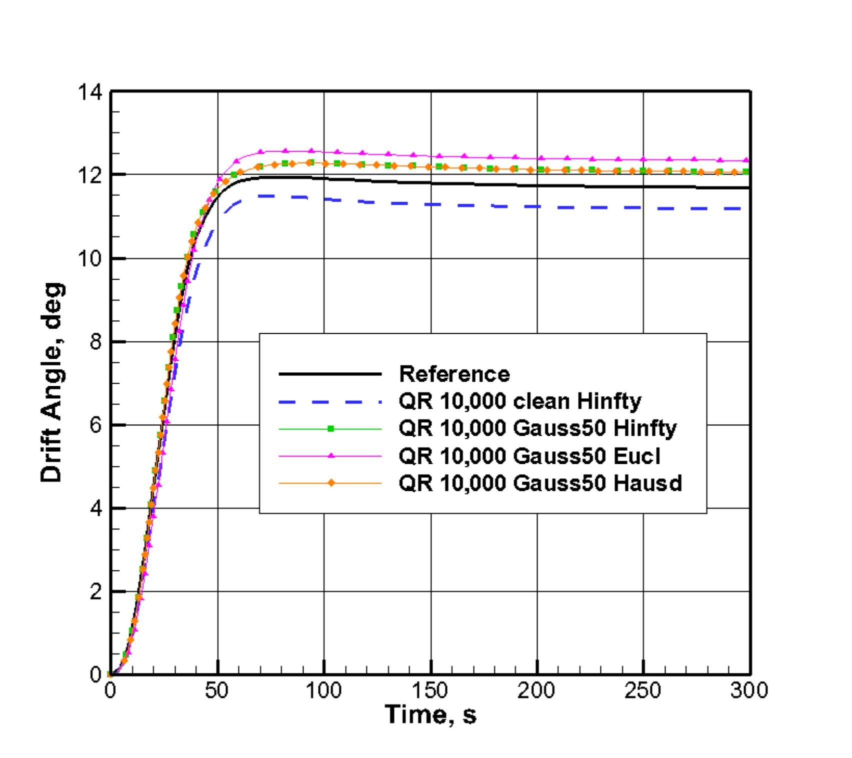

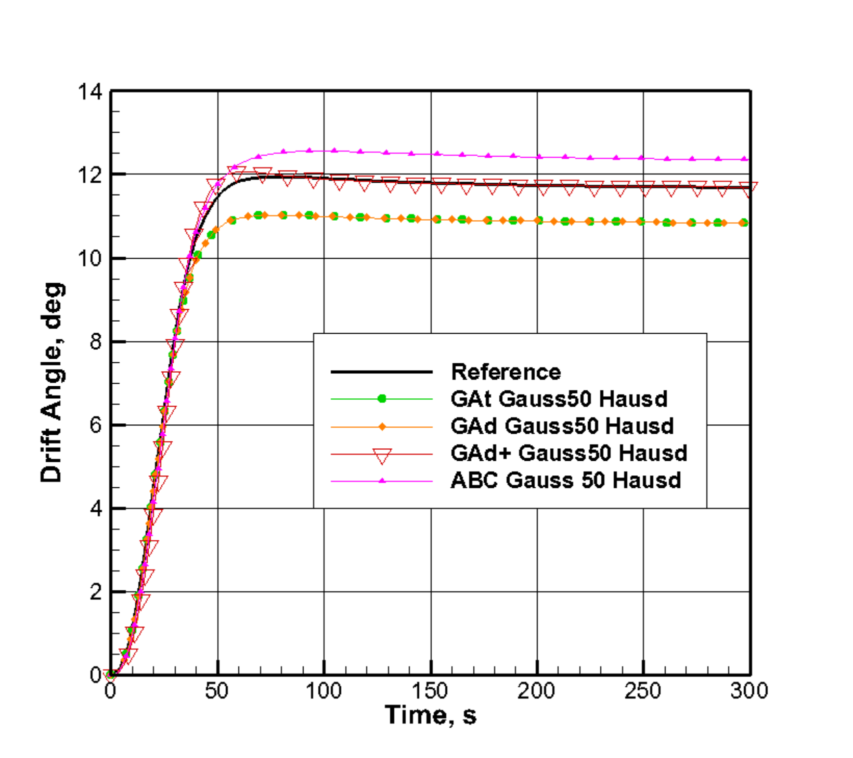

Numerical results: 35deg turn, speed

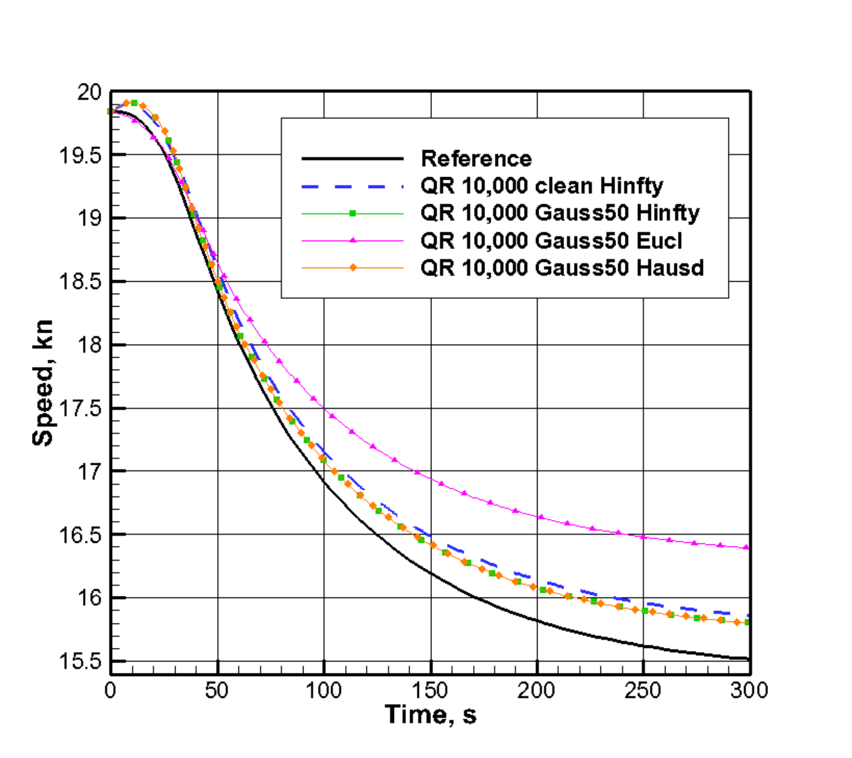

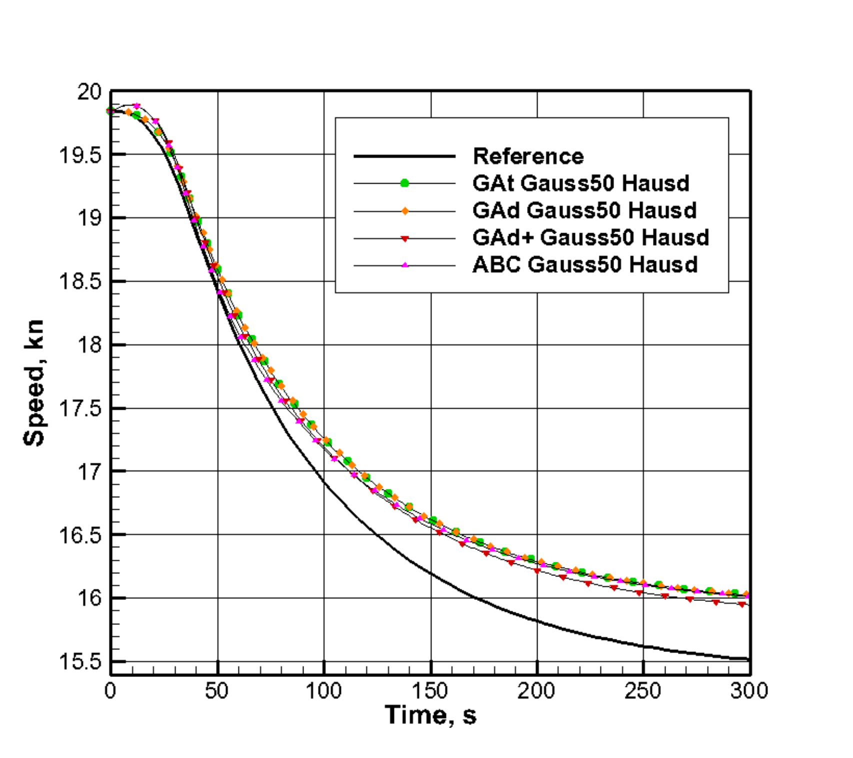

Numerical results: spiral curves

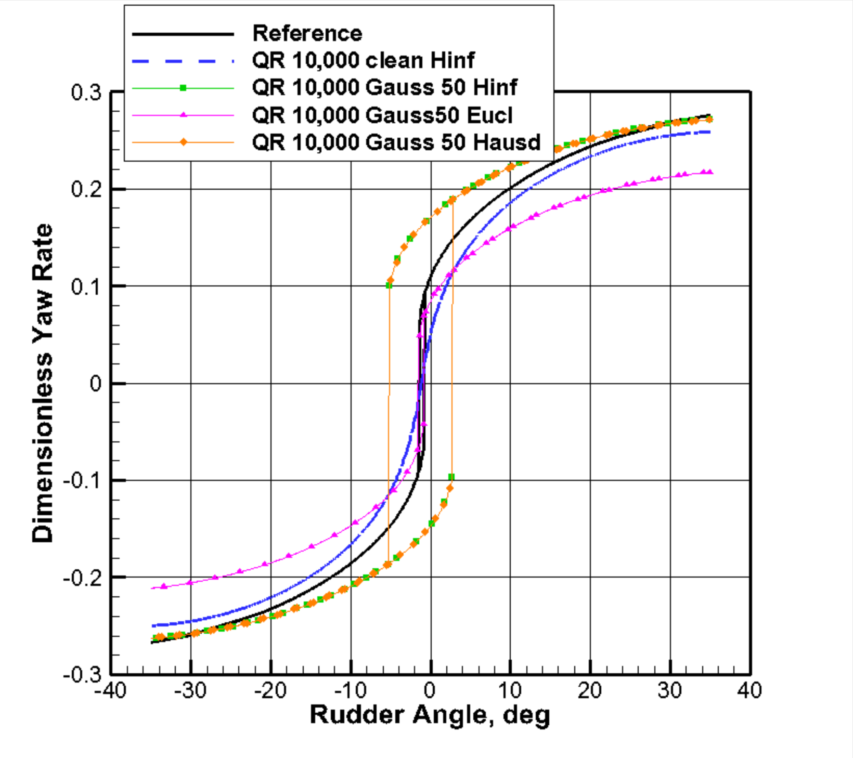

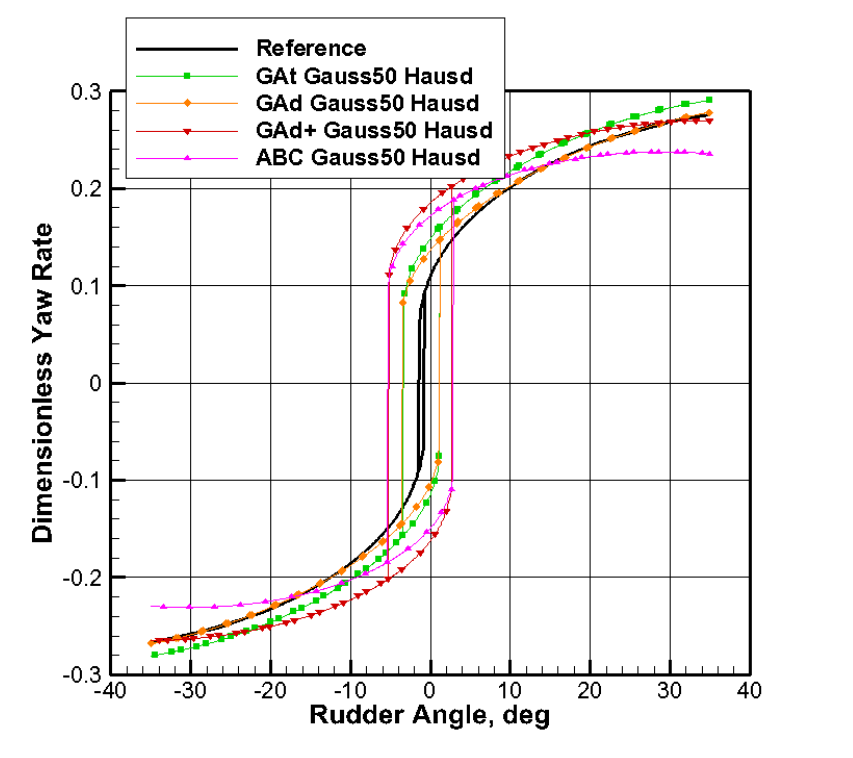

Numerical results: spiral curves---drift angle

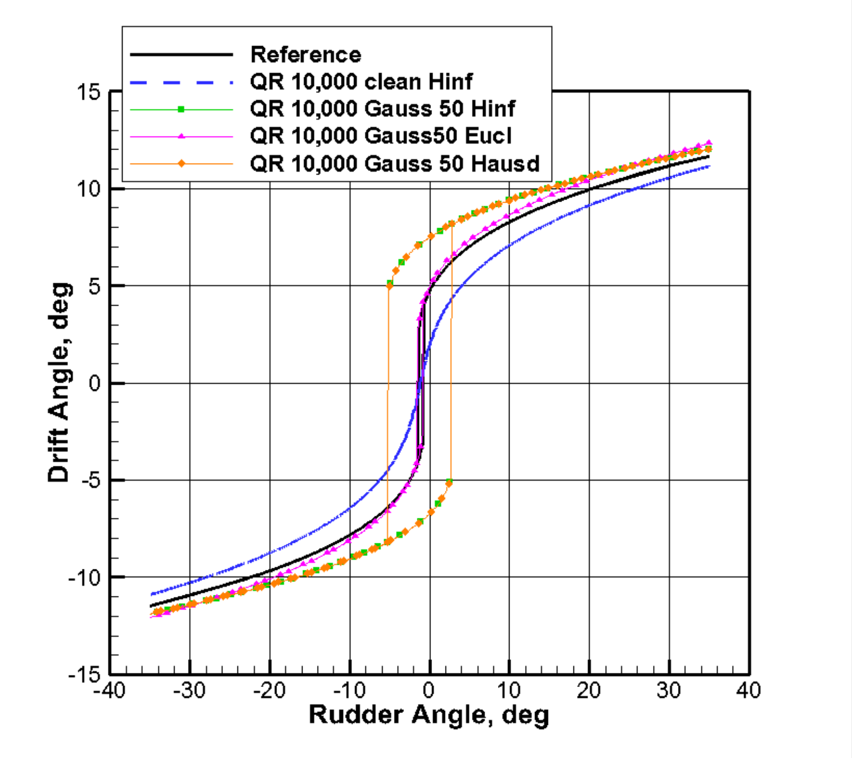

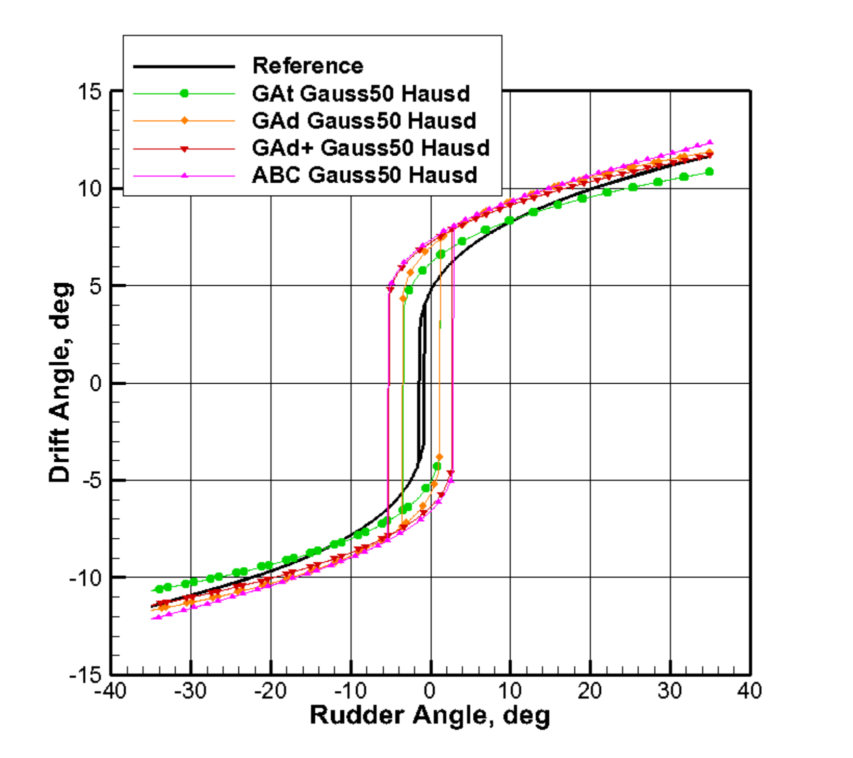

Conclusions

1. **Inferiority of the quasi-random search confirmed**
2. **A somewhat poorer performance of the ABC algorithm confirmed**
3. **The Dieudonné spiral should be considered as a critical validation manoeuvre**
4. **The algorithm is not fast and its detailed exploration and meta-optimization are different**
5. **Superiority of the Hausdorff metric confirmed**
6. **Inferiority of the Euclidean metric confirmed**
7. **The method can be assessed as sufficiently robust and reliable**

Linearisation: Motivation

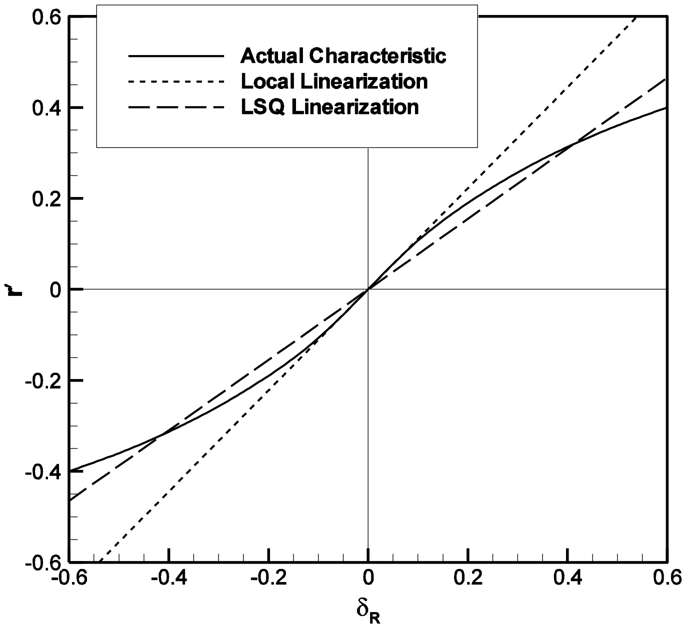

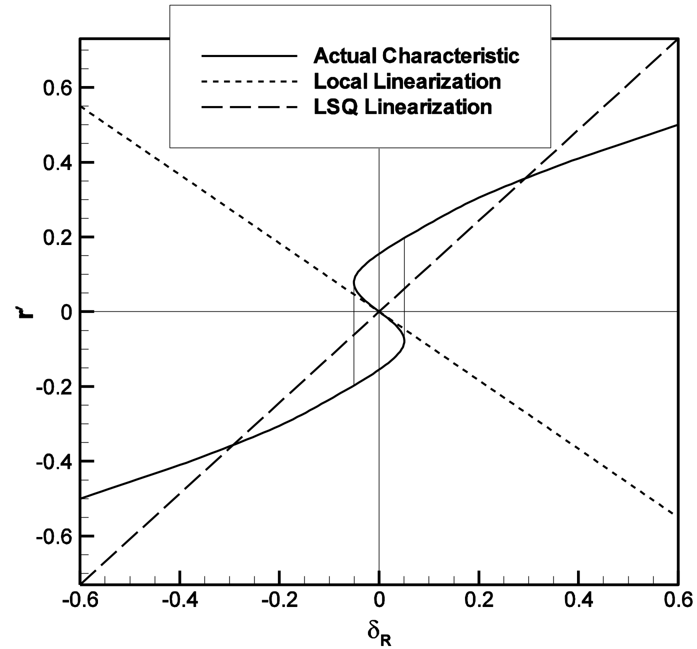

- Bang-Bang Time-Optimal Control Synthesis:

  Linear models may result in a closed-form description of the switching surface

Linearisation: Problem Statement

- Primary nonlinear partial ship model

$$M\dot{x} = G(x) \qquad (n \text{ states})$$

- Linearized partial model

$$M\dot{x} = Lx \quad \text{or} \quad \dot{x} = Ax, \quad A = M^{-1}L$$

- LSQ fit: $$\int_{\mathrm{D}} [G(x) - Lx]^2 \, \mathrm{d}\, x = \min$$

Linearisation: Discretized Least-Square Approximation--1

- Discrete set $\quad \mathrm{D} = \{x^{(1)}, \ldots, x^{(N)}\} \subset \mathrm{D}, \quad N \geq n$
- Responses of nonlinear model

$$G(x^{(i)}) = y^{(i)} = (y_1^{(i)}, \ldots, y_m^{(i)})^T, \; i = 1, \ldots, N$$

- Response and design matrices:

$$Y = \begin{pmatrix} y_1^{(1)} & \cdots & y_m^{(1)} \\ \vdots & \ddots & \vdots \\ y_1^{(N)} & \cdots & y_m^{(N)} \end{pmatrix}, \quad X = \begin{pmatrix} x_1^{(1)} & \cdots & x_n^{(1)} \\ \vdots & \ddots & \vdots \\ x_1^{(N)} & \cdots & x_n^{(N)} \end{pmatrix}$$

INSTITUTO SUPERIOR TÉCNICO

Discretized Least-Square Approximation--2

- Linear matrix equation

$$Y = XL^T$$

- Its LSQ solution:

$$L = ((X^T X)^{-1} X^T Y)^T$$

Quasi-Random Points Generation: Sobol Sequence

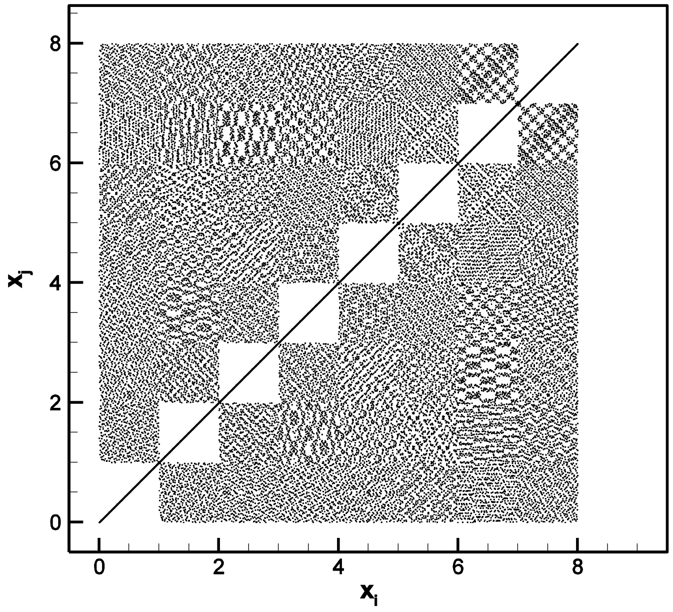

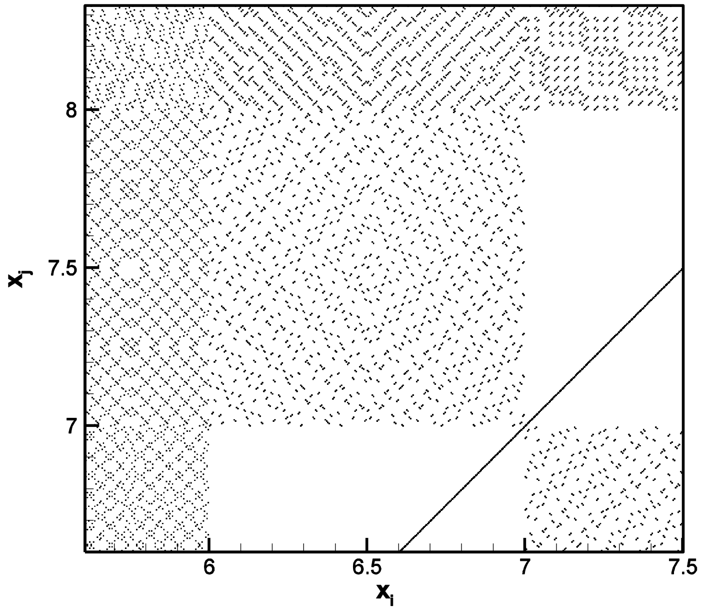

Numerical Example: 3DOF model

Container ship *S-175*:

Length between PP---175m,

Mass---24570t,

Constant speed---16.7kn

Linearization around straight-path motion

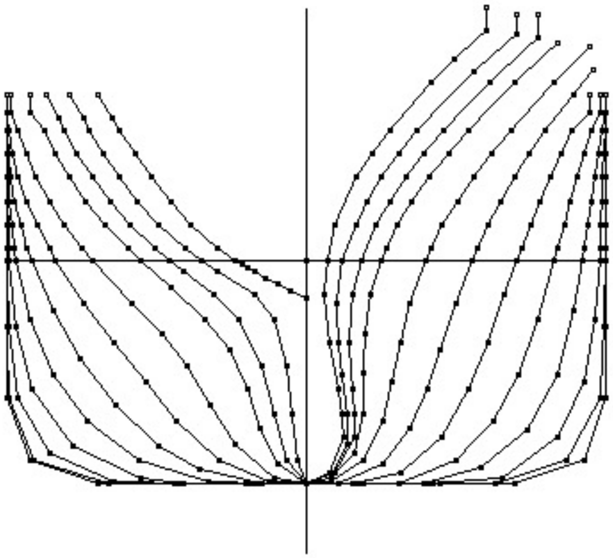

Linerisation: Numerical Example-1

- Submodel to be linearized:

$$
\begin{aligned}
&(m+\mu_{11})\dot{u} - mvr - mx_G r^2 = X_H(u,v,r) + X_P(u,n) + X_R(u,v,r,\delta_R),\\
&(m+\mu_{22})\dot{v} + (mx_G + \mu_{26})\dot{r} + mur = Y_H(u,v,r) + Y_R(u,v,r,\delta_R),\\
&(mx_G + \mu_{26})\dot{v} + (I_{zz} + \mu_{66})\dot{r} + mx_G ur = N_H(u,v,r) + N_R(u,v,r,\delta_R),
\end{aligned}
$$

- Linearization domain defined by:

$$u = u_0 \pm \Delta u;\ \ n = n_0 \pm \Delta n;\ \ v = \pm \Delta v;\ \ r = \pm \Delta r;\ \ \delta_R = \pm \Delta \delta_R$$

$$u_0 = 8\mathrm{m/s}; \quad \mathrm{n}_0 = 120\mathrm{rpm}$$

Linearisation: Numerical Example--2

- Linearisation domains' parameters:

Domain	Δu	Δv	Δr	$\Delta\delta$	Δn
Large	2.0m/s	2.4m/s	0.16 deg/s	35deg	0.5rps
Small	2.0m/s	0.024 m/s	0.0016 deg/s	0.5deg	0.5rps

Numerical Example--3

- Dynamics matrix of the linearized model

$$A = \begin{pmatrix} a_X^u & a_X^v & a_X^r & a_X^\delta & a_X^n \\ a_Y^u & a_Y^v & a_Y^r & a_Y^\delta & a_Y^n \\ a_N^u & a_N^v & a_N^r & a_N^\delta & a_N^n \end{pmatrix}$$

- Linearized submodel to analyze:

$$\begin{aligned} \dot{u} &= a_X^u u + a_X^n n, \\ \dot{v} &= a_Y^v v + a_Y^r v + a_Y^v \delta_R, \\ \dot{r} &= a_N^v v + a_N^r v + a_N^v \delta_R \end{aligned}$$

INSTITUTO SUPERIOR TÉCNICO

Numerical Example--4

- The same submodel, Laplace-transformed:

$$\begin{aligned}
(p - a_X^u)U(p) &= a_X^n N(p), \\
(p - a_Y^v)V(p) - a_Y^r R(p) &= a_Y^\delta \Delta(p), \\
-a_N^v V(p) + (p - a_N^r)R(p) &= a_N^\delta \Delta(p)
\end{aligned}$$

- Eigenvalues:

$$p_L = a_X^u < 0; \quad p_{1,2} = \tfrac{1}{2}(B \pm \sqrt{B^2 - 4C});$$

$$B = a_Y^v + a_N^r; \quad C = a_N^v a_Y^r - a_Y^v a_N^r$$

Numerical Example--5

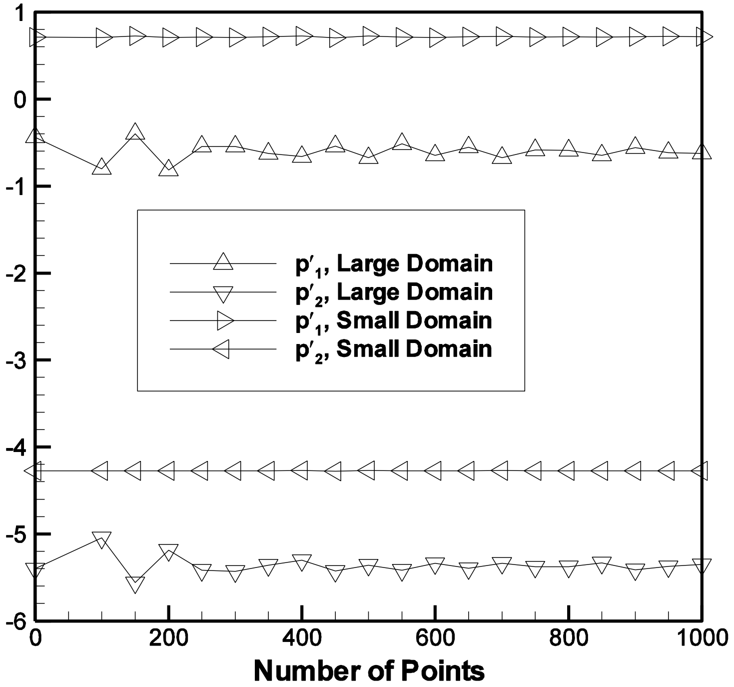

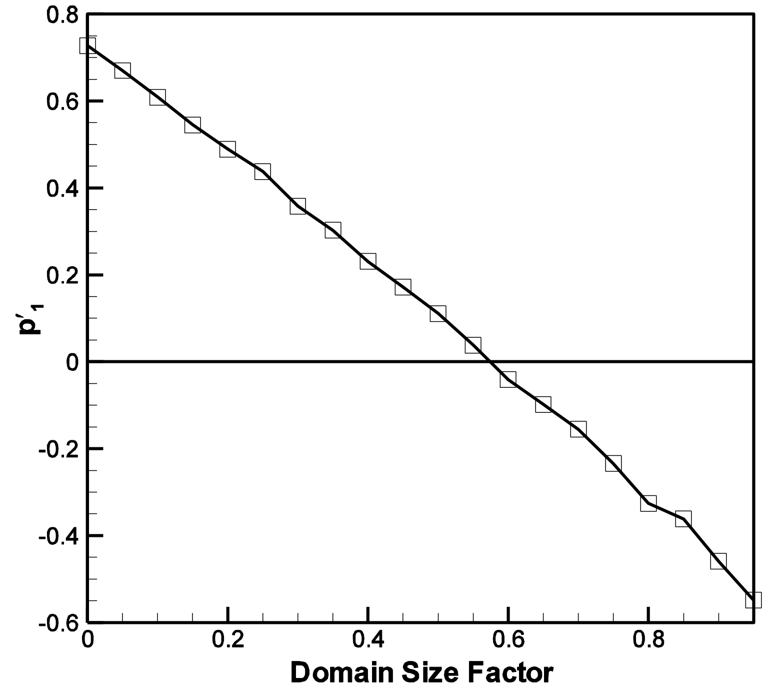

Eigenvalues vs *N* and domain size:

Linearisation: Numerical Example--5

- Nomoto equation:

$$T_1T_2\ddot{r} + (T_1 + T_2)\dot{r} + r = K(\delta_R + T_3\dot{\delta}_R).$$

- Its parameters:

$$T_1 = -1/p_1,\ T_2 = -1/p_2, T_3 = a_N^{\delta}/Q,$$
$$K = T_1T_2Q;\quad Q = a_N^{v}a_Y^{\delta} - a_Y^{v}a_N^{\delta}.$$

- Initial angular acceleration:

$$P_2 = \frac{K'T_3'}{T_1'T_2'}$$

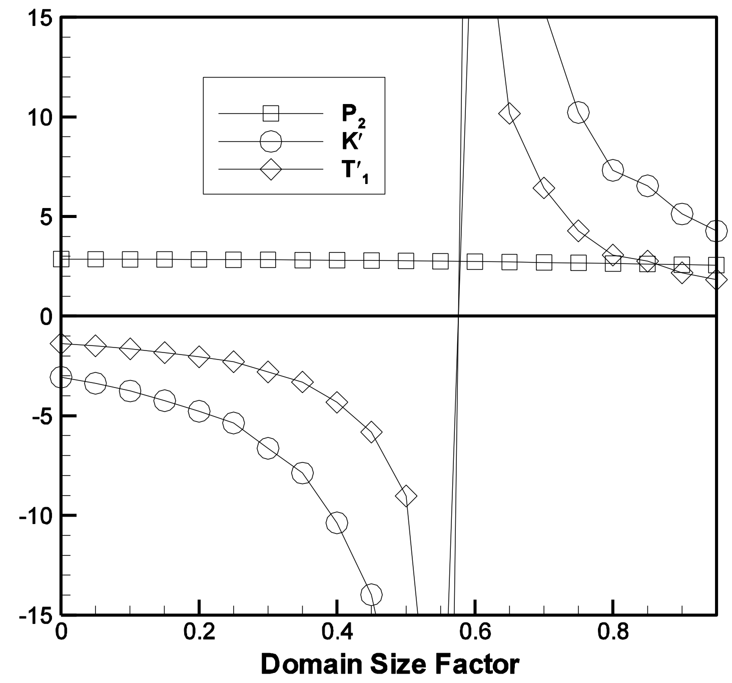

Fractional Seakeeping Model: Contents

- **Review of classic models for marine craft**
- **Simpler “fractional” issue: use of real exponents in ship resistance**
- **Non-integer derivatives/integrals**
- **Possible generalized “fractional” model for ship dynamics**
- **Behaviour in the frequency domain: fitting properties**
- **Conclusions**

INSTITUTO SUPERIOR TÉCNICO

Fractional Model: Motivation

- ***Spyrou, Niotis, Panagopoulou*** **(2008, OSAKA Colloquium)** ***Novel Modeling of Ship Rolling Based on Fractional Calculus*****:**

$$I_{xx}\ddot{\varphi} + b_{44}\varphi^{(1+\alpha)} + c_{44}\varphi = K_e(t)$$

- ***McCue, Xing*** **(2009, STAB Conference)** ***Parametric Identification for two Nonlinear Models of Ship Rolling Using Neural Networks*****---used was the model from the previous reference.**

- **Still personal curiosity: can it bring some advantages?**

Classic Time-Domain Mathematical Models---1

1. Partial Differential Equations + Ordinary Differential Equations models. E.g. Euler equations for rigid body with online solution of RANS equations at each time step (too slow).
2. Ordinary Integral-Differential Equations: presence of convolution integrals (memory functions).
3. Ordinary Differential Equations: neglecting part of memory effects (manoeuvring) or **approximating** OIDE through introduction of auxiliary fictitious state variables.

Assume an OIDE-model being conditionally adequate…

Classic Time-Domain Mathematical Models---2

- General OIDE model:

$$F(\dot{x}, x, \int_0^t x(\tau)K(t-\tau)\,\mathrm{d}\tau, u, e, t) = 0.$$

- Partly linearized (Newtonian mechanics) OIDE model:

$$\dot{x} = \int_0^t x(\tau)K(t-\tau)\,\mathrm{d}\tau + f(x,u,e,t).$$

- Simplified ODE model:

$$\dot{x} = f(x,u,e,t).$$

- Volterra IE equivalent to ODE:

$$x(t) = x_0 + \int_0^t f[x(\tau),u,e,\tau)\,\mathrm{d}\,\tau.$$

- Volterra IE equivalent to OIDE:

$$x(t) = x_0 + \int_0^t \Phi[x(\tau),u,e,\tau]\,\mathrm{d}\,\tau,$$

$$\Phi[x(\tau),u,e,\tau] = K_1(t-\tau)x(\tau) + f[x(\tau),u,e,\tau],$$

$$K_1(s) = \int_0^t K(\sigma)\,\mathrm{d}\,\sigma.$$

Analogy: fractional (real) powers in ship resistance

Extrapolation of the flat plate frictional resistance according to original Froude's method:

$$R_F = cSV^{1.825}$$

(the coefficient is here dimensional!)

Later approach:

$$R_F = C_F(\mathrm{Rn})\frac{\rho V^2}{2}S,$$

$$\mathrm{Rn} = \frac{VL}{\nu},$$

$$C_F = \frac{0.075}{(\log_{10}\mathrm{Rn} - 2)^2} \quad \text{or}$$

$$C_F = \frac{0.455}{(\log_{10}\mathrm{Rn})^{2.58}}$$

INSTITUTO SUPERIOR TÉCNICO

Fractional Derivative---Definitions

Grünwald—Post—Letnikov's definition:

$$D_x^q f(x) \equiv \frac{\mathrm{d}^q f}{\mathrm{d}x^q} = \lim_{N\to\infty} \left\{ \frac{\left(\frac{x}{N}\right)^{-q}}{\Gamma(-q)} \sum_{j=0}^{N-1} \frac{\Gamma(j-q)}{\Gamma(j+1)} f\left[x\left(1 - \frac{j-\frac{q}{2}}{N}\right)\right]\right\},$$

$q > 0$ ---derivation; $q < 0$ ---integration

Riemann—Liouville's integral (q<0)

$$\frac{\mathrm{d}^q f}{\mathrm{d}\,x^q} = \frac{1}{\Gamma(-q)} \int_0^x (x-y)^{-q-1} f(y)\,\mathrm{d}y$$

INSTITUTO SUPERIOR TÉCNICO

Fractional Derivative---Some Properties

Fractional derivative of an exponent:

$$\frac{\mathrm{d}^q\, e^{\pm x}}{\mathrm{d}\,x^q} = \frac{e^{\pm x}}{x^q}\gamma^*(-q,\pm x),\ \text{ where the incomplete gamma-function } \gamma^*(-n,\pm x) = (\pm x)^n$$

$$\text{Particular case: } \gamma^*(\tfrac{1}{2},x) = \frac{\operatorname{erf}(\sqrt{x})}{\sqrt{x}} \quad \Rightarrow \quad \frac{\mathrm{d}^{\frac{1}{2}}\, e^{\pm x}}{\mathrm{d}\,x^{\frac{1}{2}}} = \frac{1}{\sqrt{\pi x}} + e^x \operatorname{erf}(\sqrt{x})$$

Fractional derivative of a constant:

$$\frac{\mathrm{d}^q\, C}{\mathrm{d}\,x^q} = C\frac{x^{-q}}{\Gamma(1-q)}$$

Problems with Leibniz's rule for the product, chain rule for the composition etc.

Linearized models:

Classic OIDE

$$\dot{x} = \int_0^t x(\tau) K(t-\tau)\,\mathrm{d}\tau + Ax + f(t),$$

Allegedly equivalent OFDE

$$\dot{x} = \mathrm{D}_{\mathrm{t}}^{q}\, x + Ax + f(t), \quad q > 0$$

Fourier image of a fractional derivative:

$$x(t) \leftrightarrow \hat{x}(\omega) \quad \Rightarrow \quad \mathrm{D}_{\mathrm{t}}^{q}\, x(t) \leftrightarrow (i\omega)^{q}\, \hat{x}(\omega)$$

INSTITUTO SUPERIOR TÉCNICO

Generalized Rational Approximation of a Complex Added Mass Coefficient---1

$$\hat{\mu}_{ij}(\omega) - \mu_{ij\infty} = \frac{F(i\omega)^{\alpha_1} + G}{(i\omega)^{\beta_1} + B(i\omega)^{\beta_2} + C(i\omega)^{\beta_3} + D},$$

$$\hat{\mu}_{ij}(\omega) = \mu_{ij}(\omega) - \tfrac{i}{\omega}\nu_{ij}(\omega)$$

where in the classic ODE-approximation case:

$\alpha_1 = \beta_3 = 1;\ \ \beta_1 = 3;\ \ \beta_2 = 2 \quad \Rightarrow$ 5 free parameters.

OFDE $\quad\Rightarrow\quad$ up to 9 parameters.

If the number of parameters is still limited to 5, then

$$\hat{\mu}_{ij}(\omega) - \mu_{ij\infty} = \frac{G}{(i\omega)^{\beta} + C(i\omega)^{\gamma} + D}, \quad \beta > \gamma > 1$$

INSTITUTO SUPERIOR TÉCNICO

Generalized Rational Approximation of a Complex Added Mass Coefficient---2

Added mass: $\mu_{ij}(\omega) = \mu_{ij\infty} + \dfrac{G\omega^{\beta}\cos(\frac{\pi}{2}\beta) + GC\omega^{\gamma}\cos(\frac{\pi}{2}\gamma) + GD}{\Delta(\omega)}$,

Damping coefficient: $\nu_{ij}(\omega) = \dfrac{G\omega^{1+\beta}\sin(\frac{\pi}{2}\beta) + GC\omega^{1+\gamma}\sin(\frac{\pi}{2}\gamma)}{\Delta(\omega)}$,

where $\Delta(\omega) = \omega^{2\beta} + C^2\omega^{2\gamma} + 2C\omega^{\beta+\gamma}\cos(\beta-\gamma) + 2D\omega^{\beta}\cos(\frac{\pi}{2}\beta)$
$+2CD\omega^{\gamma}\cos(\frac{\pi}{2}\gamma) + D^2$.

Asymptotics: as $\omega \to 0$: $\nu_{ij} \sim \mathrm{const}\cdot\omega^{1+\gamma}$

as $\omega \to \infty$: $\nu_{ij} \sim \mathrm{const}\cdot\omega^{1-\beta}$

---consumes one of the parameters...

Similarly with the alternative

$$\frac{F(i\omega)^{\alpha} + G}{(i\omega)^{\beta} + D}$$

9-parameter function's responses for ij=22: left---added mass; right---damping coefficient

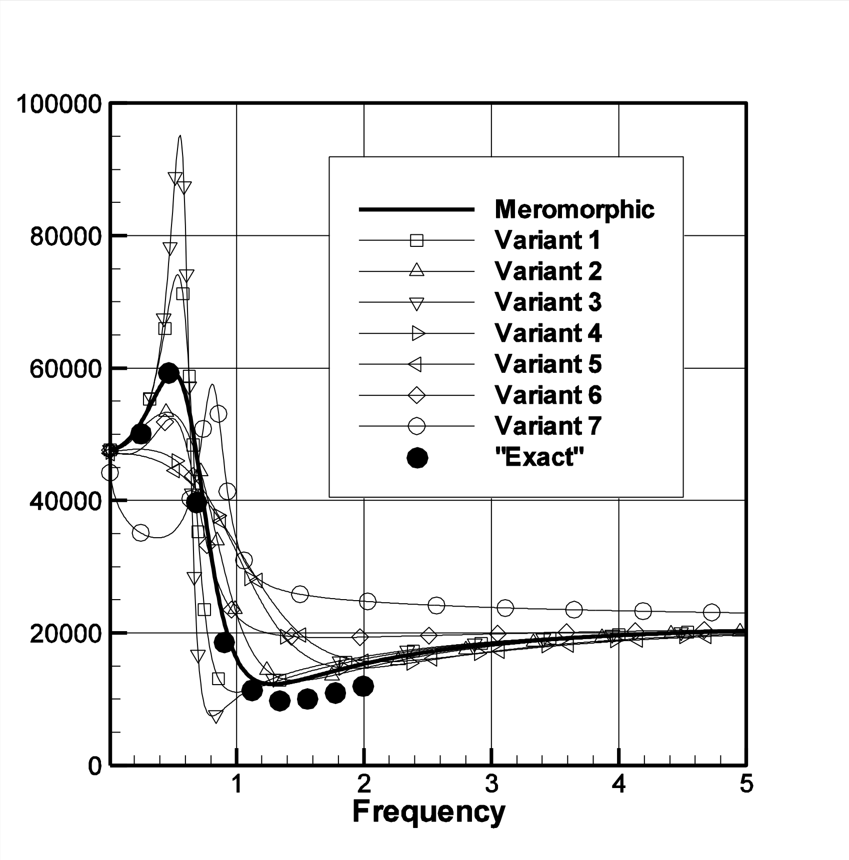

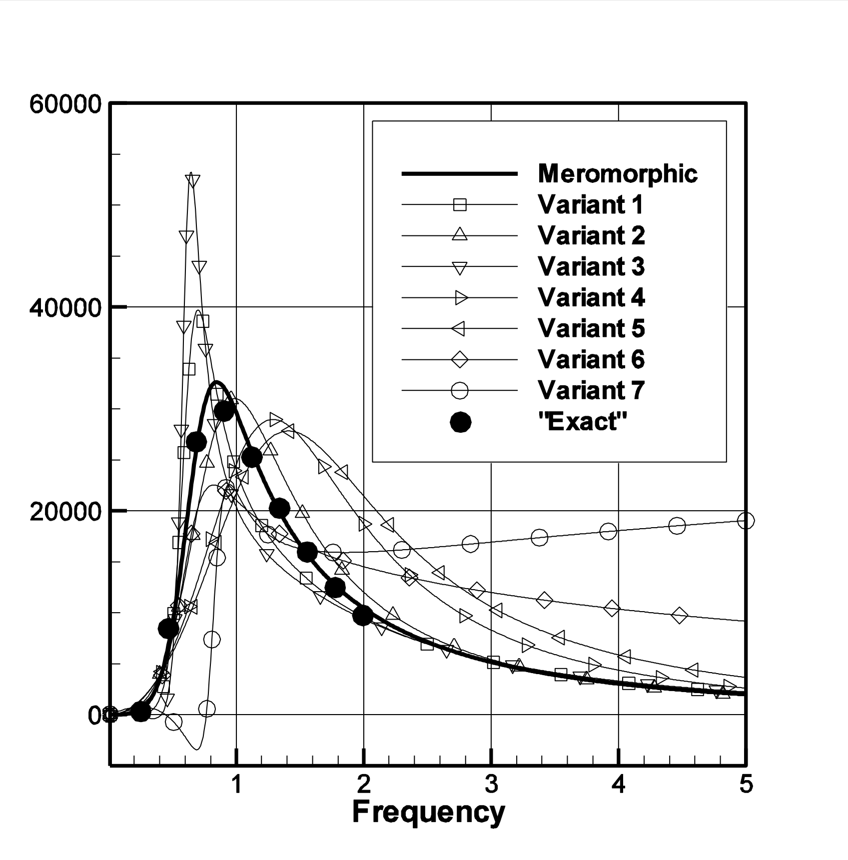

Conclusions

- Numerics related to Fractional Ordinary Differential Equations is much more complicated than in the case of ODE and not less complicated than for OIDE.
- Some convenient and precious properties of linear ODE, like conservation of a harmonic signal, are lost.
- Apparently, fractional ODE models are not more economical from the viewpoint of the number of parameters required for describing the actual frequency response.
- Dimensionality problems may arise.
- Inspiration caused by the “fractional idea” seems to be premature, at least in ship dynamics.
- Further studies in this direction do not seem justified.

INSTITUTO SUPERIOR TÉCNICO

Equipment for full-scale trials: Especificações

1. **O peso e o volume mínimos: portabilidade completa por 2–3 pessoas**
2. **Instalação rápida no navio: 20–30 minutos**
3. **Impossibilidade de efectuar ligação aos circuitos de commando e sensores próprios do navio**
4. **Gravação numérica contínua de: posição do navio, rumo (aproamento), velocidade e ângulo do vento relativos, velocidade em relação do fundo (SOG), rumo em relação do fundo (COG)**
5. **Gravação vídeo contínuo do estado dos indicadores visuais do navio: rotações das máquinas, ângulos das tubeiras dos propulsores de jacto de água, configurações dos *buckets***

INSTITUTO SUPERIOR TÉCNICO

Descrição Geral

Parâmetros	Sensor	Produtor	Marca
Coordenadas, SOG, COG (Rumo)	Receptor GPS	Thallas/ Magellan	DG14++ ou DG16--
Aproamento	Girobússola de Fibras Ópticas	iXSEA	Octans II
Vento	Anemómetro	Autohelm	ST50
Velocidade Angular de Guinada	Sensor de Velocidade Angular	Bei	Gyrochip
Parâmetros de Controlo	Câmara Vídeo de Alta Definição	Sony	HDR-HC3E

INSTITUTO SUPERIOR TÉCNICO

Receptor GPS *Magellan DG14*

Característica	Valor Numérico
Erro de posição em modo autónomo	CEP 3m, R95 5m
Erro de posição em modo diferencial (baliza)	CEP 0.7m, R95 1.6m
Erro de SOG	0.1nós (95%)
Tempo até à primeira captação	90s (cold start)
Frequência de actualização	10Hz

Girobússola *iXSEA Octans II (surface unit)*

Característica	Valor Numérico
Resolução	0.01º
Erro dinâmico	0.05º RMS ou 0.2º/cos(Latitude)
Velocidade de Guinada Máxima (Follow-up speed)	750º/s
Tempo de fixação no meridiano (settling time)	<1’ (estático) <5’ (condições quaisquer)
Massa	4.8kg

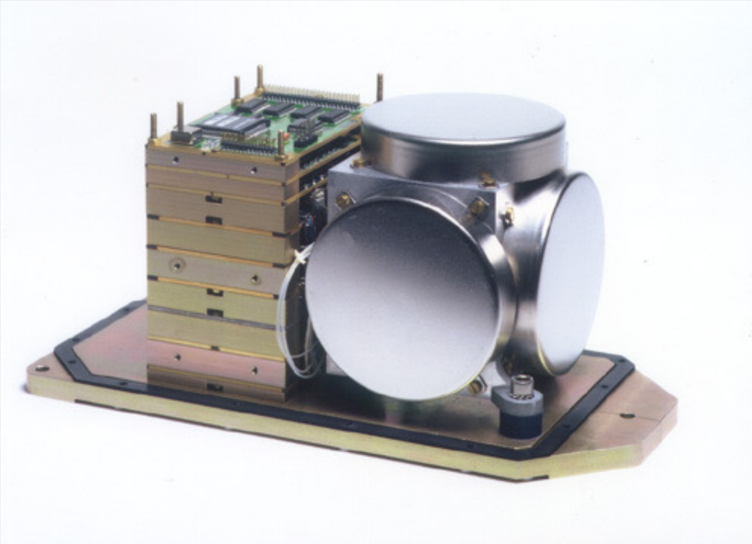

Anemómetro *Autohelm ST50*

Característica	Valor Numérico
Intervalo das velocidades	0−60nós
Incerteza estimada	±2nós
Intervalo dos ângulos	±180º
Incerteza estimada	±5º

INSTITUTO SUPERIOR TÉCNICO

Sistema de Aquisição de Dados em *LabView*—1

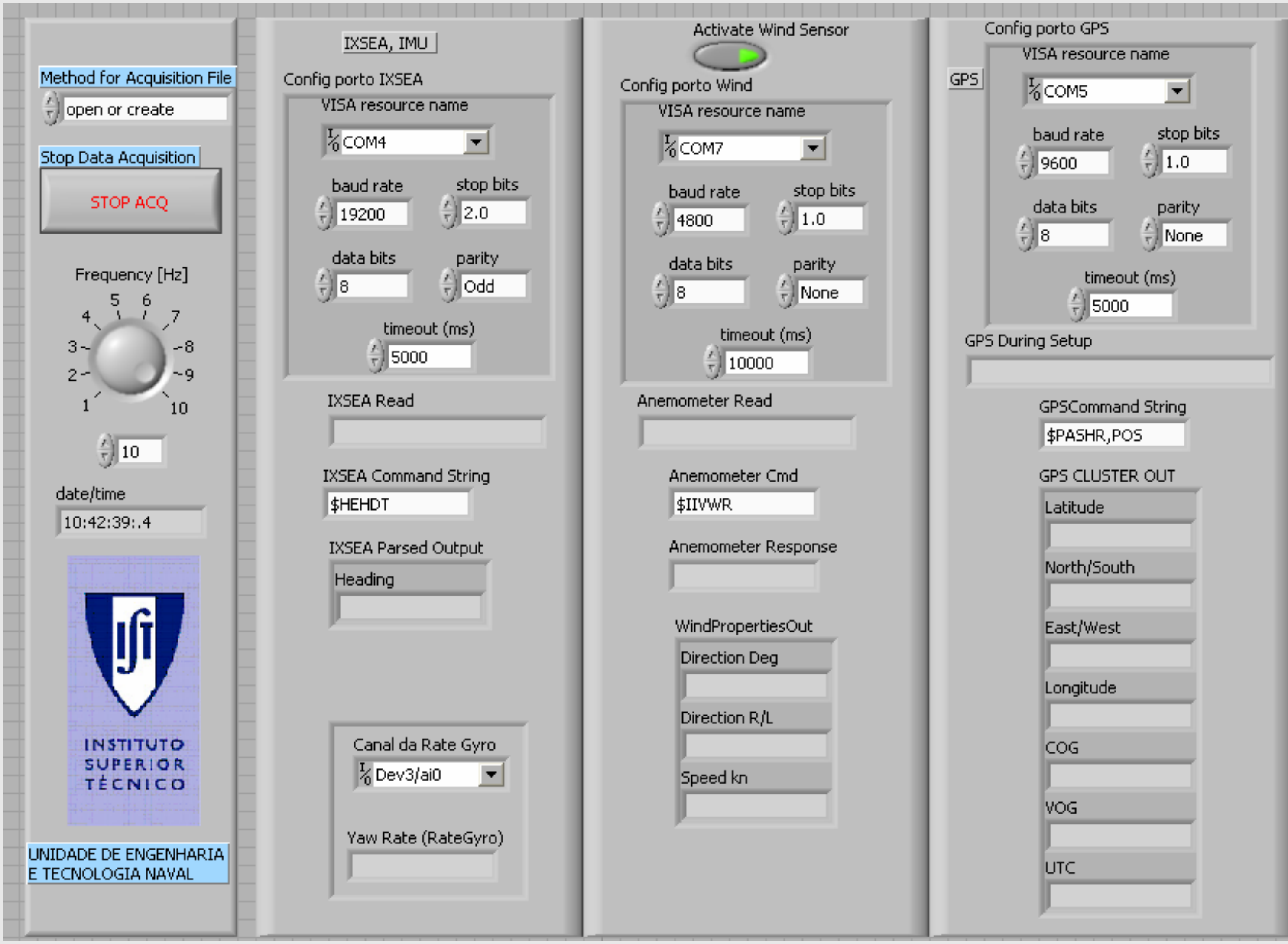

Painel frontal

Sistema de Aquisição de Dados—2

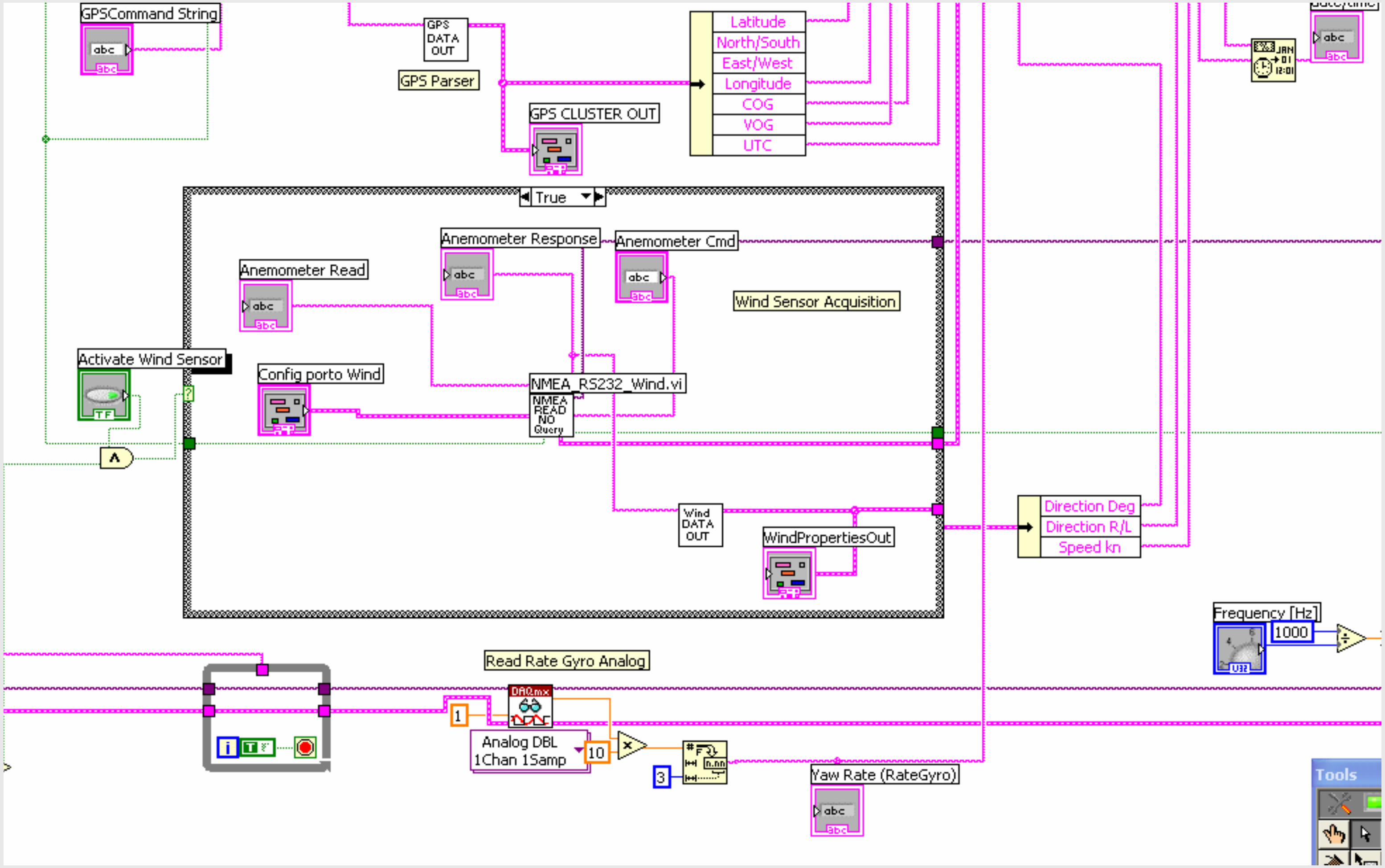

Parte do diagrama associado ao painel frontal

Sistema de Aquisição de Dados—3

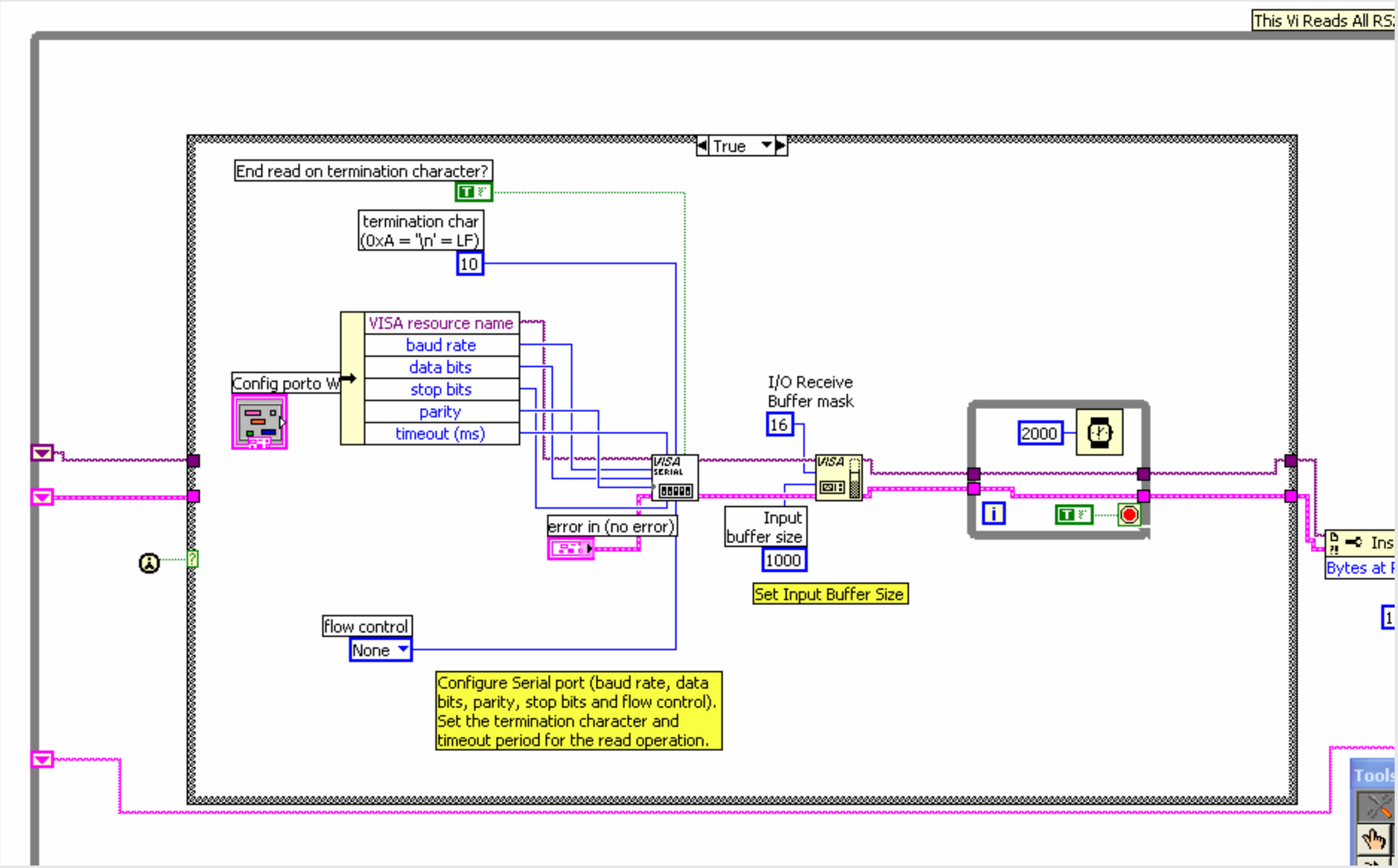

Inicialização do porto série na primeira chamada

Sistema de Aquisição de Dados—4

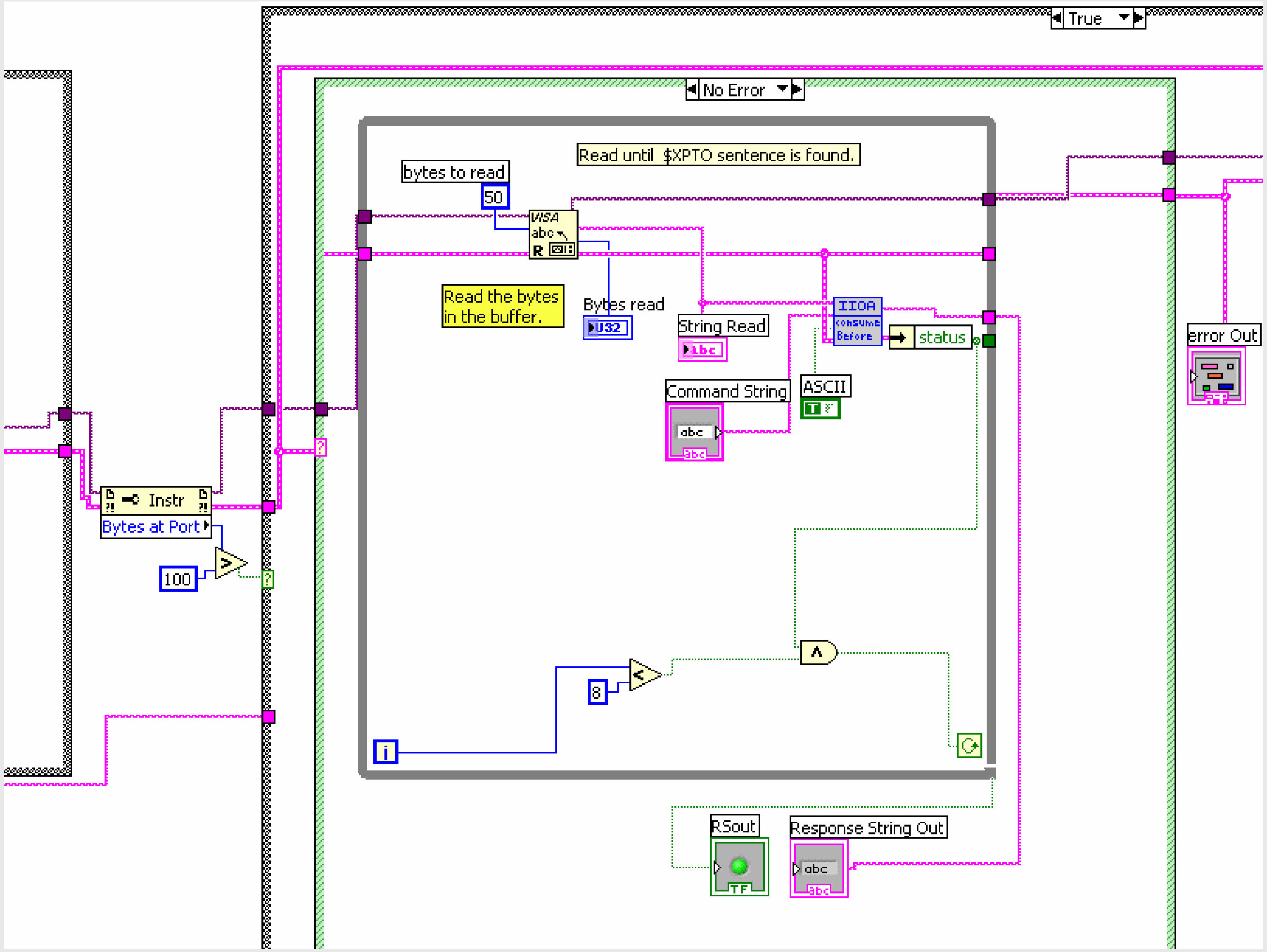

Leitura da informação existente no *buffer*, de acordo com regras estabelecidas

Sistema de Aquisição de Dados—5

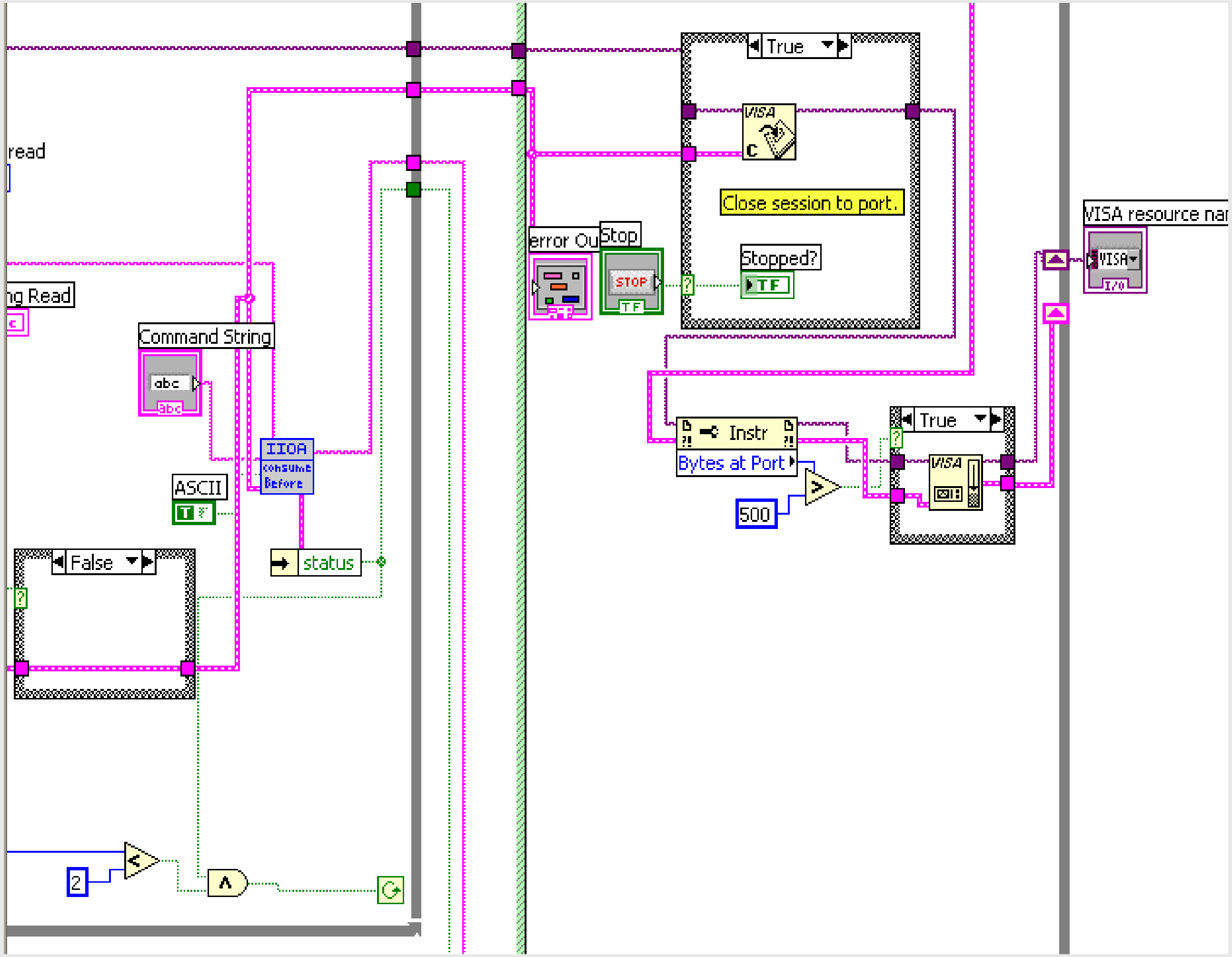

Gestão de informação presente no *buffer*

Sistema de Aquisição de Dados—6

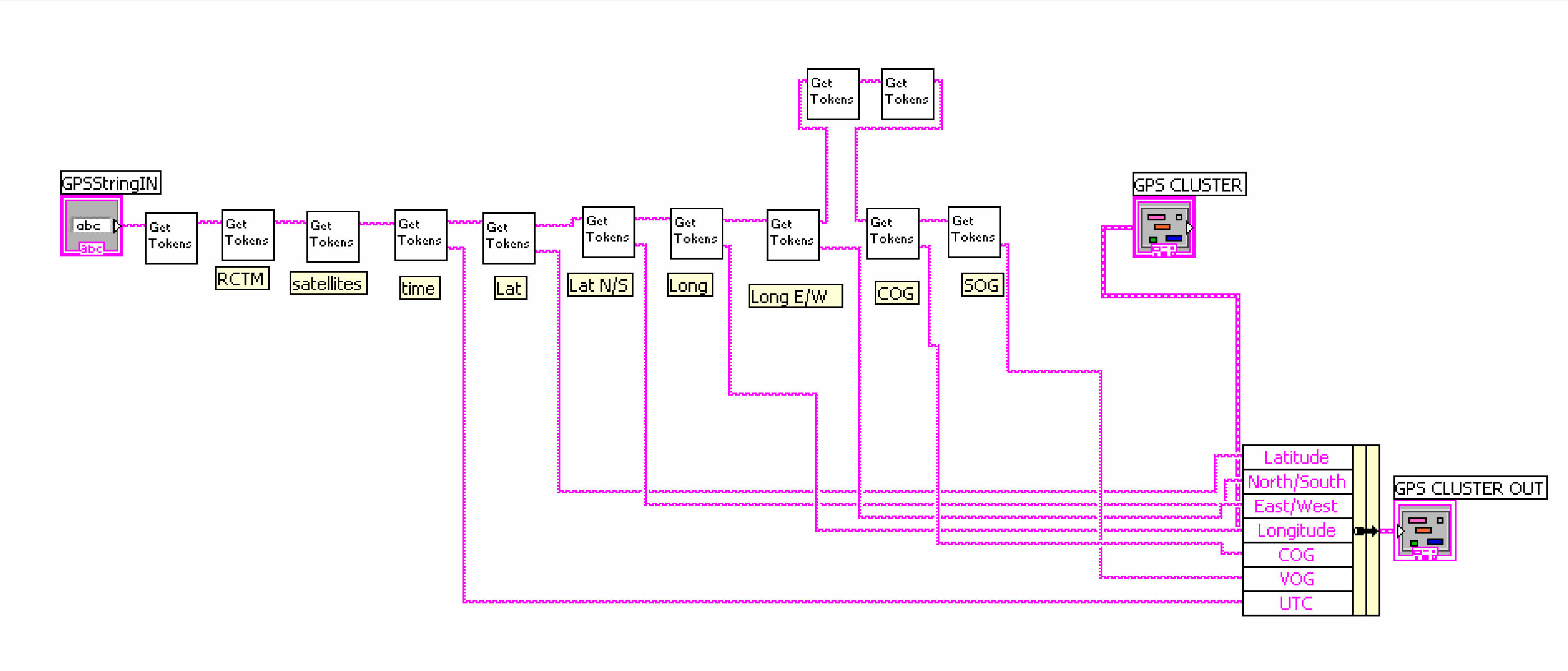

Procura de identificadores e truncatura da frase completa

Transformação dos Dados

0.342 138.80 3842.02903 00908.72744 014.65 319.28 053.0 R 17.0 135524.80 13:55:40:.39

1.099 139.41 3842.03423 00908.73311 014.41 319.71 053.0 R 17.0 135526.50 13:55:42:.41

Aproamento (0−360º) → Ângulo de guinada relativo ±180º

Coordenadas geográficas da antena (gggmmss.ss) → Coordenadas cartesianas relativas do centro do navio, m

Ângulo de vento: (0−180º L/R) → ±180º

Aproamento e rumo (COG) → Ângulo de deriva ±180º

```
TITLE="Trajectory "
VARIABLES = "Transfer, m"  "Advance, m"
ZONE T ="Trajectory"
-461.188     14.8727
-453.581     4.77048
.....................................
```

Exemplo: Trajectória—1

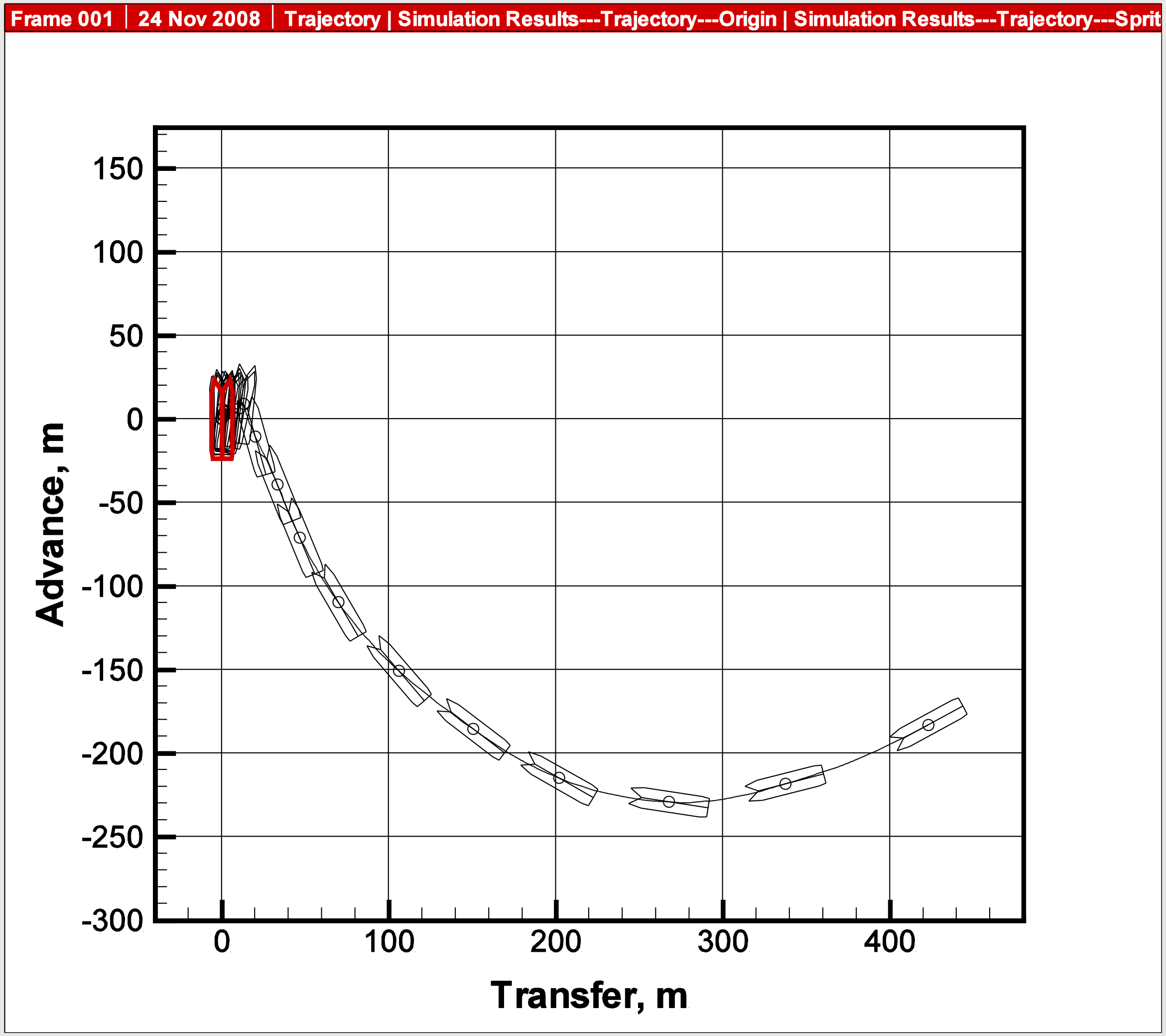

Atracamento a Cais do Sodré, São Julião, 20.03.2008, UTC1400

Exemplo: Trajectória—2

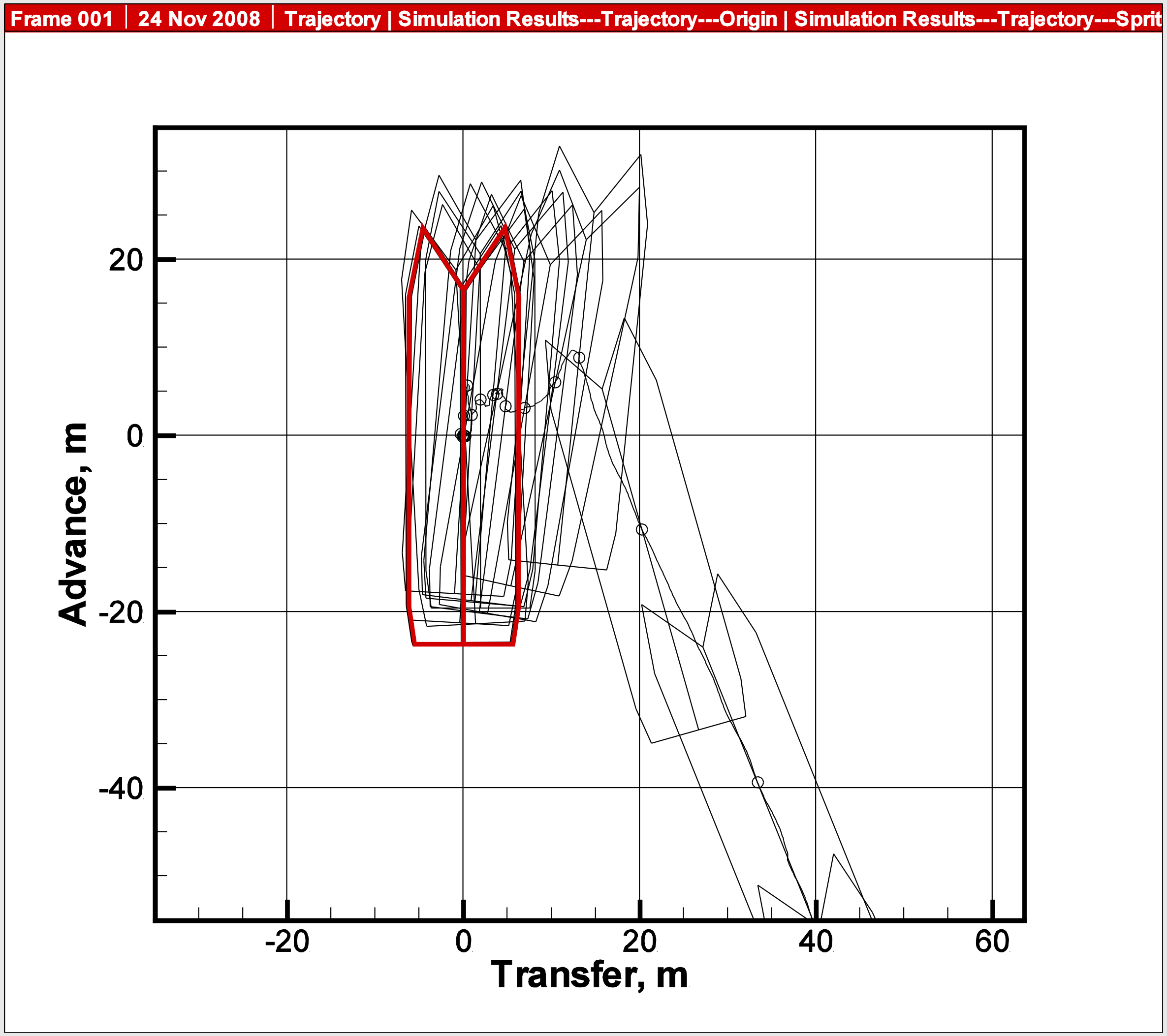

Atracamento a Cais do Sodré—Fase Final, São Julião, 20.03.2008, UTC1400

Exemplo: Respostas Temporais—1

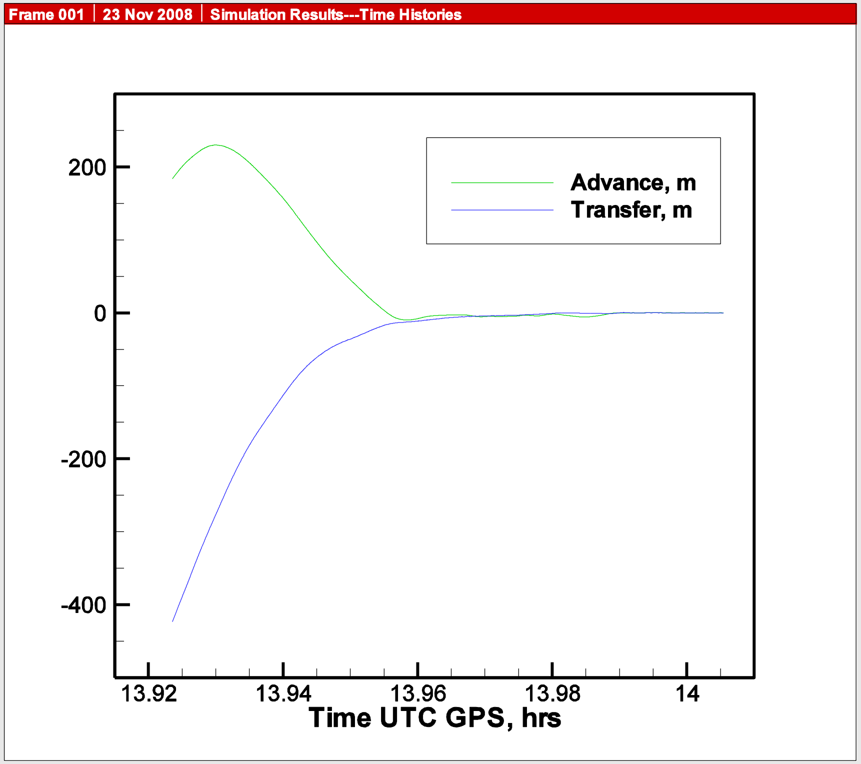

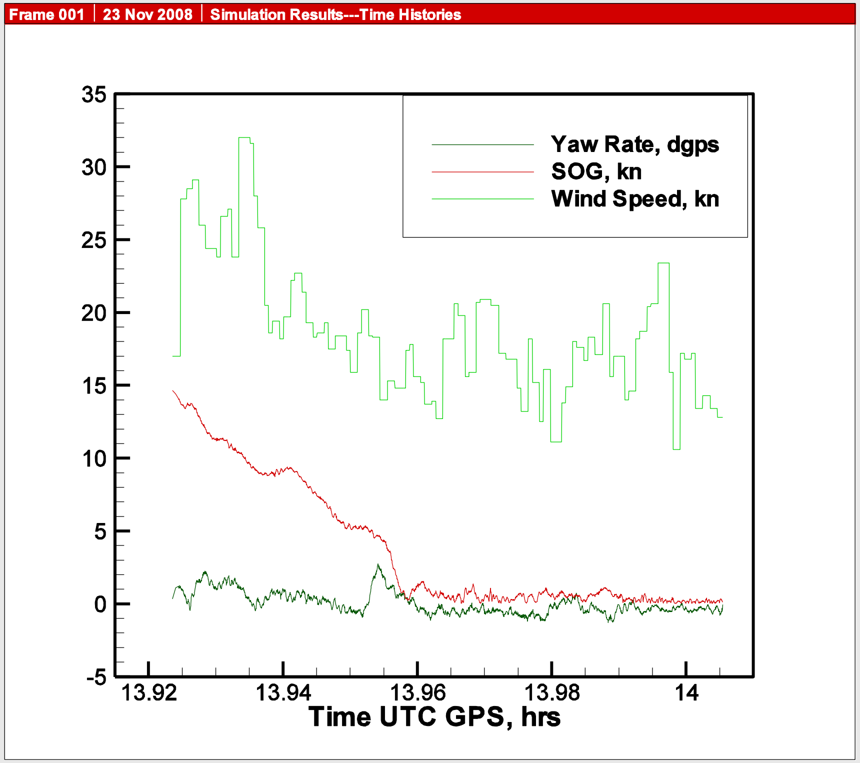

Atracamento a Cais do Sodré, São Julião, 20.03.2008, UTC1400

Exemplo: Respostas Temporais—2

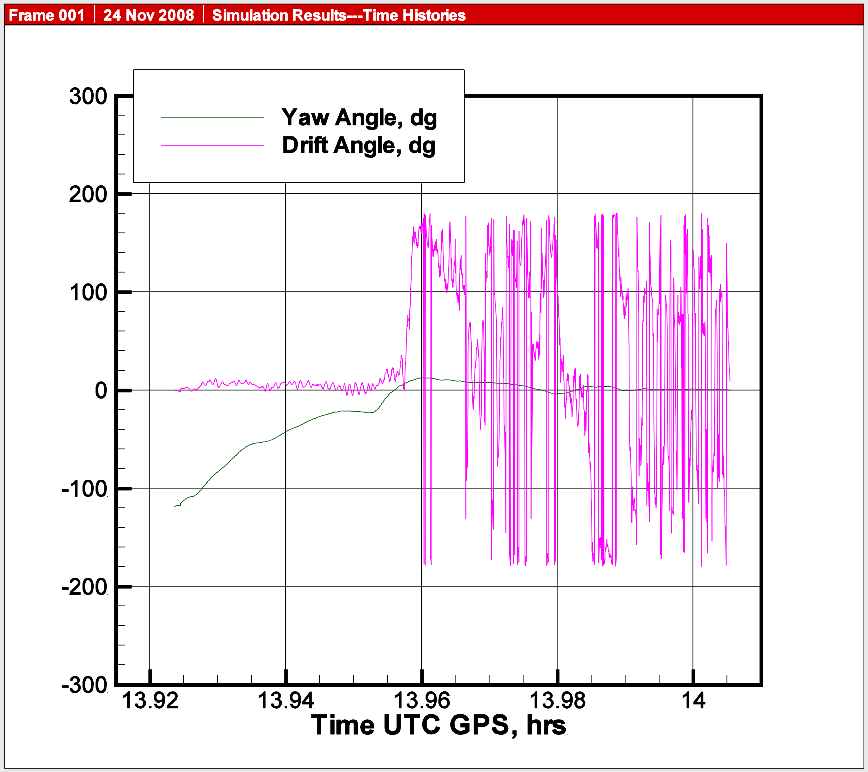

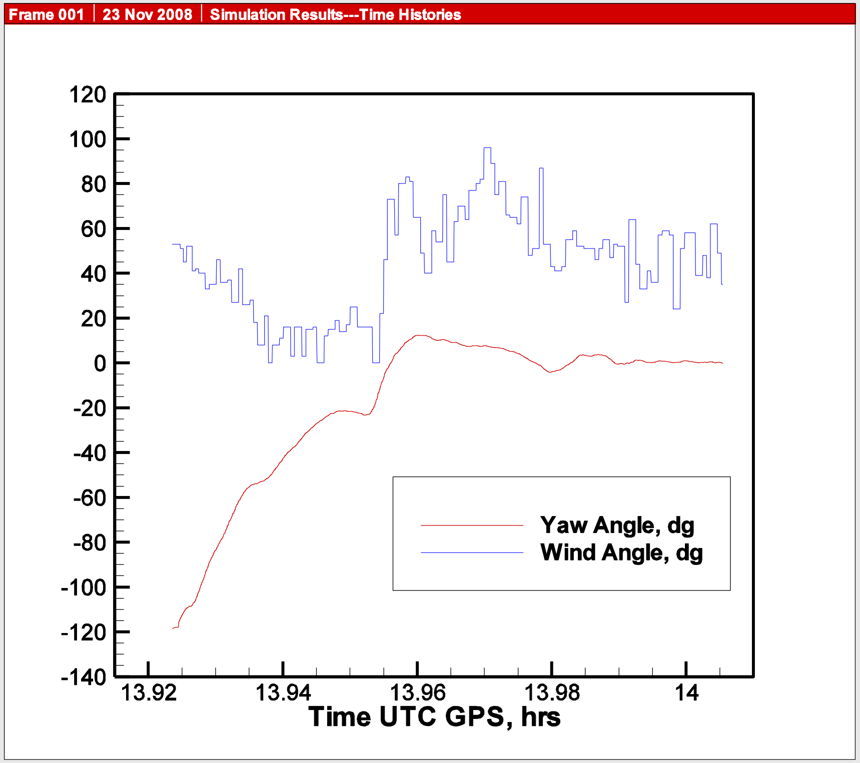

Atracamento a Cais do Sodré, São Julião, 20.03.2008, UTC1400

Exemplo: Trajectória—3

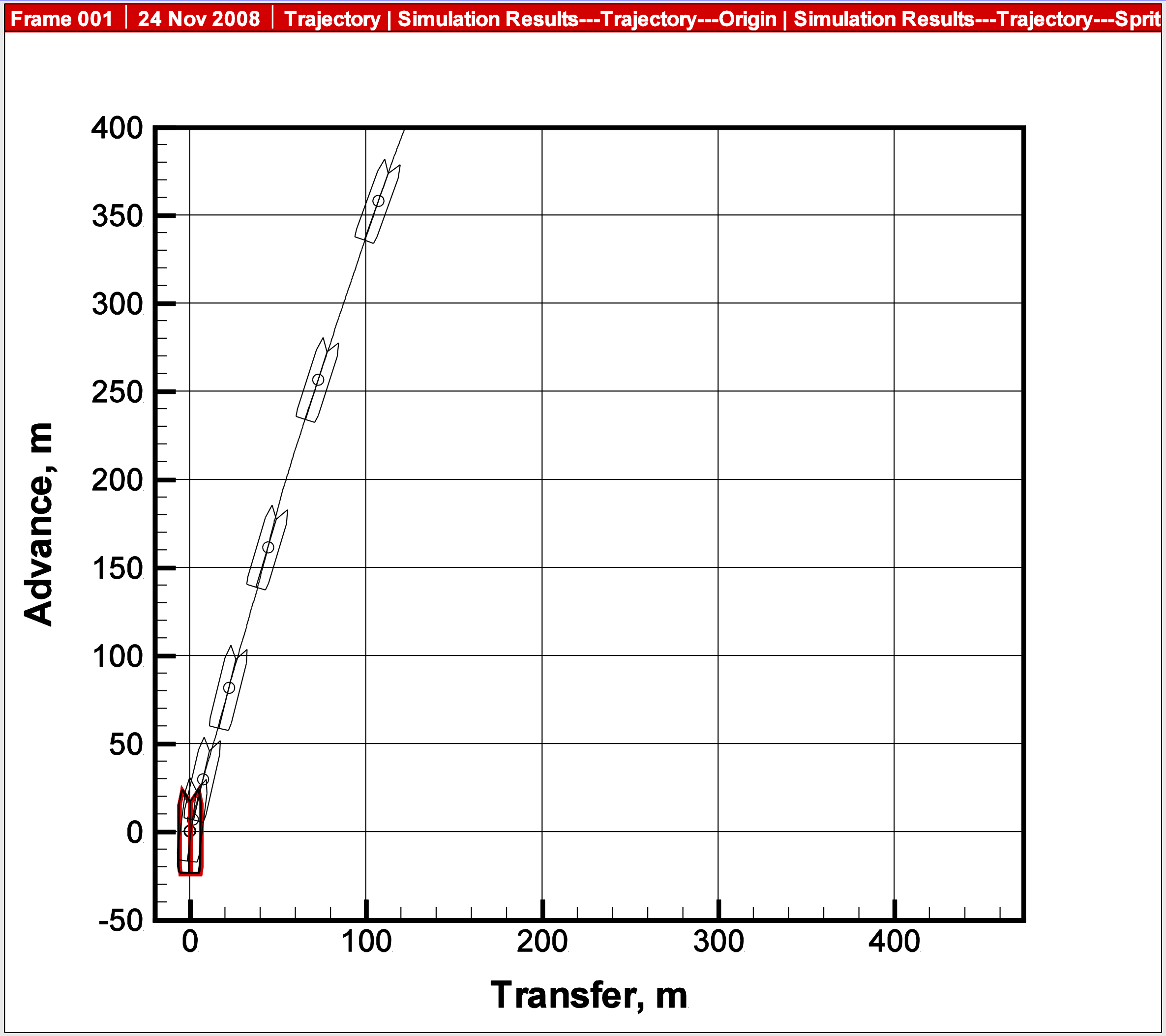

Saída de Cais do Sodré, São Julião, 20.03.2008, UTC1403

Exemplo: Trajectória—4

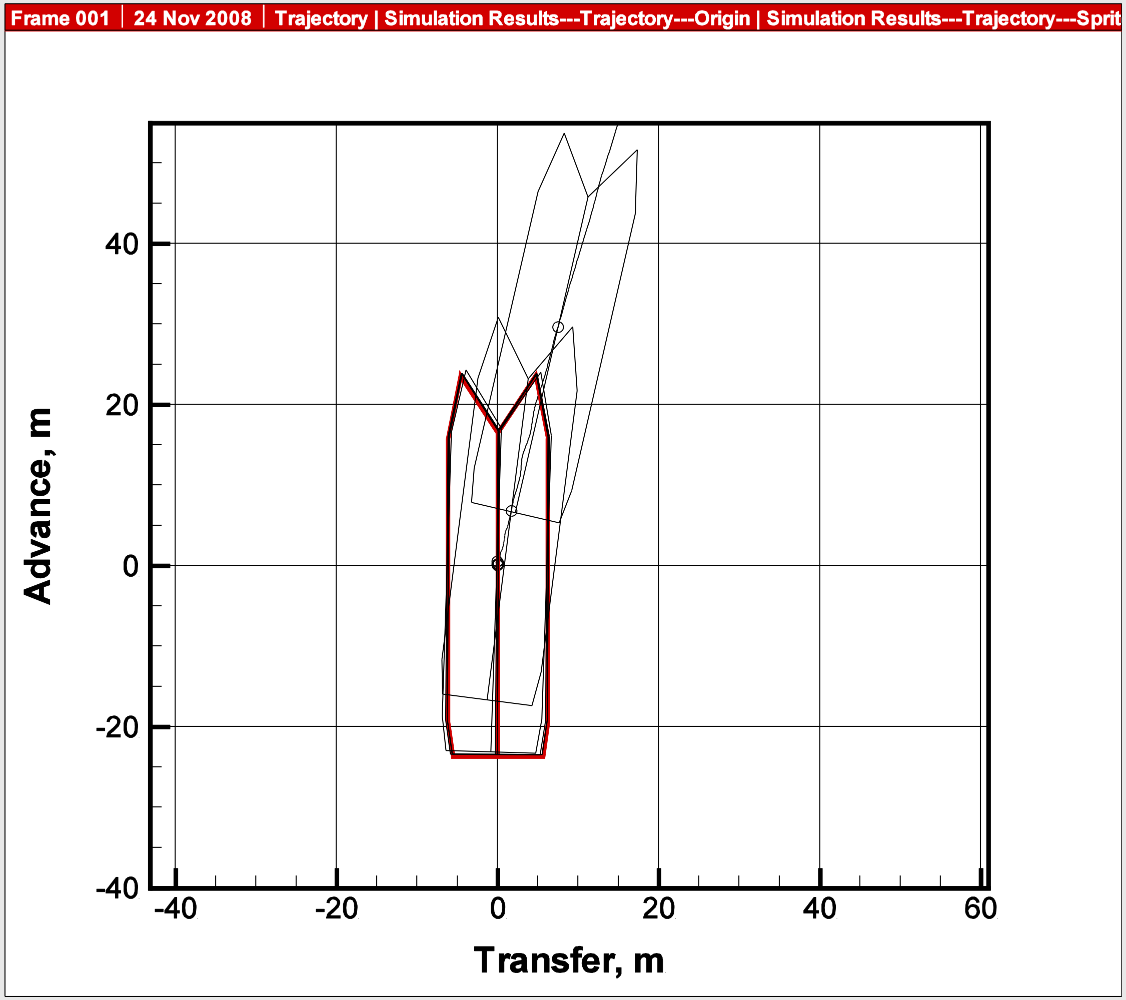

Saida de Cais do Sodré—Fase Inicial, São Julião, 20.03.2008, UTC1403

Exemplo: Respostas Temporais—3

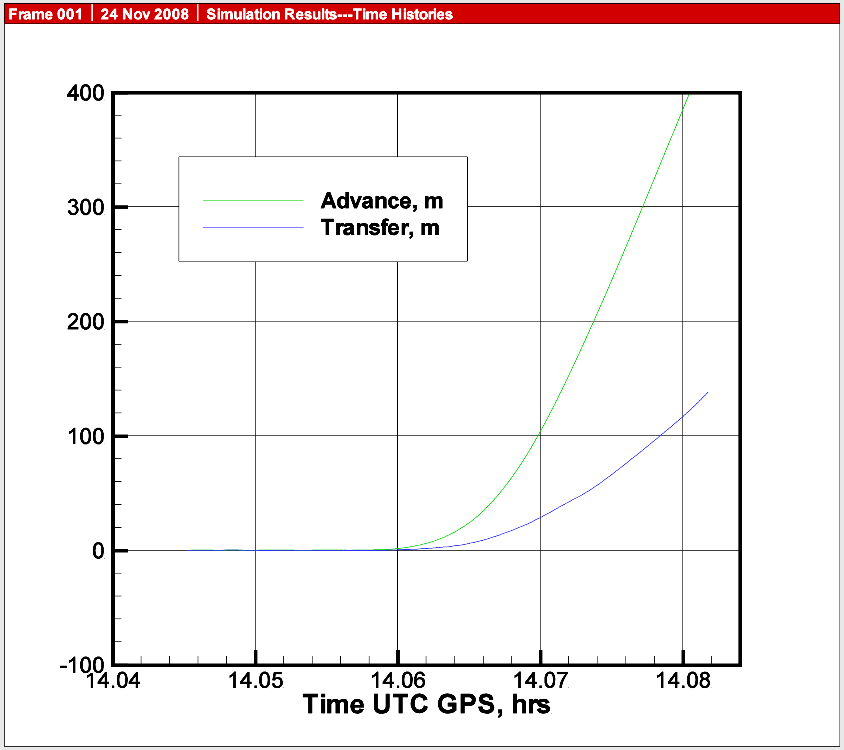

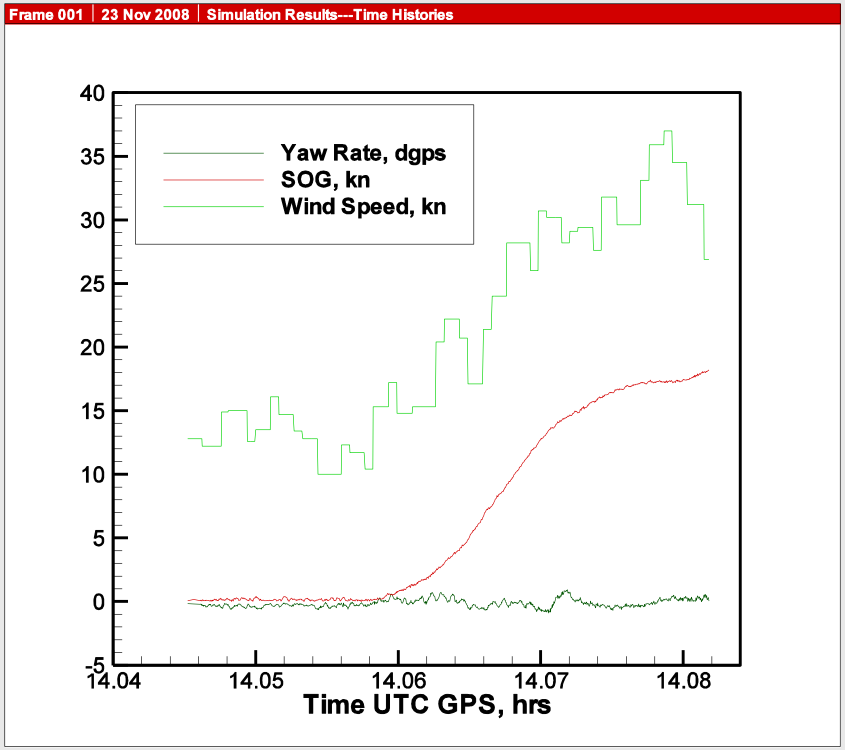

Saída de Cais do Sodré, São Julião, 20.03.2008, UTC1403

Exemplo: Respostas Temporais—4

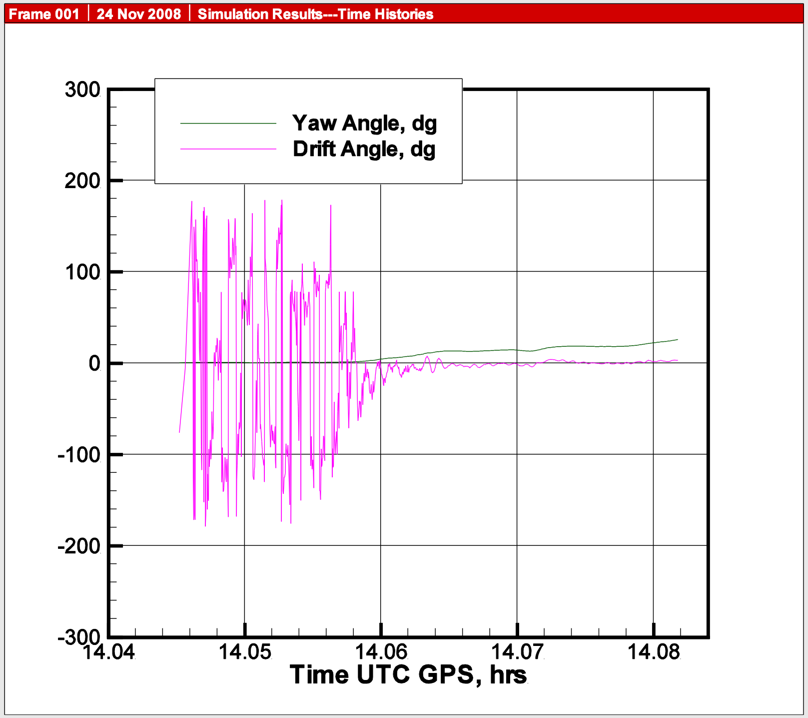

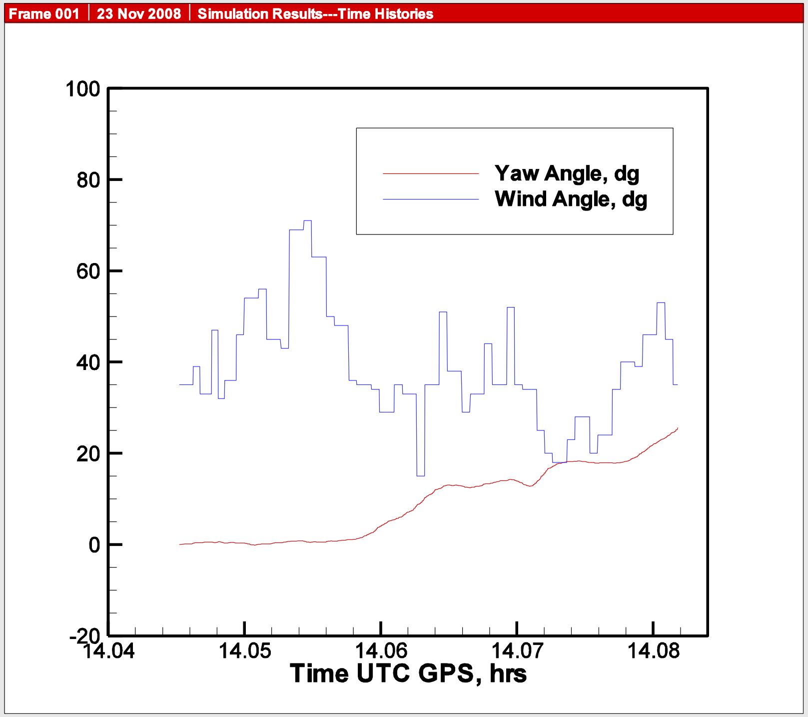

Saída de Cais do Sodré, São Julião, 20.03.2008, UTC1403

Exemplo: Imagem do Painel de Controlo

Atracamento a Cais do Sodré, São Julião, 20.03.2008

Conclusões

- Um novo conjunto de equipamento e do software para medição, gravação e pós-processamento dos parâmetros de movimento dos navios de superfície foi desenvolvido por CENTEC
- O sistema foi aplicado com êxito nos ensaios passivos com catamarãs de Transtejo/Soflusa
- A inconveniência mais grave foi causada pela necessidade de usar os cabos de ligação à antena GPS e ao sensor de vento
- O problema de gravação dos valores numéricos dos parâmetros de controlo só ficou resolvido parcialmente: em caso da necessidade dos valores precisos, ligação aos circuitos de navio é indispensável.

INSTITUTO SUPERIOR TÉCNICO

Dentro de uma mala

iXSEA e GPS

Last trials in 2015

Last trials in 2015




Numerical study of some properties of generic mathematical models of directionally unstable ships

Nomoto-type models:

$$T_1' T_2' \ddot{r}' + (T_1' + T_2')\dot{r}' + f(r') = K'(\delta_R + T_3' \dot{\delta}_R), \quad T' \dot{r}' + f(r') = K'\delta_R,$$

$$\bar{t} = \frac{t' K' \delta_m}{(T_1' + T_2') r_m'}, \quad p\ddot{\bar{r}} + \dot{\bar{r}} + F(\bar{r}) = \bar{\delta} + q\dot{\bar{\delta}}, \quad T' = T_1' + T_2' - T_3'$$

$$p = \frac{K'\delta_m T_1' T_2'}{r_m' (T_1' + T_2')^2}; \quad q = \frac{K'\delta_m T_3'}{r_m'(T_1' + T_2')^2} \qquad \dot{\bar{r}} + F(\bar{r}) = \bar{\delta}.$$

$$\bar{r} = r' / r_m'$$

$$\dot{\bar{r}} = \bar{s} + \frac{q}{p}\bar{\delta}, \qquad \bar{\delta} = \delta_R / \delta_m$$

$$\dot{\bar{s}} = \frac{1}{p}[(1 - \frac{q}{p})\bar{\delta} - \bar{s} - F(\bar{r})]. \qquad \dot{\bar{r}} = \bar{\delta} - F(\bar{r}).$$

$$\bar{\delta}(\bar{\psi}, \bar{r}) = \bar{\delta}_z \operatorname{sign}(\bar{\psi}_z \operatorname{sign} \bar{r} - \bar{\psi}), \qquad \bar{\delta}(\bar{t}) = \bar{\delta}_a \sin \bar{\omega}\bar{t}.$$

INSTITUTO SUPERIOR TÉCNICO

Static characteristic and some phase portraits

- Spiral curve and time histories

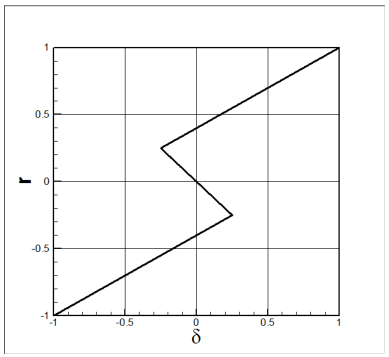

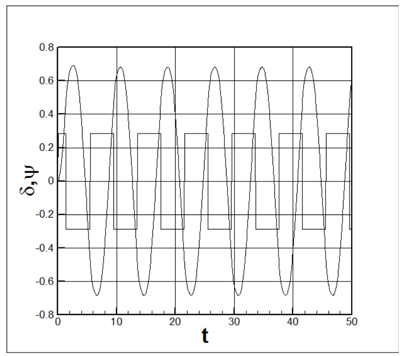

- Sine excitation

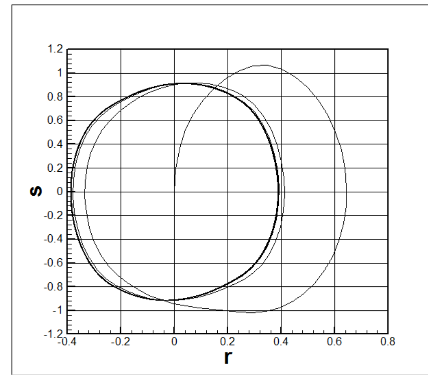

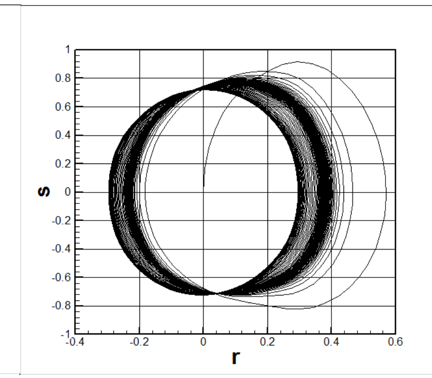

- Zigzag

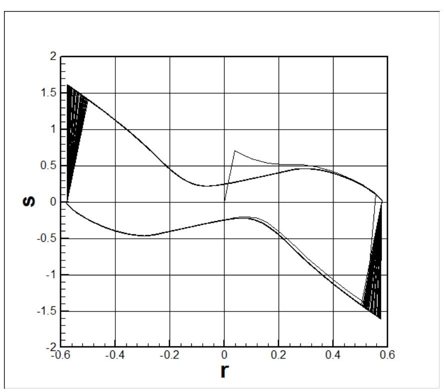

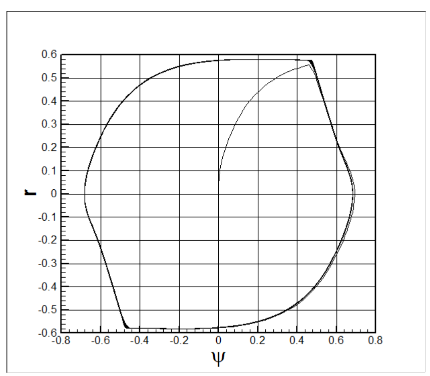

- Failed Zigzag

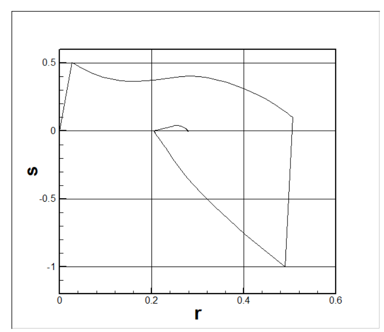

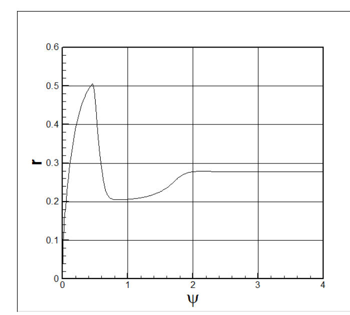

Ship aerodynamics: wind tunnel tests

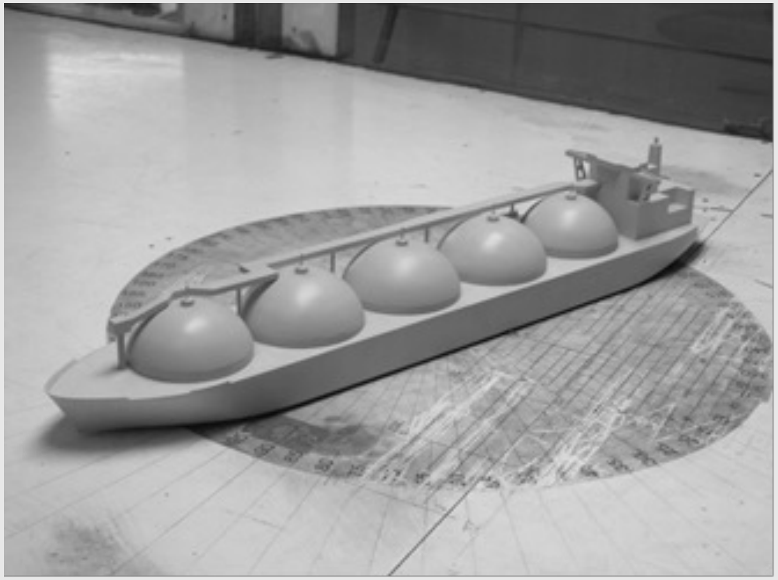

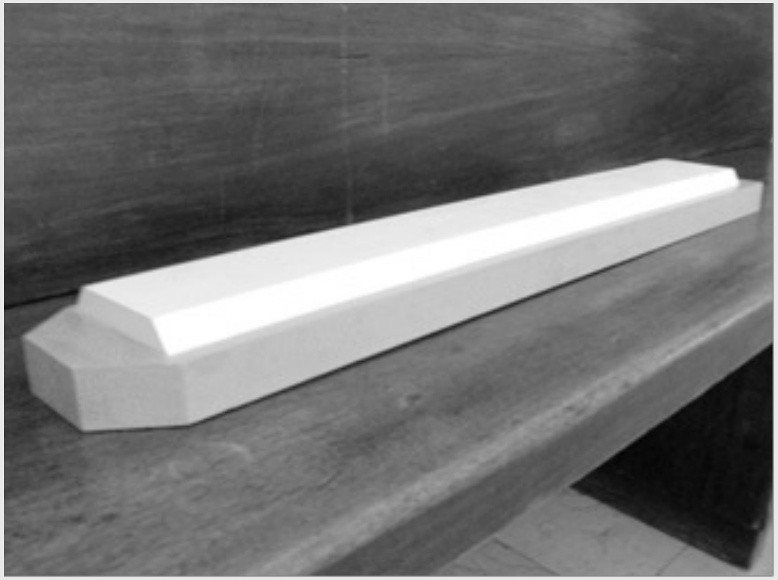

Table 1 Main characteristics of the models.

Characteristic	Value for:	
	Platform	***Galea***
Length overall L_{OA}, m	0.916	0.725
Breadth B, m	0.15	0.115
Frontal projected area A_F, m^2	0.00683	0.01051
Lateral projected area A_L, m^2	0.05275	0.05011
Reynolds number in tests **Rn**	6.2×10^5	4.9×10^5

Ship aerodynamics: Tanker and barge

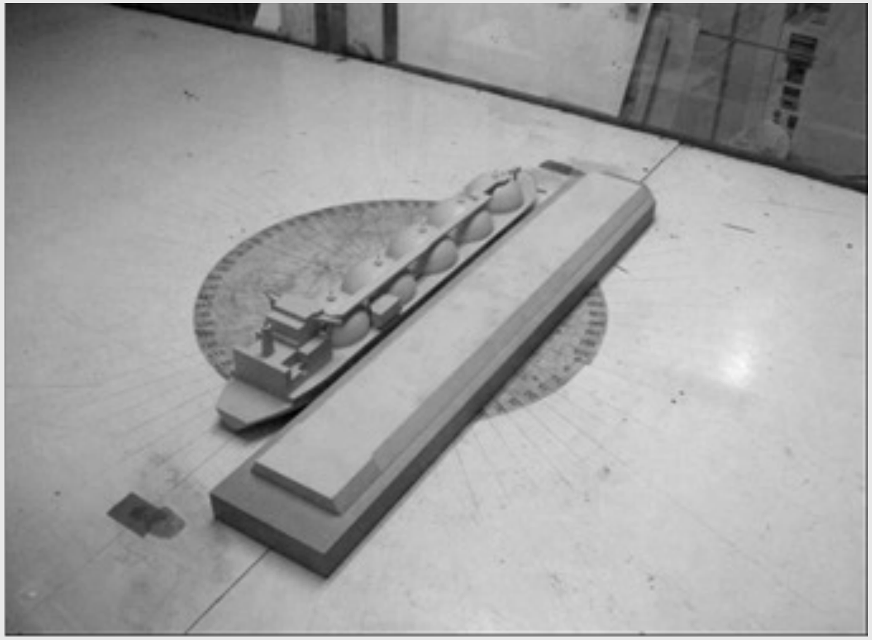

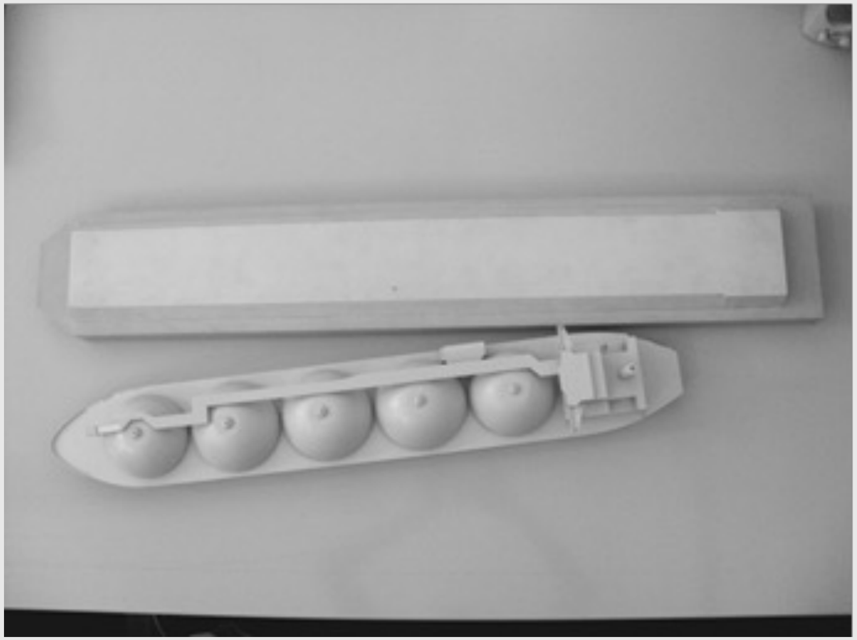

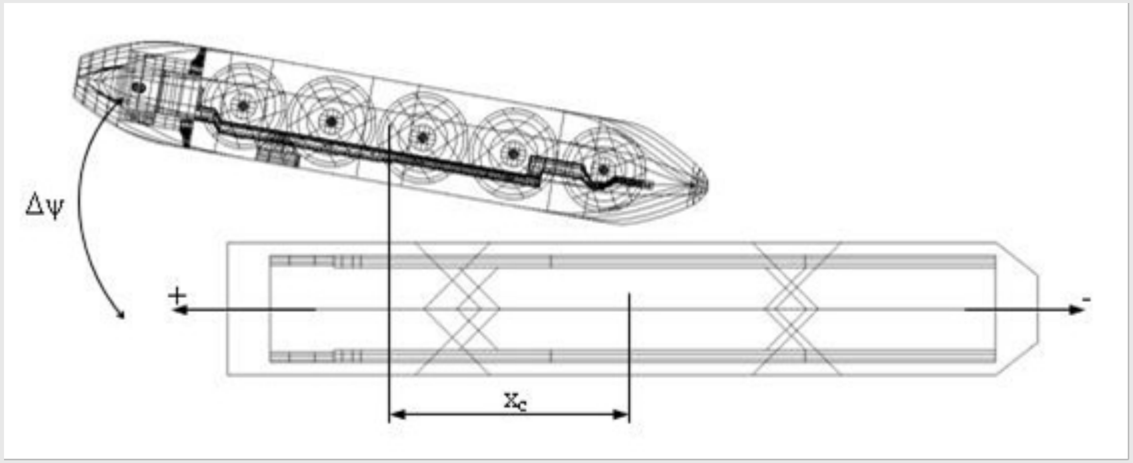

Shielded tanker: some results

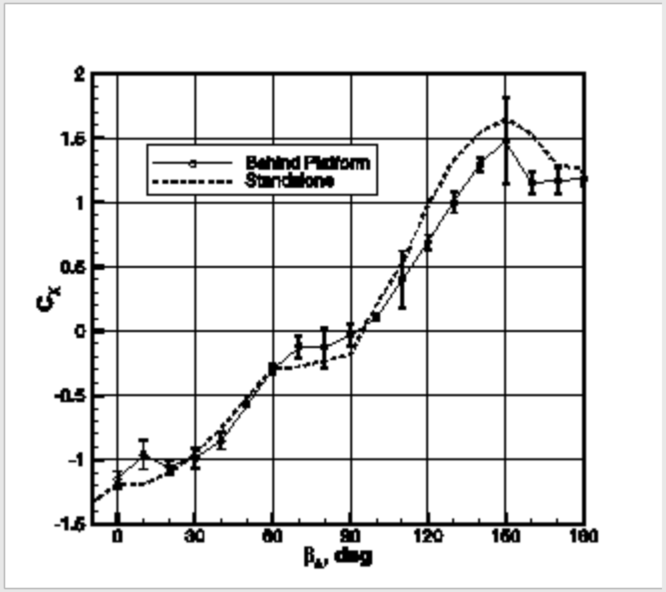

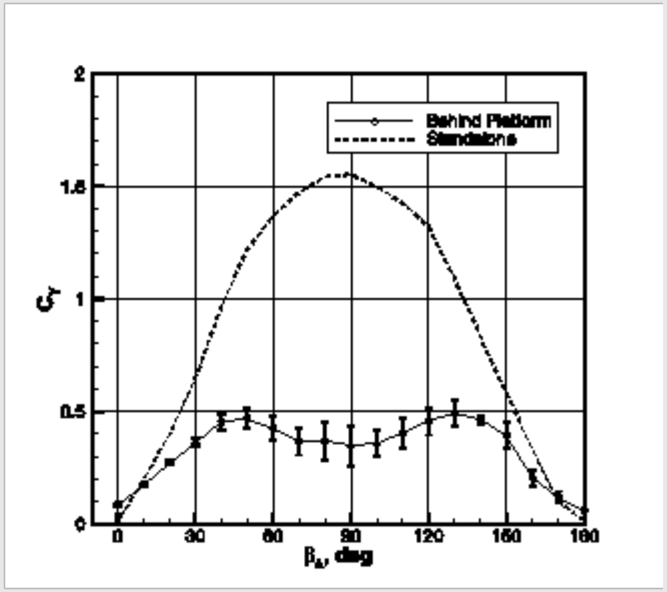

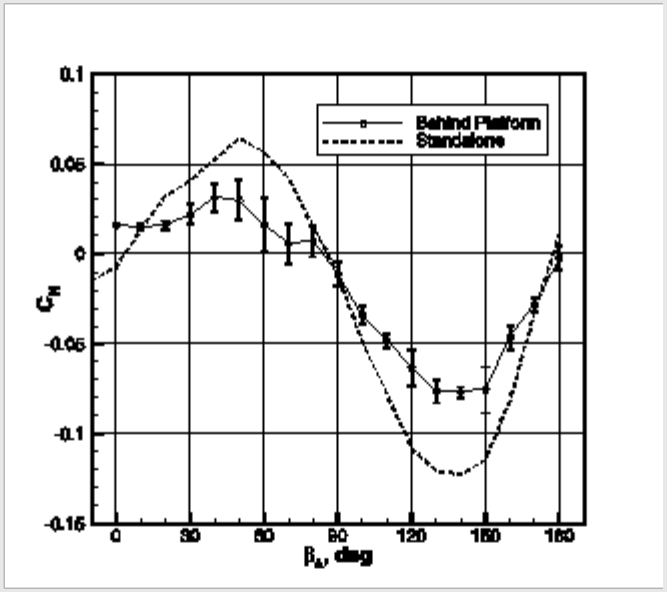

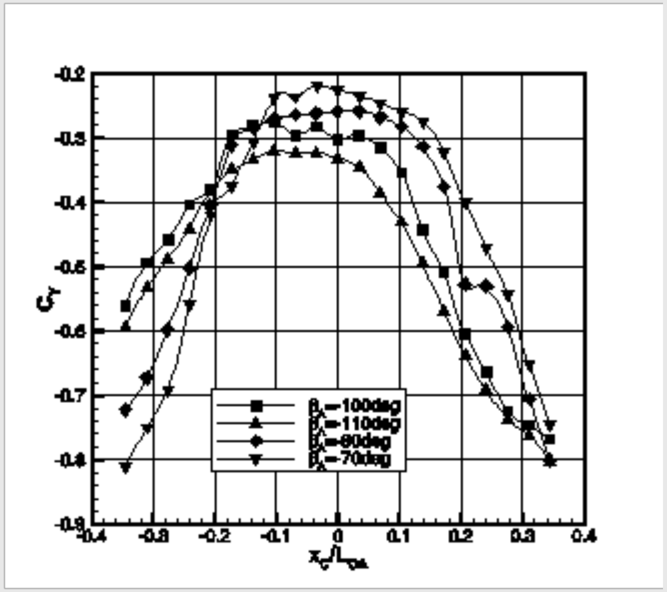

Aerodynamics: CFD --- 1

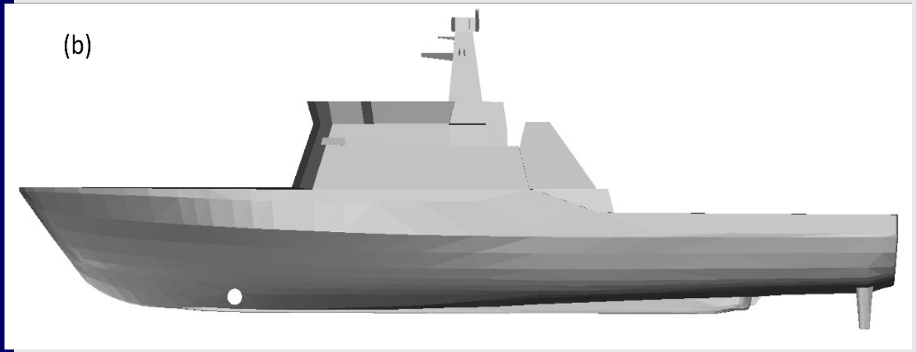

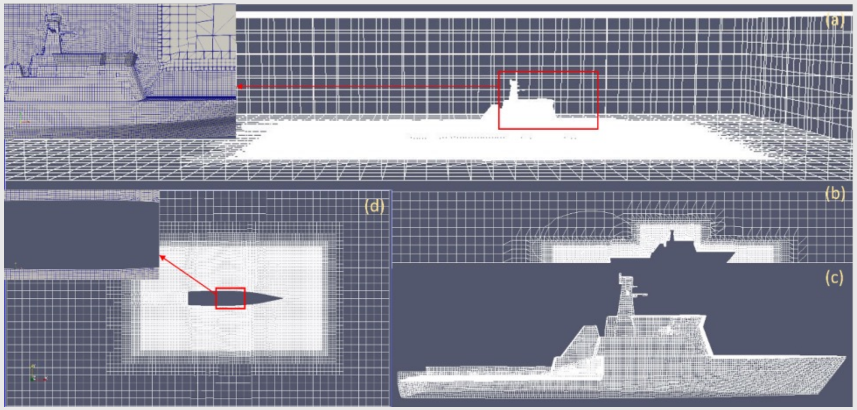

Table 1. The surge and sway force and heel and yaw moment results for the aerodynamic load-predicted using model scale simulations in OpenFOAM.

Drift Angle (Deg)	Turbulence Model	C_{XA}	C_{YA}	C_{KA}	C_{NA}
45	SST K-Omega	−0.22	0.85	−0.522	0.16
	K-Epsilon	−0.19	0.85	−0.515	0.16
	DDES	−0.13	0.92	−0.564	0.17
90	SST K-Omega	−0.04	1.10	−0.599	0.06
	K-Epsilon	0.03	1.14	−0.587	0.06
	DDES	−0.12	1.17	−0.627	0.06
135	SST K-Omega	0.36	0.93	−0.458	−0.06
	K-Epsilon	0.29	1.00	−0.484	−0.08
	DDES	0.29	0.98	−0.471	−0.06

Aerodynamics: CFD --- 2

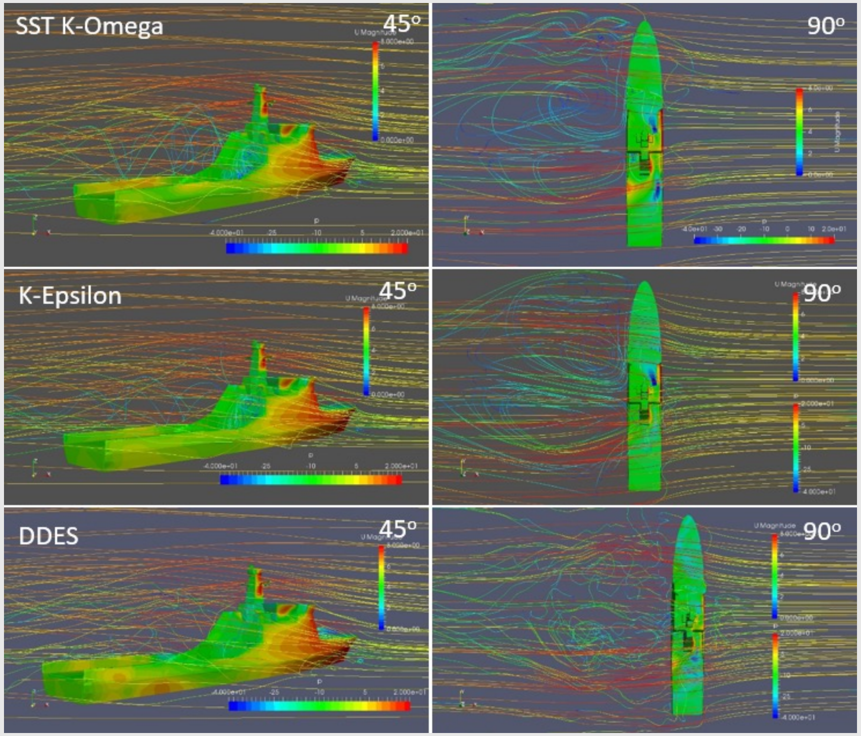

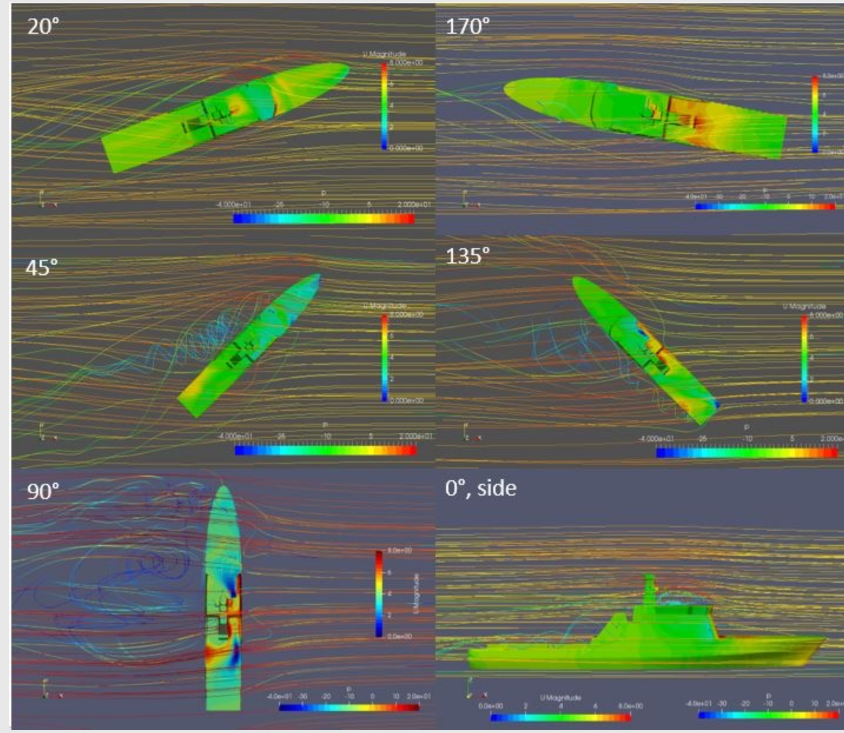

Table 2. Mesh resolutions used for the verification study for the model scale simulations.

Mesh	Total Number of Cells	Dimensions of Cells x (m)	y (m)	z (m)	Minimum Layer Thickness	Non-Dimensional Wall Distance, y+	Coarsening Ratio
1	$8.7 \cdot 10^6$	0.01953	0.01875	0.01875	0.00375	65	1.00
2	$3.95 \cdot 10^6$	0.02500	0.02500	0.02344	0.00500	87	1.30
3	$2.25 \cdot 10^6$	0.03125	0.03125	0.03125	0.00625	108	1.25

Aerodynamics: CFD --- 3

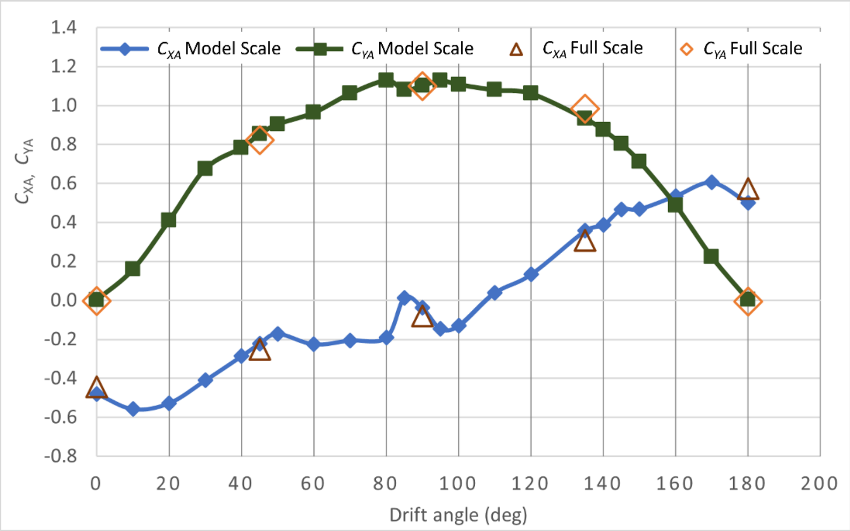

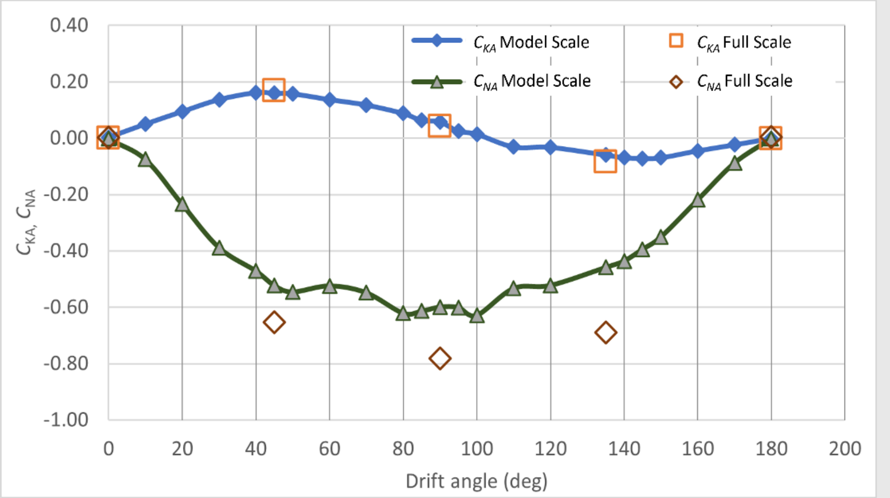

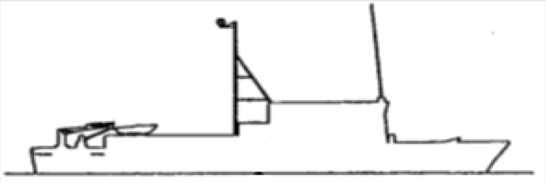

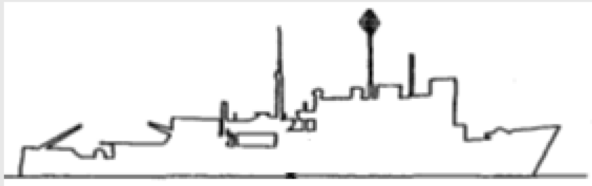

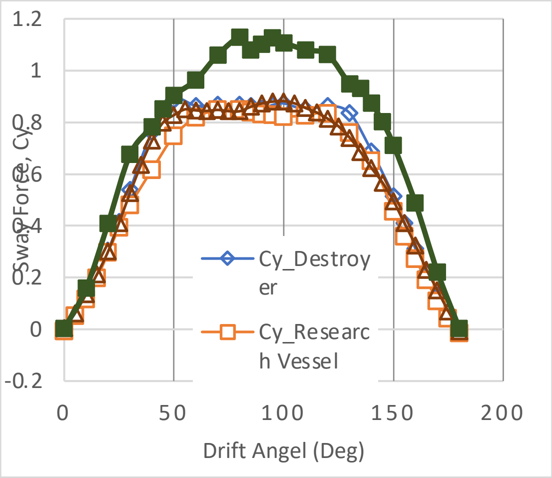

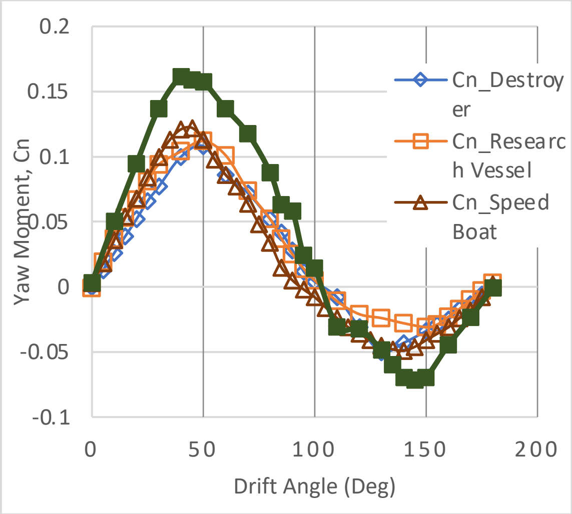

Code SLAVIB

1. Seakeeping: heading or following waves only
2. Strip theory (on the basis of STRIPmod)
3. Wagner's slamming model with empiric corrections (filtered pile-up)
4. Hybrid frequency-time domain
5. Regular and irregular seas (Donelan spectrum)
6. Rigid and elastic hull
7. Vibrations by means of modal shapes method
8. Whipping and springing accounted for
9. Equivalent static loads
10. Shear forces and bending moments at various stations
11. Fortran 90 code

Sectional Total Load

$$
\begin{aligned}
F &= \min\left[-k\rho\frac{\pi}{8}\left(b^2\frac{\mathrm{D}w}{\mathrm{D}t}+w_+\frac{\mathrm{D}b^2}{\mathrm{D}t}\right)-\rho(g-\mathsf{z}_{\mathsf{w3}}(x,z_0,t))A_0,\ (p_a-p_v)b\right]\\
&+\ f_+\left[-k\rho\frac{\pi}{8}V\left(b^2\frac{\partial w}{\partial x}+w_+\frac{\partial b^2}{\partial x}\right)-\frac{1}{2}\rho bV^2\right],
\end{aligned}
$$

where

$$
\begin{aligned}
f_+(x) &= \max(x,0),\\
w_+ &= \begin{cases} w & \text{if} \quad w_p>0 \ \text{and} \ w>0,\\ 0 & \quad\quad\ \text{otherwise} \end{cases}
\end{aligned}
$$

$$D/Dt=\frac{\partial}{\partial t}-V\frac{\partial}{\partial x},$$

$$w=\frac{\mathrm{D}r(x,t)}{\mathrm{D}t},$$

$$r(x,t)=T_0(x,t)+z_{ref}(x),$$

Vibrations and loads

$$\mu \ddot{z}_0 + \mathcal{K}(z_0) = 0, \qquad \mu(x) = m(x) + \mu_{33\infty}(x).$$

$$z_0(x,t) = \sum_j a_{0j}(t)\zeta_j(x), \qquad \mathcal{K}(\zeta_j) = \Omega_j^2 \mu(x)\zeta_j.$$

$$\mu \ddot{z} + \mathcal{K}z + \gamma \frac{\partial}{\partial t}(\mathcal{K}z) + \beta \dot{z} = F_{RB}(x,t), \qquad z(x,t) = \sum_j a_j(t)\zeta_j(x),$$

$$\ddot{a}_j + \bar{\nu}\Omega_j \dot{a}_j + \Omega_j^2 a_j = f_j(t),$$

$$f_j(t) = \frac{\int_L F_{RB}(x,t)\zeta_j(x)\mathrm{d}x}{\int_L \mu(x)\zeta_j^2(x)\mathrm{d}x}.$$

$$F_s(x,t) = \mu(x)\sum_j a_j(t)\Omega_j^2\zeta_j(x).$$

$$V_3(x,t) = \int_x^{bow} v_3(\xi,t)\mathrm{d}\xi,$$

$$v_3(x,t) = \begin{cases} F_{RB}(x,t) & \text{for the rigid hull,} \\ F_s(x,t) & \text{for the elastic hull.} \end{cases}$$

$$M_3(x,t) = \int_x^{bow} V_3(\xi,t)\mathrm{d}\xi$$

Example of output

```
SLAVIB Nonlinear Loads and Vibrations Simulation:

 Ishiguro Schiff voll beladen

Main Particulars:
   Length......... 191.230 m
   Beam...........  28.009 m
   Draught........   6.810 m
   Trim...........   0.000 m
   Displacement...   19154.4     m^3
   Speed.......... 16.90 m/s  = 32.9 kn
   Froude number..  0.390
Regular waves:
   Height:            8.000 m
   Period:           11.300 s
   Propagation angle: 180.0 deg


Simulation time:   400.0 s
```

```
Results are presented for  50 strips numbered from 1 (stern) to  50 (bow)

Extreme bending moments (still water + waves; elastic hull):
  --maximum equivalent statical value:   0.1211E+07 kN*m  at station  29
  --minimum equivalent statical value:   -5843.     kN*m  at station   6

Extreme bending moments (still water + waves; rigid hull):
```

```
  --maximum value:   0.1183E+07 kN*m  at station  28
  --minimum value:   -7779.     kN*m  at station   5

Midship extreme equivalent bending moments (still water + waves; elastic hull):
  --in hogging:     0.1157E+07 kN*m
  --in sagging:     0.3589E+06 kN*m

Midship extreme bending  moments (still water + waves; rigid hull):
  --in hogging:     0.1141E+07 kN*m
  --in sagging:     0.4706E+06 kN*m


Simulation started  on  2003.01.23  at  17:52:37.8
Simulation finished on  2003.01.23  at  19:05:50.7

Elapsed CPU time:   4392.957 seconds
```

Table 1: Influence of Discretization

n_x	n_z	Δt, s	V_{5max}, kNm	V_{5min}, kNm	Relative CPU time
50	100	0.01	0.1498e7	-8	1
100	200	0.01	0.1520e7	-4570	2.44
200	400	0.01	0.1515e7	-1757	7.41
200	400	0.005	0.1516e7	-1570	14.07
200	400	0.002	0.1516e7	-1464	34.67
200	400	0.001	0.1516e7	-1428	70.83
400	400	0.005	0.1516e7	-1807	28.1
400	600	0.005	0.1517e7	-1809	40.34

Hull description

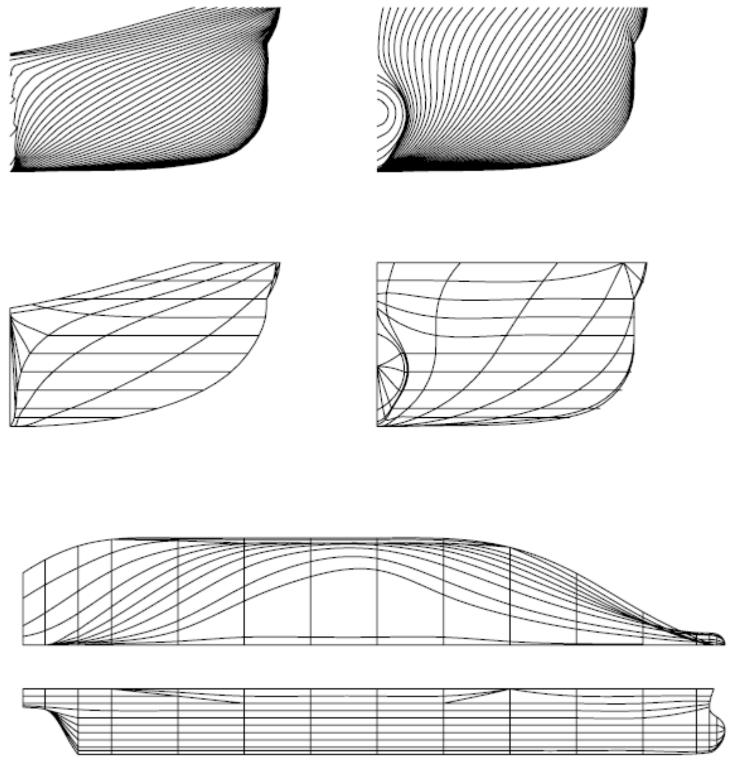

Figure 2: *Body lines of the sample ship: EUMEDES representation*

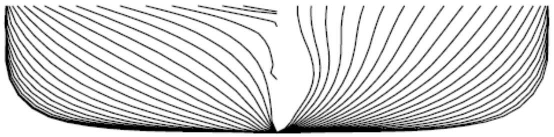

Figure 3: *Body lines of the sample ship: sections generated for STRIPmod (51 nominal sections)*

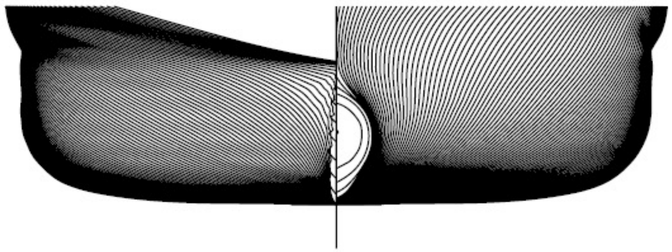

Figure 4: *Body lines of the sample ship: sections generated for SLAVIB (200 sections, 400 waterplanes*

Time histories for sectional loads

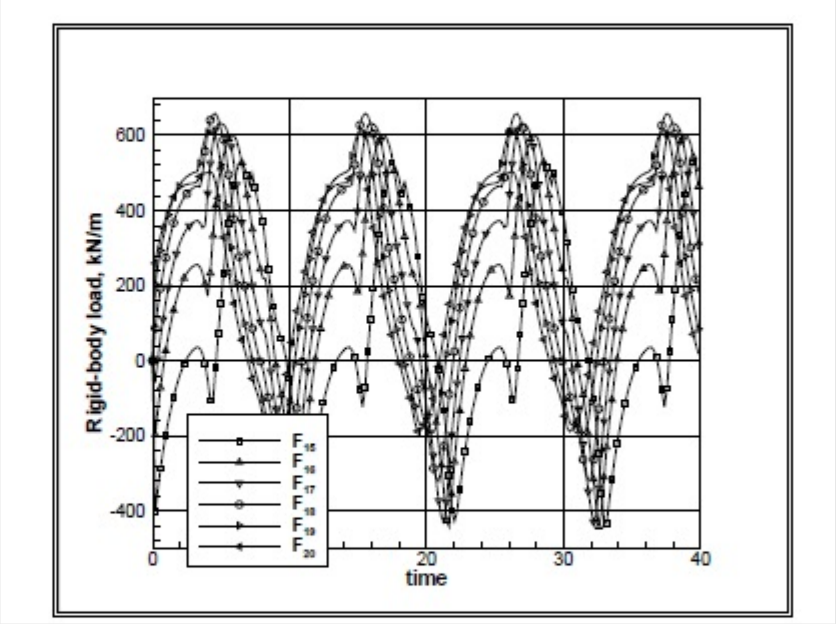

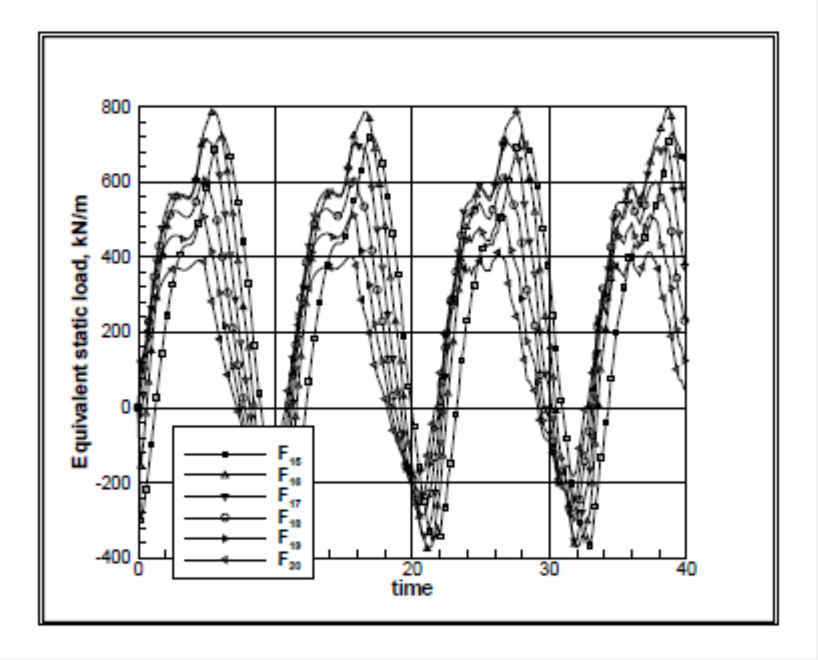

Figure 13: *Time histories for the total loading on the strips 15 to 20 (with 20th strip being the last): the ship is assumed to be rigid; head regular waves* h_w *= 8 m,* **Fn** = 0

Figure 14: *Time histories for the equivalent static load on the elastic ship*

Irregular seas

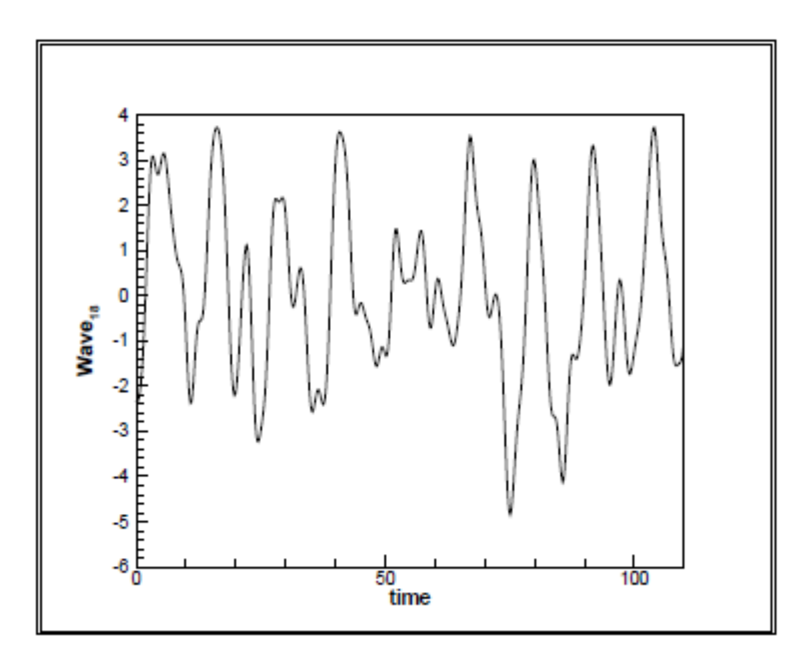

Figure 29: *Irregular head sea:* $\overline{h_{1/3}}$ = 8.0m*; Donelan spectrum; process at the station 18*
(out of 21); **Fn** = 0

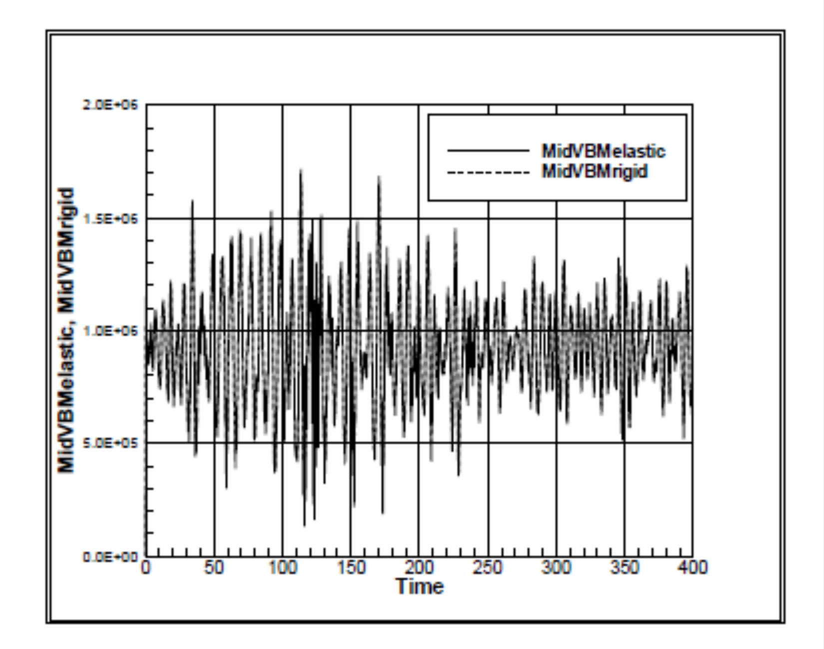

Figure 36: *Time histories for the midship bending moment in head irregular sea: rigid-body*
and elastic formulations (final variant)

Thank you!

Спасибо за внимание!